

11-22-2018 2:30 PM

# Determining the Molecular Mechanisms of PACS-1-mediated Protein Sorting

Brennan S. Dirk, *The University of Western Ontario*

Supervisor: Dikeakos, Jimmy D., *The University of Western Ontario*

A thesis submitted in partial fulfillment of the requirements for the Doctor of Philosophy degree in Microbiology and Immunology

© Brennan S. Dirk 2018

Follow this and additional works at: <https://ir.lib.uwo.ca/etd>



Part of the [Cell Biology Commons](#), and the [Virology Commons](#)

---

## Recommended Citation

Dirk, Brennan S., "Determining the Molecular Mechanisms of PACS-1-mediated Protein Sorting" (2018). *Electronic Thesis and Dissertation Repository*. 5966.  
<https://ir.lib.uwo.ca/etd/5966>

This Dissertation/Thesis is brought to you for free and open access by Scholarship@Western. It has been accepted for inclusion in Electronic Thesis and Dissertation Repository by an authorized administrator of Scholarship@Western. For more information, please contact [wlsadmin@uwo.ca](mailto:wlsadmin@uwo.ca).

## Abstract

Membrane trafficking events are required to direct proteins to their precise subcellular locations. The cellular Phosphofurin Acidic Cluster Sorting protein – 1 (PACS-1) has emerged as a protein of interest in controlling the localization of a multitude of cellular and viral proteins. Specifically, PACS-1 is hijacked by type-1 Human Immunodeficiency Virus (HIV-1) to contribute to immune evasion in addition to regulating neuroendocrine hormone storage and release. To accomplish this, PACS-1 connects the cytoplasmic tail of cellular receptors to the heterotetrameric adaptor proteins (APs) to form a functional trafficking unit. Throughout this dissertation, I explored the role of PACS-1 and AP-1 to drive the localization of unique cargo proteins; the type-1 major histocompatibility complex (MHC-I) and the adrenocorticotrophic hormone (ACTH). I have utilized the intracellular protein-protein interaction reporter assay: bimolecular fluorescence complementation (BiFC), in combination with super-resolution microscopy to uncover the membrane trafficking route undertaken by the HIV-viral accessory protein Nef and the cellular receptor MHC-I. Additionally, I have generated a tool termed “viral BiFC” to study virus:host interactions in cells. These studies revealed a mechanism by which Nef re-routes MHC-I from the cell surface, toward the trans-Golgi Network (TGN) by hijacking both early and recycling endosomes. Interestingly, Nef requires PACS-1 to permit the transport of MHC-I from the endosomes to the TGN, a process which is also dependent on AP-1 recruitment. Moreover, the role of PACS-1 extends beyond its implication in HIV-1 infection. The regulation of neuroendocrine cell hormone storage and secretion is a tightly regulated process requiring coordinated trafficking of multiple proteins. Thus, I hypothesized that PACS-1 would promote proper storage of ACTH within specialized storage granules. These studies identified a key role for PACS-1 and AP-1 in directing ACTH to the storage granule. Undoubtedly, the function of PACS-1 is important in not only the immune evasive capabilities of HIV-1 Nef, but also in the regulation of hormone secretion. By understanding how cargo molecules are targeted throughout the cell by PACS-1, we can begin to unravel the molecular details of viral pathogenesis and cellular homeostasis.

## Keywords

Membrane trafficking, Cell biology, HIV-1, Nef, Regulated secretion, PACS-1

# Co-Authorship Statement

## Chapter 2

The data within chapter 2 was published in PLoS ONE: **Dirk BS\***, Jacob RA\*, Johnson AL, Pawlak EN, Cavanagh CP, Van Nynatten L, Haeryfar SM, & Dikeakos JD. 2015. Viral bimolecular fluorescence complementation: A Novel Tool to Study Intracellular Vesicular Trafficking Pathways. *PLoS ONE*. 10(4) doi:e0125619.

The above co-authors assisted in writing and editing the manuscript, as well as cloning of some of the constructs. All microscopy data, western blots and quantifications were conducted by myself. The flow experiments were conducted in conjunction of RAJ.

## Chapter 3

A portion of the results in chapter 3 were published in Scientific Reports: **Dirk BS**, Pawlak EN, Johnson AL, Van Nynatten LR, Dr. Jacob RA, Heit B & Dikeakos JD. 2016. HIV-1 Nef sequesters MHC-I intracellularly by targeting early stages of endocytosis and recycling. *Scientific Reports*. 6:37021.

All of the above co-authors aided in the writing and editing of the manuscript. Flow cytometry experiments were done in conjunction with ENP. A portion of the cells quantified and images presented in Figures 3.10 to 3.13 were imaged by an undergraduate research project student, Christopher End, whom I directly supervised.

## Chapter 4

A portion of the results in chapter 4 was published in Biochemical and Biophysical Communications: **Dirk BS**, End C, Pawlak EN, Van Nynatten LR, Jacob RA, Heit B, Dikeakos JD. 2018. PACS-1 and adaptor proteins – 1 mediate ACTH trafficking to the regulated secretory pathway. *Biochem Biophys Res Commun*. (in press).

All data within this chapter was conducted by me, with exception of the western blots in Figure 4-1, which were conducted by Christopher End.



## Acknowledgments

Firstly, I would like to thank my supervisor Dr. Jimmy Dikeakos. Words cannot comprehend how much your support has meant to me over the course of my PhD. I thank you for the countless hours you have spent editing manuscripts, scholarship applications, presentations and my thesis. I thank you for the guidance that you have provided me through my academic career and personal life. Graduate school is very much like a roller coaster, and you have always believed in me, even when sometimes I didn't always believe in myself. Most importantly, I thank you for the friendship that you have provided over the years, as you have always treated myself and other lab members as family.

I would also like to thank the members of my thesis advisory committee; Dr. Greg Dekaban and Dr. Bryan Heit. I could not have asked for a better committee to support me throughout the past five years.

I have been fortunate enough to work with some amazing people in the lab for the past 5+ years. To all the past and present members of the Dikeakos lab, thank you for always supporting me. I would especially like to thank Aaron Johnson, Emily Pawlak, Logan Van Nynatten and Rajesh Jacob for their friendship the past 5 years. Aaron, you were always there to encourage me. Emily, thank you for keeping me on track and focused. Logan, thank you for keeping me sane, even though sometimes the microscope had other plans. Raj, thank you for always being there when I needed help with setting up virus experiments, especially early on. I would also like to send a special thank you to the current members: Mitch, Cassie, Olivia, Roy, Steven and Jason. I wish you the best luck on your next steps, you have chosen a great mentor and lab to do research.

Last, but certainly not least, I would like to thank my family and friends. The past 5+ years have not been easy. I know I have missed many family functions, and it has meant the world to have your support. Thank you Mom and Dad for supporting me through my undergraduate degree, and encouraging me to pursue my passion of science. To my wife Jade, you have been my biggest supporter and have carried me through the 5+ years of my PhD. I honestly do not think I would have been able to do this without you by my side.

# Table of Contents

Abstract.....	i
Co-Authorship Statement .....	iii
Acknowledgments .....	iv
Table of Contents.....	v
List of Tables .....	x
List of Figures.....	xi
List of Abbreviations .....	xiv
Chapter 1.....	1
1 Introduction.....	1
1.1 General introduction to membrane trafficking .....	1
1.2 Organization of the endomembrane system .....	2
1.3 Membrane trafficking and disease.....	5
1.4 Trafficking motifs and proteins .....	6
1.4.1 Sorting motifs .....	6
1.4.2 Adaptor protein complexes.....	7
1.4.3 Membrane coat proteins .....	8
1.5 The Phosphofurin Acidic Cluster Sorting proteins: multifaceted membrane trafficking regulators .....	10
1.5.1 Regulation of PACS-1 sorting.....	12
1.5.2 Receptor trafficking by PACS-1.....	13
1.6 The secretory pathway.....	16
1.6.1 Regulated secretory pathway.....	16
1.7 Introduction to viruses .....	18
1.8 Strategies for viral immune evasion: The MHC-I receptor.....	19
1.8.1 Targeting MHC-I peptide loading and trafficking .....	22

1.9 The human immunodeficiency virus (HIV-1).....	26
1.10 A key pathogenic mediator of HIV-1 disease: Nef .....	26
1.11 Thesis overview .....	31
1.12 References .....	33
Chapter 2.....	48
2 Viral Bimolecular Fluorescence Complementation: A Novel Tool to Study Intracellular Vesicular Trafficking Pathways .....	48
2.1 Introduction .....	48
2.2 Results .....	50
2.2.1 Designing a lentiviral vector enabling dual transgene expression .....	50
2.2.2 Insertion of an F2A site into a lentiviral vector allows concurrent protein production.....	52
2.2.3 Nef and Nef-interacting partners are simultaneously expressed in a lentiviral vector.....	54
2.2.4 Viral BiFC demonstrates that Nef interacts with PACS-1 in specific endosomal compartments .....	58
2.2.5 Viral BiFC can be used to study novel interactions between Nef and host cellular proteins in the endocytic network.....	65
2.3 Discussion.....	69
2.4 Materials and Methods .....	73
2.4.1 Cell Culture.....	73
2.4.2 Proviral plasmids and cloning strategy.....	73
2.4.3 Generation of the F2A cleavage site and 5' MCS .....	75
2.4.4 Pseudovirus production and processing .....	76
2.4.5 Western Blots, Antibodies and Infections .....	76
2.4.6 Microscopy .....	77
2.4.7 Flow Cytometry .....	78
2.4.8 Statistics.....	79

2.5	References .....	79
Chapter 3.....		83
3	HIV-1 Nef sequesters MHC-I intracellularly by targeting early stages of endocytosis and recycling.....	83
3.1	Introduction .....	83
3.2	Results .....	86
3.2.1	Bimolecular fluorescence complementation microscopy detects a Nef:MHC-I complex in cells .....	86
3.2.2	Nef targets recycling MHC-I prior to transit through a Rab11 compartment .....	89
3.2.3	Nef interacts with MHC-I within an early endosomal compartment .....	92
3.2.4	Nef traffics MHC-I to a late endosomal compartment .....	96
3.2.5	Nef and MHC-I are not trafficked to the lysosome, but traffic to the trans-Golgi network .....	97
3.2.6	PACS-1 recruitment by Nef alters the intracellular localization of the Nef:MHC-I complex.....	109
3.2.7	Adaptor Protein -1 recruitment is enhanced by the Nef acidic cluster ....	112
3.2.8	PACS-1 directly facilitates localization of MHC-I to the trans-Golgi Network .....	117
3.3	Discussion.....	120
3.4	Methods .....	123
3.4.1	Cells .....	123
3.4.2	Plasmids.....	124
3.4.3	Transfections .....	124
3.4.4	Western Blots .....	125
3.4.5	Immunofluorescence .....	125
3.4.6	Antibody Uptake.....	126
3.4.7	Ammonium chloride treatment of cells to assess lysosomal trafficking. ....	127
3.4.8	Microscopy .....	127

3.4.9	Flow cytometry.....	128
3.4.10	Statistics.....	129
3.5	References .....	130
Chapter 4.....		135
4	PACS-1 and Adaptor Protein 1 mediate ACTH trafficking to the regulated secretory pathway.....	135
4.1	Introduction .....	135
4.2	Results .....	137
4.2.1	PACS-1 and AP-1 promote intracellular storage of POMC.....	137
4.2.2	ACTH is not directed to a lysosomal degradation pathway .....	143
4.2.3	PACS-1: Adaptor Protein interactions modulate PACS-1:ACTH co-localization.....	145
4.2.4	PACS-1 facilitates the trafficking of ACTH to mature secretory granules .....	148
4.3	Discussion.....	151
4.4	Materials and Methods .....	154
4.4.1	Cell Culture.....	154
4.4.2	Plasmids and siRNA.....	154
4.4.3	Transfections .....	154
4.4.4	qRT-PCR .....	155
4.4.5	Western Blots .....	155
4.4.6	Extracellular ACTH Quantification.....	156
4.4.7	Widefield microscopy.....	156
4.4.8	Ground-state depletion microscopy.....	157
4.4.9	Statistics.....	157
4.5	References .....	158
Chapter 5.....		163

5 Thesis Overview .....	163
5.1 Discussion.....	163
5.1.1 General Discussion Overview .....	163
5.1.2 Summary of Findings .....	163
5.1.3 Interrogating Nef's interacting partners during MHC-I downregulation	165
5.1.4 Role of PACS-1 and AP-1 in protein sorting .....	168
5.1.5 Concluding remarks.....	169
5.2 References .....	170
Curriculum Vitae .....	177

## List of Tables

Table 1: Sorting motifs within the endomembrane system. ....	7
Table 2: Primers used for cloning viral-BiFC vectors.....	74
Table 3 Primers for mutagenesis and qRT-PCR .....	158

## List of Figures

Figure 1.1: Overview of the endomembrane system.....	3
Figure 1.2: PACS-1 structure and function .....	15
Figure 1.3: Interactions at the immunological synapse. ....	20
Figure 1.4: Viral targeting of MHC-I antigen presentation.....	24
Figure 1.5: Dual mechanisms of Nef-mediated MHC-I downregulation. ....	30
Figure 2.1: Construction of an HIV-1 derived lentiviral expression system harboring an F2A peptide and two multiple cloning sites. ....	51
Figure 2.2: Functional cleavage at the engineered F2A site.....	53
Figure 2.3: Fluorescence microscopy confirms expression of proteins from the 5' and 3' MCS.....	55
Figure 2.4: MHC-I-mCherry produced from the F2A site reaches the cell surface and is sensitive to Nef. ....	57
Figure 2.5: Visualizing the Nef/PACS-1 interaction using viral Bimolecular Fluorescence Complementation. (A).....	59
Figure 2.6: Nef-V <sub>C</sub> expressed from a viral BiFC vector expressing PACS-1-V <sub>N</sub> is able to downregulate MHC-I.....	61
Figure 2.7: Nef/PACS-1 viral BiFC signal is localized to specific Rab5 and LAMP-1 positive endosomes. ....	63
Figure 2.8: Viral BiFC signals of MHC-I/Nef and SNX18/Nef are localized to AP-1 positive endosomes. ....	66
Figure 2.9: Nef-V <sub>C</sub> expressed from a base viral BiFC vector is able to downregulate MHC-I. ....	68



Figure 3.1 Bimolecular fluorescence complementation is observed between Nef and MHC-I. .....	87
Figure 3.2: Functionality of MHC-I and Nef fusion proteins.....	88
Figure 3.3: Nef prevents MHC-I from entering into a Rab11 dependent recycling route. ....	90
Figure 3.4: Nef:MHC-I interaction occurs within Rab5-positive early endosomes.....	93
Figure 3.5: Disruption of early endosomal regulation interferes with Nef-mediated MHC-I downregulation. ....	95
Figure 3.6: Nef:MHC-I interaction occurs within Rab7-positive late endosomes. ....	99
Figure 3.7: Nef:MHC-I interaction does not occur in lysosomes.....	102
Figure 3.8: Lysosomal localization of MHC-I-eGFP.....	105
Figure 3.9: Nef targets MHC-I for sequestration within the trans-Golgi network. ....	107
Figure 3.10: The Nef acidic cluster mutant alters the intracellular localization of the Nef:MHC-I complex.....	110
Figure 3.11: Wide-field microscopy demonstrates that PACS-1 recruitment by Nef enhances the co-localization of AP-1 to the Nef:MHC-I complex. ....	114
Figure 3.12: Ground state depletion microscopy (GSDM) demonstrates that PACS-1 recruitment by Nef enhances the localization of AP-1 to the Nef:MHC-I complex. ....	116
Figure 3.13: PACS-1:Adaptor Protein interaction promotes TGN localization of Nef and MHC-I .....	118
Figure 4.1: Intracellular storage of POMC is regulated by PACS-1 and AP-1.....	139
Figure 4.2: PACS-1, AP-1 and AP-3 are required for the sorting of ACTH to the regulated secretory pathway. ....	141
Figure 4.3: ACTH is not targeted to the degradative lysosomal compartment. ....	144

Figure 4.4: PACS-1 co-localizes to POMC<sup>+</sup> vesicles in AtT-20 cells.....146

Figure 4.5: PACS-1 and AP-1 facilitate the sorting of POMC to mature secretory granules.  
.....149

## List of Abbreviations

ACTH	adrenocorticotrophic hormone
ADMUT	adaptor mutant
ADP	adenosine diphosphate
AIDS	acquired immunodeficiency syndrome
ANOVA	analysis of variance
AP	adaptor protein
APC	allophycocyanin
Arf	adenosine ribosylation factor 1
ARR	atrophin related region
B2M	beta -2-microglobulin
Bp	base pairs
BSA	bovine serum albumin
BST2	bone marrow stromal cell antigen 2
CA	constitutively active
CD	cluster of differentiation
cDNA	complementary deoxyribonucleic acid
CFTR	cystic fibrosis transmembrane conductase regulator
CI-MPR	cation independent mannose 6 phosphate receptor
CK2	casein kinase 2

COP-I	coatamer protein I
COP-II	coatamer protein 2
CPE	carboxy peptidase e
CT	cycle threshold
CTL	cytotoxic t lymphocyte
CTR	c-terminal region
DAPI	4',6-diamidino-2-phenylindole
DCSGs	dense core secretory granule
DN	dominant negative
DNA	deoxyribonucleic acid
ECL	Enhanced chemiluminescence
EDTA	Ethylenediaminetetraacetic acid
eGFP	enhanced green fluorescence protein
ER	Endoplasmic Reticulum
ERAD	endoplasmic reticulum associated degradation pathway
ERGIC	endoplasmic reticulum-Golgi intermediate compartment
F2A	auto cleavable 2a peptide
FACS	fluorescence activated cell sorting
FBR	furin binding region
FITC	Fluorescein isothiocyanate

FL1	fluorophore 1
FL2	fluorophore 2
GAP	guanine nucleotide triphosphatase activating protein
GEF	Guanine nucleotide exchange factor
GGA	Golgi-localized gamma-ear containing arf binding protein
GSDM	ground state depletion microscopy
GTPASE	Guanine triphosphatase
hCMV	human cytomegalovirus
HEPES	hydroxyethylpiperazine ethane sulfonic acid
HIV	human immunodeficiency virus
HLA	human leukocyte antigen
HRP	horse radish peroxidase
ICP47	infected cell protein 47
IRES	internal ribosomal entry site
JaCoP	just another co-localization plugin
KDa	kilodalton
LAMP1	lysosomal associated membrane protein 1
LTR	long terminal repeat
MAP	mouse anterior pituitary
MCS	multiple cloning site

MCS	multiple cloning site
MHC-I	major histocompatibility complex type - 1
MHC-II	major histocompatibility complex type II
MliSR	Molecular interactions in super resolution imaging
MR	middle region
MSH	melanocyte stimulating hormone
MW	molecular weight
NA	numerical aperture
NIH	National Institute of Health
nm	nanometer
PACS	phosphofurin acidic cluster sorting protein
PBS	phosphate buffered saline
PC	pro-hormone convertase
PFA	paraformaldehyde
PI3K	phosphoinositide 3 kinase
POMC	pro-opiomelanocortin
PP2A	protein phosphatase 2a
PTEN	phosphatase and tensin homolog
qRT-PCR	quantitative real-time polymerase chain reaction
RD1	phycoerythrin

RNA	ribonucleic acid
RT	reverse transcriptase
SDS	sodium dodecyl sulfate
SDS- PAGE	sodium dodecyl sulfate polyacrylamide gel electrophoresis
Sec	secretory
SERINC5	serine incorporator 5
siRNA	short interfering ribonucleic acid
SNARE	Soluble N-ethylmaleimide-sensitive factor attachment protein receptor
SYK	spleen tyrosine kinase
TAP	tapasin
TBST	tris-buffered saline + tween
TCR	T cell receptor
TfnR	transferrin receptor
TGN	trans-Golgi Network
TGN46	trans-Golgi Network protein 46
TSG101	tumour susceptibility gene 101
US6	unique short 6 protein
VAMP	vesicular associated membrane protein
vATPase	vacuolar adenosine triphosphatase

VC	C-terminal venus
VN	N-terminal venus
WB	Western Blot
ZAP 70	zeta chain associated protein kinase 70
μm	micrometer



# Chapter 1

## 1 Introduction

### 1.1 General introduction to membrane trafficking

Eukaryotic cells are characterized by the presence of intracellular membrane-bound compartments that are termed organelles. The development of such specialized compartments enables eukaryotic cells to carry out diverse cellular functions within precise cellular compartments (1). However, this compartmentalization also requires exquisite mechanisms that control the movement of compartmental contents from one area to another, and often relies on sub-organelle structures in the form of membrane bound vesicles. The net result of this control is a constant shuttling of vesicles and the proteins they carry, their cargo, throughout the cell. These trafficking steps are collectively controlled by the endomembrane system and the membrane trafficking machinery. Millions of years of evolution have led to a full network of interconnected organelles each with their own specialized functions, and controlled by multiple adaptor and connector proteins (Fig 1.1)(1-3).

More specifically, eukaryotic cells contain a defined set of organelles that are critical for membrane trafficking. One such organelle, the endoplasmic reticulum (ER), is required for protein synthesis (4-6). Conversely, the Golgi apparatus fulfills a role of sorting proteins to their correct destination while also ensuring a diverse array of post-translational modifications take place along the way (7-10). In addition, eukaryotic cells contain a plethora of vesicles, which can also be considered organelles. These vesicles include multiple types of endosomal vesicles and lysosomes, which together form the endolysosomal network (Fig 1.1).

The identity of the various eukaryotic organelles is not only defined by their function but also by the proteins that coat their outer. Genomic studies have demonstrated that eukaryotes contain groups of proteins that form the basis of membrane trafficking and also define organelle identity (1, 2). These groups of proteins include: coat proteins which can induce membrane curvature and budding; guanine nucleotide exchange factors

(GEFs) and GTPase activating proteins (GAPs), which control the identity of endosomal membranes (11-13); vacuolar ATPases (14), which modulate intraluminal pH; and soluble N-ethylmaleimide sensitive factor attachment protein receptor (SNARE) proteins that primarily serve to dock and fuse vesicles (15, 16). Taken together, this basic set of proteins provides the basis for membrane trafficking.

## 1.2 Organization of the endomembrane system

Within the endomembrane system exists two primary trafficking routes; the retrograde transport system (movement from the plasma membrane to the cell interior; encompassing the endolysosomal network), and the secretory transport system (10, 17) (movement of newly synthesized proteins to the cell surface). Elements encompassing the endolysosomal machinery include pathways that recycle cell surface proteins (18-20), and target cellular proteins for degradation via the acidic lysosomal organelle or traffic cellular receptors to the Golgi-network (21). Moreover, secretory transport can be further subdivided into the regulated, and constitutive secretion of proteins depending on specific cell types (22).

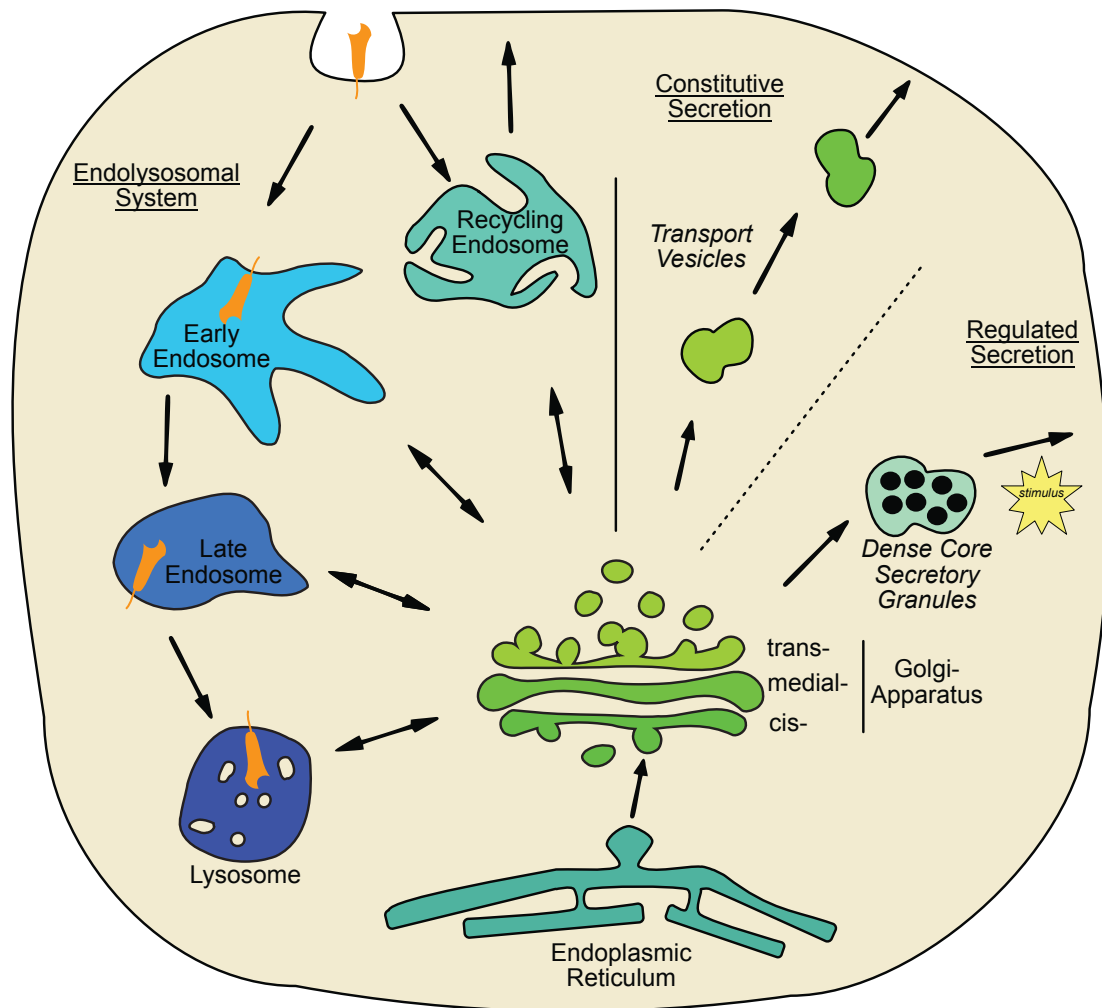


**Figure 1.1: Overview of the endomembrane system**

The endomembrane system can be classified into two primary networks; the endolysosomal network (retrograde transport; left), and the secretory network (anterograde transport; right). The endolysosomal network is responsible for sorting newly endocytosed molecules within the cell. Destinations include the recycling endosome; where molecules can be rapidly returned back to the cell surface, early and late endosomes; which represent increasingly acidifying compartments where molecules can be sorted to either the degradative lysosomal compartment, or back to the TGN to be further modified or sequestered. The secretory network (right) primarily targets newly synthesized proteins to the cell surface or for secretion. Two primary pathways exist: constitutive secretion or regulated secretion. Constitutive secretion is present within all

cell types, and utilizes the ER to synthesize proteins, which are subsequently modified within the Golgi apparatus, and transported to the cell surface through transport vesicles. Regulated secretion is present within specialized cell types such as endocrine and neuroendocrine cells, and packages cargo within a dense core secretory granule organelle for subsequent secretion upon a physiological stimulation.

### 1.3 Membrane trafficking and disease

While membrane trafficking is fundamental in nature, it plays a critical role in health and disease (23). For example, within the regulated secretory pathway of neuroendocrine cells (Fig. 1.1), neurotransmitter synthesis and release will require fine-tuned intracellular storage and release mechanisms (24, 25). Similarly, hormonal regulation also requires the regulated secretory pathway (26). Moreover, the trafficking of functional receptors to the cell surface for immune cell signaling and communication is critical for cellular homeostasis and immunity (27-30). As such, multiple human diseases are the result of defects in membrane trafficking. Cystic fibrosis patients, for example, may carry mutations within the cystic fibrosis conductance regulator gene (*ctfr*)(31, 32), which results in the intracellular mis-localization of CFTR. Conversely, patients with Hermansky-Pudlak syndrome, a rare disorder resulting in albinism and bleeding problems, carry mutations within the trafficking machinery involved in the formation of vesicles, resulting in platelet dysfunction and decreased melanin storage (33-35).

These fundamental membrane trafficking processes are also utilized by pathogens such as viruses, which have evolved methods to traffic within eukaryotic cells. As viruses are unable to replicate in the absence of their host, they hijack components of the endomembrane system in order to gain access to sites permissive for viral replication and assembly within the cell (36). This viral manipulation of the endolysosomal network is required by multiple viruses to ensure the completion of viral lifecycles (37-39). For example, viral proteins can alter the location of host cellular proteins normally located on the cell surface thereby inhibiting antiviral signaling pathways, apoptosis, and communication (40-42). These activities can render the cellular environment more permissive to viral replication. The type-1 human immune deficiency virus (HIV-1) is no exception to this as the viral accessory proteins Nef and Vpu modify the surface expression of over 35 receptors for the purposes of viral immune evasion, propagation and cell-to-cell signaling (41). Thus, the endomembrane system while fundamental in nature is a central component that is often deregulated during diseased states.

## 1.4 Trafficking motifs and proteins

### 1.4.1 Sorting motifs

The movement of proteins within the cell is not a random process. For example, proteins that contain transmembrane domains are properly routed to the cell surface where they fulfill critical cellular functions dependent on their differential abilities to bind or transport ligands, thereby serving as functional receptors (43, 44). The trafficking of receptors is dependent on sorting motifs within their cytoplasmic domains. These motifs enable key interactions with cytosolic trafficking molecules (45). Sorting motifs were initially proposed by the Nobel Prize laureate Gunter Blobel (46, 47). They are amino acid sequences that direct proteins to a precise subcellular locale. Several motifs have been described in eukaryotes that traffic proteins containing transmembrane domains to and from the cell surface, between endosomes, the endoplasmic reticulum, and the Golgi apparatus (See Table 1) (45). Interestingly, these sorting motifs have evolved to be specific as different sorting motifs can recruit various trafficking proteins, termed adaptor proteins (APs)(48). In general, adaptor proteins interact with cytoplasmic tails of cellular receptors and allow the recruitment of additional structural and movement proteins required for vesicular trafficking (48, 49).

One of the most well studied set of adaptor proteins are the heterotetrameric clathrin adaptor proteins (APs) (49). Most notably, these proteins directly interact with sorting motifs and permit the formation of vesicles by recruiting the structural coat protein clathrin. Two well described sorting motifs characteristic of this family are the tyrosine, and dileucine sorting motifs (48, 50). An additional mode of controlling vesicular trafficking is through post-transcriptional modifications, which can also serve as sorting signals. For example, the phosphorylation of two serine residues within the furin's endopeptidase's acidic cluster (S<sub>773</sub>DS<sub>775</sub>EEDE) directs furin's recycling between the TGN and endosomes (51, 52). Furthermore, newly synthesized transmembrane proteins requiring exit from the ER possess ER exit signals (di-acidic motifs)(53). In contrast, ER resident receptors contain di-basic motifs (KKxx/ KxKxx)(54). Importantly, these motifs allow the recruitment of various connector, adaptor and structural proteins to facilitate vesicle biogenesis, movement and docking which will be discussed below.

**Table 1: Sorting motifs within the endomembrane system.**

Sorting Motifs	Examples of Receptors with Sorting Motifs	Trafficking Protein(s) Recruited by Sorting Motif	Subcellular Trafficking Location (s)
Tyrosine motif (Yxx $\theta$ )	Furin, CI-MPR	AP-1/2/3/4/5	Endosome - TGN
Dileucine motif (LL)	CD4, CD28	COPII, AP-1/2/3/4/5	Plasma membrane - Endosomes
Di-basic Motif (KKxx/KxKxx)	KDEL-receptor	COP-I	Cis-Golgi to ER
Di-Acidic Motif (D/E)xx(D/E),	ERGIC-53	COP-II	ER exit signal
Acidic Cluster Motif (E/D) <sub>4</sub>	Furin, VAMP4	PACS-1	Endosomes – TGN

#### 1.4.2 Adaptor protein complexes

One of the most well studied family of trafficking molecules that bind and recognize sorting motifs to traffic receptors within cells is the heterotetrameric adaptor proteins (APs) complex family. Currently, five AP complex types (AP-1 through 5) have been described to mediate trafficking to diverse locations within the cell (49, 55). Each AP complex contains four subunits; two large subunits (either an  $\alpha$ ,  $\gamma$ ,  $\delta$ ,  $\epsilon$  or  $\zeta$  plus a  $\beta$ 1- $\beta$ 5 subunit), one medium ( $\mu$ 1- $\mu$ 5), and one small subunit ( $\sigma$ 1- $\sigma$ 5) (55). Each subunit, of the heterotetramer has a specific function. The  $\alpha$ ,  $\gamma$ ,  $\delta$  and  $\epsilon$  large subunits associate with specific lipids on membranes (56, 57), and the  $\beta$  subunits recruit the coat protein clathrin through the L $\theta$ x $\theta$ D/E amino acid motif, where  $\theta$  represents a bulky hydrophobic residue. The medium subunit primarily recognizes tyrosine (Yxx $\theta$ ) and dileucine sorting (LL) motifs, and is also able to interact with lipids located in membranes. The small  $\sigma$  subunits ( $\sigma$ 1-5) do not have a defined role in receptor or lipid binding, and instead provide stability to the AP complex (58).

Each AP controls distinct trafficking steps within cells. AP-1 is primarily found within endosomes and the Golgi apparatus (59). Its principal function is to traffic receptors to and from the Golgi apparatus and endosomes (59). Alternatively, AP-2 is localized to the plasma membrane and recycling endosomes, where it controls clathrin-mediated

endocytosis of cargo and recycling (60). Like AP-1, AP-3 is also localized to the Golgi and endosomes, but primarily regulates cargo destined for lysosomal organelles and synaptic vesicles (33, 61). Unlike the other APs, both AP-4 and AP-5 are much less studied and mediate cargo movement from the Golgi to the plasma membrane (62, 63).

During membrane trafficking, APs can directly interact with cytoplasmic domains of trans-membrane receptors (64). A sample of these interactions have been described (Table 1). In addition, APs themselves interact with other trafficking molecules to form trafficking complexes. Indeed, AP-1 and AP-3 are in complex with the phosphofurin acidic cluster sorting proteins (PACS) membrane trafficking molecules (65). These AP-PACS interactions occur independently of their canonical sorting motifs and are believed to assist in the recruitment of various coat proteins which are essential components of the membrane trafficking machinery (66, 67). Indeed, clathrin is believed to coat vesicles that mediate PACS-1/AP-1-dependent trafficking whereas COP-I coats vesicles are mediated by PACS-2-dependent trafficking (68). These trafficking paradigms will serve as a model for the remainder of this dissertation.

### 1.4.3 Membrane coat proteins

#### *Clathrin*

Vesicles require a structural component to induce the mechanical forces implicated in the bending and curvature processes which ensure movement during membrane trafficking events. Membrane morphology is critical for the binding of several different effector molecules which sense membrane curvature (69). This is often ensured by membrane coat proteins. The clathrin coat protein, initially described by Roth and Porter in 1964, represents this class of protein (70). These scientists used electron microscopy to identify an electron dense lattice formed on invaginated membranes in mosquito oocytes (70). Further biochemical characterization later identified clathrin as a hexamer composed of 3 heavy subunit and 3 light subunit domains, that self-assemble along membranes to form an ordered lattice (71). This structure can ultimately shape and form vesicles. These sites of clathrin assembly often include AP-1, AP-2, AP-3 or AP-4 proteins, which potently recruit clathrin to the cytoplasmic tails of cargo containing tyrosine and dileucine sorting



motifs (72) (Table 1). Trafficking of the cellular endopeptidase furin, requires the interactions with both AP-2 and AP-1 via furin's dileucine/isoleucine motif (LI<sub>756</sub>) and tyrosine motif (Y<sub>759</sub>KGL) to facilitate clathrin-dependent endocytosis and subsequent intracellular sorting (51, 73). Clathrin can recruit additional proteins that also serve as effector molecules, such as dynamin (74), a protein which polymerizes along the neck of the newly budding vesicle. Indeed, dynamin is required to pinch off newly formed vesicles via the constriction of the dynamin ring catalyzed by its GTPase activity (74, 75). Importantly, the membrane trafficking regulator protein PACS-1 is central to AP-1-dependent trafficking events which in turn can also be clathrin-dependent.

### *Coatmer proteins*

In addition to clathrin, another family of coat proteins are also implicated in the formation of trafficking vesicles within the secretory network. This family represent an additional class of eukaryotic coat proteins and consists of coatmer protein – I (COPI) and coatmer protein II (COPII)(76). In contrast to clathrin, COP-I and COP-II complexes primarily function during trafficking events that occur between the ER and the cis-Golgi compartments (76).

### *COP-II*

The minimal COP-II complex contains the small GTPase Sar1p, and the translocation secretory machinery proteins Sec23/24p and Sec13/31p (75). Sar1p regulates recruitment of the COP-II complex by acting as GTP-regulated on/off switch (77, 78). In its GDP-bound state, it is primarily cytosolic, and cannot recruit the COP-II coat. Recruitment to ER-membranes is controlled by the guanine exchange factor Sec13, which exchanges GDP for GTP, thereby turning the COP-II complex “on”(79, 80). Once recruited, both Sec23/24p and Sec13/31p heterodimers can assemble to promote membrane curvature. It is unclear whether transmembrane proteins destined for ER exit are targeted prior to Sec23/24p and Sec13/31p recruitment (81). Two sorting motifs have been identified for COP-II trafficking; the di-acidic motif and a modified tyrosine motif (Table 1). It is these cytoplasmic sequences which directly interact with Sec23/24p at sites of membrane curvature (81).

### *COP-I*

The COP-I complex functions similarly to COP-II, but regulates the retrograde transport of receptors from the cis-Golgi to the ER. The basic components of the of COP-I complex includes the GTPase Arf1 (82), and seven coatomer proteins  $\alpha$ -,  $\beta$ -,  $\beta'$ -,  $\gamma$ -,  $\delta$ -,  $\epsilon$ - and  $\zeta$ -COP(83). Similar to Sar1p of the COP-II initiation complex, vesicle formation from the cis-Golgi membrane is initiated when GTP-bound Arf1 embeds into the lipid bilayer (82). The coatomer can then self-assemble, resulting in the recruitment of proteins which provide the structural basis for membrane curvature. *In vitro* studies have provided evidence supporting the role of  $\alpha$ -COP,  $\beta$ -COP, and  $\delta$ -COP in the direct recognition and binding of dibasic motif (KKXX)-containing receptors, allowing for the concentration of multiple COP-I-specific proteins to a single vesicle (84, 85).

The second member of the PACS family of membrane trafficking proteins, PACS-2, has been implicated in a functional interaction that implicates a COP family protein. Simmen et al. demonstrated that PACS-2 regulates ER-mitochondrial communication in a manner dependent on an interaction between PACS-2 and COP-I (86). Indeed, disruption of this interaction resulted in the induction of the intrinsic apoptotic pathway, marked by the translocation of the pro-apoptotic receptor Bid to the mitochondrial membrane (86). PACS-2 involvement in COP-I trafficking is not limited to ER-mitochondrial communication, but also in the relocalization of the non-selective cation channel polycystin-2 from the plasma membrane to the ER (87).

Overall, the roles of PACS-1 and PACS-2 in pathways implicating clathrin and COP-I, respectively, highlight the essential role of this family of proteins in the regulation of membrane trafficking.

## 1.5 The Phosphofurin Acidic Cluster Sorting proteins: multifaceted membrane trafficking regulators

The increased complexity of the tree of life required a corresponding increase in the complexity of the endomembrane system. This complexity requires specific membrane trafficking regulators, such as the PACS proteins, to shuttle diverse cargo in an

increasingly sophisticated manner throughout the cell (88, 89). A single PACS protein made its first appearance in lower metazoans, such as arthropods and nematodes, and was almost exclusively mediating membrane trafficking events (90). It was not until the evolution of vertebrates, that the *PACS* gene duplicated, giving rise to *PACS-1* and *PACS-2* (88). The duplicated PACS proteins were expressed in order to accommodate the many client cargo proteins and act in concert with the greater quantities of multiple APs and coat proteins found in higher order metazoans (2). PACS-1 was originally discovered in 1998 by Gary Thomas and colleagues (66). The group performed a yeast-two hybrid screen to identify protein binding partners of the endopeptidase furin, a key molecule implicated in regulated secretion (66). These seminal studies demonstrated that PACS-1 acts as a cytosolic molecular trafficking regulator that targets furin to the TGN (66). PACS-2 was subsequently discovered in 2005, as a membrane trafficking regulator protein that mediates cell death pathways (86). Together, these proteins have been studied for the last two decades and have been ascribed multiple roles in cellular homeostasis (88, 89). Unsurprisingly, the degree of homology between the two proteins is quite high (54%). The most significant of these homologies lies within the Furin Binding Region (FBR; 75% homology) of both PACS-1 and PACS-2, as this region has been repeatedly demonstrated to interact with client cargo molecules (91). Indeed, as the name suggests, it is the FBR region of PACS-1 that mediates the interaction with furin.

Functionally, the PACS proteins serve as connector molecules between the coat proteins clathrin or COP-I, and the specific cargo proteins that are being transported within the cell. Interestingly, the PACS proteins have also evolved a degree of specificity in their interactions with cargo molecules. PACS-1 and PACS-2 both predominantly recognize cargo molecules that contain stretches of acidic amino acids, often referred to as “acidic clusters” (87, 92-95). The original acidic cluster binding motif was defined in the cytoplasmic tail of furin which is phosphorylated by Casein Kinase 2 (CK2) in order to bind PACS-1 (66). It is the latter mechanism which gave rise to the PACS name.

In certain instances, the trafficking of cargo molecules is governed by both PACS-1 and PACS-2. For example, trafficking of the cation-independent mannose-6-phosphate receptor (CI-MPR) requires PACS-1 to mediate its shuttling from the cell surface in

addition to requiring PACS-2 to sort CI-MPR to additional endosomal locations (95). CI-MPR trafficking demonstrates the potential interplay between PACS-1 and PACS-2 needed to traffic certain cargo (96). Despite this interplay, my thesis will primarily focus on specific PACS-1-dependent trafficking steps.

### 1.5.1 Regulation of PACS-1 sorting

PACS-1 is a central membrane trafficking regulator protein that mediates the trafficking of multiple different proteins. A sampling of these receptors include: furin (66), CI-MPR (95), vesicular membrane associated protein-4 (VAMP4)(94), and the pro-hormone convertase 6B (97). The primary role of PACS-1 is to link acidic cluster containing cargo to a clathrin adaptor protein and induce their transport from an endosomal compartment to the TGN (Fig. 2.1A)(66). However, not all PACS-1-dependent trafficking is clathrin-dependent. PACS-1 also utilizes the ADP ribosylation factor family of GTP binding protein 6 (ARF6), a protein which localizes to the plasma membrane, alters membrane lipid composition, and induces actin remodeling (98, 99). For example, the HIV-1 viral protein Nef commandeers both Arf6 and PACS-1 to induce the endocytosis of the MHC-I receptor from the surface of infected cells.

During transcription PACS-1 is differentially spliced into two isoforms, a 104 KDa protein termed PACS-1a and a 97 KDa protein termed PACS-1b (100). The entire scientific literature on PACS-1 has been described using the 104 KDa isoform, PACS-1a, which is ubiquitously expressed and will be referred to as PACS-1 in this thesis for simplicity. PACS-1 possesses four domains (Figure 1.2B); the atrophin-1 related region (ARR), the furin binding region (FBR), the middle region (MR), and the C-terminal region (CTR)(65, 66). The roles of these domains have been described to varying degrees. Both the FBR and MR have designated roles in receptor trafficking by directly binding client proteins. These domains also mediate the phosphorylation-dependent auto-regulation of PACS-1 (101). In addition, the MR domain contains a predicted poly-basic nuclear localization signal (NLS), however, whether this latter domain functions as a true NLS remains to be seen (88). As studies of both the ARR and CTR are limited, these domains currently have unknown functions (88).

*In vitro* and cell-based assays have demonstrated that the FBR contains motifs that directly link it to the adaptor coat proteins. Specifically, PACS-1 ETELQLTF<sub>175</sub> is required for binding to AP-1 and AP-3 (65, 66). Furthermore, the PACS-1 MR region contains an auto-regulatory region, which mediates PACS-1's ability to bind cargo. Obtaining additional details on PACS-1 regulation and on the role of the various PACS-1 domains have been partially hampered by the intrinsically disordered nature of PACS-1. Indeed, over half of PACS-1 is predicted to lack tertiary structure (Figure 1-2C). Despite this, details on the regulation of PACS-1 via phosphorylation emerged in the early 2000s.

### 1.5.2 Receptor trafficking by PACS-1

The initial description of PACS-1 regulation was described in relation to the phosphorylation of PACS-1 S278 located in the MR region. This phosphorylation is achieved by CK2, a ubiquitous serine/threonine kinase (102). In its dephosphorylated form, the PACS-1 MR adopts a conformation which blocks receptor binding due to the folding of the MR domain onto the FBR (95). However, CK2 phosphorylation at PACS-1 S278 enables receptor binding (67, 94, 95). This process is inhibited by PACS-1 S278 dephosphorylation by the protein phosphatase 2A (PP2A)(96). These elegant regulatory steps controlling PACS-1, were highlighted during studies of CI-MPR trafficking. CI-MPR is a receptor that acts a chaperone protein that interacts with lysosomal hydrolases and cathepsins, to permit their trafficking to a pre-lysosomal compartment (103, 104). The retrieval of CI-MPR back to the Golgi is necessary to ensure the receptor is not degraded within the lysosome (95). This represents a model in which cells can maximize their energy by not degrading cellular proteins which can be used again. Additional studies are needed to fully grasp the extent of PACS-1 in preventing lysosomal degradation of receptors, and whether additional receptors follow the same pathway.

The best-documented PACS-1 cargo is the cellular endopeptidase furin (105). Furin cleaves and activates multiple proteins to ensure they are in an active state. Furin substrates are numbered in the thousands and are implicated in diverse roles such as embryogenesis and bone development (106). These activities occur within the secretory pathway which ensures protein localization to the cell surface and/or extracellular protein secretion. Within the endomembrane system, furin localization is tightly regulated by

PACS-1 to ensure furin substrates are cleaved and activated (73, 107). This sorting activity is dependent on the phosphorylation by CK2 of both serines within the furin acidic cluster motif S<sub>773</sub>DS<sub>775</sub>EEDE (51), and the S<sub>278</sub> within the PACS-1 autoregulatory region. The phosphorylation of furin promotes its recycling back to the plasma membrane, whereas, dephosphorylation by PP2A favors its progression to the late endosome (51). Within the late endosomal compartment, PACS-1 can then interact with furin to facilitate its retrograde transport to the Golgi (51, 107). Both recycling back to the plasma membrane, and transport to the TGN require the interaction of PACS-1 with the phosphorylated tail of furin (51, 73). However, it remains unclear how PACS-1 distinguishes between furin returning back to the cell surface and furin transiting to the TGN. Ultimately, this elegant regulation of furin trafficking by PACS-1 highlights the key role of PACS-1 within the endomembrane system.

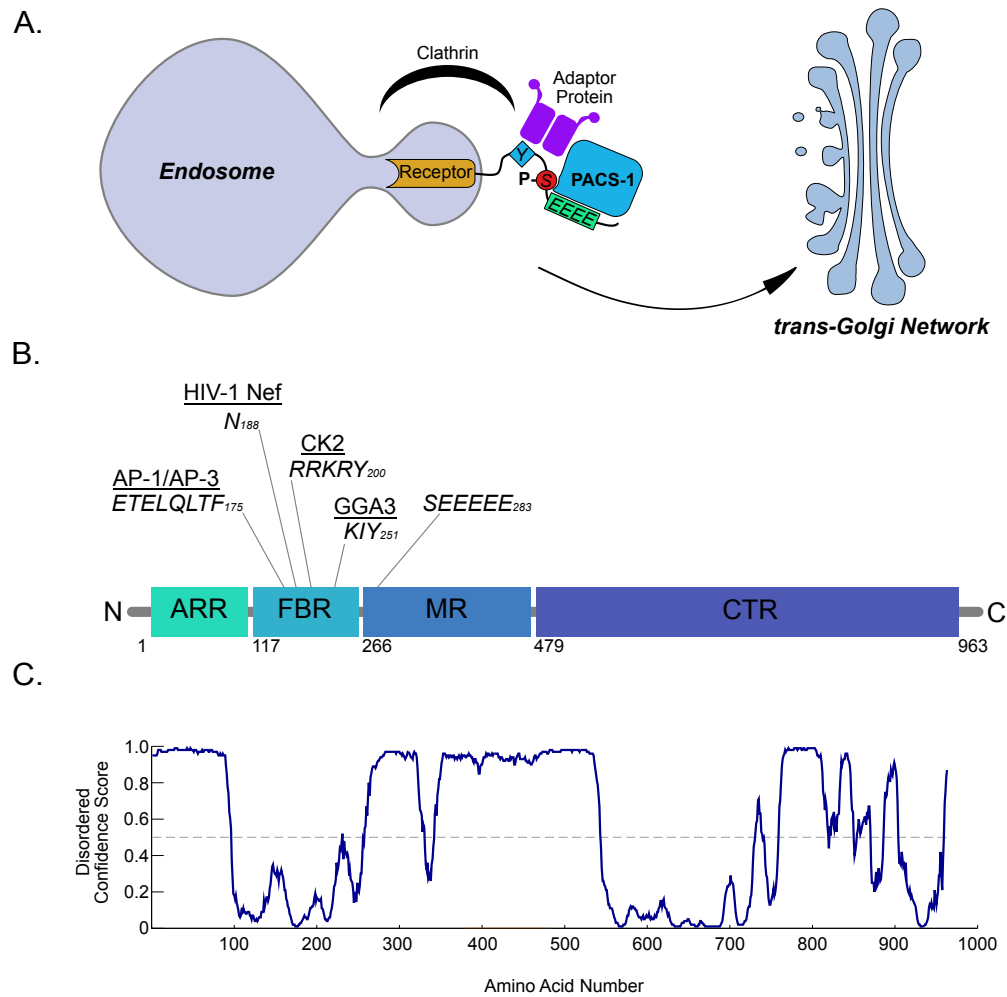


**Figure 1.2: PACS-1 structure and function**

(A) Within the cell, PACS-1 acts as a connector which interacts with the acidic clusters (green) adjacent to phosphorylated serine/threonine residues (red), to recruit the clathrin adaptor proteins (purple), and subsequently clathrin (black) to induce vesicle formation, and retrograde transport to the TGN. (B) Shown is a diagram depicting the 4 domains of PACS-1: Atrophin related region (ARR), furin binding region (FBR), middle region (MR), and the C-terminal region (CTR). Indicated above are the various motifs which engage in specific interactions with the indicated proteins. (C) A graphical depiction of the PACS-1 disordered regions as determined by PSIPRED secondary structure predictor (108). (disordered confidence score > 0 indicates greater intrinsic disorder).

## 1.6 The secretory pathway

As was briefly introduced in Section 1.1, proteins that localize to the plasma membrane or that will be secreted, traffic within the secretory pathway and in particular via the constitutive secretion pathway. These events are due to the presence of signal peptides that are expressed at the amino terminus of proteins and are subsequently recognized by the ER secretory complex; Sec61 translocon, which marks the gateway to the secretory pathway (109, 110). This intraluminal trafficking pathway transports proteins through the various compartments of the ER and Golgi. Specifically, coat proteins such as COP-II will mediate the trafficking of vesicles within the Golgi complex where secretory pathway proteins can be subjected to post-translational modifications such as glycosylation (81). A critical sorting station within the secretory pathway is the TGN, which is also the ultimate trafficking locale within the Golgi apparatus (7). As noted earlier, secretory pathway cargo proteins such as the PACS-1-trafficked furin are shuttled to and from the TGN (65, 66). Further trafficking of proteins within the secretory pathway occurs upon the recognition of sorting motifs within these proteins by connector and adaptor proteins which include AP-1 and clathrin (49). As these two proteins are often found in the same location as PACS-1, it is not surprising that PACS-1 itself plays distinct roles in secretory pathway trafficking that have yet to be fully explored in this thesis. To fully appreciate these events, a specialized organelle, the dense core secretory granule (DCSG) will be introduced as it is a vesicle that buds from the TGN and is exclusively present within endocrine and neuroendocrine cells (111). Taken together, the TGN and DCSG trafficking events that involve PACS-1 comprise key elements of the regulated secretory pathway.

### 1.6.1 Regulated secretory pathway

Whereas most eukaryotic cell types contain a constitutive secretory pathway which traffics proteins to the cell surface, endocrine and neuroendocrine cells contain a regulated secretory pathway. This specialized form of secretion is characterized by the presence of a unique organelle termed the DCSG (112). DCSGs are dense vesicles that concentrate their contents, typically peptide hormones, and only release their contents upon receiving a physiological stimulus (113, 114). Thus, the specific cargo that are



trafficked from the TGN to the DCSGs are often peptide hormones that are released via exocytosis in a regulated fashion in order to avoid excessive secretion (114).

An example of a cargo molecule that traffics through the regulated secretory pathway and that will be further explored in Chapter 4 is the pro-opiomelanocortin hormone (POMC) (115). Primarily synthesized in the anterior pituitary gland, POMC is the precursor peptide to multiple biologically active peptide hormones (116, 117). Specifically, POMC is processed into these active peptide hormones within DCSGs and the latter active hormones are only released upon the appropriate stimulus. Examples of the diverse hormones that are generated from POMC within DCSGs include  $\alpha$ -melanin stimulating hormone (MSH), which controls critical functions such as sex behavior, appetite, and melanin production (118). Furthermore, the adrenocorticotrophic hormone (ACTH) is also produced from POMC and controls the hypothalamic-pituitary-adrenal signaling axis (119). ACTH is also a potent stimulator of cortisol from the adrenal gland (119).

Multiple proposed models exist to distinguish the trafficking of cargo between the regulated and constitutive pathways. Two models however, predominate; the “sorting by entry model” (120), and the “sorting by retention model” (120, 121). Both models imply that cargo traversing the secretory pathway will transit from the ER, through the Golgi apparatus and subsequently make a fate decision between the constitutive and regulated sorting pathways (120). In the sorting by entry model, cargo destined for DCSGs would contain appropriate sorting signals and be targeted to DCSGs (122). Examples of these sorting signals include recognition of receptor sequences, secondary structural elements and cleavage sites that serve as the very bait that cleaves precursor molecules into smaller molecules within DCSGs (123, 124). Conversely, in the “sorting by retention model”, all cargo, irrespective of whether they reside or not in DCSGs, will enter the regulated secretory pathway. Subsequent to this initial sorting event, cargo that is not a resident DCSGs protein will be removed or extruded from these vesicles and diverted to the constitutive secretory pathway (125). The remaining cargo located within DCSGs will thus have been sorted “by retention” to DCSGs and consequentially to the regulated secretory pathway. While both models are not mutually exclusive, PACS-1 has been defined as a key component of the sort by retention pathway. PACS-1 is capable of

removing the SNARE protein VAMP4 from the regulated secretory pathway and traffic it to the TGN (94). This PACS-1 dependent retrieval of VAMP4 from the regulated secretory pathway is dependent on VAMP4's interaction with AP-1, PACS-1, and is regulated by the phosphorylation of S<sub>30</sub> within the VAMP4 cytoplasmic tail (E<sub>27</sub>DDSDDEED) by CK2 (94). PACS-1- and AP-1 also mediate the retrieval of both furin and CI-MPR from the regulated secretory pathway (95).

As highlighted in the previous sections, PACS-1 is a critical trafficking regulator that enables the trafficking of multiple cargo protein to various subcellular locales. It is thus unsurprising to discover that pathogens have subverted this protein to ensure their specific components are targeted to the correct subcellular locale often at the expense of deleterious effects on the host. The function of PACS-1 is subverted by viruses such as the human cytomegalovirus (hCMV) and HIV-1 (126, 127). The following sections will highlight this subversion of PACS-1 by viruses by emphasizing the example of the HIV-1 Nef protein (92, 93, 126, 128).

## 1.7 Introduction to viruses

When compared to the human genome, viruses have on average a 100-1000 fold decrease in their genome's coding capacity (129). This limited coding capacity results in a perceived deficiency in the diversity of viral proteins that would be required for the virus to complete its replication cycle. To overcome this, viral proteins seek and subsequently interact with host proteins located within the very cells they infect. The resulting viral-host protein-protein interactions represent key events that the virus uses to complete its replication cycle often by fending off the host immune response. Indeed, viruses modulate the host cell to evade immune surveillance. Consequently, viruses encode proteins aimed at modulating the host cell trafficking machinery thereby evading the immune response and consequentially optimizing viral replication (130). An example where key viral-host protein interactions mediate the immune response include the modulation of the presence of host receptors on the cell surface (130-135). This virus-dependent receptor modulation can occur due to multiple trafficking mechanisms such as preventing receptors from exiting the ER, blocking receptor transport through the Golgi apparatus or their sequestration within cellular compartments due to endocytosis or

degradation (93, 136-139). Specifically, controlling the ability of infected cells to traffic the MHC-I receptor to the cell surface where it would normally present viral antigens to cytotoxic T cells represents a mechanism by which viral proteins interact with host proteins to ensure viral persistence (140-145).

## 1.8 Strategies for viral immune evasion: The MHC-I receptor

The type I major histocompatibility complex (MHC-I) receptor is encoded by the human leukocyte antigen (HLA) allele and represents a primary antiviral signaling molecule that is ultimately trafficked to the cell surface of all nucleated cells (29, 146). The HLA locus is highly polymorphic and gives rise to thousands of unique HLA alleles (147, 148). The diversity of peptides loaded within the MHC-I cleft is determined by the variable  $\alpha 1$  and  $\alpha 2$  domains of the trans-membrane spanning alpha chain (Fig. 1.3) (149). Classically, the peptide-binding cleft can accommodate peptides ranging from 8-10 amino acids in length, which are anchored between tyrosine residues on the  $\alpha 1$  or  $\alpha 2$  domains (150). There are three classical MHC-I types termed HLA-A, HLA-B, and HLA-C, and four non-classical types termed HLA-E, HLA-F, HLA-G and HLA-H (151). HLA-A and HLA-B are primarily loaded with endogenous or exogenous antigens and interact directly with the CD8<sup>+</sup> T cells via their T cell receptor (TCR) which recognizes presented antigens on MHC-I. The latter interaction has been termed the immunological synapse (151, 152).

Within the immunological synapse, additional proteins also play important physiological roles (Fig. 1.3). CD3 is in complex with the TCR, and upon receptor binding, can engage in a phosphorylation dependent interaction with the Zeta-chain associated protein kinase 70 kinase (ZAP-70), resulting in cellular activation (153). CD8 acts as a co-receptor for the TCR, and is specific for the binding of MHC-I (154). Upon receptor engagement with MHC-I, CD8 initiates downstream signaling cascades for activation involving the Src-Family kinase (SFK) Lck (155). The presence of additional co-stimulatory molecules such as CD28 ensures the immune response occurs only when required (156). CD28 interacts with CD80/86 on the antigen-presenting cell to promote downstream activation of the SFK, Lck, similar to CD8 (156). Ultimately, the plethora of interactions within the

immunological synapse trigger cytoskeleton remodeling, and activation of genes and kinases required for cytolysis of the infected cell (156-158). Coincidentally, viruses have targeted many steps along the viral antigen processing and presentation of MHC-I (135, 136, 142).

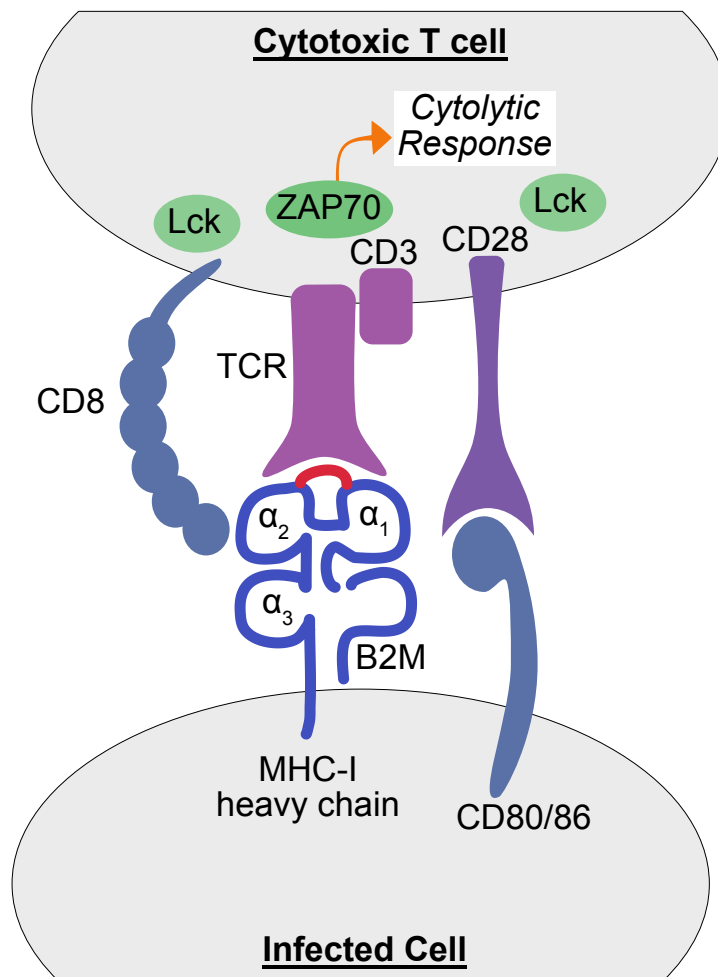


**Figure 1.3: Interactions at the immunological synapse.**

Infected cells display viral peptides (red) within the  $\alpha_1$  and  $\alpha_2$  cleft of MHC-I heavy chain. Engagement of MHC-I by the TCR and CD8 mark the initiation of the immunological synapse. Key interactions between the co-stimulatory receptor CD86 and CD80 ensure that immune responses are appropriately directed at the infected cell. The numerous contact points between the infected cell and cytotoxic T cell initiate a signaling cascade resulting in the activation of the CTL, and a cytolytic response via the cellular

kinases ZAP70 and Lck. (MHC-I: type 1 major histocompatibility complex 1, B2M; Beta-2-microglobulin, TCR; T cell receptor, ZAP70; zeta-chain associated protein kinase 70, Lck; tyrosine protein kinase).

### 1.8.1 Targeting MHC-I peptide loading and trafficking

First, viruses can mediate the localization of MHC-I on the cell surface by interfering with viral peptide loading at the ER. Targeting the early stages of MHC-I peptide loading, represents a mechanism that interferes with viral antigen presentation. Multiple viruses have evolved mechanisms to target this stage of peptide loading (Fig. 1.4). Herpes simplex virus (HSV) encodes the viral protein ICP47 which targets early peptide loading to the transporter associated with antigen presentation (TAP) (159, 160). Specifically, ICP47 binds TAP directly preventing peptide translocation (160). The human cytomegalovirus US6 protein can also prevent peptide loading by preventing TAP ATP hydrolysis (161). Normally, TAP ensures the proper loading of peptides into the MHC-I alpha cleft, and the proper addition of  $\beta$ 2-microglobulin to the MHC-I complex in an ATP-dependent manner (162). Similarly, the US3 protein from hCMV binds to the TAP complex and interferes with peptide loading (139, 163). Targeting TAP is not only limited to the Herpesvirus family. Other diverse viruses also target this assembly complex. The cowpox virus protein CPXV012 prevents ATP binding to the TAP complex, (164) whereas the adenovirus E3-19K protein competes for TAP binding, and prevents MHC-I recruitment and subsequent peptide loading. Adenovirus E3-19K can also directly bind MHC-I to prevent peptide loading (145, 165, 166).

Once MHC-I complexes have been successfully loaded in the ER, they transit through the Golgi apparatus, where post-translational modifications such as glycosylation occur (Fig. 1.4) (167, 168). The MHC-I ER-to-Golgi transit step represents an attractive viral protein target. One such viral mechanism is dictated by the endoplasmic reticulum associated degradation pathway (ERAD) (169, 170). Under physiological conditions, the ERAD pathway degrades MHC-I heavy chains lacking associated  $\beta$ 2-microglobulin, or improperly folded proteins (170, 171). Normally, only a small fraction of MHC-I undergoes ERAD (172). However, specific viral proteins can induce ERAD targeting of functional MHC-I as the receptor exits the ER. Viral proteins such as hCMV US2 and US11 translocate MHC-I into the cytosol for ERAD proteasomal degradation (173, 174). Specific mechanisms that mediate these translocation events are not yet fully understood,

but are believed to involve the recruitment of the dissociation complex Sec61b and ubiquitination of the cytoplasmic tail of MHC-I to facilitate its premature ER exit (173).

Additional viral mechanisms that occur outside of the ER also prevent MHC-I Golgi trafficking. For example, poxviruses usurp the retrograde transport machinery between the Golgi and ER. To accomplish this, the poxvirus protein CPXV203 hijacks the COP-I ER retention pathway to induce the retrograde transport of MHC-I from the cis-Golgi back to the ER by binding to the MHC-I cytoplasmic tail (175).

Other viruses have evolved alternative mechanisms that target cell surface MHC-I. Kaposi's sarcoma-associated herpesvirus K3 and K5 proteins redirect MHC-I to the endolysosomal pathway for degradation within lysosomes (Fig. 1.4) (136, 137). This activity is ensured by the homology between both K3 and K5 and the host ubiquitin ligase machinery (137). The latter host machinery can post-translationally add ubiquitin to cellular proteins to ensure their degradation (176). In the context of K3 and K5, ubiquitination of MHC-I leads to the recruitment of the tumor susceptibility gene 101 (TSG101), which targets MHC-I to lysosomal compartments of the endolysosomal network (177).

The HIV-1 Nef protein also modulates cell surface MHC-I levels. Much like K3 and K5, Nef primarily targets cell surface MHC-I for rapid endocytosis (Fig. 1.4) (178). In the next section, I will review the ability of the HIV-1 Nef protein to modulate the cell surface levels of MHC-I. This activity is also dependent on key viral host interactions that subvert the membrane trafficking machinery including a critical interaction with PACS-1 (92, 179-181).

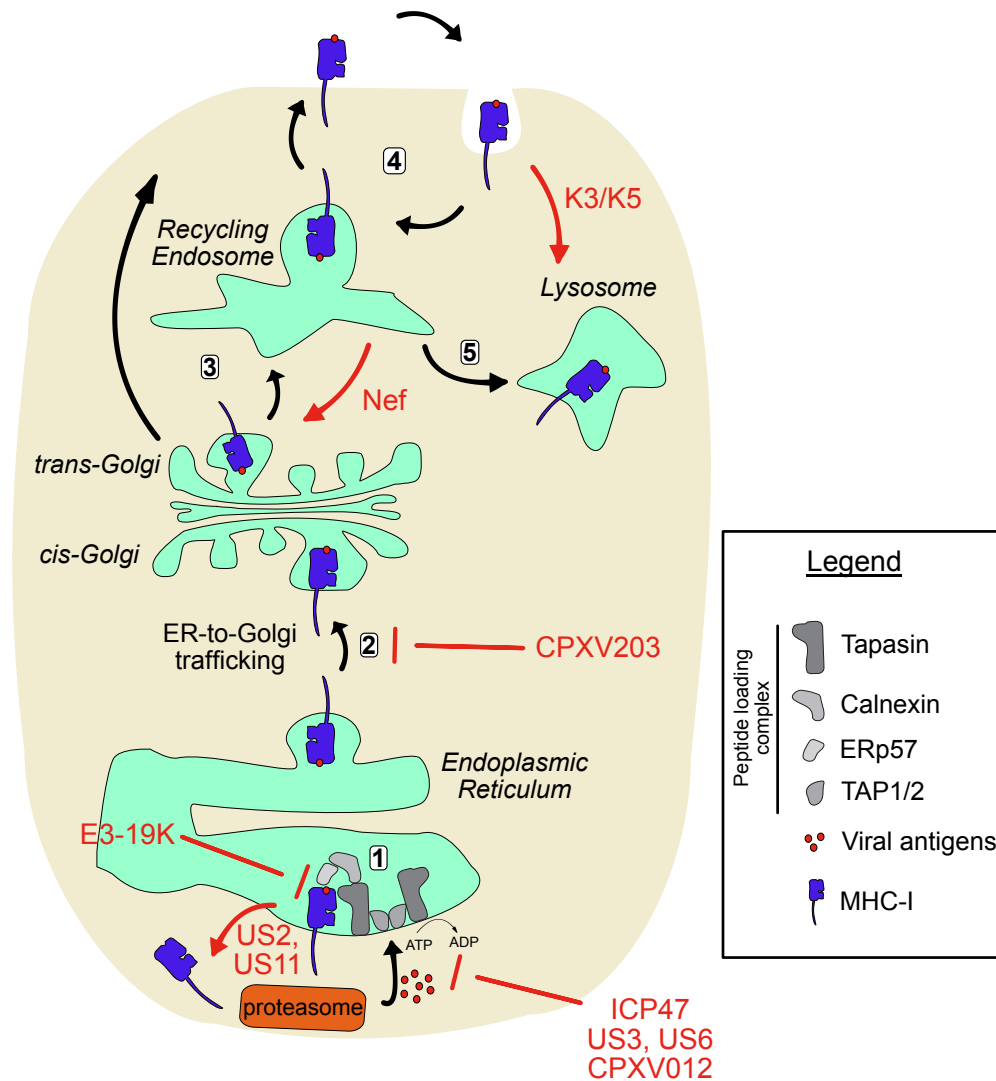


**Figure 1.4: Viral targeting of MHC-I antigen presentation**

(1) MHC-I heavy chain associates with the tapasin peptide loading complex to allow processed viral antigens to fill the alpha cleft, a process inhibited by Adenovirus E3-19K protein. Additionally, hCMV US2 and US11 can translocate the MHC-I heavy chain into the cytosol for proteasomal degradation. Once MHC-I is fully associated with the peptide loading complex, peptides are translocated into the ER lumen through the ATP-dependent transporter associated with antigen presentation (TAP1/2); Herpes simplex virus proteins ICP47, human cytomegalovirus US3 and U6, and cowpox virus protein CPX012 all inhibit efficient peptide translocation. (2) Once loaded, MHC-I transits through the ER to the cis-Golgi to be post translationally modified by the addition of N-



linked glycosylation, which can be inhibited by the Cowpox virus CPXV203 protein. (3) MHC-I can either transit to the cell surface directly from the Golgi, or through an intermediate recycling endosome. (4) Cell surface MHC-I levels are maintained through a homeostatic recycling loop; a process which can be hijacked by the HIV-1 Nef protein. (5) Improperly loaded MHC-I is directed for lysosomal degradation, a process similar to the method used by the Kaposi sarcoma associated herpes virus K3 and K5 proteins.

## 1.9 The human immunodeficiency virus (HIV-1)

Human immunodeficiency virus type 1 (HIV-1) is a member of the *Retroviridae* family that belongs to the lentivirus subfamily (182). Retroviruses are characterized by their ability to reverse transcribe a positive sense strand of RNA into DNA due to the presence of the viral RNA-dependent DNA polymerase, also known as reverse transcriptase (182). In the early 1980's, otherwise healthy individuals became susceptible to opportunistic infections. This condition was subsequently termed Acquired Immunodeficiency Syndrome (183, 184). Shortly thereafter, the causative agent was determined to be HIV-1 (183, 184). Ever since that initial recognition, HIV-1 has become one of the most destructive infectious diseases in modern times, infecting over 76 million people, and, so far, claiming the lives of over half of these infected individuals (185). Currently, infected patients who can access treatment can benefit from anti-retroviral therapy which effectively controls viral replication and prolongs a patient's lifespan when compared to untreated patients (186-188). Despite this, there are currently nearly 2 million new infections per year globally (185, 189). With no prophylactic vaccine available, understanding the HIV-1 lifecycle to generate new, more effective anti-retrovirals is a top priority. Therefore, determining the mechanisms and cellular factors governing viral persistence within the cell is of critical importance.

## 1.10 A key pathogenic mediator of HIV-1 disease: Nef

A mechanism that HIV-1 uses to thwart the immune system is its ability to hijack membrane trafficking pathways for the purposes of viral immune evasion. One such pathway is the retrograde transport of MHC-I from the cell surface to an intracellular location (141, 142, 144, 145, 175, 177). Whereas MHC-I down-regulation by DNA viruses often requires multiple proteins, HIV can use a single protein, Nef, to facilitate this form of immune evasion (143, 190). More recently, MHC-I downregulation during HIV-1 infection has expanded to include the viral protein Vpu (191). Both, Nef and Vpu alter host membrane trafficking and signaling pathways to disrupt immune cell signaling. Moreover, their importance to viral pathogenesis has been well documented (192, 193).

The importance of Nef during HIV-1 pathogenesis has been demonstrated in both patients and in animal models (194-198). Nef has been described as critical for HIV-1 pathogenesis and disease progression to AIDS (199-201). Indeed, individuals infected with an HIV-1 deleted for the *nef* gene displayed a delayed progression to AIDS (202). Moreover, a transgenic Nef mouse model was previously developed to highlight the importance of Nef in disease progression. In these studies pioneered by Paul Jolicoeur, 1998, Nef was expressed under the control of the CD4 promoter, thereby allowing all CD4-positive cells within a transgenic mouse line to express the Nef protein (196). Transgenic mice expressing Nef exhibited a rapid CD4 T cell decline, significant weight loss, and overall a phenotype that resembled AIDS when compared to their littermates that did not express Nef (196, 197). Overall, this animal model highlighted the pathogenic nature of Nef protein even in the absence of any viral replication. Importantly, the importance of Nef could also be recapitulated in a simian model of disease during infection by simian immunodeficiency virus (SIV)(194, 195, 203). These studies illustrated not only that Nef was important for pathogenesis, but also that SIV harboring a mutated Nef sequence could revert back to its wildtype sequence, ultimately resulting the infected macaque to develop simian AIDS (194).

Nef is a 27-34 kDa protein which is myristoylated at its amino terminus. This co-translational modification is key as it enables Nef to associate with membranes, thereby permitting the protein to traffic to various membrane subcellular locations (204). Nef has no known enzymatic functions, and therefore must interact with numerous host cell proteins to benefit viral persistence (205). These viral-host protein interactions result in Nef mediating pathways implicated in programmed cell death, T-cell activation, B-cell immunoglobulin class switching, and the down-regulation of many host cell receptors (206-211).

Perhaps the most profound consequence of Nef expression in cells during infection is its ability to modify the cellular localization of over 35 different host receptors. Most notably, cell surface receptor CD4 (212), MHC-I (213), and more recently, host restriction factor serine incorporator 5 (SERINC5) (214, 215), have been extensively studied. The down regulation of CD4 from the cell surface prevents HIV-1 superinfection

(216) and decreases antibody-dependent cellular cytotoxicity (ADCC)(217, 218). To achieve this, Nef interacts with the cytoplasmic tail of CD4 to recruit AP-2 via the Nef LL<sub>64-65</sub> motif (209, 212, 219). Nef and CD4 subsequently traffic to the acidified lysosomal compartment for degradation, further requiring the interaction of Nef (DE<sub>178-179</sub>) with the vacuolar ATPase (vATPase), which aids in lysosomal acidification (220). The apparent downregulation of CD4 allows the HIV-1 envelope glycoprotein gp120 to be present on the cell surface in a closed conformation. Adopting this conformation prevents high affinity antibody binding and associated effector cell recruitment (218).

Recently however, these and other Nef functions were reevaluated in the context of a newly discovered cellular restriction factor that restricts HIV infectivity. As such, SERINC5 was identified as a potent inhibitor of viral particle infectivity (214, 215). However, once again, HIV-1 has developed a mechanism to negate SERINC5 effects by downregulating this receptor from the cell surface and thereby inhibiting the incorporation of this restriction factor in newly formed virions (215, 221). Trafficking of SERINC5 away from the budding virion seems to follow a similar trafficking pathway to CD4 downregulation by Nef (222). To this end, SERINC5 downregulation is dependent on the Nef dileucine motif (LL<sub>164-165</sub>)(222). Microscopy studies have examined the interaction between Nef and SERINC5, and identified that it accumulates within a late endosome or lysosome(222). Importantly, knockdown of AP-2 partially restored the restrictive abilities of SERINC5 in the presence of Nef, further highlighting similarities between CD4 and SERINC5 downregulation (223).

In contrast to the downregulation of CD4 and SERINC5, the Nef-dependent downregulation of MHC-I follows a distinct pathway, requiring a different set of viral-host interactions. Two primary models exist to explain how Nef down-regulates MHC-I (Fig. 1.5). The first is termed the ‘signaling model’ and indicates that Nef affects the retrograde transport of cell surface MHC-I(180). The signaling model further proposes that Nef interacts with PACS-1 and PACS-2 to facilitate MHC-I endocytosis (128). Specifically, Nef’s interaction with PACS-2, localizes Nef to the TGN where it interacts and activates the Src family kinases (SFKs) Hck, Lyn, Syk or c-Src (92). In turn, activated SFKs activate ZAP-70, followed by the phosphorylation of phosphoinositide-3-

kinase (PI3K) (92). Upon PI3K activation, the incorporation of PIP<sub>3</sub> into the membrane permits the clathrin-independent endocytosis of MHC-I from the cell surface (93). The mechanism by which this endocytosis takes place is not completely understood, however this process is thought to be partly regulated by the small guanine nucleotide exchange factors Arf6 and Arf1(93). Subsequent to MHC-I endocytosis, AP-1 interacts with Nef via its  $\mu$ 1 subunit and targets the MHC-I cytoplasmic tail through the tyrosine motif (Y<sub>320</sub>SQA) (224, 225). It is hypothesized that a ternary complex between Nef/MHC-I/AP-1 prevents MHC-I from recycling back to the cell surface; however, visualization of this ternary complex within a defined cellular compartment has yet to be conducted (225). In addition, the “signaling model” demonstrated that MHC-I ultimately accumulates in a para-nuclear region, characteristic of the TGN (226). In this case, MHC-I would be sequestered at TGN and away from the cell surface where it would fail to present viral antigens to anti-HIV CTLs (127, 190). This sequestration of MHC-I within the cell is PACS-1 dependent and is believed to involve AP-1 as well (127). However, the mechanism governing this event has yet to be defined.

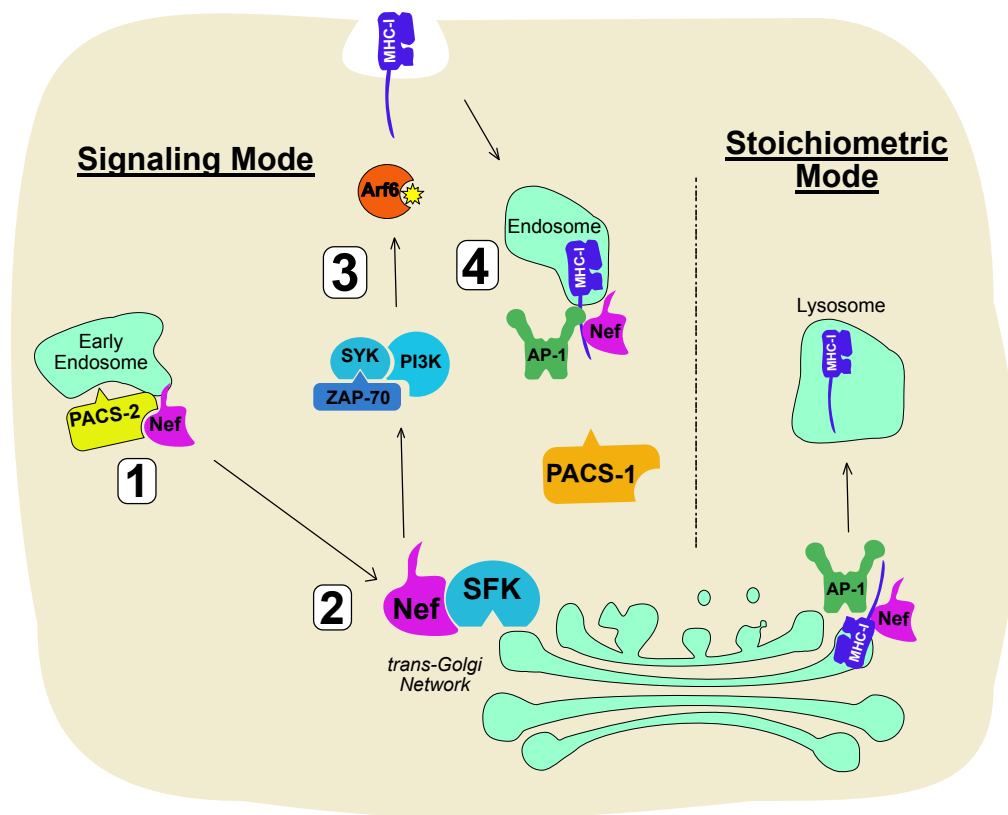


**Figure 1.5: Dual mechanisms of Nef-mediated MHC-I downregulation.**

Within the signaling mode (left) of MHC-I downregulation, (1) Nef is localized from the early endosome to the TGN through its interaction with PACS-2. (2) Nef interacts, and activates Golgi-resident Src-Family kinases to initiate a signaling cascade involving ZAP-70, PI3K, and SYK (a Src-Family Kinase). (3) Arf6/Arf1 becomes activated to induce the endocytosis of MHC-I from the cell surface. (4) Once within the cell, MHC-I is targeted by both Nef and AP-1, and through a PACS-1-dependent trafficking step, becomes localized to a paranuclear compartment. The stoichiometric mode (right) involves the targeting of newly synthesized MHC-I at the Golgi, and its rapid trafficking to the lysosome for degradation in an AP-1-dependent manner.

A contrasting model of Nef-dependent MHC-I downregulation occurs during the latter stages of infection and involves the inhibition of newly synthesized MHC-I trafficking to the cell surface (180). This model, termed the “stoichiometric mode” involves Nef binding to the MHC-I cytosolic tail during transport through the Golgi by an undefined mechanism. As with the signaling mode, a MHC-I/Nef/AP-1 ternary complex is formed, thus preventing MHC-I from trafficking to the cell surface (224). In contrast, this model proposes that MHC-I is routed toward the degradative lysosomal compartment where MHC-I is degraded (225, 227, 228).

It is likely these mechanisms of MHC-I downregulation are not mutually exclusive, and in fact, represent redundant approaches to evade the cytotoxic T cell responses (130, 180). In fact, studies identified that Nef can downregulate MHC-I by both the signaling mode, and the stoichiometric mode (180). However, the mechanism by which this mode switch occurs remains elusive. Moreover, the precise contribution of PACS-1 in the intracellular trafficking of MHC-I has yet to be defined.

## 1.11 Thesis overview

Throughout this thesis, I will outline the role of PACS-1 in the sorting of cellular proteins in two contexts. First, I will explore the role of PACS-1 in Nef-mediated MHC-I downregulation. This function of Nef has been described in some detail, yet, many of the specific cellular trafficking steps have not yet been elucidated. It is known that the rate of MHC-I endocytosis is increased in the presence of Nef, and that this is dependent on the PACS proteins. Moreover, we know that once internalized, MHC-I is trafficked to a para-nuclear compartment, however, the exact subcellular location remains elusive (179, 181). Structural studies have proposed a ternary complex model by which both Nef and AP-1 cooperatively bind the cytoplasmic tail of MHC-I to alter its cellular location (205). This model is attractive, but has not been completely confirmed within cell, nor does it fully integrate PACS-1 in the cellular sorting of MHC-I. Importantly, Nef and PACS-1 have been shown to interact directly through multiple interaction assays, and its importance to Nef function has been well documented (92, 127, 128, 181, 226). The role of PACS-1 in the cellular receptor sorting is based on the premise that PACS-1 connects acidic cluster containing cargo to the clathrin adaptor protein machinery (66, 95). Thus, I *hypothesize*

*that Nef and PACS-1 interact, and facilitates the recruitment of AP-1 to the cytoplasmic tail of MHC-I to induce its retrograde transport to the TGN.*

My second objective revolves around examining the role of PACS-1 in the uninfected cell. Specifically, I explored how PACS-1 controls the localization and secretion of the small peptide hormone ACTH. PACS-1 has been implicated in the routing of cellular receptors within the regulated secretory network of neuroendocrine cells (65, 66, 94). However, the role of PACS-1 in controlling the trafficking of small peptides within the lumen of vesicles has yet to be defined. Thus, I hypothesize that *PACS-1 and AP-1 are integral trafficking proteins which regulate the localization of ACTH within neuroendocrine cells.*

Overall, defining the PACS-1-dependent trafficking steps in homeostasis and disease will aid in the understanding of the regulation of AP recruitment to mediate the movement of a diverse array of receptors and cargo. Importantly, this will define the cellular compartments important for MHC-I downregulation by Nef, as well as identify the role of PACS-1 in protein sorting in neuroendocrine cell.



## 1.12 References

1. Field MC, Dacks JB. First and last ancestors: reconstructing evolution of the endomembrane system with ESCRTs, vesicle coat proteins, and nuclear pore complexes. *Current opinion in cell biology*. 2009;21(1):4-13.
2. Dacks JB, Field MC. Evolution of the eukaryotic membrane-trafficking system: origin, tempo and mode. *Journal of cell science*. 2007;120(17):2977-2985.
3. Gould SB, Garg SG, Martin WF. Bacterial vesicle secretion and the evolutionary origin of the eukaryotic endomembrane system. *Trends in microbiology*. 2016;24(7):525-534.
4. Rapoport TA, Jungnickel B, Kutay U. Protein transport across the eukaryotic endoplasmic reticulum and bacterial inner membranes. *Annual review of biochemistry*. 1996;65(1):271-303.
5. Shibata Y, Voeltz GK, Rapoport TA. Rough sheets and smooth tubules. *Cell*. 2006;126(3):435-439.
6. Voeltz GK, Rolls MM, Rapoport TA. Structural organization of the endoplasmic reticulum. *EMBO reports*. 2002;3(10):944-950.
7. Griffiths G, Simons K. The trans Golgi network: sorting at the exit site of the Golgi complex. *Science*. 1986;234(4775):438-443.
8. Orci L, Glick BS, Rothman JE. A new type of coated vesicular carrier that appears not to contain clathrin: its possible role in protein transport within the Golgi stack. *Cell*. 1986;46(2):171-184.
9. Rambourg A, Clermont Y. Three-dimensional electron microscopy: structure of the Golgi apparatus. *European journal of cell biology*. 1990;51(2):189.
10. Traub LM, Kornfeld S. The trans-Golgi network: a late secretory sorting station. *Current opinion in cell biology*. 1997;9(4):527-533.
11. Pfeffer SR. Rab GTPases: specifying and deciphering organelle identity and function. *Trends in cell biology*. 2001;11(12):487-491.
12. Gorvel J-P, Chavrier P, Zerial M, Gruenberg J. rab5 controls early endosome fusion in vitro. *Cell*. 1991;64(5):915-925.
13. Stenmark H, Olkkonen VM. The rab gtpase family. *Genome biology*. 2001;2(5):reviews3007. 3001.
14. Finbow ME, Eliopoulos EE, Jackson PJ, Keen JN, Meagher L, Thompson P, et al. Structure of a 16 kDa integral membrane protein that has identity to the putative proton channel of the vacuolar H<sup>+</sup>-ATPase. *Protein Engineering, Design and Selection*. 1992;5(1):7-15.
15. Block MR, Glick BS, Wilcox CA, Wieland FT, Rothman JE. Purification of an N-ethylmaleimide-sensitive protein catalyzing vesicular transport. *Proc Natl Acad Sci U S A*. 1988;85(21):7852-7856.
16. Wilson DW, Wilcox CA, Flynn GC, Chen E, Kuang W-J, Henzel WJ, et al. A fusion protein required for vesicle-mediated transport in both mammalian cells and yeast. *Nature*. 1989;339(6223):355.
17. Burgess TL, Kelly RB. Constitutive and regulated secretion of proteins. *Annual review of cell biology*. 1987;3(1):243-293.
18. Ullrich O, Reinsch S, Urbé S, Zerial M, Parton RG. Rab11 regulates recycling through the pericentriolar recycling endosome. *The Journal of cell biology*. 1996;135(4):913-924.

19. Schmid SL, Fuchs R, Male P, Mellman I. Two distinct subpopulations of endosomes involved in membrane recycling and transport to lysosomes. *Cell*. 1988;52(1):73-83.
20. Bonifacino JS, Rojas R. Retrograde transport from endosomes to the trans-Golgi network. *Nat Rev Mol Cell Biol*. 2006;7(8):568-579.
21. Sorkin A, Von Zastrow M. Endocytosis and signalling: intertwining molecular networks. *Nature reviews Molecular cell biology*. 2009;10(9):609.
22. Burgess TL, Kelly RB. Constitutive and regulated secretion of proteins. *Annu Rev Cell Biol*. 1987;3:243-293.
23. De Matteis MA, Luini A. Mendelian disorders of membrane trafficking. *New England Journal of Medicine*. 2011;365(10):927-938.
24. Buckley K, Kelly RB. Identification of a transmembrane glycoprotein specific for secretory vesicles of neural and endocrine cells. *The Journal of cell biology*. 1985;100(4):1284-1294.
25. Reigada D, Díez-Pérez I, Gorostiza P, Verdaguer A, de Aranda IG, Pineda O, et al. Control of neurotransmitter release by an internal gel matrix in synaptic vesicles. *Proceedings of the National Academy of Sciences*. 2003;100(6):3485-3490.
26. Dannies PS. Concentrating hormones into secretory granules: layers of control. *Molecular and cellular endocrinology*. 2001;177(1-2):87-93.
27. Wang D, Lou J, Ouyang C, Chen W, Liu Y, Liu X, et al. Ras-related protein Rab10 facilitates TLR4 signaling by promoting replenishment of TLR4 onto the plasma membrane. *Proceedings of the National Academy of Sciences*. 2010;107(31):13806-13811.
28. Gangloff M. Different dimerisation mode for TLR4 upon endosomal acidification? *Trends in biochemical sciences*. 2012;37(3):92-98.
29. Grommé M, Uytdehaag FG, Janssen H, Calafat J, Van Binnendijk RS, Kenter MJ, et al. Recycling MHC class I molecules and endosomal peptide loading. *Proceedings of the National Academy of Sciences*. 1999;96(18):10326-10331.
30. Wolf PR, Ploegh HL. How MHC class II molecules acquire peptide cargo: biosynthesis and trafficking through the endocytic pathway. *Annual review of cell and developmental biology*. 1995;11(1):267-306.
31. Riordan JR, Rommens JM, Kerem B-s, Alon N, Rozmahel R, Grzelczak Z, et al. Identification of the cystic fibrosis gene: cloning and characterization of complementary DNA. *Science*. 1989;245(4922):1066-1073.
32. Cheng SH, Gregory RJ, Marshall J, Paul S, Souza DW, White GA, et al. Defective intracellular transport and processing of CFTR is the molecular basis of most cystic fibrosis. *Cell*. 1990;63(4):827-834.
33. Dell'Angelica EC, Shotelersuk V, Aguilar RC, Gahl WA, Bonifacino JS. Altered trafficking of lysosomal proteins in Hermansky-Pudlak syndrome due to mutations in the  $\beta$ 3A subunit of the AP-3 adaptor. *Molecular cell*. 1999;3(1):11-21.
34. Li W, Zhang Q, Oiso N, Novak EK, Gautam R, O'Brien EP, et al. Hermansky-Pudlak syndrome type 7 (HPS-7) results from mutant dysbindin, a member of the biogenesis of lysosome-related organelles complex 1 (BLOC-1). *Nature genetics*. 2003;35(1):84.
35. Wei ML. Hermansky-Pudlak syndrome: a disease of protein trafficking and organelle function. *Pigment Cell Research*. 2006;19(1):19-42.

36. Froshauer S, Kartenbeck J, Helenius A. Alphavirus RNA replicase is located on the cytoplasmic surface of endosomes and lysosomes. *The Journal of cell biology*. 1988;107(6):2075-2086.
37. Mercer J, Schelhaas M, Helenius A. Virus entry by endocytosis. *Annual review of biochemistry*. 2010;79:803-833.
38. Bayer N, Schober D, Prchla E, Murphy RF, Blaas D, Fuchs R. Effect of bafilomycin A1 and nocodazole on endocytic transport in HeLa cells: implications for viral uncoating and infection. *Journal of virology*. 1998;72(12):9645-9655.
39. Siczekarski SB, Whittaker GR. Differential requirements of Rab5 and Rab7 for endocytosis of influenza and other enveloped viruses. *Traffic*. 2003;4(5):333-343.
40. Pawlak EN, Dikeakos JD. HIV-1 Nef: a master manipulator of the membrane trafficking machinery mediating immune evasion. *Biochimica et Biophysica Acta (BBA)-General Subjects*. 2015;1850(4):733-741.
41. Haller C, Müller B, Fritz JV, Lamas-Murua M, Stolp B, Pujol FM, et al. HIV-1 Nef and Vpu are functionally redundant broad-spectrum modulators of cell surface receptors, including tetraspanins. *Journal of virology*. 2014;88(24):14241-14257.
42. Tokarev A, Guatelli J. Misdirection of membrane trafficking by HIV-1 Vpu and Nef: Keys to viral virulence and persistence. *Cell Logist*. 2011;1(3):90-102.
43. Dautry-Varsat A, Ciechanover A, Lodish HF. pH and the recycling of transferrin during receptor-mediated endocytosis. *Proceedings of the National Academy of Sciences*. 1983;80(8):2258-2262.
44. French AR, Tadaki DK, Niyogi SK, Lauffenburger DA. Intracellular trafficking of epidermal growth factor family ligands is directly influenced by the pH sensitivity of the receptor/ligand interaction. *Journal of Biological Chemistry*. 1995;270(9):4334-4340.
45. Bonifacino JS, Traub LM. Signals for sorting of transmembrane proteins to endosomes and lysosomes. *Annual review of biochemistry*. 2003;72(1):395-447.
46. Blobel G. Intracellular protein topogenesis. *Proceedings of the National Academy of Sciences*. 1980;77(3):1496-1500.
47. Blobel G, Dobberstein B. Transfer of proteins across membranes. I. Presence of proteolytically processed and unprocessed nascent immunoglobulin light chains on membrane-bound ribosomes of murine myeloma. *The Journal of cell biology*. 1975;67(3):835-851.
48. Bonifacino JS, Dell'Angelica EC. Molecular bases for the recognition of tyrosine-based sorting signals. *The Journal of cell biology*. 1999;145(5):923-926.
49. Nakatsu F, Ohno H. Adaptor protein complexes as the key regulators of protein sorting in the post-Golgi network. *Cell structure and function*. 2003;28(5):419-429.
50. Letourneur F, Klausner RD. A novel di-leucine motif and a tyrosine-based motif independently mediate lysosomal targeting and endocytosis of CD3 chains. *Cell*. 1992;69(7):1143-1157.
51. Jones B, Thomas L, Molloy S, Thulin C, Fry M, Walsh K, et al. Intracellular trafficking of furin is modulated by the phosphorylation state of a casein kinase II site in its cytoplasmic tail. *The EMBO journal*. 1995;14(23):5869-5883.
52. Dittié AS, Thomas L, Thomas G, Tooze SA. Interaction of furin in immature secretory granules from neuroendocrine cells with the AP-1 adaptor complex is modulated by casein kinase II phosphorylation. *The EMBO Journal*. 1997;16(16):4859-4870.

53. Letourneur F, Gaynor EC, Hennecke S, Démollière C, Duden R, Emr SD, et al. Coatamer is essential for retrieval of dilysine-tagged proteins to the endoplasmic reticulum. *Cell*. 1994;79(7):1199-1207.
54. Nishimura N, Balch WE. A di-acidic signal required for selective export from the endoplasmic reticulum. *Science*. 1997;277(5325):556-558.
55. Park SY, Guo X. Adaptor protein complexes and intracellular transport. *Bioscience reports*. 2014;34(4):e00123.
56. Wang YJ, Wang J, Sun HQ, Martinez M, Sun YX, Macia E, et al. Phosphatidylinositol 4 phosphate regulates targeting of clathrin adaptor AP-1 complexes to the Golgi. *Cell*. 2003;114(3):299-310.
57. Gaidarov I, Keen JH. Phosphoinositide-AP-2 interactions required for targeting to plasma membrane clathrin-coated pits. *The Journal of cell biology*. 1999;146(4):755-764.
58. Collins BM, McCoy AJ, Kent HM, Evans PR, Owen DJ. Molecular architecture and functional model of the endocytic AP2 complex. *Cell*. 2002;109(4):523-535.
59. Fölsch H, Pypaert M, Schu P, Mellman I. Distribution and function of AP-1 clathrin adaptor complexes in polarized epithelial cells. *The Journal of cell biology*. 2001;152(3):595-606.
60. Robinson MS. 100-kD coated vesicle proteins: molecular heterogeneity and intracellular distribution studied with monoclonal antibodies. *The Journal of cell biology*. 1987;104(4):887-895.
61. Faúndez V, Horng J-T, Kelly RB. A function for the AP3 coat complex in synaptic vesicle formation from endosomes. *Cell*. 1998;93(3):423-432.
62. Hirst J, Barlow LD, Francisco GC, Sahlender DA, Seaman MN, Dacks JB, et al. The fifth adaptor protein complex. *PLoS biology*. 2011;9(10):e1001170.
63. Yap CC, Murate M, Kishigami S, Muto Y, Kishida H, Hashikawa T, et al. Adaptor protein complex-4 (AP-4) is expressed in the central nervous system neurons and interacts with glutamate receptor  $\delta 2$ . *Molecular and Cellular Neuroscience*. 2003;24(2):283-295.
64. Traub LM. Common principles in clathrin-mediated sorting at the Golgi and the plasma membrane. *Biochimica et Biophysica Acta (BBA)-Molecular Cell Research*. 2005;1744(3):415-437.
65. Crump CM, Xiang Y, Thomas L, Gu F, Austin C, Tooze SA, et al. PACS-1 binding to adaptors is required for acidic cluster motif-mediated protein traffic. *The EMBO journal*. 2001;20(9):2191-2201.
66. Wan L, Molloy SS, Thomas L, Liu G, Xiang Y, Rybak SL, et al. PACS-1 defines a novel gene family of cytosolic sorting proteins required for trans-Golgi network localization. *Cell*. 1998;94(2):205-216.
67. Schermer B, Höpker K, Omran H, Ghenoïu C, Fliegauf M, Fekete A, et al. Phosphorylation by casein kinase 2 induces PACS-1 binding of nephrocystin and targeting to cilia. *The EMBO journal*. 2005;24(24):4415-4424.
68. Werneburg NW, Bronk SF, Guicciardi ME, Thomas L, Dikeakos JD, Thomas G, et al. Tumor necrosis factor-related apoptosis-inducing ligand (TRAIL) protein-induced lysosomal translocation of proapoptotic effectors is mediated by phosphofurin acidic cluster sorting protein-2 (PACS-2). *J Biol Chem*. 2012;287(29):24427-24437.

69. Frost A, Perera R, Roux A, Spasov K, Destaing O, Egelman EH, et al. Structural basis of membrane invagination by F-BAR domains. *Cell*. 2008;132(5):807-817.
70. Roth TF, Porter KR. Yolk protein uptake in the oocyte of the mosquito *Aedes aegypti*. *L. The Journal of cell biology*. 1964;20(2):313-332.
71. Cheng Y, Boll W, Kirchhausen T, Harrison SC, Walz T. Cryo-electron tomography of clathrin-coated vesicles: structural implications for coat assembly. *Journal of molecular biology*. 2007;365(3):892-899.
72. Loerke D, Mettlen M, Schmid SL, Danuser G. Measuring the hierarchy of molecular events during clathrin-mediated endocytosis. *Traffic*. 2011;12(7):815-825.
73. Molloy S, Thomas L, VanSlyke J, Stenberg P, Thomas G. Intracellular trafficking and activation of the furin proprotein convertase: localization to the TGN and recycling from the cell surface. *The EMBO journal*. 1994;13(1):18-33.
74. Sweitzer SM, Hinshaw JE. Dynamin undergoes a GTP-dependent conformational change causing vesiculation. *Cell*. 1998;93(6):1021-1029.
75. Matsuoka K, Orci L, Amherdt M, Bednarek SY, Hamamoto S, Schekman R, et al. COPII-coated vesicle formation reconstituted with purified coat proteins and chemically defined liposomes. *Cell*. 1998;93(2):263-275.
76. Gomez-Navarro N, Miller E. Protein sorting at the ER–Golgi interface. *J Cell Biol*. 2016;jcb. 201610031.
77. Nakano A, Muramatsu M. A novel GTP-binding protein, Sar1p, is involved in transport from the endoplasmic reticulum to the Golgi apparatus. *The Journal of cell biology*. 1989;109(6):2677-2691.
78. Oka T, Nakano A. Inhibition of GTP hydrolysis by Sar1p causes accumulation of vesicles that are a functional intermediate of the ER-to-Golgi transport in yeast. *The Journal of cell biology*. 1994;124(4):425-434.
79. Yoshihisa T, Barlowe C, Schekman R. Requirement for a GTPase-activating protein in vesicle budding from the endoplasmic reticulum. *Science*. 1993;259(5100):1466-1468.
80. Barlowe C, Schekman R. SEC12 encodes a guanine-nucleotide-exchange factor essential for transport vesicle budding from the ER. *Nature*. 1993;365(6444):347.
81. Aridor M, Weissman J, Bannykh S, Nuoffer C, Balch WE. Cargo selection by the COPII budding machinery during export from the ER. *The Journal of cell biology*. 1998;141(1):61-70.
82. Serafini T, Orci L, Amherdt M, Brunner M, Kahn RA, Rothmant JE. ADP-ribosylation factor is a subunit of the coat of Golgi-derived COP-coated vesicles: a novel role for a GTP-binding protein. *Cell*. 1991;67(2):239-253.
83. Waters MG, Serafini T, Rothman JE. 'Coatomer': a cytosolic protein complex containing subunits of non-clathrin-coated Golgi transport vesicles. *Nature*. 1991;349(6306):248.
84. Ma W, Goldberg J. Rules for the recognition of dilysine retrieval motifs by coatomer. *The EMBO journal*. 2013;32(7):926-937.
85. Vincent MJ, Martin AS, Compans RW. Function of the KKXX motif in endoplasmic reticulum retrieval of a transmembrane protein depends on the length and structure of the cytoplasmic domain. *Journal of Biological Chemistry*. 1998;273(2):950-956.
86. Simmen T, Aslan JE, Blagoveshchenskaya AD, Thomas L, Wan L, Xiang Y, et

- al. PACS-2 controls endoplasmic reticulum–mitochondria communication and Bid-mediated apoptosis. *The EMBO journal*. 2005;24(4):717-729.
87. Köttgen M, Benzing T, Simmen T, Tauber R, Buchholz B, Feliciangeli S, et al. Trafficking of TRPP2 by PACS proteins represents a novel mechanism of ion channel regulation. *The EMBO journal*. 2005;24(4):705-716.
  88. Thomas G, Aslan JE, Thomas L, Shinde P, Shinde U, Simmen T. Caught in the act—protein adaptation and the expanding roles of the PACS proteins in tissue homeostasis and disease. *J Cell Sci*. 2017;jcs. 199463.
  89. Youker RT, Shinde U, Day R, Thomas G. At the crossroads of homeostasis and disease: roles of the PACS proteins in membrane traffic and apoptosis. *Biochem J*. 2009;421(1):1-15.
  90. Sieburth D, Ch'ng Q, Dybbs M, Tavazoie M, Kennedy S, Wang D, et al. Systematic analysis of genes required for synapse structure and function. *Nature*. 2005;436(7050):510.
  91. Youker R, Shinde U, Day R, Thomas G. At the crossroads of homeostasis and disease: roles of the PACS proteins in membrane traffic and apoptosis. *Biochem J*. 2009;421:1-15.
  92. Atkins KM, Thomas L, Youker RT, Harriff MJ, Pissani F, You H, et al. HIV-1 Nef Binds PACS-2 to Assemble a Multikinase Cascade That Triggers Major Histocompatibility Complex Class I (MHC-I) Down-regulation ANALYSIS USING SHORT INTERFERING RNA AND KNOCK-OUT MICE. *Journal of Biological Chemistry*. 2008;283(17):11772-11784.
  93. Blagoveshchenskaya AD, Thomas L, Feliciangeli SF, Hung CH, Thomas G. HIV-1 Nef downregulates MHC-I by a PACS-1- and PI3K-regulated ARF6 endocytic pathway. *Cell*. 2002;111(6):853-866.
  94. Hinnert I, Wendler F, Fei H, Thomas L, Thomas G, Tooze SA. AP-1 recruitment to VAMP4 is modulated by phosphorylation-dependent binding of PACS-1. *EMBO reports*. 2003;4(12):1182-1189.
  95. Scott GK, Fei H, Thomas L, Medigeschi GR, Thomas G. A PACS-1, GGA3 and CK2 complex regulates CI-MPR trafficking. *The EMBO journal*. 2006;25(19):4423-4435.
  96. Molloy SS, Thomas L, Kamibayashi C, Mumby MC, Thomas G. Regulation of endosome sorting by a specific PP2A isoform. *The Journal of cell biology*. 1998;142(6):1399-1411.
  97. Xiang Y, Molloy SS, Thomas L, Thomas G. The PC6B cytoplasmic domain contains two acidic clusters that direct sorting to distinct trans-Golgi network/endosomal compartments. *Molecular biology of the cell*. 2000;11(4):1257-1273.
  98. Maranda B, Brown D, Bourgoin S, Casanova JE, Vinay P, Ausiello DA, et al. Intra-endosomal pH-sensitive recruitment of the Arf-nucleotide exchange factor ARNO and Arf6 from cytoplasm to proximal tubule endosomes. *Journal of Biological Chemistry*. 2001;276(21):18540-18550.
  99. D'Souza-Schorey C, Li G, Colombo MI, Stahl PD. A regulatory role for ARF6 in receptor-mediated endocytosis. *Science*. 1995;267(5201):1175-1178.
  100. Thanaraj TA, Stamm S, Clark F, Riethoven JJ, Le Texier V, Muilu J. ASD: the

- alternative splicing database. *Nucleic acids research*. 2004;32(suppl\_1):D64-D69.
101. Scott GK, Gu F, Crump CM, Thomas L, Wan L, Xiang Y, et al. The phosphorylation state of an autoregulatory domain controls PACS-1-directed protein traffic. *The EMBO journal*. 2003;22(23):6234-6244.
  102. Litchfield DW. Protein kinase CK2: structure, regulation and role in cellular decisions of life and death. *Biochemical Journal*. 2003;369(1):1-15.
  103. Lobel P, Dahms N, Kornfeld S. Cloning and sequence analysis of the cation-independent mannose 6-phosphate receptor. *Journal of Biological Chemistry*. 1988;263(5):2563-2570.
  104. Braulke T, Bonifacino JS. Sorting of lysosomal proteins. *Biochimica et Biophysica Acta (BBA)-Molecular Cell Research*. 2009;1793(4):605-614.
  105. Van den Ouweland A, Van Duijnhoven H, Keizer GD, Dorssers L, Van de Ven W. Structural homology between the human fur gene product and the subtilisin-like protease encoded by yeast KEX2. *Nucleic Acids Research*. 1990;18(3):664.
  106. Thomas G. Furin at the cutting edge: from protein traffic to embryogenesis and disease. *Nature reviews Molecular cell biology*. 2002;3(10):753.
  107. Bosshart H, Humphrey J, Deignan E, Davidson J, Drazba J, Yuan L, et al. The cytoplasmic domain mediates localization of furin to the trans-Golgi network en route to the endosomal/lysosomal system. *The Journal of Cell Biology*. 1994;126(5):1157-1172.
  108. McGuffin LJ, Bryson K, Jones DT. The PSIPRED protein structure prediction server. *Bioinformatics*. 2000;16(4):404-405.
  109. Hessa T, Kim H, Bihlmaier K, Lundin C, Boekel J, Andersson H, et al. Recognition of transmembrane helices by the endoplasmic reticulum translocon. *Nature*. 2005;433(7024):377.
  110. Pfeffer S, Burbaum L, Unverdorben P, Pech M, Chen Y, Zimmermann R, et al. Structure of the native Sec61 protein-conducting channel. *Nature communications*. 2015;6:8403.
  111. Bennett HS. Cytological manifestations of secretion in the adrenal medulla of the cat. *American Journal of Anatomy*. 1941;69(3):333-381.
  112. Kim T, Gondré-Lewis MC, Arnaoutova I, Loh YP. Dense-core secretory granule biogenesis. *Physiology*. 2006;21(2):124-133.
  113. Tooze SA. Biogenesis of secretory granules in the trans-Golgi network of neuroendocrine and endocrine cells. *Biochimica et Biophysica Acta (BBA)-Molecular Cell Research*. 1998;1404(1-2):231-244.
  114. Meldolesi J, Chieregatti E, Malosio ML. Requirements for the identification of dense-core granules. *Trends in cell biology*. 2004;14(1):13-19.
  115. Cawley NX, Li Z, Loh YP. 60 YEARS OF POMC: Biosynthesis, trafficking, and secretion of pro-opiomelanocortin-derived peptides. *Journal of molecular endocrinology*. 2016;56(4):T77-T97.
  116. Mains RE, Eipper BA. Synthesis and secretion of corticotropins, melanotropins, and endorphins by rat intermediate pituitary cells. *Journal of Biological Chemistry*. 1979;254(16):7885-7894.
  117. Crine P, Gossard F, Seidah N, Blanchette L, Lis M, Chrétien M. Concomitant synthesis of beta-endorphin and alpha-melanotropin from two forms of pro-opiomelanocortin in the rat pars intermedia. *Proceedings of the National Academy of Sciences*. 1979;76(10):5085-5089.

118. Gantz I, Fong TM. The melanocortin system. *American Journal of Physiology-Endocrinology And Metabolism*. 2003;284(3):E468-E474.
119. Tsigos C, Chrousos GP. Hypothalamic–pituitary–adrenal axis, neuroendocrine factors and stress. *Journal of psychosomatic research*. 2002;53(4):865-871.
120. Kuliawat R, Arvan P. Distinct molecular mechanisms for protein sorting within immature secretory granules of pancreatic beta-cells. *The Journal of Cell Biology*. 1994;126(1):77-86.
121. Rothman JE. Protein sorting by selective retention in the endoplasmic reticulum and Golgi stack. *Cell*. 1987;50(4):521.
122. Cool DR, Normant E, Shen F-s, Chen H-C, Pannell L, Zhang Y, et al. Carboxypeptidase E is a regulated secretory pathway sorting receptor: genetic obliteration leads to endocrine disorders in Cpefat mice. *Cell*. 1997;88(1):73-83.
123. Che FY, Biswas R, Fricker LD. Relative quantitation of peptides in wild-type and Cpefat/fat mouse pituitary using stable isotopic tags and mass spectrometry. *Journal of mass spectrometry*. 2005;40(2):227-237.
124. McGirr R, Guizzetti L, Dhanvantari S. The Sorting of Proglucagon to Secretory Granules is Mediated by CPE and Intrinsic Sorting Signals. *Journal of Endocrinology*. 2013;JOE-12-0468.
125. Sobota JA, Ferraro F, Bäck N, Eipper BA, Mains RE. Not all secretory granules are created equal: Partitioning of soluble content proteins. *Molecular biology of the cell*. 2006;17(12):5038-5052.
126. Crump CM, Hung C-H, Thomas L, Wan L, Thomas G. Role of PACS-1 in trafficking of human cytomegalovirus glycoprotein B and virus production. *Journal of virology*. 2003;77(20):11105-11113.
127. Piguet V, Wan L, Borel C, Mangasarian A, Demaurex N, Thomas G, et al. HIV-1 Nef protein binds to the cellular protein PACS-1 to downregulate class I major histocompatibility complexes. *Nature cell biology*. 2000;2(3):163-167.
128. Dikeakos JD, Thomas L, Kwon G, Elferich J, Shinde U, Thomas G. An interdomain binding site on HIV-1 Nef interacts with PACS-1 and PACS-2 on endosomes to down-regulate MHC-I. *Molecular biology of the cell*. 2012;23(11):2184-2197.
129. Venter JC, Adams MD, Myers EW, Li PW, Mural RJ, Sutton GG, et al. The sequence of the human genome. *science*. 2001;291(5507):1304-1351.
130. Pawlak EN, Dikeakos JD. HIV-1 Nef: A Master Manipulator of the Membrane Trafficking Machinery Mediating Immune Evasion. *Biochimica et Biophysica Acta (BBA)-General Subjects*. 2015.
131. Lodoen MB, Lanier LL. Viral modulation of NK cell immunity. *Nature Reviews Microbiology*. 2005;3(1):59.
132. Collins DR, Collins KL. HIV-1 accessory proteins adapt cellular adaptors to facilitate immune evasion. *PLoS Pathog*. 2014;10(1):e1003851.
133. Kirchhoff F. Immune evasion and counteraction of restriction factors by HIV-1 and other primate lentiviruses. *Cell Host Microbe*. 2010;8(1):55-67.
134. Li K, Foy E, Ferreón JC, Nakamura M, Ferreón AC, Ikeda M, et al. Immune evasion by hepatitis C virus NS3/4A protease-mediated cleavage of the Toll-like receptor 3 adaptor protein TRIF. *Proceedings of the National Academy of Sciences*. 2005;102(8):2992-2997.



135. Loenen WA, Bruggeman C, Wiertz E, editors. Immune evasion by human cytomegalovirus: lessons in immunology and cell biology. Seminars in immunology; 2001: Elsevier.
136. Ishido S, Wang C, Lee B-S, Cohen GB, Jung J. Downregulation of major histocompatibility complex class I molecules by Kaposi's sarcoma-associated herpesvirus K3 and K5 proteins. *Journal of Virology*. 2000;74(11):5300-5309.
137. Lehner PJ, Hoer S, Dodd R, Duncan LM. Downregulation of cell surface receptors by the K3 family of viral and cellular ubiquitin E3 ligases. *Immunological reviews*. 2005;207(1):112-125.
138. Nair-Gupta P, Baccarini A, Tung N, Seyffer F, Florey O, Huang Y, et al. TLR signals induce phagosomal MHC-I delivery from the endosomal recycling compartment to allow cross-presentation. *Cell*. 2014;158(3):506-521.
139. Park B, Kim Y, Shin J, Lee S, Cho K, Früh K, et al. Human cytomegalovirus inhibits tapasin-dependent peptide loading and optimization of the MHC class I peptide cargo for immune evasion. *Immunity*. 2004;20(1):71-85.
140. Dirk BS, Pawlak EN, Johnson AL, Van Nynatten LR, Jacob RA, Heit B, et al. HIV-1 Nef sequesters MHC-I intracellularly by targeting early stages of endocytosis and recycling. *Scientific reports*. 2016;6:37021.
141. Lybarger L, Wang X, Harris MR, Virgin IV HW, Hansen TH. Virus subversion of the MHC class I peptide-loading complex. *Immunity*. 2003;18(1):121-130.
142. Coscoy L, Ganem D. Kaposi's sarcoma-associated herpesvirus encodes two proteins that block cell surface display of MHC class I chains by enhancing their endocytosis. *Proceedings of the National Academy of Sciences*. 2000;97(14):8051-8056.
143. Collins KL, Chen BK, Kalams SA, Walker BD, Baltimore D. HIV-1 Nef protein protects infected primary cells against killing by cytotoxic T lymphocytes. *Nature*. 1998;391(6665):397-401.
144. Hengel H, Flohr T, Hämmerling GJ, Koszinowski UH, Momburg F. Human cytomegalovirus inhibits peptide translocation into the endoplasmic reticulum for MHC class I assembly. *Journal of General Virology*. 1996;77(9):2287-2296.
145. Beier DC, Cox JH, Vining DR, Cresswell P, Engelhard VH. Association of human class I MHC alleles with the adenovirus E3/19K protein. *The Journal of Immunology*. 1994;152(8):3862-3872.
146. Donaldson JG, Williams DB. Intracellular assembly and trafficking of MHC class I molecules. *Traffic*. 2009;10(12):1745-1752.
147. Stephens HA. HIV-1 diversity versus HLA class I polymorphism. *Trends in immunology*. 2005;26(1):41-47.
148. Bukur J, Jasinski S, Seliger B, editors. The role of classical and non-classical HLA class I antigens in human tumors. Seminars in cancer biology; 2012: Elsevier.
149. Rohren EM, Pease LR, Ploegh HL, Schumacher T. Polymorphisms in pockets of major histocompatibility complex class I molecules influence peptide preference. *Journal of Experimental Medicine*. 1993;177(6):1713-1721.
150. Rammensee H-G, Friede T, Stevanović S. MHC ligands and peptide motifs: first listing. *Immunogenetics*. 1995;41(4):178-228.
151. O'Callaghan CA, Bell JL. Structure and function of the human MHC class Ib molecules HLA-E, HLA-F and HLA-G. *Immunological reviews*. 1998;163(1):129-138.
152. Jondal M, Schirmbeck R, Reimann J. MHC class I-restricted CTL responses to

- exogenous antigens. *Immunity*. 1996;5(4):295-302.
153. Iwashima M, Irving BA, Van Oers N, Chan AC, Weiss A. Sequential interactions of the TCR with two distinct cytoplasmic tyrosine kinases. *Science*. 1994;263(5150):1136-1139.
  154. Wang R, Natarajan K, Margulies DH. Structural basis of the CD8 $\alpha\beta$ /MHC class I interaction: focused recognition orients CD8 $\beta$  to a T cell proximal position. *The Journal of Immunology*. 2009;jimmunol. 0901276.
  155. Artyomov MN, Lis M, Devadas S, Davis MM, Chakraborty AK. CD4 and CD8 binding to MHC molecules primarily acts to enhance Lck delivery. *Proceedings of the National Academy of Sciences*. 2010;107(39):16916-16921.
  156. Pentcheva-Hoang T, Egen JG, Wojnoonski K, Allison JP. B7-1 and B7-2 selectively recruit CTLA-4 and CD28 to the immunological synapse. *Immunity*. 2004;21(3):401-413.
  157. Lee K-H, Holdorf AD, Dustin ML, Chan AC, Allen PM, Shaw AS. T cell receptor signaling precedes immunological synapse formation. *Science*. 2002;295(5559):1539-1542.
  158. Stinchcombe JC, Bossi G, Booth S, Griffiths GM. The immunological synapse of CTL contains a secretory domain and membrane bridges. *Immunity*. 2001;15(5):751-761.
  159. Tomazin R, van Schoot NE, Goldsmith K, Jugovic P, Sempé P, Früh K, et al. Herpes simplex virus type 2 ICP47 inhibits human TAP but not mouse TAP. *Journal of virology*. 1998;72(3):2560-2563.
  160. Tomazin R, Hill AB, Jugovic P, York I, Van Endert P, Ploegh HL, et al. Stable binding of the herpes simplex virus ICP47 protein to the peptide binding site of TAP. *The EMBO journal*. 1996;15(13):3256-3266.
  161. Lehner PJ, Karttunen JT, Wilkinson GW, Cresswell P. The human cytomegalovirus US6 glycoprotein inhibits transporter associated with antigen processing-dependent peptide translocation. *Proceedings of the National Academy of Sciences*. 1997;94(13):6904-6909.
  162. Ortmann B, Copeman J, Lehner PJ, Sadasivan B, Herberg JA, Grandea AG, et al. A critical role for tapasin in the assembly and function of multimeric MHC class I-TAP complexes. *Science*. 1997;277(5330):1306-1309.
  163. Ahn K, Angulo A, Ghazal P, Peterson PA, Yang Y, Früh K. Human cytomegalovirus inhibits antigen presentation by a sequential multistep process. *Proceedings of the National Academy of Sciences*. 1996;93(20):10990-10995.
  164. Luteijn RD, Hoelen H, Kruse E, Van Leeuwen WF, Grootens J, Horst D, et al. Cowpox virus protein CPXV012 eludes CTLs by blocking ATP binding to TAP. *The Journal of Immunology*. 2014;1400964.
  165. Burgert H-G, Maryanski JL, Kvist S. "E3/19K" protein of adenovirus type 2 inhibits lysis of cytolytic T lymphocytes by blocking cell-surface expression of histocompatibility class I antigens. *Proceedings of the National Academy of Sciences*. 1987;84(5):1356-1360.
  166. Burgert H-G, Kvist S. The E3/19K protein of adenovirus type 2 binds to the domains of histocompatibility antigens required for CTL recognition. *The EMBO journal*. 1987;6(7):2019-2026.
  167. Barbosa JA, Santos-Aguado J, Mentzer SJ, Strominger JL, Burakoff SJ, Biro PA. Site-directed mutagenesis of class I HLA genes. Role of glycosylation in surface

- expression and functional recognition. *Journal of Experimental Medicine*. 1987;166(5):1329-1350.
168. Mandal TK, Mukhopadhyay C. Effect of glycosylation on structure and dynamics of MHC class I glycoprotein: a molecular dynamics study. *Biopolymers: Original Research on Biomolecules*. 2001;59(1):11-23.
  169. Wiertz EJ, Tortorella D, Bogoy M, Yu J, Mothes W, Jones TR, et al. Sec61-mediated transfer of a membrane protein from the endoplasmic reticulum to the proteasome for destruction. *Nature*. 1996;384(6608):432.
  170. Pilon M, Schekman R, Römisch K. Sec61p mediates export of a misfolded secretory protein from the endoplasmic reticulum to the cytosol for degradation. *The EMBO journal*. 1997;16(15):4540-4548.
  171. Paulsson KM, Jevon M, Wang JW, Li S, Wang P. The double lysine motif of tapasin is a retrieval signal for retention of unstable MHC class I molecules in the endoplasmic reticulum. *The Journal of Immunology*. 2006;176(12):7482-7488.
  172. Hughes EA, Hammond C, Cresswell P. Misfolded major histocompatibility complex class I heavy chains are translocated into the cytoplasm and degraded by the proteasome. *Proceedings of the National Academy of Sciences*. 1997;94(5):1896-1901.
  173. Wiertz EJ, Jones TR, Sun L, Bogoy M, Geuze HJ, Ploegh HL. The human cytomegalovirus US11 gene product dislocates MHC class I heavy chains from the endoplasmic reticulum to the cytosol. *Cell*. 1996;84(5):769-779.
  174. Gewurz BE, Gaudet R, Tortorella D, Wang EW, Ploegh HL, Wiley DC. Antigen presentation subverted: Structure of the human cytomegalovirus protein US2 bound to the class I molecule HLA-A2. *Proceedings of the National Academy of Sciences*. 2001;98(12):6794-6799.
  175. McCoy IV WH, Wang X, Yokoyama WM, Hansen TH, Fremont DH. Structural mechanism of ER retrieval of MHC class I by cowpox. *PLoS biology*. 2012;10(11):e1001432.
  176. Katzmann DJ, Babst M, Emr SD. Ubiquitin-dependent sorting into the multivesicular body pathway requires the function of a conserved endosomal protein sorting complex, ESCRT-I. *Cell*. 2001;106(2):145-155.
  177. Hewitt EW, Duncan L, Mufti D, Baker J, Stevenson PG, Lehner PJ. Ubiquitylation of MHC class I by the K3 viral protein signals internalization and TSG101-dependent degradation. *The EMBO Journal*. 2002;21(10):2418-2429.
  178. Benichou S, Benmerah A. The HIV nef and the Kaposi-sarcoma-associated virus K3/K5 proteins: "parasites" of the endocytosis pathway. *Medecine sciences: M/S*. 2003;19(1):100-106.
  179. Dikeakos JD, Thomas L, Kwon G, Elferich J, Shinde U, Thomas G. An interdomain binding site on HIV-1 Nef interacts with PACS-1 and PACS-2 on endosomes to down-regulate MHC-I. *Molecular biology of the cell*. 2012;23(11):2184-2197.
  180. Dikeakos JD, Atkins KM, Thomas L, Emert-Sedlak L, Byeon IJ, Jung J, et al. Small molecule inhibition of HIV-1-induced MHC-I down-regulation identifies a temporally regulated switch in Nef action. *Molecular biology of the cell*. 2010;21(19):3279-3292.
  181. Hung CH, Thomas L, Ruby CE, Atkins KM, Morris NP, Knight ZA, et al. HIV-1 Nef assembles a Src family kinase-ZAP-70/Syk-PI3K cascade to downregulate cell-

- surface MHC-I. *Cell Host Microbe*. 2007;1(2):121-133.
182. Frankel AD, Young JA. HIV-1: fifteen proteins and an RNA. *Annu Rev Biochem*. 1998;67:1-25.
  183. Gallo RC, Sarin PS, Gelmann E, Robert-Guroff M, Richardson E, Kalyanaraman V, et al. Isolation of human T-cell leukemia virus in acquired immune deficiency syndrome (AIDS). *Science*. 1983;220(4599):865-867.
  184. Barré-Sinoussi F, Chermann J-C, Rey F, Nugeyre MT, Chamaret S, Gruest J, et al. Isolation of a T-lymphotropic retrovirus from a patient at risk for acquired immune deficiency syndrome (AIDS). *Science*. 1983;220(4599):868-871.
  185. HIV/AIDS JUNPo. Global AIDS update 2016. Geneva: UNAIDS. 2016.
  186. Cohen MS, Chen YQ, McCauley M, Gamble T, Hosseinipour MC, Kumarasamy N, et al. Prevention of HIV-1 infection with early antiretroviral therapy. *New England journal of medicine*. 2011;365(6):493-505.
  187. Egger M, May M, Chêne G, Phillips AN, Ledergerber B, Dabis F, et al. Prognosis of HIV-1-infected patients starting highly active antiretroviral therapy: a collaborative analysis of prospective studies. *The Lancet*. 2002;360(9327):119-129.
  188. Donnell D, Baeten JM, Kiarie J, Thomas KK, Stevens W, Cohen CR, et al. Heterosexual HIV-1 transmission after initiation of antiretroviral therapy: a prospective cohort analysis. *The Lancet*. 2010;375(9731):2092-2098.
  189. HIV/AIDS JUNPo. Global report: UNAIDS report on the global AIDS epidemic. UNAIDS Programme, Geneva, Switzerland. 2013.
  190. Schwartz O, Maréchal V, Le Gall S, Lemonnier F, Heard J-M. Endocytosis of major histocompatibility complex class I molecules is induced by the HIV-1 Nef protein. *Nature medicine*. 1996;2(3):338-342.
  191. Apps R, Del Prete GQ, Chatterjee P, Lara A, Brumme ZL, Brockman MA, et al. HIV-1 vpu mediates HLA-C downregulation. *Cell host & microbe*. 2016;19(5):686-695.
  192. Hout DR, Gomez ML, Pacyniak E, Gomez LM, Inbody SH, Mulcahy ER, et al. Scrambling of the amino acids within the transmembrane domain of Vpu results in a simian-human immunodeficiency virus (SHIVTM) that is less pathogenic for pig-tailed macaques. *Virology*. 2005;339(1):56-69.
  193. Nomaguchi M, Fujita M, Adachi A. Role of HIV-1 Vpu protein for virus spread and pathogenesis. *Microbes and infection*. 2008;10(9):960-967.
  194. Schindler M, Münch J, Brenner M, Stahl-Hennig C, Skowronski J, Kirchhoff F. Comprehensive analysis of nef functions selected in simian immunodeficiency virus-infected macaques. *Journal of virology*. 2004;78(19):10588-10597.
  195. Schindler M, Schmökel J, Specht A, Li H, Münch J, Khalid M, et al. Inefficient Nef-mediated downmodulation of CD3 and MHC-I correlates with loss of CD4<sup>+</sup> T cells in natural SIV infection. *PLOS pathogens*. 2008;4(7):e1000107.
  196. Hanna Z, Kay DG, Rebai N, Guimond A, Jothy S, Jolicoeur P. Nef harbors a major determinant of pathogenicity for an AIDS-like disease induced by HIV-1 in transgenic mice. *Cell*. 1998;95(2):163-175.
  197. Hanna Z, Weng X, Kay DG, Poudrier J, Lowell C, Jolicoeur P. The pathogenicity of human immunodeficiency virus (HIV) type 1 Nef in CD4C/HIV transgenic mice is abolished by mutation of its SH3-binding domain, and disease development is delayed in the absence of Hck. *Journal of virology*. 2001;75(19):9378-9392.
  198. Learmont JC, Geczy AF, Mills J, Ashton LJ, Raynes-Greenow CH, Garsia RJ, et

- al. Immunologic and virologic status after 14 to 18 years of infection with an attenuated strain of HIV-1. A report from the Sydney Blood Bank Cohort. *N Engl J Med*. 1999;340(22):1715-1722.
199. Swingler S, Zhou J, Swingler C, Dauphin A, Greenough T, Jolicoeur P, et al. Evidence for a pathogenic determinant in HIV-1 Nef involved in B cell dysfunction in HIV/AIDS. *Cell host & microbe*. 2008;4(1):63-76.
200. Kirchhoff F, Greenough TC, Brettler DB, Sullivan JL, Desrosiers RC. Absence of intact nef sequences in a long-term survivor with nonprogressive HIV-1 infection. *New England Journal of Medicine*. 1995;332(4):228-232.
201. Miller MD, Warmerdam MT, Gaston I, Greene WC, Feinberg MB. The human immunodeficiency virus-1 nef gene product: a positive factor for viral infection and replication in primary lymphocytes and macrophages. *Journal of Experimental Medicine*. 1994;179(1):101-113.
202. Mariani R, Kirchhoff F, Greenough TC, Sullivan JL, Desrosiers RC, Skowronski J. High frequency of defective nef alleles in a long-term survivor with nonprogressive human immunodeficiency virus type 1 infection. *Journal of virology*. 1996;70(11):7752-7764.
203. Kestier III HW, Ringler DJ, Mori K, Panicali DL, Sehgal PK, Daniel MD, et al. Importance of the nef gene for maintenance of high virus loads and for development of AIDS. *Cell*. 1991;65(4):651-662.
204. Gerlach H, Laumann V, Martens S, Becker CF, Goody RS, Geyer M. HIV-1 Nef membrane association depends on charge, curvature, composition and sequence. *Nature chemical biology*. 2010;6(1):46-53.
205. Jia X, Singh R, Homann S, Yang H, Guatelli J, Xiong Y. Structural basis of evasion of cellular adaptive immunity by HIV-1 Nef. *Nature structural & molecular biology*. 2012;19(7):701-706.
206. Rasola A, Gramaglia D, Boccaccio C, Comoglio PM. Apoptosis enhancement by the HIV-1 Nef protein. *J Immunol*. 2001;166(1):81-88.
207. Schragar JA, Marsh JW. HIV-1 Nef increases T cell activation in a stimulus-dependent manner. *Proc Natl Acad Sci U S A*. 1999;96(14):8167-8172.
208. Qiao X, He B, Chiu A, Knowles DM, Chadburn A, Cerutti A. Human immunodeficiency virus 1 Nef suppresses CD40-dependent immunoglobulin class switching in bystander B cells. *Nature immunology*. 2006;7(3):302-310.
209. Bresnahan PA, Yonemoto W, Ferrell S, Williams-Herman D, Geleziunas R, Greene WC. A dileucine motif in HIV-1 Nef acts as an internalization signal for CD4 downregulation and binds the AP-1 clathrin adaptor. *Current biology*. 1998;8(22):1235-S1231.
210. Chaudhry A, Verghese DA, Das SR, Jameel S, George A, Bal V, et al. HIV-1 Nef promotes endocytosis of cell surface MHC class II molecules via a constitutive pathway. *J Immunol*. 2009;183(4):2415-2424.
211. Leonard JA, Filzen T, Carter CC, Schaefer M, Collins KL. HIV-1 Nef disrupts intracellular trafficking of major histocompatibility complex class I, CD4, CD8, and CD28 by distinct pathways that share common elements. *J Virol*. 2011;85(14):6867-6881.
212. Aiken C, Konner J, Landau NR, Lenburg ME, Trono D. Nef induces CD4 endocytosis: requirement for a critical dileucine motif in the membrane-proximal CD4

cytoplasmic domain. *Cell*. 1994;76(5):853-864.

213. Collins KL, Chen BK, Kalams SA, Walker BD, Baltimore D. HIV-1 Nef protein protects infected primary cells against killing by cytotoxic T lymphocytes. *Nature*. 1998;391(6665):397.

214. Usami Y, Wu Y, Göttlinger HG. SERINC3 and SERINC5 restrict HIV-1 infectivity and are counteracted by Nef. *Nature*. 2015;526(7572):218.

215. Rosa A, Chande A, Ziglio S, De Sanctis V, Bertorelli R, Goh SL, et al. HIV-1 Nef promotes infection by excluding SERINC5 from virion incorporation. *Nature*. 2015;526(7572):212.

216. Benson R, Sanfridson A, Ottinger J, Doyle C, Cullen B. Downregulation of cell-surface CD4 expression by simian immunodeficiency virus Nef prevents viral super infection. *Journal of Experimental Medicine*. 1993;177(6):1561-1566.

217. Veillette M, Désormeaux A, Medjahed H, Gharsallah N-E, Coutu M, Baalwa J, et al. Interaction with cellular CD4 exposes HIV-1 envelope epitopes targeted by antibody-dependent cell-mediated cytotoxicity. *Journal of virology*. 2014;88(5):2633-2644.

218. Richard J, Veillette M, Brassard N, Iyer SS, Roger M, Martin L, et al. CD4 mimetics sensitize HIV-1-infected cells to ADCC. *Proceedings of the National Academy of Sciences*. 2015:201506755.

219. Chaudhuri R, Lindwasser OW, Smith WJ, Hurley JH, Bonifacino JS. Downregulation of CD4 by human immunodeficiency virus type 1 Nef is dependent on clathrin and involves direct interaction of Nef with the AP2 clathrin adaptor. *J Virol*. 2007;81(8):3877-3890.

220. Lu X, Yu H, Liu S-H, Brodsky FM, Peterlin BM. Interactions between HIV1 Nef and vacuolar ATPase facilitate the internalization of CD4. *Immunity*. 1998;8(5):647-656.

221. Usami Y, Wu Y, Göttlinger HG. SERINC3 and SERINC5 restrict HIV-1 infectivity and are counteracted by Nef. *Nature*. 2015;526(7572):218-223.

222. Shi J, Xiong R, Zhou T, Su P, Zhang X, Qiu X, et al. HIV-1 Nef antagonizes SERINC5 restriction by downregulation of SERINC5 via the endosome/lysosome system. *Journal of virology*. 2018:JVI. 00196-00118.

223. Trautz B, Pierini V, Wombacher R, Stolp B, Chase AJ, Pizzato M, et al. Antagonism of the SERINC5 Particle Infectivity Restriction by HIV-1 Nef Involves Counteraction of Virion-associated Pools of the Restriction Factor. *Journal of virology*. 2016:JVI. 01246-01216.

224. Roeth JF, Williams M, Kasper MR, Filzen TM, Collins KL. HIV-1 Nef disrupts MHC-I trafficking by recruiting AP-1 to the MHC-I cytoplasmic tail. *J Cell Biol*. 2004;167(5):903-913.

225. Wonderlich ER, Williams M, Collins KL. The tyrosine binding pocket in the adaptor protein 1 (AP-1)  $\mu$ 1 subunit is necessary for Nef to recruit AP-1 to the major histocompatibility complex class I cytoplasmic tail. *Journal of Biological Chemistry*. 2008;283(6):3011-3022.

226. Blagoveshchenskaya AD, Thomas L, Feliciangeli SF, Hung C-H, Thomas G. HIV-1 Nef downregulates MHC-I by a PACS-1-and PI3K-regulated ARF6 endocytic pathway. *Cell*. 2002;111(6):853-866.

227. Schaefer MR, Wonderlich ER, Roeth JF, Leonard JA, Collins KL. HIV-1 Nef targets MHC-I and CD4 for degradation via a final common beta-COP-dependent pathway in T cells. *PLoS Pathog*. 2008;4(8):e1000131.

228. Kasper MR, Roeth JF, Williams M, Filzen TM, Fleis RI, Collins KL. HIV-1 Nef disrupts antigen presentation early in the secretory pathway. *Journal of Biological Chemistry*. 2005;280(13):12840-12848.

## Chapter 2

# 2 Viral Bimolecular Fluorescence Complementation: A Novel Tool to Study Intracellular Vesicular Trafficking Pathways

## 2.1 Introduction

The sub-cellular localization of mammalian proteins is coordinated by the membrane trafficking machinery, including a vast network of membrane-bound vesicles and adaptor molecules (1, 2). Viruses, such as Human Immunodeficiency Virus type 1 (HIV-1), are able to exploit the host membrane trafficking machinery and key cellular components to favour viral replication. HIV-1 produces 15 viral proteins (3, 4), including a 27 kDa accessory protein termed Nef, which lacks any known enzymatic activity, but is essential for viral pathogenesis (5, 6). Nef mediates its pathogenic effects by modulating membrane trafficking in infected cells. Notably, Nef facilitates downregulation of various cell surface molecules, including major histocompatibility complex-I (MHC-I), which results in attenuation of the immune response by impairing the presentation of viral antigens to cytotoxic T-lymphocytes (CTLs) (7, 8).

Nef-mediated MHC-I downregulation is primarily orchestrated by protein-protein interactions between Nef and various host cellular proteins (7, 9-12). This includes the membrane trafficking regulators phosphofurin acidic cluster sorting proteins 1 and 2 (PACS-1 and PACS-2), which form specific protein complexes with Nef at distinct sub-cellular locations in order to downregulate MHC-I (7, 9, 12, 13). In turn, PACS-1 can specifically interact with the clathrin adaptor protein-1 (AP-1) to facilitate Nef mediated sequestration of MHC-I away from the cell surface (7, 13, 14). The PACS-1/AP-1 interaction, as well as the crystal structure of Nef in complex with AP-1 and MHC-I, demonstrate that host membrane trafficking regulator proteins, such as AP-1 and PACS-1, are key for HIV-1 immune evasion (14). Recently, the interactions between Nef and PACS proteins have been visualized using bimolecular fluorescence complementation (BiFC). BiFC is a microscopy technique that localizes protein interactions through the reconstitution of a functional fluorophore upon the interaction of two protein-binding



partners each fused to a non-fluorescent fragment of a fluorophore (15-17). Although BiFC has demonstrated that PACS-1 or PACS-2 and Nef interact at distinct sub-cellular compartments, it has not been shown with concurrent expression from a single plasmid or in the context of viral infection with other HIV-1 proteins present (9).

This study addresses the current limitations of using BiFC to investigate viral protein interactions through the development of a lentiviral vector that enables simultaneous expression of Nef with various binding partners from the same vector in the context of a viral infection. To accomplish this, we utilized a lentiviral expression system yielding pseudovirions modified such that they only undergo a single round of replication, but are still capable of genomic integration (18). The co-expression of transgenes of interest was achieved by inserting the autocleavable 2a (F2A) coding sequence from the foot and mouth disease virus into the previously described HIV-1 based vector pNL4-3  $\Delta$ gag/pol eGFP (19-22). Previous reports have demonstrated that insertion of an F2A site stalls translation, resulting in the production of cleaved polyproteins containing a 21 residue carboxy terminal F2A tag and a single proline addition at the amino terminus (23). We have used this unique system to express multiple transgenes fused to split fluorophores, thereby permitting analysis of protein-protein interactions using BiFC. Our results demonstrate that viral BiFC can be used to study the interaction between HIV-1 Nef and PACS-1 at both early and late endosomal compartments. The utility of viral BiFC is highlighted by its ability to provide the distinct sub-cellular localization of the interaction between Nef and MHC-I. In addition, viral BiFC can be used to study novel interactions between Nef and host membrane trafficking regulators. Indeed, using viral BiFC we demonstrate for the first time an interaction between Nef and the sorting nexin 18 (SNX18) protein. Viral BiFC represents a unique tool enabling the visualization of Nef interactions at specific sub-cellular locations in the context of an HIV-1 infection.

## 2.2 Results

### 2.2.1 Designing a lentiviral vector enabling dual transgene expression

Multiple Nef-interacting proteins have been identified using *in vitro* interaction assays, cellular co-immunoprecipitation analyses, and more recently by fluorescence resonance energy transfer and mass spectrometry (7, 9, 10, 13, 24-31). However, the Nef protein-protein interaction network has never been defined in the context of expression from a single vector that mimics the conditions present during a viral infection. To address this, we constructed a lentiviral vector containing an F2A cleavage site or the non-functional mutant, F2A (null), as a control, thereby facilitating concurrent expression of Nef and a potential Nef-interacting partner (Fig. 2.1). Vector assembly was initiated using the previously described pNL4-3  $\Delta$ gag/pol eGFP vector as a base (Fig. 2.1; top panel) (19, 20). This base vector contains intact 5' and 3' long terminal repeat (LTR) regions and expresses all HIV-1 viral proteins except full-length Gag and Pol. These genes are mutated in the base vector to generate truncated proteins and must be supplied in trans for productive pseudovirion synthesis (Fig. 2.1; top panel) (20, 32). To facilitate gene insertion, two multiple cloning sites (MCSs) were introduced into the base vector: a 3' MCS containing the XmaI, AgeI and NotI restriction sites and a 5' MCS containing the ApaI, SphI and SpeI restriction sites (Fig. 2.1; bottom panel). We inserted HIV-1 Nef fused with the eGFP fluorescent tag into the 3' MCS whereas the 5' MCS was used to insert potential Nef-interacting partners.

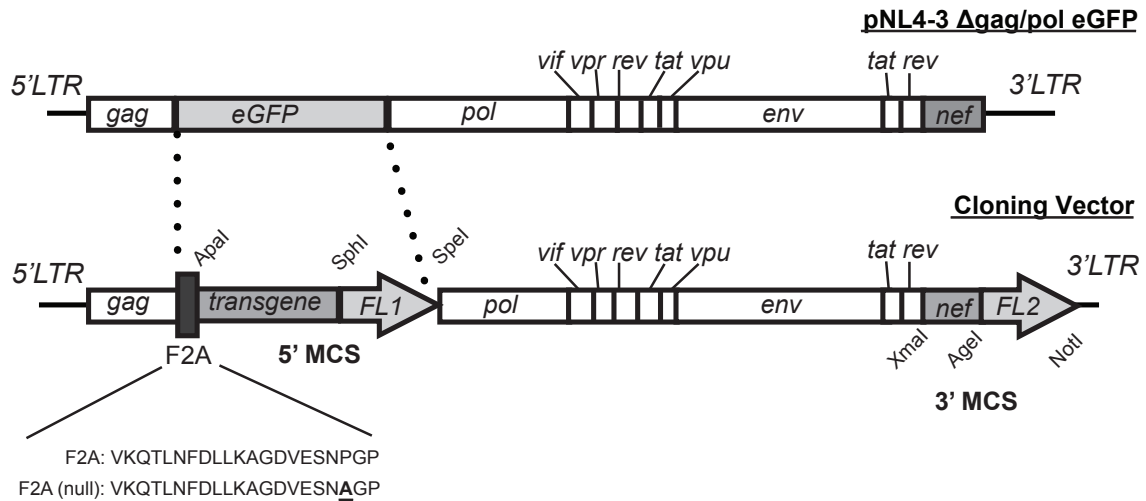


**Figure 2.1: Construction of an HIV-1 derived lentiviral expression system harboring an F2A peptide and two multiple cloning sites.**

The pNL4-3 Δgag/pol eGFP vector (top) was engineered to contain the self-cleaving F2A peptide followed by a 5' MCS (ApaI, SphI and SpeI), to introduce various transgene fusion proteins of interest. A MCS was introduced at the 3' end in order to insert various Nef fusion proteins (XmaI, AgeI and NotI). (MCS: multiple cloning site; *FL1*: fluorophore fused to transgene of interest in the 5' MCS; *FL2*: fluorophore fused to Nef in the 3' MCS).

### 2.2.2 Insertion of an F2A site into a lentiviral vector allows concurrent protein production

To avoid the production of proteins fused to truncated Gag/Pol proteins from the 5' MCS, we exploited the self-cleaving property of the 2A peptide (F2A) derived from the foot and mouth disease virus by inserting the 21 amino acid F2A site between the Gag/Pol fusion protein and the 5' MCS (Fig. 2.1; bottom panel). The resulting vector, pNL4-3 F2A-X Nef-eGFP (Fig. 2.2A) has an empty 5' MCS in order to accommodate future gene insertions. To test the cleavage efficiency of the F2A site, we constructed a lentiviral vector containing a Flag-tagged mStrawberry (mSB) fluorophore in the 5' MCS (Fig. 2.2A). Pseudovirus from the resulting pNL4-3 F2A-mSB-Flag Nef-eGFP construct was then used to infect Jurkat E6.1 T-cells. In order to directly quantitate the cleavage efficiency, a control vector with an inactive F2A site was constructed (Fig. 2.1 & 2.2; F2A (null)). Site-directed mutagenesis of the penultimate proline residue to alanine has been demonstrated to render the F2A site inactive (33). In agreement with cleavage mediated at the F2A site, western blot analysis demonstrated the production of a cleaved Flag-tagged mStrawberry protein that migrated just below the 35 kDa molecular weight marker (Fig. 2.2B; ++ Flag blot). Consistent with mutation of the penultimate proline in the F2A site to produce a defective cleavage site (22, 33, 34), cells infected with pNL4-3 F2A (null)-mSB-Flag Nef-eGFP pseudovirus produced a Flag-tagged mStrawberry protein fused to the HIV-1 Gag/Pol protein that migrated above the 48 kDa molecular weight marker (Fig. 2.2B; + Flag blot). Quantification of the cleavage efficiency between the F2A and the F2A (null) site was determined by dividing the densitometry measurement of the cleaved product by the sum of both the cleaved and uncleaved products. We observed a 6-fold increase in cleavage efficiency in the presence of a functional F2A site, confirming that the cleavage is F2A-dependent (Fig. 2.2C). Moreover, the pNL4-3 F2A-mSB-Flag Nef-eGFP construct efficiently produced Nef-eGFP, confirming that the 3' MCS can also produce a fluorophore-tagged protein of interest (Fig. 2.2B; lane 3 GFP blot). Overall, these results demonstrate the 3' and 5' MCSs can be used to produce conjugated proteins and the proteins expressed from the 5' MCS are cleaved from truncated Gag/Pol.

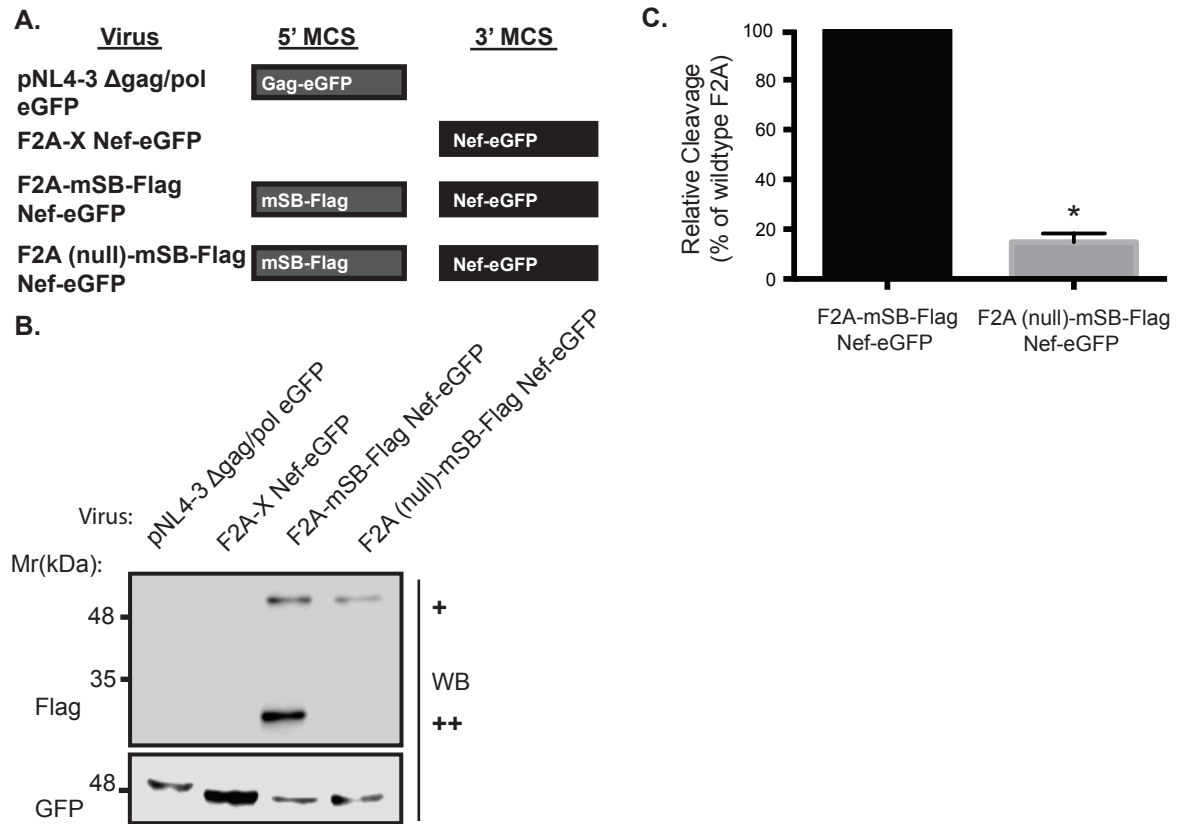


**Figure 2.2: Functional cleavage at the engineered F2A site.**

Viruses were engineered with various proteins within the 5' MCS and/or the 3' MCS and Jurkat E6.1 T-cells were infected with the resulting pseudoviruses. Flag and GFP specific western blots were performed on lysates collected 48 hours post infection to verify protein expression levels. (A) Schematic representation of proteins produced from lentiviral expression system. (B) A Flag specific western blot was used to quantitate the cleavage efficiency at the F2A site in the F2A-mSB-Flag Nef-eGFP virus, compared to the F2A mutant, F2A (null)-mSB-Flag Nef-eGFP, which lacks cleavage activity (+ uncleaved product, ++ cleaved product). GFP specific western blots confirmed the presence of the Gag-eGFP fusion protein (lane 1) or Nef-eGFP fusion proteins (lanes 2-4). (C) Cleavage efficiency at the F2A site was 6-fold higher compared to the F2A (null) virus (\* indicates p-value < 0.05). Details on how the cleavage efficiency was calculated are included in Materials and Methods. Error bars calculated from 3 independent experiments. p-value was determined by paired t-test.

### 2.2.3 Nef and Nef-interacting partners are simultaneously expressed in a lentiviral vector

The Nef-dependent endocytosis of cell surface MHC-I during an HIV-1 infection leads to evasion of CTL killing, thereby contributing to continued viral replication (35). Nef-mediated MHC-I downregulation requires subversion of multiple membrane trafficking regulators, including binding to PACS-1 (7, 9, 10, 12, 13, 36). Therefore, to evaluate the simultaneous expression of Nef with PACS-1 or MHC-I, specifically the HLA-A2 allele, we engineered constructs containing different fluorophores for all genes inserted in the 5' or 3' MCS, respectively (Fig. 2.3A). The resulting vectors (pNL4-3 F2A-MHC-I-mCherry Nef-eGFP and pNL4-3 F2A-PACS-1-mCherry Nef-eGFP) were designed to include an mCherry tag at the 5' site and an eGFP tag at the 3' site. To confirm the presence of the different fluorophores fused to proteins of interest, we infected HeLa cells with pseudovirions encoding the MHC-I or PACS-1 genes and visualized cells by widefield fluorescence microscopy. This demonstrated simultaneous expression of both mCherry-tagged MHC-I or PACS-1 and eGFP tagged Nef (Fig. 2.3B, column 2 and 3). Similar infection of Jurkat E6.1 T-cells with pseudovirions generated from the respective vectors confirmed their simultaneous expression by western blot (Fig. 2.3C, lane 4 and 5). Importantly, the conjugation of mCherry to MHC-I did not alter its localization within the cell as flow cytometry measurements indicated that mCherry-tagged MHC-I expressed in Jurkat E6.1 T-cells infected with the pNL4-3 F2A-MHC-I-mCherry  $\Delta$ Nef pseudovirus, was correctly routed to the cell surface (Fig. 2.3D & 2.4). Moreover, MHC-I-mCherry was sensitive to Nef activity as Jurkat E6.1 T-cells infected with pNL4-3 F2A-MHC-I-mCherry Nef-eGFP resulted in less MHC-I-mCherry on the cell surface compared to cells infected with pNL4-3 F2A-MHC-I-mCherry  $\Delta$ Nef (Fig. 2.3D and 2.4). These results indicate that co-expression of PACS-1-mCherry or MHC-I-mCherry and Nef-eGFP is achievable. Moreover, using different fluorophores for Nef and its binding partners allows for simultaneous observation of both proteins in infected cells without compromising their functionality.

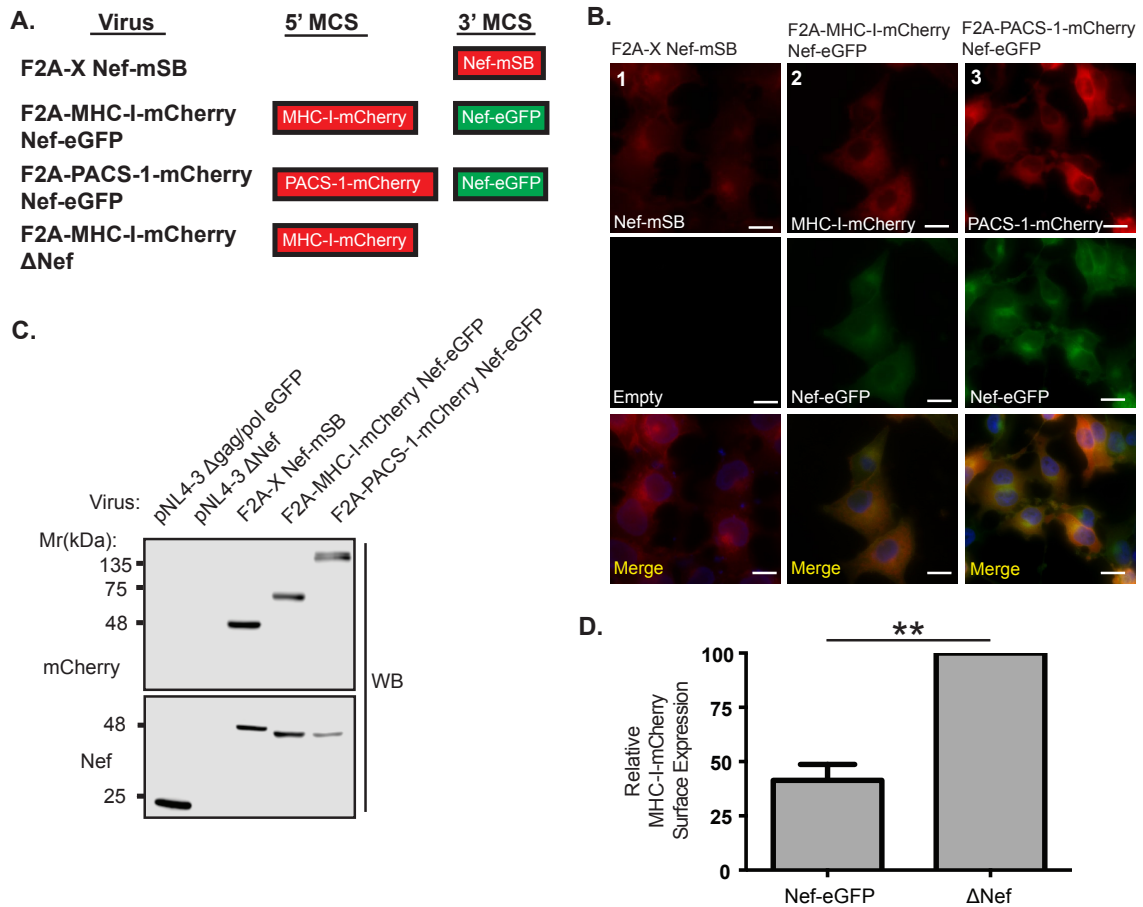


**Figure 2.3: Fluorescence microscopy confirms expression of proteins from the 5' and 3' MCS.**

Viruses were engineered to produce MHC-I-mCherry or PACS-1-mCherry from the 5' MCS in combination with Nef-eGFP from the 3' MCS. (A) Schematic representation of proteins produced from lentiviral expression system. (B) To detect the fluorescent fusion proteins, HeLa cells were infected and visualized 48 hours post infection by widefield fluorescence microscopy. Expression of the Nef-mSB fusion protein was confirmed (column 1), along with concurrent expression of MHC-I or PACS-1-mCherry fusions with Nef-eGFP (columns 2 and 3). Cell nuclei were stained using Hoescht nuclear stain (blue). Scale bars represent 15 $\mu$ m. (C) mCherry and Nef specific western blots were performed to confirm the expression of the fusion proteins. (D) Jurkat E6.1 T-cells were infected with pNL4-3 F2A-MHC-I-mCherry Nef-eGFP (Nef-eGFP) or pNL4-3 F2A-MHC-I-mCherry  $\Delta$ Nef ( $\Delta$ Nef). At 48 hours post infection, cells were surface stained for

MHC-I-mCherry (BB7.2 antibody), fixed, permeabilized and stained for intracellular p24 (KC57-RD1 antibody). Columns represent relative MHC-I-mCherry surface expression calculated from the geometric mean fluorescent intensity (gMFI) of surface MHC-I-mCherry on infected cells and normalized to the cell surface MHC-I-mCherry levels of  $\Delta$ Nef-infected cells. Error bars were calculated from four independent repeats. (\* indicates  $p$ -value  $< 0.01$ ).



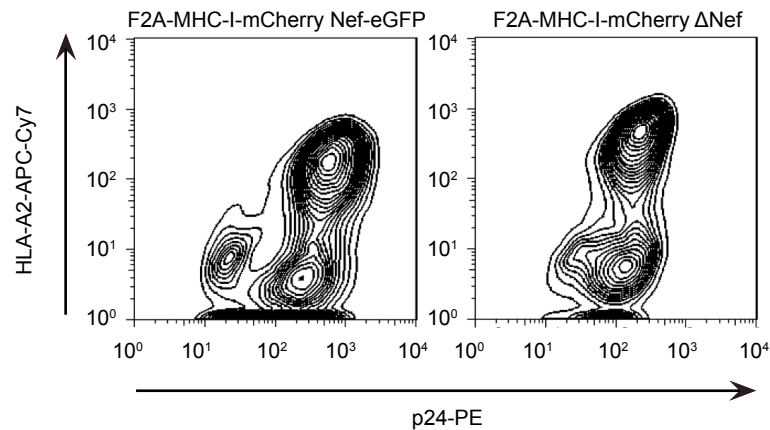


**Figure 2.4: MHC-I-mCherry produced from the F2A site reaches the cell surface and is sensitive to Nef.**

Jurkat E6.1 T-cells were infected with a virus expressing MHC-I-mCherry in the presence (F2A-MHC-I-mCherry Nef-eGFP) or absence (F2A MHC-I mCherry  $\Delta$ Nef) of eGFP-tagged Nef. At 48 hours post infection cells were washed and stained for surface HLA-A2 using APC/Cy7 conjugated BB7.2 monoclonal antibody. Cells were then washed, fixed, and permeabilized to allow for intracellular staining of p24 (using a PE conjugated anti-p24 antibody).

## 2.2.4 Viral BiFC demonstrates that Nef interacts with PACS-1 in specific endosomal compartments

To investigate the utility of our lentiviral vector system for studying protein-protein interactions, we constructed lentiviral BiFC vectors (Fig. 2.5A). These were designed such that a functional Venus fluorophore was reconstituted when proteins fused to the amino ( $V_N$  [1-173]) and carboxy ( $V_C$  [155-238]) fragments of Venus were in close proximity. Indeed, vectors were designed to contain PACS-1- $V_N$  in the 5' MCS and Nef- $V_C$  in the 3' MCS (pNL4-3 F2A-PACS-1- $V_N$  Nef- $V_C$ ). Strikingly, infection of HeLa cells revealed that PACS-1 and Nef reconstitute a functional fluorophore when expressed from the pNL4-3 F2A-PACS-1- $V_N$  Nef- $V_C$  vector, indicating that PACS-1 and Nef are expressed and are in close proximity (Fig. 2.5B, column 3). Analysis at the protein level revealed PACS-1- $V_N$  and Nef- $V_C$  are both expressed (Fig. 2.5C). To rule out possible auto-fluorescence of the individual split fluorophores, we also infected HeLa cells with viruses expressing the individual split fluorophores (Nef- $V_C$  or PACS-1- $V_N$ ; Fig. 2.5B), in combination with either PACS-1-mCherry or Nef-mSB (Fig. 2.5A). Indeed, sole expression of PACS-1- $V_N$  or Nef- $V_C$  did not result in fluorescence (Fig. 2.5B; column 1, 2), even though these proteins were efficiently produced (Fig. 2.5C) and red fluorescence was observed indicating protein expression from the other MCS (Fig. 2.5B; column 1, 2). Moreover, to determine if the Nef protein produced from our viral BiFC vector system was functional, we used flow cytometry to test the ability of Nef produced from pNL4-3 F2A-PACS-1- $V_N$  Nef- $V_C$  to downregulate endogenous MHC-I in Jurkat E6.1 T-cells. Our analysis demonstrated that Nef- $V_C$  downregulated MHC-I efficiently when compared to Jurkat E6.1 T-cells infected with a virus lacking Nef (pNL4-3 F2A-PACS-1- $V_N$   $\Delta$ Nef) (Fig. 2.5D and 2.6).

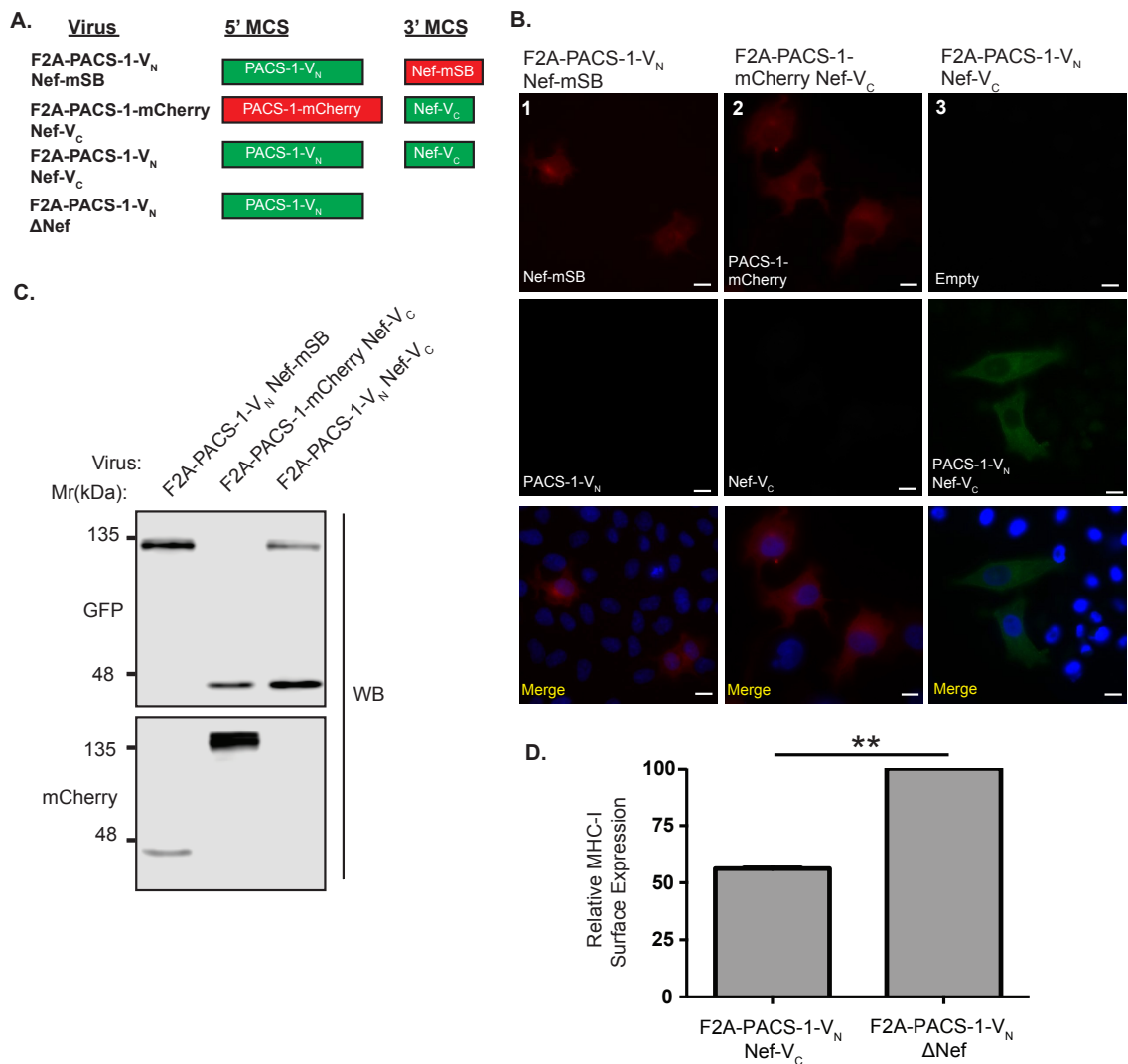


**Figure 2.5: Visualizing the Nef/PACS-1 interaction using viral Bimolecular Fluorescence Complementation. (A)**

Schematic representation of proteins produced from lentiviral expression system. (B) HeLa cells were infected with various viruses encoding different fusion proteins and visualized using widefield fluorescence microscopy. BiFC (green, column 3) was visualized in the F2A-PACS-1-V<sub>N</sub> Nef-V<sub>C</sub> infected HeLa cells and not the control BiFC viral infections (columns 1 and 2). Cells were mounted in DAPI Fluoromount G media for nuclear staining (blue). Scale bars represent 15µm. (C) Expression of the V<sub>N</sub> or V<sub>C</sub> fragment was detected by a GFP specific Western blot, whereas the mCherry and mSB fusions, which acted as controls, were detected by an mCherry specific western blot.

Densitometry measurements for PACS-1-V<sub>N</sub> and Nef-V<sub>C</sub> were 10,500 and 29,200 arbitrary units, respectively, as determined by Licor C-Digit. (D) Jurkat E6.1 T-cells were infected with F2A-PACS-1-V<sub>N</sub> Nef-V<sub>C</sub> and the corresponding non-functional Nef mutant (F2A-PACS-1-V<sub>N</sub> ΔNef). At 72 hours post infection, cells were surface stained for MHC-I (W6/32 antibody), fixed, permeabilized and stained for intracellular p24 (KC57-RD1 antibody). Columns represent relative MHC-I surface expression calculated from the geometric mean fluorescent intensity (gMFI) of surface MHC-I on infected cells and normalized to cell surface MHC-I levels of ΔNef-infected cells. Error bars were calculated from four independent repeats. (\* indicates  $p$ -value < 0.01).

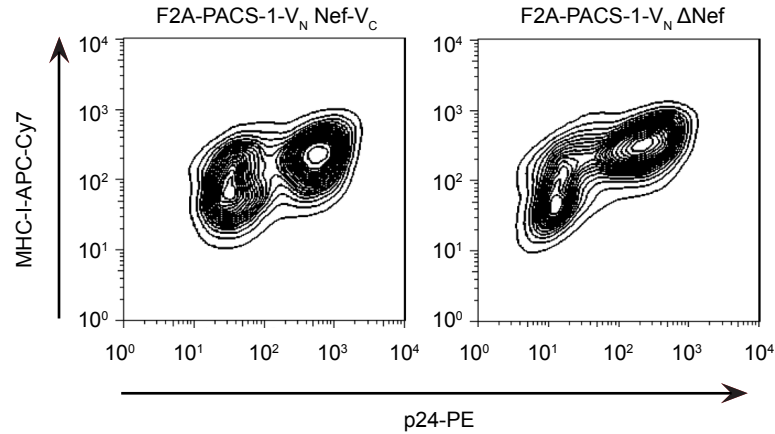


**Figure 2.6: Nef- $V_C$  expressed from a viral BiFC vector expressing PACS-1- $V_N$  is able to downregulate MHC-I**

Jurkat E6.1 T-cells infected with a virus expressing PACS-1- $V_N$  in the presence (F2A-PACS-1- $V_N$  Nef- $V_C$ ) or absence (F2A-PACS-1- $V_N$   $\Delta$ Nef) of Nef- $V_C$ . At 72 hours post-infection cells were washed and stained for surface MHC-I (using an APC/Cy7 conjugated pan-selective monoclonal antibody). Cells were then washed, fixed, permeabilized and stained for intracellular p24 (using a PE-conjugated anti-p24 antibody).

To test if the viral BiFC signal between PACS-1-V<sub>N</sub> and Nef-V<sub>C</sub> was localized to a specific sub-cellular compartment, we performed an immunofluorescence analysis (Fig. 2.7A) using markers of the endocytic pathway previously identified as co-localizing with Nef/PACS-1 complexes (9). HeLa cells infected with pNL4-3 F2A-PACS-1-V<sub>N</sub> Nef-V<sub>C</sub> and exhibiting viral BiFC were stained with markers for late or early endosomes. We observed 21% and 34% co-localization with markers for Rab5 and LAMP-1, consistent with a Nef/PACS-1 interaction on early and late endosomes, respectively (Fig. 2.7B). Together these experiments indicate that viral BiFC can be applied to study protein-protein interactions between Nef and host cellular binding partners, and is particularly effective for mapping the sub-cellular locations of their interactions during viral infection. In addition, viral BiFC produces a functional Nef protein that has the ability to downregulate MHC-I.

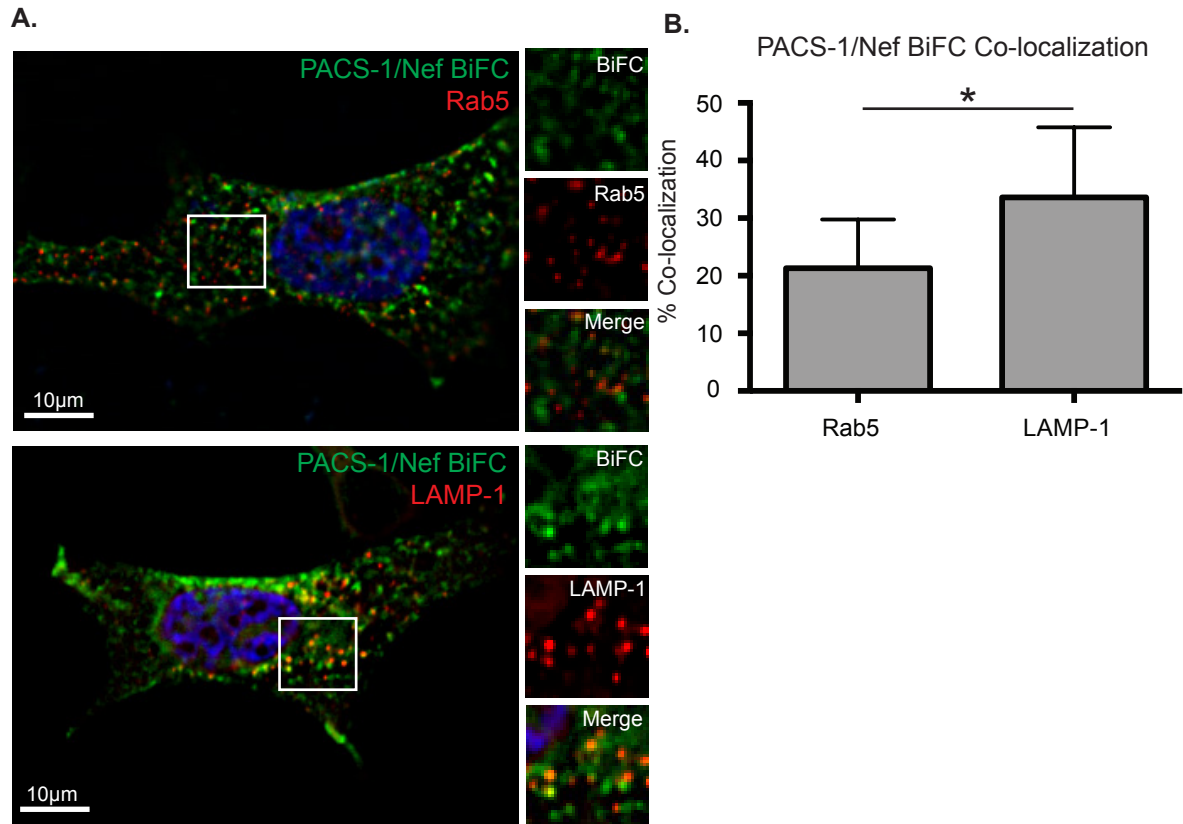


**Figure 2.7: Nef/PACS-1 viral BiFC signal is localized to specific Rab5 and LAMP-1 positive endosomes.**

(A) HeLa cells were infected with the F2A-PACS-1- $V_N$  Nef- $V_C$  virus and immunostained for Rab5 or LAMP-1. Cells were fixed, permeablized and stained using Rab5 or LAMP-1 specific primary antibodies. Viral BiFC (green) was observed under the FITC channels and Rab5/LAMP-1 (red) fluorescence was observed under the Far-Red channel. Cells were mounted in DAPI Fluoromount G media for nuclear staining (blue). Scale bars represent 10 $\mu$ m. Panels on the right represent a magnification of the boxed region from the left panel. (B) Twenty-one percent of the viral BiFC signal co-localized with Rab5, whereas 34% co-localized with LAMP-1. Co-localization was determined by the Manders Coefficient. Pearson's correlation values were determined to be 0.36 and 0.42 for Rab5 and LAMP-1 co-localization, respectively. Error bars were calculated from 3

independent experiments and quantification of at least 25 different cells. (\* indicates p value  $< 0.05$ ).



### 2.2.5 Viral BiFC can be used the study novel interactions between Nef and host cellular proteins in the endocytic network

We demonstrated that viral BiFC can recapitulate previously characterized interactions between Nef and host cellular proteins, such as the Nef/PACS-1 interactions, and can be used to examine the sub-cellular localization of such interactions (Fig. 2.7). Therefore, we decided to test if viral BiFC can spatially define the interaction between Nef and additional interacting partners. We first tested the ability of Nef to interact with the cell surface receptor MHC-I. Indeed, the Nef/MHC-I interaction has been demonstrated both *in vitro* and by crystallography, but this complex has never been demonstrated within cells. Thus, we inserted the MHC-I allele HLA-A2 into the 5' MCS of our viral BiFC vector to generate the vector pNL4-3 F2A-MHC-I-V<sub>N</sub> Nef-V<sub>C</sub>. To test for an interaction between MHC-I-V<sub>N</sub> and Nef-V<sub>C</sub>, HeLa cells were infected and observed under widefield fluorescence microscopy. Interestingly, BiFC was observed, demonstrating an interaction between Nef and MHC-I in cells (Fig. 2.8A). Furthermore, we co-localized this interaction to vesicles that are positive for AP-1 (Fig. 2.8B) consistent with the *in vitro* Nef/MHC-I/AP-1 crystal structure (14).

Since both PACS-1 and AP-1 are implicated in the Nef mediated downregulation of MHC-I, we explored the possibility that Nef associates with another host cellular membrane trafficking regulator, sorting nexin 18 (SNX18). We pursued SNX18 since this protein co-localizes with both PACS-1 and AP-1 within the endocytic network (37). To test if there is an association between Nef and SNX18, we inserted the *SNX18* gene in the 5' MCS of our viral BiFC vector to produce pNL4-3 F2A-SNX18-V<sub>N</sub> Nef-V<sub>C</sub>. We then infected HeLa cells with pNL4-3 F2A-SNX18-V<sub>N</sub> Nef-V<sub>C</sub> and tested for BiFC. As for our previously tested interactions, BiFC was observed between SNX18 and Nef demonstrating for the first time the close proximity between Nef and SNX18 (Fig. 2.8A; bottom panels). Furthermore, this association co-localized with AP-1, consistent with SNX18's localization in the endosomal network (Fig. 2.8A) (37). Importantly, infection with a vector harboring an empty 5' MCS (pNL4-3 F2A-X Nef-V<sub>C</sub>) demonstrated that Nef-V<sub>C</sub> expressed from this vector can downregulate endogenous MHC-I in Jurkat E6.1

T-cells (Fig. 2.8C and 2.9). This indicates that Nef fused to a split fluorophore is functional. Overall, viral BiFC can be used to further study previously described interactions as well as identify novel interactions between Nef and host cellular partners, and spatially define these interactions within the cell.

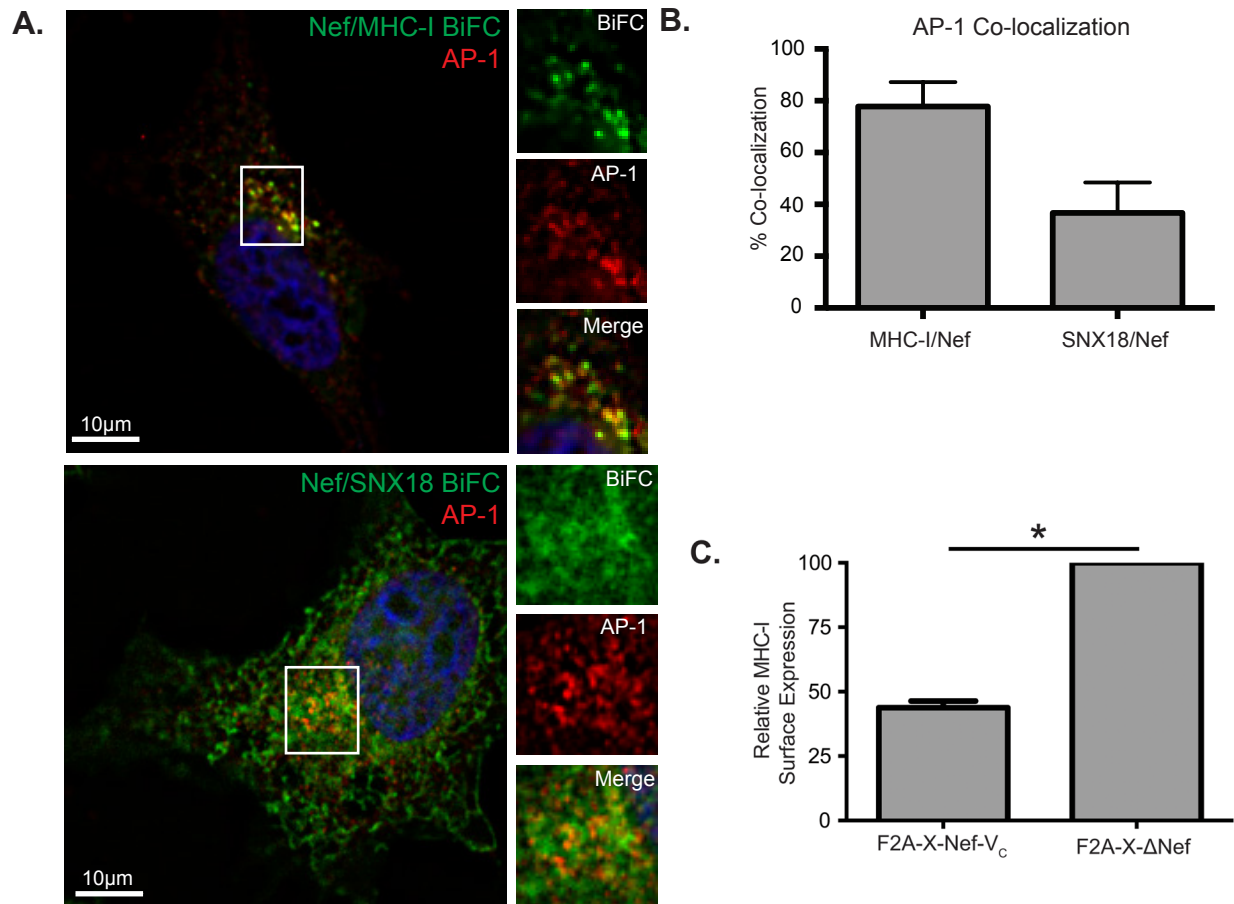


**Figure 2.8: Viral BiFC signals of MHC-I/Nef and SNX18/Nef are localized to AP-1 positive endosomes.**

(A) HeLa cells were infected with either the F2A-MHC-I-V<sub>N</sub> Nef-V<sub>C</sub> virus (top) or the F2A-SNX18-V<sub>N</sub> Nef-V<sub>C</sub> virus (bottom) and immunostained for AP-1. Cells were fixed, permeabilized and stained using an AP-1 specific primary antibody. Viral BiFC fluorescence (green) was observed under the FITC channels and AP-1 fluorescence (red)

was observed under the Far-Red channel. Cells were mounted in DAPI Fluoromount G media for nuclear staining (blue). Scale bars represent 10 $\mu$ m. Panels on the right represent a magnification of the boxed region from the left panel. (B) 78% percent of the Nef/MHC-I BiFC signal co-localized with AP-1, whereas 37% of the Nef/SNX18 BiFC signal co-localized with AP-1. Co-localization was determined by the Manders Coefficient, and mean Pearson's correlation was determined to be 0.74 and 0.40 for Nef/MHC-I and Nef/SNX18, respectively. Error bars were calculated by 3 independent experiments and quantification of at least 25 different cells. (C) Jurkat E6.1 T-cells were infected with F2A-X Nef-V<sub>C</sub> virus and the corresponding non-functional Nef mutant (F2A-X  $\Delta$ Nef). At 72 hours post infection, cells were surface stained for MHC-I (W6/32 antibody), fixed, permeabilized and stained for intracellular p24 (KC57-RD1 antibody). Columns represent relative MHC-I surface expression calculated from the geometric mean fluorescent intensity (gMFI) of surface MHC-I on infected cells and normalized to the cell surface MHC-I levels of  $\Delta$ Nef-infected cells. Error bars were calculated from four independent repeats. (\*\* indicates  $p$ -value < 0.01).

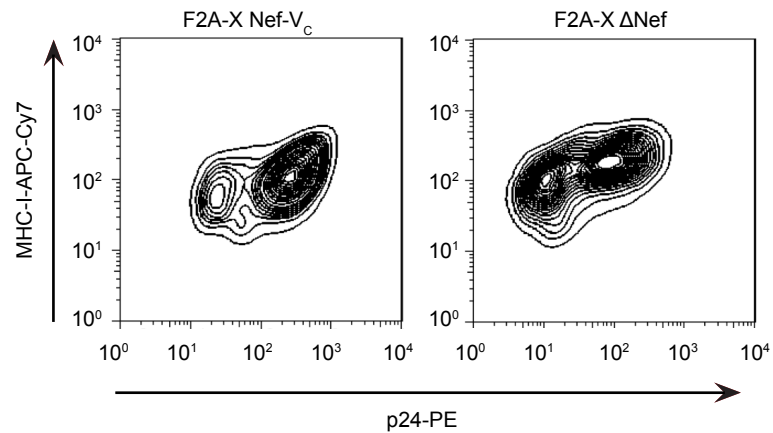


**Figure 2.9: Nef-V<sub>C</sub> expressed from a base viral BiFC vector is able to downregulate MHC-I.**

Jurkat E6.1 T-cells were infected with a base viral BiFC virus containing Nef-V<sub>C</sub> (F2A-X Nef-V<sub>C</sub>) or a virus that does not produce Nef (F2A-X ΔNef). At 72 hours post-infection cells were washed and stained for surface MHC-I (using an APC/Cy7 conjugated pan-selective monoclonal antibody). Cells were then washed, fixed, permeabilized and stained for intracellular p24 (using a PE-conjugated anti-p24 antibody).

## 2.3 Discussion

This study describes viral BiFC, a novel lentiviral expression system designed for studying protein-protein interactions and mapping their sub-cellular locations. This vector has the unique capability of enabling the use of bimolecular fluorescence complementation from a single vector in the context of a viral infection. We demonstrate the application and utility of viral BiFC for understanding the membrane trafficking pathways of cellular proteins interacting with the HIV-1 protein Nef (Fig. 2.7 and 2.8). This is of utmost importance as Nef is considered the pathogenic factor responsible for the progression to AIDS (38). Moreover, since Nef lacks any enzymatic activity its ability to interact with cellular partners is key to define its pathogenic nature.

Lentiviral vectors are ideal vehicles for introducing genes at high expression levels inside a heterologous cell {for review see (18, 39, 40)}. However, the study of protein interactions often requires gene expression from multiple vectors, which may result in suboptimal or differential expression of the proteins of interest. One approach to express multiple genes with lentiviral vectors involves using an internal ribosome entry site (IRES) (41). However, significant differences in IRES activity have been reported in different cell types, thereby decreasing the utility of these vectors (42, 43). Moreover, the use of an IRES is limited, as there are significant restrictions imposed when cloning due to the substantial size of IRES sequences (23) and multiple reports suggest certain cistrons inhibit IRES element activity (44, 45).

In contrast, effective protein expression from polycistronic RNA can be achieved using plasmids harboring the 2A peptide sequence, such as in this study, which permits independent translation of coding sequences from a single transcript (23, 46, 47). This approach allowed for co-expression of PACS-1-mCherry or MHC-I-mCherry and Nef-eGFP, demonstrating that Nef and host cell proteins can be efficiently expressed from a single integrating vector (Fig. 2.3). We validated the cleavage efficiency of the 2A site by constructing a modified vector with a mutated F2A site (Fig. 2.2). Production of cleaved mStrawberry-Flag was significantly reduced (a six-fold decrease;  $p < 0.05$ ) in the vector encoding the mutated F2A site (Fig. 2.2B, C), directly confirming the efficiency of cleavage mediated by the F2A site.

BiFC is a valuable tool for visualizing protein-protein interactions within a cell {for review see (15, 16)}. This powerful technique can be used to identify the specific sub-cellular locations where protein interactions occur, and to define protein interaction interfaces by elucidating the residues critical for a protein interaction to occur (9, 15, 16, 48). In the case of Nef, previous reports have utilized BiFC to demonstrate the dimerization of Nef and to study the interaction between Nef and the host cellular proteins PACS-1 and PACS-2 (9, 48-50). However, these studies utilized a dual vector expression system, which may result in the need to laboriously optimize the expression levels of two different plasmids in order to observe BiFC (48, 50). This fine-tuning of plasmid levels is effectively removed in our system, which relies on protein expression from a single vector. In addition, previous studies were not conducted under the conditions of viral infection, precluding generalizability of these studies to the nature of HIV-1 infection. Our single vector expression system has the added advantage that all infected cells express both proteins of interest concomitantly within the context of a viral infection (Fig. 2.3, 2.5, 2.8). This is of particular interest when studying interactions between Nef and PACS-1. Indeed, the Nef/PACS-1 interaction modulates the downregulation of cell surface MHC-I via a mechanism that depends on the length of infection (13). Our viral BiFC system will facilitate full elucidation of the mechanisms governing the influence of the HIV-1 genome on the time-dependent action of the Nef/PACS-1 interaction through deletion of specific HIV-1 proteins within our viral vector. This molecular dissection will be possible using a single vector system that detects Nef interactions (Fig. 2.7A, 2.8) and is functionally capable of downregulating MHC-I (Fig. 2.3D, 2.5C).

Interestingly, our observation of the Nef/PACS-1 interaction at distinct endosomal compartments (Fig. 2.7) is in accordance with the previously defined sub-cellular localization of this interaction (9), thereby validating that viral BiFC demonstrates protein interactions between Nef and host proteins at *bone fide* cellular compartments. Indeed, this system can define the interacting interfaces between Nef and multiple Nef-binding partners as well as map the sub-cellular location of their interactions. Specifically, the interaction between Nef, MHC-I, and the membrane adaptor protein-1 (AP-1) is critical in orchestrating the downregulation of MHC-I to evade immune detection and this

interaction has been studied *in vitro* (36, 51, 52). However, the exact sub-cellular localization of these interactions currently remains unknown. By inserting the MHC-I gene into our viral BiFC system and co-localizing the Nef/MHC-I interaction to AP-1 positive endosomes we effectively recapitulated the Nef/MHC-I/AP-1 interaction in HIV-1 infected cells (Fig. 2.8). This information is critical to understand the exact molecular players that are subverted by Nef in order to traffic MHC-I molecules from the plasma membrane. A novel membrane trafficking regulator that may play a role in this process is SNX18. Our analysis is the first to demonstrate that SNX18 associates with Nef in an AP-1 positive compartment (Fig. 2.8). This is consistent with the reported presence of SNX18 in compartments that are PACS-1 and AP-1 positive (37). Future studies will be required to correctly decipher the role of SNX18 in Nef mediated MHC-I downregulation and to confirm if the Nef/SNX18 interaction is direct. An attractive hypothesis is a required role for SNX18 in biogenerating specific vesicles required for Nef to correctly remove MHC-I from the cell surface. This implies that Nef may require the fissionogenic ability of proteins such as dynamin, which is recruited by SNX18 to correctly shuttle host proteins such as MHC-I to sub-cellular locales (37).

Although constructed as a robust tool to decipher membrane trafficking networks in HIV-1 infected cells, our vector system also has potential as a drug discovery tool. Recently, Poe *et al.* elegantly demonstrated that BiFC can be utilized for high-throughput screening of small molecule inhibitor libraries for molecules that block specific protein-protein interactions (49). By performing small-molecule screens of compound libraries in cells infected with our viral BiFC system we will be able to identify compounds that disrupt the interactions between Nef and Nef-binding partners such as PACS-1 or the Nef/MHC-I/AP-1 complex. Our system will allow for identification of novel inhibitors of these interactions in a model of infection, thereby affording us key information about the Nef interaction interfaces that mediate immune evasion during HIV-1 infection.

Due to the essential role Nef plays in HIV-1 pathogenesis, our viral BiFC system was designed to study the many interactions Nef must make to modulate infected cells. However, it will be interesting to determine in future studies if removal of Nef from the 3' MCS will allow viral BiFC to be applicable to any protein-protein interaction analysis.

Given that Nef itself has been determined to play a role in viral replication (53), additional studies are required to determine if Nef can be replaced by a heterologous sequence. Previous studies suggest that viruses harboring a Nef gene deletion could still efficiently replicate suggesting that heterologous sequences can be placed in the 3' MCS (53). Moreover, the MCSs in our lentiviral system will not only enable insertion of genes of interest, but also sequences capable of silencing host genes, such as short hairpin RNA sequences (54, 55).

In summary, viral BiFC is a powerful tool that enables the study of vesicular trafficking in the context of HIV-1 infection and provides an efficient method to introduce transgenes directly into a lentiviral vector. Viral BiFC will enable researchers to study Nef interactions at specific sub-cellular locales, thereby elucidating key cellular events that mediate HIV-1 pathogenesis.



## 2.4 Materials and Methods

### 2.4.1 Cell Culture

HeLa (ATCC, Manassas, VA) and HEK 293T cells (Life Technologies, Carlsbad, CA) were grown in complete DMEM containing 10% fetal bovine serum (Life Technologies, Waltham, WA), 100µg/ml penicillin-streptomycin (Hyclone, Logan, UT), 1% sodium pyruvate, 1% non-essential amino acids and 2mM L-glutamine (Hyclone). Jurkat E6.1 T-cells (Catalog number 177; National Institutes of Health, AIDS Research and Reference Reagent Program) were cultured in RPMI 1640 with supplements as mentioned above. All cell lines were grown at 37°C in the presence of 5% CO<sub>2</sub> and sub-cultured in accordance with supplier's recommendations.

### 2.4.2 Proviral plasmids and cloning strategy

3' cloning site for Nef fusion proteins: The previously described pNL4-3 Δgag/pol eGFP replication incompetent HIV-1 proviral vector (19, 20) was used as the base template for modification into our final expression vector system. First, primer overlap extension mutagenesis (56) was used to amplify two fragments flanking the Nef coding sequence in order to remove Nef and insert XmaI, AgeI and NotI restriction sites, termed the 3' multiple cloning site (MCS). Specifically, an initial PCR reaction (Reaction I) was performed with primers JD 14 and JD 37 (Table 2) in order to amplify a 316 bp fragment upstream of Nef, containing the 3' MCS restriction sites. A subsequent PCR reaction (Reaction II) amplified a 1157 bp fragment immediately after the Nef stop codon using primers JD 38 and JD 15 (Table 2). The forward primer in Reaction II contained complementary nucleotides to the 3' MCS restriction sites in JD 37. Products from Reaction I and II were purified, mixed and amplified (Reaction III) using the flanking JD 14 and JD 15 primers (Table 2). The Reaction III product was inserted into the pNL4-3 Δgag/pol eGFP base vector using BamHI and NcoI restriction sites in order to generate a pNL4-3 Δgag/pol eGFP with the 3' MCS in lieu of Nef (Fig. 2.1). This 3' MCS is capable of accepting Nef fusion proteins with various fluorophores. The mStrawberry (mSB) fragment was amplified from Addgene plasmid 20970 (57). For the BiFC experiments regions expressing the amino portion of the Venus fluorophore (V<sub>N</sub>; amino

acids 1-173) or the carboxy portion of the Venus fluorophore (V<sub>c</sub>; amino acids 155-238) (15) were inserted in either MCS.

**Table 2: Primers used for cloning viral-BiFC vectors**

Primer	Sequence
JD 14	GTGAACGGATCCTTAGCAC
JD 15	CCTGCACTCCATGGATCA
JD 37	CCTTGGGCGGCCGCATATAACCGGTAAATTCCCGGGCTTATA GCAAAATCCTTTCCAAGCCCT
JD 38	CCTTGGCCCGGGAAATTTACCGGTATATGCGGCCGCCATCGA GCTTGCTACAAGGGAC
JD 42	GTTGTTGCAGAATTCTTATTATGGCTTCCAC
JD 43	CCTTGGTTGGCCAGGGCCCGTAAAAACAGTACATACAGACA ATGGC
JD 106	TAGTGAAACAGACTTTGAATTTTGACCTTCTCAAGTTGGCGG GAGACGTGGAGTCCAACCCCGGGCCCGCAGCAGCATGCGCA GCAACTAGTTAATGGCC
JD 107	CTTAAGTAGTTGCTGCGCATGCTGCTGCGGGCCCGGGGTTGG ACTCCACGTCTCCCGCCAACTTGAGAAGGTCAAATTCAAAG TCTGTTTCACTACATG
JD 132	GGTTGGGCATGCATGGCGCTGCGCGCCCGG
JD 142	GCAGCAACTAGTTTACTTATCGTCGTCATCCTTGTAATCTCCG TCCTCGATGTTGTGGCGGATC
JD 144	GCTGCTGCATGCATGGCCGTZATGGCGCCC
JD 165	TGAAGCGCGCACGGCAAG
JD 166	TGCTGCGGGCCCGGCGTTGGACTCCACGTCTCCCGC

### 2.4.3 Generation of the F2A cleavage site and 5' MCS

An ApaI site was inserted directly after eGFP in the pNL4-3  $\Delta$ gag/pol eGFP plasmid (JD 43 and JD 42). Briefly, a PCR reaction was conducted to produce the desired ApaI restriction site directly adjacent to the MscI restriction site already present in the proviral vector. The product was then digested with MscI and EcoRI and cloned into the parent vector. Subsequently, to insert the F2A sequences and the 5' MCS, two complementary primers (JD 106 and 107, Table 2) were engineered to contain the F2A sequence (VKQTLNFDLLKAGDVESNPGP) in addition to ApaI, SphI and SpeI restriction sites, termed the 5' MCS, plus a 2 bp overhang that is complementary to the ApaI and SphI cut sites. These primers were annealed together and ligated into pNL4.3  $\Delta$ Gag/pol eGFP with the inserted ApaI cut site (Fig. 2.1; bottom), which was cut with SphI and ApaI. The resulting plasmid contained unique 5' restriction cut sites in order to permit insertion of foreign genes. To generate the F2A (null) control vector, primer overlap extension mutagenesis was performed to mutate the penultimate proline to an alanine. First, a forward primer was generated upstream of the F2A site containing a PstI restriction site (JD 165). Second, a reverse primer was engineered to contain the F2A mutation with an adjacent ApaI site (JD 166). A subsequent PCR was conducted using F2A mSB-Flag Nef-eGFP as a template, and the product was inserted into the F2A vector utilizing the PstI and ApaI restriction sites, thereby replacing the functionally active F2A with the non-functional mutant.

To generate the MHC-I (HLA-A2 allele) and SNX18 BiFC constructs, products were amplified from expression plasmids containing cDNA sequences for MHC-I-V<sub>N</sub> (JD 144 and JD 142; Table 2) or SNX18-V<sub>N</sub>, (JD 132 and JD 142; Table 2, SNX18 cDNA was provided by Rytis Prekaris; University of Colorado Denver) then cloned into the viral vector using the SpeI and SphI cut sites. To engineer the F2A-MHC-I-mCherry  $\Delta$ Nef viral vector, we digested the parental backbone of F2A-MHC-I-mCherry Nef-GFP with PstI and EcoRI and cloned the product into a pNL4-3  $\Delta$ Nef construct generating an F2A-MHC-I-mCherry  $\Delta$ Nef viral vector.

#### 2.4.4 Pseudovirus production and processing

Pseudovirions were produced in HEK 293T cells. Cells were triple transfected using PolyJet (FroggaBio, Toronto, ON) with pNL4-3  $\Delta$ gag/pol eGFP or the modified variants, as well as pdR8.2 and pMD2.G as previously described (32). Pseudovirus was harvested 48 hours post-transfection. Briefly, virus-containing media was first centrifuged at 3000xg for 5 minutes and subsequently filtered. The filtered supernatant was supplemented with an additional 10% FBS prior to storage at -80°C.

#### 2.4.5 Western Blots, Antibodies and Infections

Jurkat E6.1 T-cells or HeLa cells were infected with various pseudoviruses for 48 hours, at which point infected cells were washed once with phosphate buffered saline (PBS) and subsequently lysed in lysis buffer (0.5M HEPES, 1.25M NaCl, 1M MgCl<sub>2</sub>, 0.25M EDTA, 0.1% Triton X-100 and 1X complete Protease inhibitor Tablets (Roche, Indianapolis, IN). Cells were incubated on a rotator for 20 minutes at 4°C before removing insoluble cellular debris by centrifugation at 20,000xg for 20 minutes. Lysates were boiled at 98°C in 5X SDS-PAGE sample buffer (0.312M Tris pH 6.8, 25% 2-Mercaptoethanol, 50% glycerol, 10% SDS) and proteins were separated on a 12% SDS-PAGE gel and subsequently transferred to nitrocellulose membranes. Membranes were blocked in 5% non-fat skimmed milk (Bioshop, Burlington, ON) in TBST containing 0.1% Triton X-100 for 1 hour, then incubated overnight at 4°C with various antibodies: rabbit anti-Nef polyclonal antibody (1:4000; catalog number 2949, NIH AIDS Research and Reference Reagent Program, USA), rabbit anti-GFP polyclonal antibody (1:2000; Clontech; Mountain View, CA), rat anti-DYKDDDK monoclonal IgG (1:2500; BioLegend, San Diego, CA), or rabbit anti-mCherry monoclonal IgG (1:2000; Thermo Scientific). Membranes were then washed and incubated for two hours with the appropriate species-specific HRP-conjugated antibodies (1:5000; Thermo Scientific). All blots were developed and quantified using ECL substrates (Millipore Inc., Billerica, MA) and a C-DiGit chemiluminescence Western blot scanner (LI-COR Biosciences, Lincoln, NE).

Cleavage efficiency of the F2A site was calculated by dividing the signal intensity of the cleaved product by the sum of both the cleaved and un-cleaved product. Efficiencies were then normalized to the wildtype F2A cleavage. Subsequently, a ratio was obtained by comparing the wildtype functional F2A cleavage efficiency to the mutant.

For flow cytometry the following antibodies were used: W6/32 (anti-MHC-I; pan-selective, provided by D. Johnson, Oregon Health and Sciences University), antibody conjugated to APC/Cy7 (1:25, Biolegend, San Diego, CA), anti-p24 clone KC57 conjugated to RD1 (phycoerythrin) (1:50, Beckman Coulter, Brea, CA), anti BB7.2 conjugated to APC/Cy7 (1:25, Biolegend, San Diego, CA).

For immunofluorescence, rabbit anti-Rab5 (clone C8B1; 1:200, Cell Signaling), mouse anti-LAMP-1 (clone H4A3, 1:100, obtained from the Developmental Studies Hybridoma Bank) and mouse anti-AP-1 $\gamma$  (Sigma Aldrich) antibodies were used.

#### 2.4.6 Microscopy

HeLa cells were seeded onto sterile glass coverslips at  $5 \times 10^5$  cells per coverslip for 16 hours prior to infection. Cells were infected for 48 hours before processing for immunofluorescence. Briefly, cells were washed three times with PBS before fixation in 4% paraformaldehyde for 20 minutes at room temperature. Cells were subsequently washed with PBS twice prior to nuclear staining. Immediately prior to imaging, Hoechst nuclear stain (1 $\mu$ g/ml; Thermo Scientific) was added to the coverslip and incubated for 10 minutes. Cells were imaged on the Leica DMI6000 B on 63X objective using the FITC, CY3 and DAPI filter settings using the Hamamatsu Orca-flash 4.0 Camera.

For BiFC experiments, infections were set as above. Prior to fixation, the cells were incubated at room temperature for 2 hours to allow the reconstituted fluorophore to mature. The fixation protocol was then carried out as described above. To visualize early or late endosomes, cells were stained with rabbit anti-Rab5 or mouse anti-LAMP-1 antibodies, respectively. Samples were incubated in a permeabilization buffer containing 1% BSA in PBS and 0.2% Triton X-100 for 5 minutes, then blocked in a buffer containing 5% BSA in PBS for 1 hour. Anti-Rab5 or LAMP-1 antibodies were then

diluted in 1% BSA and 0.2% Triton X-100 (1:200 and 1:100, Jackson ImmunoResearch). Cells were then washed three times in PBS (2 minutes each) before adding the secondary donkey anti-rabbit AlexaFluor 647 or donkey anti-mouse Alexafluor 647 (1:1000; Jackson ImmunoResearch) in the same manner as the primary antibody. AP-1 staining was carried out as mentioned above using mouse anti-AP-1 $\gamma$  (1:200; Sigma Aldrich) primary antibody and donkey anti-mouse Alexafluor 647 (1:1000; Jackson ImmunoResearch). Samples were washed three times in PBS (1 minute each) prior to imaging and mounted onto glass slides using DAPI Fluormount-G (Southern Biotech, Birmingham, AL). Cells were imaged on the Leica DMI6000 B on 100X objective using the FITC, CY5 and DAPI filter settings using the Hamamatsu Photometrics Delta Evolve camera. Images were subsequently deconvolved using the Advanced Fluorescence Deconvolution application on the Leica Application Suite software. Co-localization analysis was conducted using the Manders Coefficient and Pearson Correlation from the Image J plugin as described previously (58).

### 2.4.7 Flow Cytometry

To quantify the cell surface expression levels of MHC-I, Jurkat E6.1 T-cells were infected with the appropriate viruses and 72 hours post infection cells were surface stained for MHC-I using W6/32 antibody conjugated to APC/Cy7 (Biolegend, San Diego, CA). Following fixation in 1% paraformaldehyde, cells were permeabilized with cold methanol. Subsequently, intracellular staining with RD1 (phycoerythrin) conjugated anti-p24 (Beckman Coulter) was performed to gate for infected cells. Cell surface MHC-I expression was quantified by flow cytometry (BD FACS Canto II) and the data analyzed using FlowJo software (version 9.6.4, Treestar, Ashland, OR).

The ability of the MHC-I-mCherry fusion protein to be trafficked to the membrane was tested using an allele specific antibody. Jurkat E6.1 T-cells were infected with the appropriate virus and 48 hours post-infection, cell surface staining was performed using the BB7.2 antibody (Biolegend) which recognizes only MHC-I molecules encoded by A\*02 alleles. Cells were then fixed in 1% paraformaldehyde and permeabilized with cold methanol and intracellularly stained with RD1 (phycoerythrin) conjugated anti-p24 to

gate for infected cells. MHC-I-mCherry cell surface expression was quantified by flow cytometry (BD FACS Canto II) and the data analyzed using FlowJo software (version 9.6.4)

## 2.4.8 Statistics

All statistics were conducted using a paired T-test on Graph Pad Prism (Graph Pad Software Inc., La Jolla, CA)

## 2.5 References

1. Pfeffer SR. Entry at the trans-face of the Golgi. *Cold Spring Harb Perspect Biol.* 2011;3(3).
2. Bonifacino JS, Rojas R. Retrograde transport from endosomes to the trans-Golgi network. *Nat Rev Mol Cell Biol.* 2006;7(8):568-579.
3. Frankel AD, Young JA. HIV-1: fifteen proteins and an RNA. *Annu Rev Biochem.* 1998;67:1-25.
4. Swanson CM, Malim MH. SnapShot: HIV-1 proteins. *Cell.* 2008;133(4):742, 742 e741.
5. Kestler HW, 3rd, Ringler DJ, Mori K, Panicali DL, Sehgal PK, Daniel MD, et al. Importance of the nef gene for maintenance of high virus loads and for development of AIDS. *Cell.* 1991;65(4):651-662.
6. Fackler OT, Baur AS. Live and let die: Nef functions beyond HIV replication. *Immunity.* 2002;16(4):493-497.
7. Blagoveshchenskaya AD, Thomas L, Feliciangeli SF, Hung CH, Thomas G. HIV-1 Nef downregulates MHC-I by a PACS-1- and PI3K-regulated ARF6 endocytic pathway. *Cell.* 2002;111(6):853-866.
8. Collins KL, Chen BK, Kalams SA, Walker BD, Baltimore D. HIV-1 Nef protein protects infected primary cells against killing by cytotoxic T lymphocytes. *Nature.* 1998;391(6665):397-401.
9. Dikeakos JD, Thomas L, Kwon G, Elferich J, Shinde U, Thomas G. An interdomain binding site on HIV-1 Nef interacts with PACS-1 and PACS-2 on endosomes to down-regulate MHC-I. *Molecular biology of the cell.* 2012;23(11):2184-2197.
10. Hung CH, Thomas L, Ruby CE, Atkins KM, Morris NP, Knight ZA, et al. HIV-1 Nef assembles a Src family kinase-ZAP-70/Syk-PI3K cascade to downregulate cell-surface MHC-I. *Cell Host Microbe.* 2007;1(2):121-133.
11. Renkema GH, Saksela K. Interactions of HIV-1 NEF with cellular signal transducing proteins. *Front Biosci.* 2000;5:D268-283.
12. Pawlak EN, Dikeakos JD. HIV-1 Nef: a master manipulator of the membrane trafficking machinery mediating immune evasion. *Biochimica et biophysica acta.* 2015;1850(4):733-741.
13. Dikeakos JD, Atkins KM, Thomas L, Emert-Sedlak L, Byeon IJ, Jung J, et al. Small molecule inhibition of HIV-1-induced MHC-I down-regulation identifies a

temporally regulated switch in Nef action. *Molecular biology of the cell*. 2010;21(19):3279-3292.

14. Jia X, Singh R, Homann S, Yang H, Guatelli J, Xiong Y. Structural basis of evasion of cellular adaptive immunity by HIV-1 Nef. *Nat Struct Mol Biol*. 2012;19(7):701-706.
15. Kerppola TK. Bimolecular fluorescence complementation (BiFC) analysis as a probe of protein interactions in living cells. *Annu Rev Biophys*. 2008;37:465-487.
16. Kerppola TK. Visualization of molecular interactions by fluorescence complementation. *Nat Rev Mol Cell Biol*. 2006;7(6):449-456.
17. Kerppola TK. Design and implementation of bimolecular fluorescence complementation (BiFC) assays for the visualization of protein interactions in living cells. *Nat Protoc*. 2006;1(3):1278-1286.
18. Kay MA, Glorioso JC, Naldini L. Viral vectors for gene therapy: the art of turning infectious agents into vehicles of therapeutics. *Nat Med*. 2001;7(1):33-40.
19. Adachi A, Gendelman HE, Koenig S, Folks T, Willey R, Rabson A, et al. Production of acquired immunodeficiency syndrome-associated retrovirus in human and nonhuman cells transfected with an infectious molecular clone. *J Virol*. 1986;59(2):284-291.
20. Husain M, Gusella GL, Klotman ME, Gelman IH, Ross MD, Schwartz EJ, et al. HIV-1 Nef induces proliferation and anchorage-independent growth in podocytes. *J Am Soc Nephrol*. 2002;13(7):1806-1815.
21. Ryan MD, King AM, Thomas GP. Cleavage of foot-and-mouth disease virus polyprotein is mediated by residues located within a 19 amino acid sequence. *J Gen Virol*. 1991;72 ( Pt 11):2727-2732.
22. Donnelly ML, Luke G, Mehrotra A, Li X, Hughes LE, Gani D, et al. Analysis of the aphthovirus 2A/2B polyprotein 'cleavage' mechanism indicates not a proteolytic reaction, but a novel translational effect: a putative ribosomal 'skip'. *J Gen Virol*. 2001;82(Pt 5):1013-1025.
23. Szymczak AL, Vignali DA. Development of 2A peptide-based strategies in the design of multicistronic vectors. *Expert Opin Biol Ther*. 2005;5(5):627-638.
24. Benson RE, Sanfridson A, Ottinger JS, Doyle C, Cullen BR. Downregulation of cell-surface CD4 expression by simian immunodeficiency virus Nef prevents viral super infection. *J Exp Med*. 1993;177(6):1561-1566.
25. Cai CY, Zhang X, Sinko PJ, Burakoff SJ, Jin YJ. Two sorting motifs, a ubiquitination motif and a tyrosine motif, are involved in HIV-1 and simian immunodeficiency virus Nef-mediated receptor endocytosis. *J Immunol*. 2011;186(10):5807-5814.
26. Chaudhry A, Verghese DA, Das SR, Jameel S, George A, Bal V, et al. HIV-1 Nef promotes endocytosis of cell surface MHC class II molecules via a constitutive pathway. *J Immunol*. 2009;183(4):2415-2424.
27. Leonard JA, Filzen T, Carter CC, Schaefer M, Collins KL. HIV-1 Nef disrupts intracellular trafficking of major histocompatibility complex class I, CD4, CD8, and CD28 by distinct pathways that share common elements. *J Virol*. 2011;85(14):6867-6881.
28. Saksela K, Cheng G, Baltimore D. Proline-rich (PxxP) motifs in HIV-1 Nef bind to SH3 domains of a subset of Src kinases and are required for the enhanced growth of



- Nef<sup>+</sup> viruses but not for down-regulation of CD4. *EMBO J.* 1995;14(3):484-491.
29. Wolf D, Witte V, Laffert B, Blume K, Stromer E, Trapp S, et al. HIV-1 Nef associated PAK and PI3-kinases stimulate Akt-independent Bad-phosphorylation to induce anti-apoptotic signals. *Nat Med.* 2001;7(11):1217-1224.
  30. Mukerji J, Olivieri KC, Misra V, Agopian KA, Gabuzda D. Proteomic analysis of HIV-1 Nef cellular binding partners reveals a role for exocyst complex proteins in mediating enhancement of intercellular nanotube formation. *Retrovirology.* 2012;9:33.
  31. Banning C, Votteler J, Hoffmann D, Koppensteiner H, Warmer M, Reimer R, et al. A flow cytometry-based FRET assay to identify and analyse protein-protein interactions in living cells. *PLoS One.* 2010;5(2):e9344.
  32. Carlotti F, Bazuine M, Kekarainen T, Seppen J, Pognonec P, Maassen JA, et al. Lentiviral vectors efficiently transduce quiescent mature 3T3-L1 adipocytes. *Mol Ther.* 2004;9(2):209-217.
  33. Donnelly ML, Hughes LE, Luke G, Mendoza H, ten Dam E, Gani D, et al. The 'cleavage' activities of foot-and-mouth disease virus 2A site-directed mutants and naturally occurring '2A-like' sequences. *J Gen Virol.* 2001;82(Pt 5):1027-1041.
  34. Szymczak AL, Workman CJ, Wang Y, Vignali KM, Dilioglou S, Vanin EF, et al. Correction of multi-gene deficiency in vivo using a single 'self-cleaving' 2A peptide-based retroviral vector. *Nat Biotechnol.* 2004;22(5):589-594.
  35. Roeth JF, Collins KL. Human immunodeficiency virus type 1 Nef: adapting to intracellular trafficking pathways. *Microbiol Mol Biol Rev.* 2006;70(2):548-563.
  36. Youker RT, Shinde U, Day R, Thomas G. At the crossroads of homeostasis and disease: roles of the PACS proteins in membrane traffic and apoptosis. *Biochem J.* 2009;421(1):1-15.
  37. Haberg K, Lundmark R, Carlsson SR. SNX18 is an SNX9 paralog that acts as a membrane tubulator in AP-1-positive endosomal trafficking. *Journal of cell science.* 2008;121(Pt 9):1495-1505.
  38. Hanna Z, Kay DG, Rebai N, Guimond A, Jothy S, Jolicoeur P. Nef harbors a major determinant of pathogenicity for an AIDS-like disease induced by HIV-1 in transgenic mice. *Cell.* 1998;95(2):163-175.
  39. Kafri T. Gene delivery by lentivirus vectors an overview. *Methods Mol Biol.* 2004;246:367-390.
  40. Cockrell AS, Kafri T. Gene delivery by lentivirus vectors. *Mol Biotechnol.* 2007;36(3):184-204.
  41. Martinez-Salas E. Internal ribosome entry site biology and its use in expression vectors. *Curr Opin Biotechnol.* 1999;10(5):458-464.
  42. Borman AM, Le Mercier P, Girard M, Kean KM. Comparison of picornaviral IRES-driven internal initiation of translation in cultured cells of different origins. *Nucleic Acids Res.* 1997;25(5):925-932.
  43. Roberts LO, Seamons RA, Belsham GJ. Recognition of picornavirus internal ribosome entry sites within cells; influence of cellular and viral proteins. *RNA.* 1998;4(5):520-529.
  44. Mizuguchi H, Xu Z, Ishii-Watabe A, Uchida E, Hayakawa T. IRES-dependent second gene expression is significantly lower than cap-dependent first gene expression in a bicistronic vector. *Mol Ther.* 2000;1(4):376-382.
  45. Hennecke M, Kwissa M, Metzger K, Oumard A, Kroger A, Schirmbeck R, et al.

Composition and arrangement of genes define the strength of IRES-driven translation in bicistronic mRNAs. *Nucleic Acids Res.* 2001;29(16):3327-3334.

46. Kim JH, Lee SR, Li LH, Park HJ, Park JH, Lee KY, et al. High cleavage efficiency of a 2A peptide derived from porcine teschovirus-1 in human cell lines, zebrafish and mice. *PLoS One.* 2011;6(4):e18556.
47. Ryan MD, Drew J. Foot-and-mouth disease virus 2A oligopeptide mediated cleavage of an artificial polyprotein. *EMBO J.* 1994;13(4):928-933.
48. Poe JA, Smithgall TE. HIV-1 Nef dimerization is required for Nef-mediated receptor downregulation and viral replication. *J Mol Biol.* 2009;394(2):329-342.
49. Poe JA, Vollmer L, Vogt A, Smithgall TE. Development and validation of a high-content bimolecular fluorescence complementation assay for small-molecule inhibitors of HIV-1 Nef dimerization. *J Biomol Screen.* 2014;19(4):556-565.
50. Ye H, Choi HJ, Poe J, Smithgall TE. Oligomerization is required for HIV-1 Nef-induced activation of the Src family protein-tyrosine kinase, Hck. *Biochemistry.* 2004;43(50):15775-15784.
51. Schaefer MR, Wonderlich ER, Roeth JF, Leonard JA, Collins KL. HIV-1 Nef targets MHC-I and CD4 for degradation via a final common beta-COP-dependent pathway in T cells. *PLoS Pathog.* 2008;4(8):e1000131.
52. Roeth JF, Williams M, Kasper MR, Filzen TM, Collins KL. HIV-1 Nef disrupts MHC-I trafficking by recruiting AP-1 to the MHC-I cytoplasmic tail. *J Cell Biol.* 2004;167(5):903-913.
53. Emert-Sedlak L, Kodama T, Lerner EC, Dai W, Foster C, Day BW, et al. Chemical library screens targeting an HIV-1 accessory factor/host cell kinase complex identify novel antiretroviral compounds. *ACS Chem Biol.* 2009;4(11):939-947.
54. Manjunath N, Wu H, Subramanya S, Shankar P. Lentiviral delivery of short hairpin RNAs. *Adv Drug Deliv Rev.* 2009;61(9):732-745.
55. Singer O, Verma IM. Applications of lentiviral vectors for shRNA delivery and transgenesis. *Curr Gene Ther.* 2008;8(6):483-488.
56. Bryksin AV, Matsumura I. Overlap extension PCR cloning: a simple and reliable way to create recombinant plasmids. *Biotechniques.* 2010;48(6):463-465.
57. Nam HS, Benezra R. High levels of Id1 expression define B1 type adult neural stem cells. *Cell Stem Cell.* 2009;5(5):515-526.
58. Cordelieres FP, Bolte S. Experimenters' guide to colocalization studies: finding a way through indicators and quantifiers, in practice. *Methods Cell Biol.* 2014;123:395-408.

## Chapter 3

### 3 HIV-1 Nef sequesters MHC-I intracellularly by targeting early stages of endocytosis and recycling

#### 3.1 Introduction

The human immunodeficiency virus type 1 (HIV-1) encodes a class of proteins that lack any known enzymatic activity. These proteins, termed “accessory proteins”, include Nef, Vpr, Vpu and Vif. Accessory proteins can promote viral fitness by allowing infected cells to evade the host immune response (1). The ability of Nef to promote HIV-1 immune evasion has been ascribed to its extensive interaction network with host proteins (2-4). Indeed, Nef interacts with multiple proteins implicated in membrane trafficking in order to downregulate cell surface levels of major histocompatibility complex class I (MHC-I), resulting in a decreased ability of infected CD4<sup>+</sup> T-cells to be detected and killed by CD8<sup>+</sup> cytotoxic T lymphocytes (CTLs)(5). This rerouting of MHC-I away from the cell surface is an example of a viral protein usurping host cell functions to ensure viral replication.

Currently, two models explain how Nef orchestrates the re-localization of MHC-I away from the cell surface (reviewed in (6)). The first model, termed the signaling model of downregulation, is activated early during infection and involves the targeting of Nef to the trans-Golgi network (TGN) by the host membrane trafficking regulator protein phosphofurin acidic cluster sorting protein 2 (PACS-2)(2, 7). Once at the TGN, Nef binds and activates specific Src-family kinases (SFKs), which subsequently trigger the phosphoinositide 3-kinase (PI3K)-dependent endocytosis of cell surface MHC-I (3). Internalized MHC-I is then sequestered in an intracellular compartment by a process involving the cytoplasmic tail of MHC-I (8) and the membrane trafficking regulator phosphofurin acidic cluster sorting protein 1 (PACS-1), which has previously been identified to interact with the membrane adaptor protein-1 (AP-1)(2, 3, 9). Interestingly, Nef, AP-1 and MHC-I have been described to form a ternary complex which depends on the cytoplasmic tail of MHC-I (10). Structural information obtained by Jia *et al.* revealed that residues Y<sub>320</sub> and D<sub>327</sub> in the cytoplasmic tail of MHC-I bridge key interactions with

Nef and AP-1, supporting Nef-dependent downregulation of MHC-I (10). The role of PACS-1, in Nef-mediated MHC-I downregulation has remained understudied. Indeed, knockdown of PACS-1, or inhibition of a PACS-1:AP-1 interaction hinders MHC-I downregulation. PACS-1 plays important roles in receptor trafficking in the uninfected cell. Classically, PACS-1 recognizes the presence of an acidic cluster motif in the cytoplasmic tail of cargo molecules and is able to connect the itinerant cargo to AP-1. The PACS-1:AP-1 interaction is required for proper regulation of the cellular protease furin in the Golgi, as well as the correct localization of the cation-independent mannose-6-phosphate receptor in late endosomes (11, 12). Thus, recognition of cargo molecules by AP-1 is tightly regulated by PACS-1; however, the role of PACS-1 in the recruitment of AP-1 to the MHC-I cytoplasmic tale has yet to be defined.

The second model of Nef-dependent MHC-I downregulation, termed the stoichiometric mode, occurs at later stages of infection (7). In this model, Nef interacts with the cytoplasmic tail of MHC-I and traffics the receptor to a degradative compartment in a process that also involves the membrane trafficking regulators AP-1 in addition to coat protein 1 (COPI) (13). The signaling and stoichiometric models are not mutually exclusive and appear to be temporally linked (7). Moreover, the signaling model may be more prominent in T-cells, as they have a relatively short half-life, whereas, the stoichiometric model may be more relevant in longer lived monocytes (7).

Despite having identified multiple membrane trafficking regulator proteins implicated in the removal of MHC-I from the cell surface, it remains unknown what cellular compartments Nef uses during this process precluding our understanding of the pathway subverted by HIV-1 to evade immune surveillance. In addition, prior analysis of pathways implicated in Nef-dependent MHC-I downregulation have primarily relied on the co-localization of Nef or MHC-I with markers of the membrane trafficking apparatus without analyzing Nef and MHC-I in complex, which is essential for Nef's ability to downregulate MHC-I (14, 15). Importantly, the various compartments implicated in the trafficking of receptors such as MHC-I play distinct functional roles within the endosomal trafficking system (2). Vesicles, such as early and late endosomes, are often implicated in the movement of cargo from the plasma membrane to distinct subcellular

locations (16, 17). Moreover, late endosomes can also facilitate trafficking of cargo to degradative lysosomal compartments (18). In parallel, recycling endosomes will continuously deplete proteins from the cell surface and return them to this location (19). Fortunately the identity of the various intracellular compartments that comprise the endosomal trafficking system can be distinguished by specific effector molecules that coat the cytosolic face of these vesicles (20).

We have previously localized interactions at the subcellular level between Nef and membrane trafficking regulators PACS-1 and PACS-2 using bimolecular fluorescence complementation (BiFC) (2). This technique is used to study protein-protein interactions within cells and involves the reconstitution of a visible fluorophore from split fluorescent molecules expressed as fusion proteins on two distinct putative protein binding partners (21-23). BiFC has enabled us and others to identify locations inside the cell where Nef can interact with itself or cytosolic binding partners, such as the trafficking regulator sorting nexin 18 (SNX18) (23-25).

In the current report, we sought to determine the trafficking route undertaken by MHC-I in complex with Nef, and determine the role of PACS-1 in the subversion of MHC-I, in order to determine the fate of MHC-I in Nef-expressing cells. Using BiFC, we demonstrate that the Nef:MHC-I interaction is dependent on key residues in the cytoplasmic tail of MHC-I and we localize the Nef:MHC-I interaction within cells. Specifically, we show that Nef interacts with MHC-I in both early and late endosomes, and at the TGN, but that the Nef:MHC-I interaction is not detectable in lysosomes. Interestingly, we show that Nef depletes the amount of MHC-I in Rab11-positive recycling endosomes, and that a functional early endosomal compartment is required for Nef-dependent MHC-I downregulation. This Nef-mediated rerouting eventually sequesters MHC-I at the TGN, which is dependent on presence of PACS-1 and AP-1. Taken together, these results, demonstrate for the first time, the specific endocytic compartments utilized by Nef to orchestrate MHC-I downregulation and support a model that results in the sequestration of MHC-I by Nef in a non-degradative compartment.

## 3.2 Results

### 3.2.1 Bimolecular fluorescence complementation microscopy detects a Nef:MHC-I complex in cells

The immunoevasive capabilities of HIV-1 are largely mediated by the ability of Nef to remove MHC-I from the cell surface (26). The crystal structure of a Nef:MHC-I complex revealed that this interaction is stabilized by AP-1, demonstrating that Nef, MHC-I and AP-1 are able to form a ternary complex (26). To validate the Nef:MHC-I interaction in cells, we performed a bimolecular fluorescence complementation (BiFC) assay. BiFC entails the expression of a split Venus fluorophore from two distinct plasmids in the form of fusion proteins, and results in a reconstituted, functional Venus fluorophore when the two fusion proteins are within 100 nm (22). Co-transfection of HeLa cells with plasmids encoding Nef- $V_C$  and MHC-I- $V_N$ -Flag, more specifically Nef and MHC-I fused to carboxy ( $V_C$ ) or amino ( $V_N$ ) fragments of Venus, respectively, revealed that Nef and MHC-I form a complex (Fig. 3.1A). In order to test for the requirement of AP-1 in the formation of the Nef:MHC-I complex in cells, we tested Nef:MHC-I BiFC with MHC-I encoding mutations in residues previously implicated in interacting with AP-1 when MHC-I is in complex with Nef (MHC-I  $Y_{320}$  or  $D_{327}$ ). Co-transfection of plasmids encoding MHC-I  $Y_{320}A$ - $V_N$  or MHC-I  $D_{327}N$ - $V_N$  and Nef- $V_C$  into HeLa cells revealed a decrease in the BiFC signal relative to wild type MHC-I (Fig. 3.1A), as measured by Venus mean fluorescence intensity in cells expressing both Nef and Flag tagged MHC-I (Fig. 3.1B). Similarly, co-expression of Nef- $V_C$  and a MHC-I double mutant (MHC-I  $Y_{320}A/D_{327}N$ ) resulted in a 2-fold reduction in BiFC signal (Fig. 3.1A and 3.1B), indicating that interactions between MHC-I and AP-1 are critical to observe a Nef:MHC-I BiFC signal, supporting the formation of a Nef:MHC-I:AP-1 ternary complex in cells. Importantly, the reductions in BiFC signal with the various MHC-I mutants were not due to differences in protein expression, as revealed by Western blot analysis (Fig. 3.1C). Furthermore, we demonstrate that the fusion of  $V_N$  or  $V_C$  to MHC-I or Nef respectively, did not alter protein function with respect to downregulation, as we previously demonstrated (24). Specifically, wildtype MHC-I- $V_N$  is downregulated by Nef (Fig. 3.2), unlike the double mutant ( $Y_{320}A/D_{327}N$ ) (Fig. 3.2). Similarly, Nef- $V_C$  is able to efficiently downregulate cell surface MHC-I (Fig. 3.2).

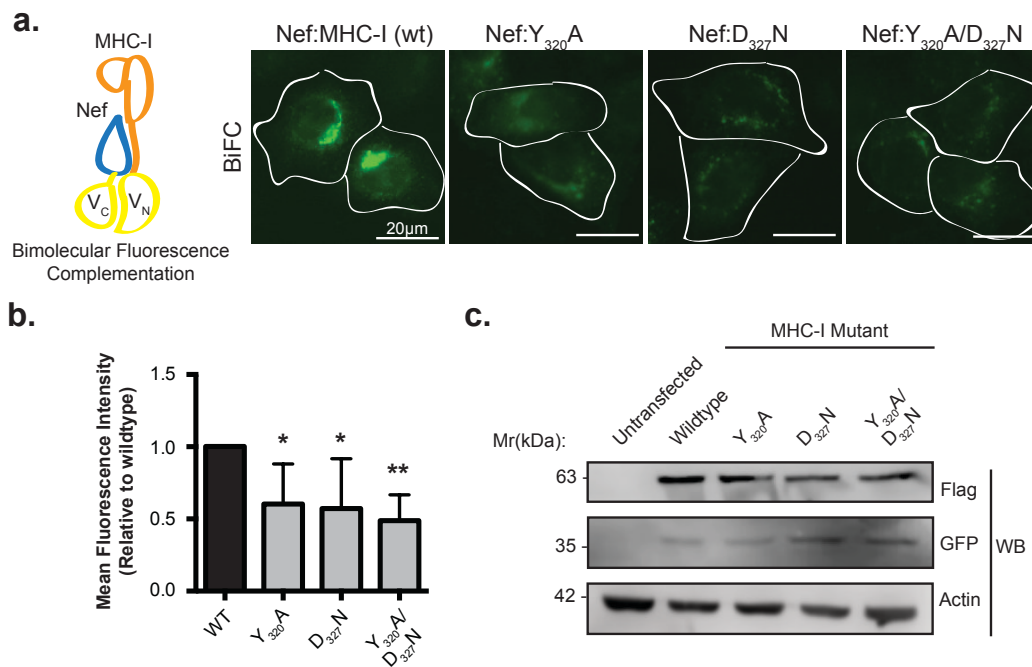


**Figure 3.1 Bimolecular fluorescence complementation is observed between Nef and MHC-I.**

(A) Left: Schematic representation of the BiFC reporter system. Right: Nef-V<sub>C</sub> and either wildtype MHC-I-V<sub>N</sub>-Flag or the indicated mutants were transfected into HeLa cells, 24 hrs later cells were fixed, and BiFC fluorescence (green) was observed under the FITC channel. Scale bars represent 20µm. (B) Fluorescence intensities of Nef and MHC-I-V<sub>N</sub>-Flag positive cells were quantified in ImageJ, minus the background signal, to observe a decrease in fluorescence in the presence of the MHC-I mutations (n = 100, \* indicates p-value < 0.05, \*\* indicates p-value < .01). (C) Flag and GFP specific Western blots were conducted to ensure equal expression of both the MHC-I-V<sub>N</sub>-Flag mutants and Nef-V<sub>C</sub>, respectively. An actin specific Western blot was conducted as a loading control.

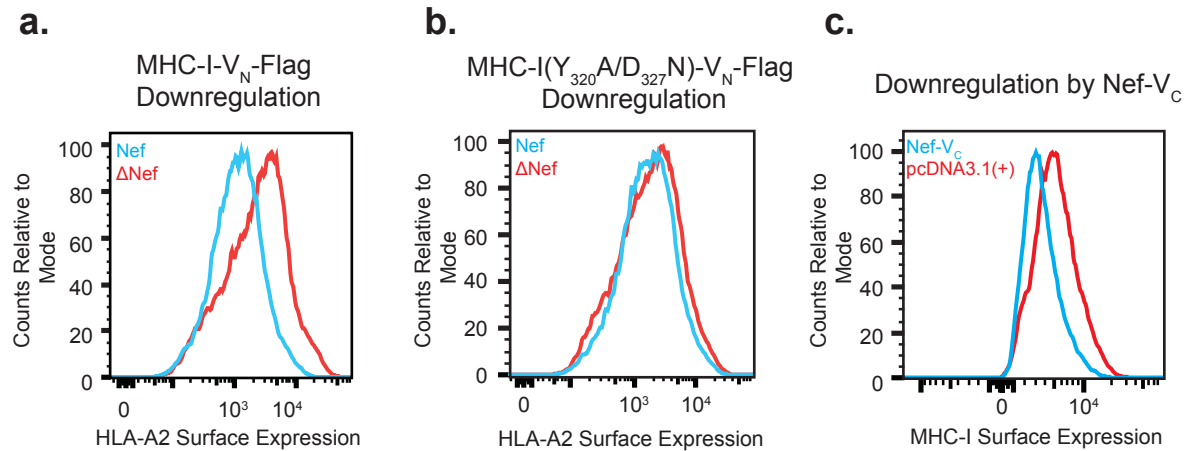


**Figure 3.2: Functionality of MHC-I and Nef fusion proteins.**

(A and B) MHC-I- $V_N$ -Flag or MHC-I- $Y_{320}A/D_{327}N$ - $V_N$ -Flag and Nef-eGFP (blue line) or eGFP (red line) were co-transfected in HeLa cells and surface stained with BB7.2 (HLA-A2 specific antibody) and surface levels of MHC-I were quantified by flow cytometry upon gating on eGFP positive cells. (C) Nef- $V_C$  or empty backbone (pcDNA3.1) and eGFP were co-transfected and surface stained with W6/32 MHC-I antibody and surface levels of MHC-I were quantified by flow cytometry after upon on GFP positive cells. Histograms are representative of 3 independent experiments.



### 3.2.2 Nef targets recycling MHC-I prior to transit through a Rab11 compartment

An obligate step in cellular homeostasis involves the rapid recycling of MHC-I to and from the cell surface in Rab11-positive recycling endosomes (27). We first tested if Nef disrupts this rapid recycling step. To test this, we co-transfected HeLa cells with plasmids encoding MHC-I-eGFP and Rab11a-dsRed (Fig. 3.3A; panel 2), which labels recycling endosomes (28). We then compared this to cells expressing Nef:MHC-I BiFC and Rab11-dsRed, in order to focus specifically on the MHC-I molecules that are targeted by Nef (Fig. 3.3A: panel 1). Pearson's correlation analysis revealed that there was ~1.6 fold less co-localization between Rab11-dsRed and Nef:MHC-I BiFC than between Rab11-dsRed and MHC-I-eGFP, suggesting that Nef targets MHC-I prior to MHC-I entering a Rab11 dependent recycling route. Furthermore, an antibody uptake experiment confirmed that the majority of MHC-I that is being targeted by Nef originates from the cell surface (Fig. 3.3C), as the Nef-MHC-I BiFC signal originating from Nef-V<sub>C</sub> and MHC-I-V<sub>N</sub>-Flag strongly co-localized with the BB7.2 antibody (Fig. 3.3D).

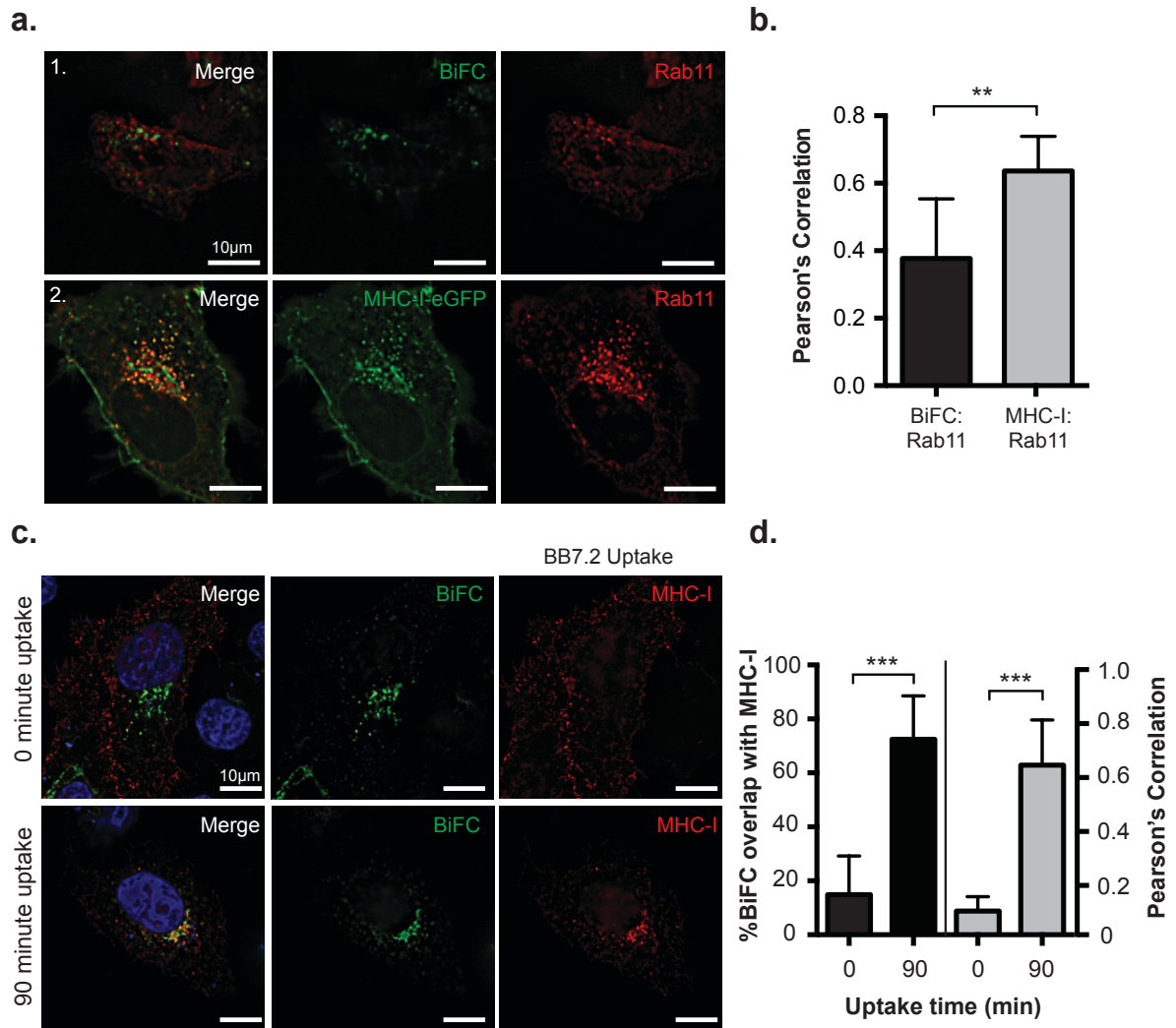


**Figure 3.3: Nef prevents MHC-I from entering into a Rab11 dependent recycling route.**

(A) Nef- $V_C$  and MHC-I- $V_N$ -Flag (panel 1) MHC-I-eGFP (panel 2) and dsRed-Rab11 were co-transfected into HeLa cells. 24hrs post transfection, cells were fixed and mounted onto coverslips. GFP and BiFC fluorescence was observed under the FITC channel, and dsRed-Rab11a was observed under the Cy3 channel. (B) Co-localization was quantified by using the Pearson's correlation through the JaCoP Plug-in on ImageJ. (C) MHC-I (BB7.2) uptake experiments were performed as described in the materials and methods. BiFC signal is visualized in green, and MHC-I uptake was pseudocolored in red, nuclei were counterstained in blue. (D) Percent of co-localization (left axis and black

bars), and Pearson's correlation (right axis and grey bars) were determined using the Mander's and Pearson's correlation respectively through the JaCoP Plug-in on ImageJ. Error bars were calculated by quantification of at least 50 cells between 3 independent experiments. (\*\* Indicates p-value < 0.01, \*\*\* indicates p-value < 0.001).

### 3.2.3 Nef interacts with MHC-I within an early endosomal compartment

Since Nef reroutes cell surface MHC-I away from recycling endosomes (Fig. 3.3A and B), we next tested if a Nef:MHC-I complex would be located in early endosomes. Early endosomes constitute the initial compartment implicated in the endocytosis and sorting of cell surface cargo (17, 29). We co-transfected HeLa cells with plasmids encoding Nef- $V_C$ , MHC-I- $V_N$ -Flag and the early endosomal effector molecule mCherry-Rab5. Fluorescence microscopy analysis revealed that the Nef:MHC-I interaction co-localized with mCherry-Rab5, suggesting that the complex is present in early endosomes (Fig. 3.4A; Pearson's = 0.612). Furthermore, in order to confirm that the Nef:MHC-I complex localizes to early endosomes, we co-expressed a constitutively active mCherry-tagged Rab5 molecule (mCherry-Rab5-CA; mCherry-Rab5 Q67L) with Nef- $V_C$  and MHC-I- $V_N$ -Flag. Expression of Rab5-CA has previously been associated with a build-up of cargo molecules in early endosomes resulting in their subsequent enlargement (30). Rab5-CA expression modified the co-localization of the Nef:MHC-I BiFC signal, wherein the BiFC signal was more prominent within Rab5 positive early endosomes (Pearson's = 0.89), confirming that these vesicles are indeed a transiting point for Nef:MHC-I complexes (Fig. 3.4A and B). Furthermore, expression of Rab5-CA reduced Nef's ability to downregulate MHC-I, demonstrating that a functional early endosomal compartment through which Nef-MHC-I complexes can transit is required for optimal downregulation of MHC-I from the cell surface (Fig. 3.5).

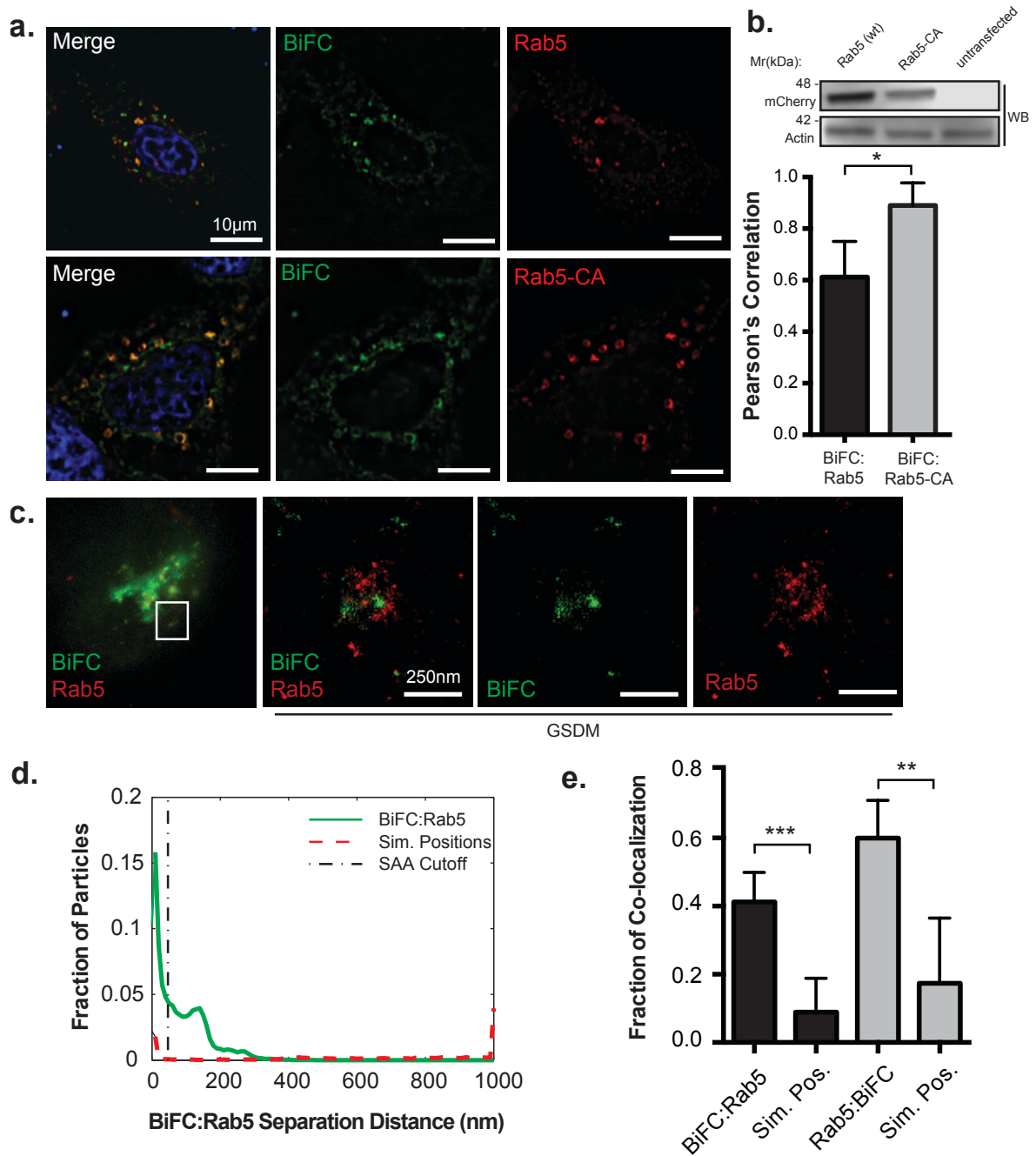


**Figure 3.4: Nef:MHC-I interaction occurs within Rab5-positive early endosomes.**

(A) HeLa cells were co-transfected with plasmids encoding Nef- $V_C$ , MHC-I- $V_N$ -Flag and the indicated mCherry-tagged Rab5 constructs (wildtype and constitutively active (CA)). Twenty-four hours post transfection cells were fixed and mounted with DAPI Fluoromount-G. BiFC fluorescence (green) was detected under the FITC channel, while the mCherry-tagged Rab5 constructs were visualized under the Cy3 filter settings. Nuclei were visualized under the DAPI

channel (scale bars represent 10 $\mu$ m). (B) Co-localization of Nef:MHC-I BiFC with the mCherry tagged Rab5 constructs was quantified by the Pearson's correlation through the JaCoP Plug-in on ImageJ. Error bars were calculated by quantification of at least 25 cells between 3 independent experiments (\* Indicates p-value < 0.05). Western blot analysis for mCherry to confirm expression levels of Rab5 and Rab5-CA, with actin as a loading control. (C) Cells were transfected with Nef-V<sub>C</sub> and MHC-I-V<sub>N</sub>-Flag and immunostained for Rab5 and subsequently imaged utilizing ground state depletion microscopy (GSDM). (D) A histogram plotting the intermolecular distances between the nearest neighbor, representing either BiFC:Rab5 (Solid line) or BiFC:Simulated random positions (Sim. Positions; Dashed line). (E) A graphical representation of the fraction of co-localized particles observed in (D) which were observed to be under the cut-off value of ~40nm. Error bars were calculated by quantification of 10 cells in 3 independent experiments (\*\* indicates p-value < .01, \*\*\* indicates p-value <.001).

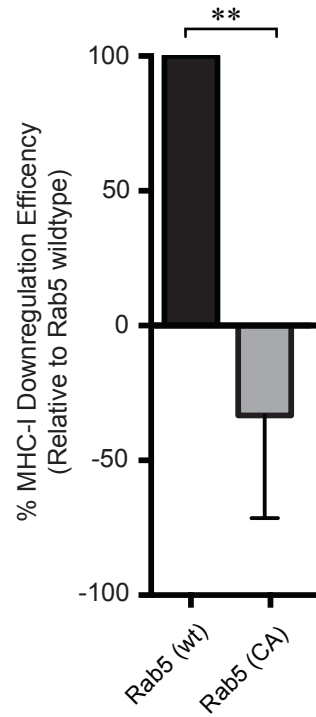


**Figure 3.5: Disruption of early endosomal regulation interferes with Nef-mediated MHC-I downregulation.**

HeLa cells were co-transfected with mCherry-tagged Rab5-constitutively active (CA) or Rab5 and Nef-eGFP or empty eGFP encoding backbone. Twenty-four hours post transfection, cell surface levels of MHC-I were measured by flow cytometry by gating on GFP and mCherry positive cells. Downregulation efficiency was calculated relative to Rab5 (wt) using the following formula:  $\text{Relative MFI} = \left( \frac{[1 - \text{Rab5}_{\text{mut}}\text{Nef}/\text{Rab5}_{\text{mut}}\Delta\text{Nef}]}{[1 - (\text{Rab5}_{\text{wt}}\text{Nef}/\text{Rab5}_{\text{wt}}\Delta\text{Nef})]} \right) \times 100$ .

Current resolution limits of conventional widefield microscopy do not allow for the visualization of discrete vesicular structures. To determine whether the Nef:MHC-I complex is contained within Rab5 early endosomes, we imaged the Rab5-dependent sorting step using the super-resolution microscopy technique of ground-state depletion microscopy (GSDM). This technique allows for visualization of cellular compartments with a resolution 10X greater than conventional microscopy (31). To visualize early endosomes by GSDM, HeLa cells were transfected with the BiFC plasmids (Nef-V<sub>C</sub> and MHC-I-V<sub>N</sub>-Flag), and immunostained for Rab5. The 10.25 fold gain in resolution provided by GSDM allowed for the detection of single Nef:MHC-I positive vesicles coated with the early endosomal effector Rab5 (Fig. 3.4C). Quantification of the association between Nef:MHC-I and Rab5 using the spatial association algorithm (SAA), which calculates the distance between punctate structures of different acquisition channels to determine if they are co-localizing together (32). The SAA analysis revealed that the association of the Nef:MHC-I BiFC complex with Rab5 is significantly greater than that of randomly simulated positions in either acquisition channel (Fig. 3.4D and E). Taken together, multiple imaging techniques have demonstrated the close association of the Nef:MHC-I complex with early endosomes suggesting that this organelle plays a key role in the immunoevasive capabilities of HIV-1.

### 3.2.4 Nef traffics MHC-I to a late endosomal compartment

Early endosomes mature to form late endosomes within the endocytic network (16). In order to test if the Nef:MHC-I complex is present in late endosomes we visualized the Nef:MHC-I BiFC signal in the presence of the late endosomal marker Rab7, an effector molecule specifically loaded onto late endosomes (33). HeLa cells expressing Nef-V<sub>C</sub> and MHC-I-V<sub>N</sub>-Flag were co-transfected with a plasmid encoding mCherry tagged wild type Rab7 (mCherry-Rab7). We observed that the Nef:MHC-I interaction occurs in late endosomes that are positive for mCherry-Rab7 (Fig. 3.6A). To further control for the Rab7 localization of Nef and MHC-I we utilized dominant-negative mCherry-tagged Rab7 (mCherry-Rab7-DN; Rab7 T22N). Previous expression of Rab7-DN has resulted in defects in trafficking of cargo transiting through late endosomes (34). When testing the co-localization of the Nef:MHC-I BiFC with overexpressed mCherry-Rab7-DN, we



observed no significant difference in colocalization between the wildtype and dominant-negative Rab7 (Fig. 3.6A and B). To confirm the late endosomal localization of the Nef:MHC-I complex, we utilized ground-state depletion super-resolution microscopy to gain the resolution needed to identify Rab7-positive vesicles containing the Nef:MHC-I complex (Fig. 3.6C). We observed that the Nef:MHC-I complex associated closely with Rab7. The SAA analysis revealed that the association of the Nef:MHC-I BiFC complex with Rab7 is significantly greater than that of randomly simulated positions in either acquisition channel (Fig. 3.6D and E). Taken together, these data demonstrate the localization of the Nef:MHC-I complex within Rab7 positive late endosomes, thereby implicating the late endosome in the re-routing of MHC-I away from the plasma membrane.

### 3.2.5 Nef and MHC-I are not trafficked to the lysosome, but traffic to the trans-Golgi network

Consistent with the maturation of certain late endosomes to lysosomes (29), we next tested if the Nef:MHC-I complex is present in lysosomes. HeLa cells overexpressing Nef-V<sub>C</sub> and MHC-I-V<sub>N</sub>-Flag were immunostained with an antibody recognizing LAMP-1, a marker of lysosomes (35) (Fig. 3.7A; panel 1). Immunofluorescence analysis revealed no significant co-localization of the Nef-MHC-I complex with lysosomes (Pearson's = 0.15), suggesting that the complex does not traffic through this compartment. As lysosomes are a prime site of proteolytic degradation (36, 37), we sought to control for any degradation of Nef:MHC-I complexes that may occur within lysosomes and thereby mask our ability to detect these complexes within this compartment prior to imaging. Accordingly, HeLa cells were treated with ammonium chloride (NH<sub>4</sub>Cl) at 20 hours post transfection for 4 hours, which will block lysosomal degradation by increasing the cellular pH and thereby inactivating protease activity within lysosomes (Fig. 3.7A; panel 2)(37). Despite increasing the cellular pH, we were unable to visualize the presence of the Nef:MHC-I complex within LAMP-1 positive lysosomes. In order to confirm that our NH<sub>4</sub>Cl treatment was sufficient to block lysosomal acidification we treated cells with LysoTracker, an agent retained in acidic compartments or we treated cells with complete media. Fluorescence intensity analysis

revealed that Lysotracker dye fluorescence intensity was decreased, and not retained within distinct vesicular structures in the presence of  $\text{NH}_4\text{Cl}$ , confirming that our  $\text{NH}_4\text{Cl}$  treatment sufficiently inhibits the acidification of lysosomes (Fig. 3.7C and D).

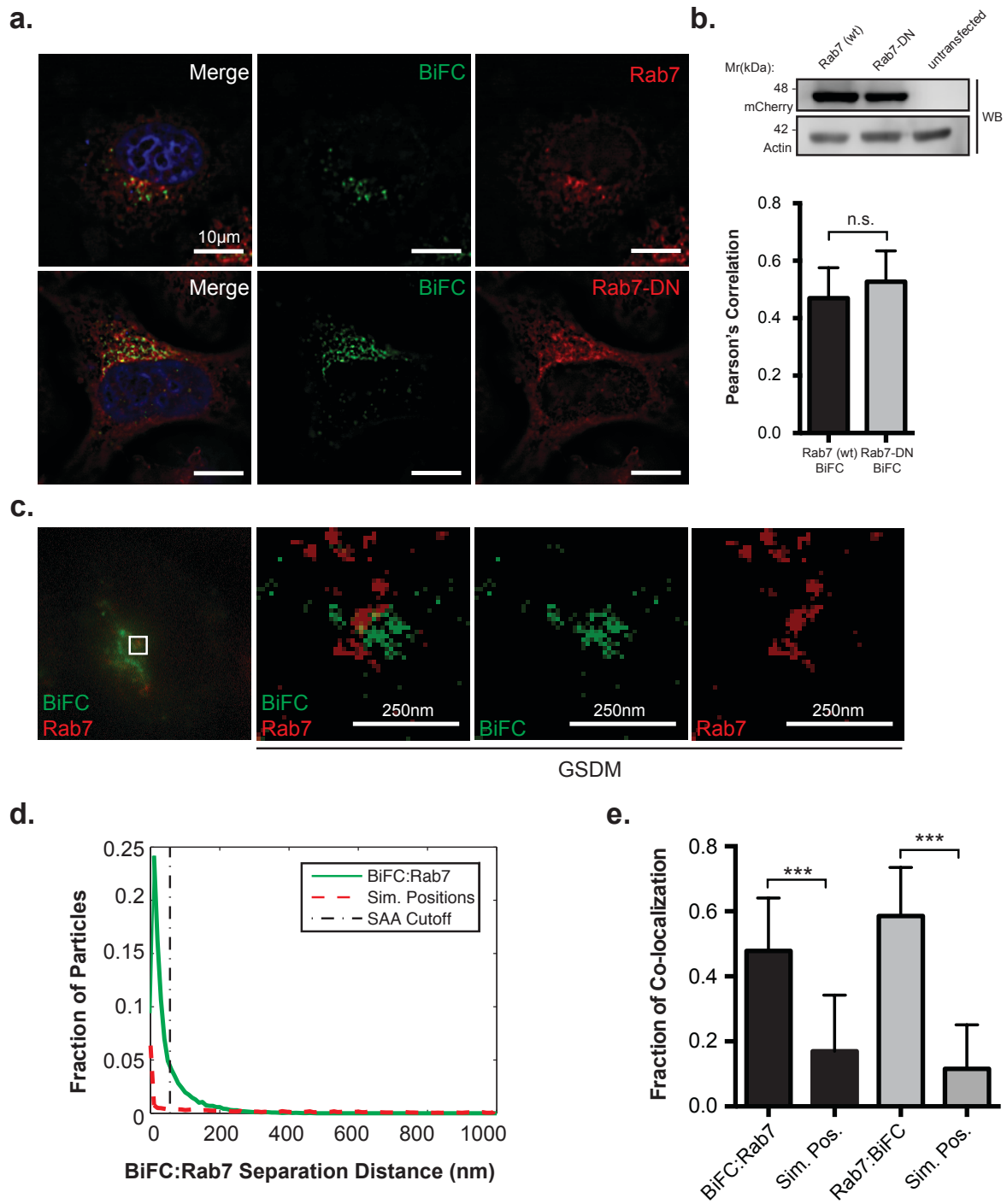


**Figure 3.6: Nef:MHC-I interaction occurs within Rab7-positive late endosomes.**

(A) HeLa cells were co-transfected with Nef- $V_C$  and MHC-I- $V_N$ -Flag encoding constructs along with constructs encoding wildtype mCherry-Rab7 or dominant negative

mCherry-Rab7 (mCherry-Rab7-DN). BiFC fluorescence (green) was visualized under the FITC channel, mCherry-Rab7 (red) was detected under the Cy3 channel. Nuclei were stained with DAPI (scale bars represent 10 $\mu$ m). (B) Co-localization was quantified by using the Pearson's correlation through the JaCoP Plug-in on ImageJ. Error bars were calculated by quantification of at least 40 cells between 3 independent experiments. Western blot analysis for mCherry to confirm expression levels of Rab7 and Rab7-DN, with actin as a loading control. (C) Cells were transfected with Nef-V<sub>C</sub> and MHC-I-V<sub>N</sub>-Flag and immunostained for Rab7 and subsequently imaged utilizing ground state depletion microscopy (GSDM). (D) A histogram plotting the intermolecular distances between the nearest neighbor, representing either BiFC:Rab7 (Solid line) or BiFC:Simulated random positions (Sim. Positions; Dashed line). (E) A graphical representation of the fraction of co-localized particles observed in (D) which were observed to be under the cut-off value of ~40nm. Error bars were calculated by quantification at least 10 cells in 3 independent experiments (\*\* indicates p-value < .01, \*\*\* indicates p-value <.001).

In order to test the functional consequence of the Nef:MHC-I complex trafficking through early and late endosomes, we designed a lentiviral vector that expressed Flag-tagged MHC-I simultaneously with HIV-1 viral proteins (Fig. 3.7E). This vector system, which we have previously described (24), utilizes the self-cleaving property of the 2A peptide (F2A) from the foot and mouth virus to express MHC-I that is not linked to HIV-1 Gag/Pol. The infection of SupT1 cells with pNL4-3 F2A-MHC-I-Flag Nef and subsequent Western blotting demonstrated that the presence of Nef does not alter the protein expression levels of MHC-I, confirming that Nef does not direct MHC-I to degradative lysosomal compartment, consistent with previous experiments (Fig. 3.7E)(7, 24). Conversely, infection of SupT1 cells with a virus that overexpresses the CD4 receptor, pNL4-3 F2A-CD4-Flag  $\Delta$ Vpu Nef demonstrated that Nef is capable of reducing total cellular CD4 (Fig. 3.7E), which is consistent with previous reports of Nef-mediated degradation of CD4 (38). Thus, the functional consequence of Nef on MHC-I and CD4 expression is different. In addition, to confirm that Nef expression was not sufficient to traffic MHC-I to lysosomes, we expressed MHC-I-eGFP and Nef-mCherry under non-BiFC conditions and found no significant localization of MHC-I-eGFP with the LAMP-1 lysosomal marker in the presence of Nef, with or without ammonium chloride treatment (Fig. 3.8).

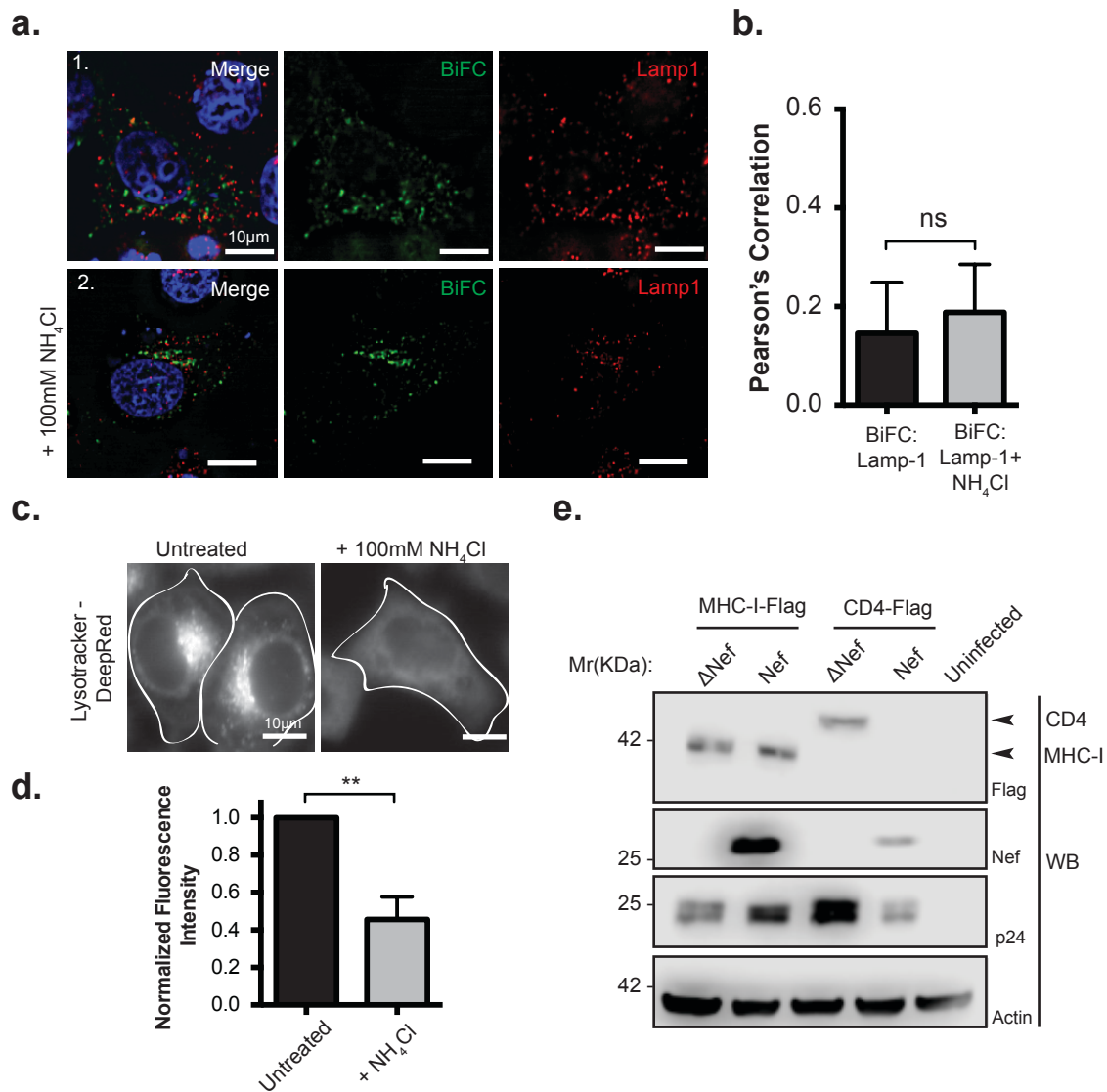
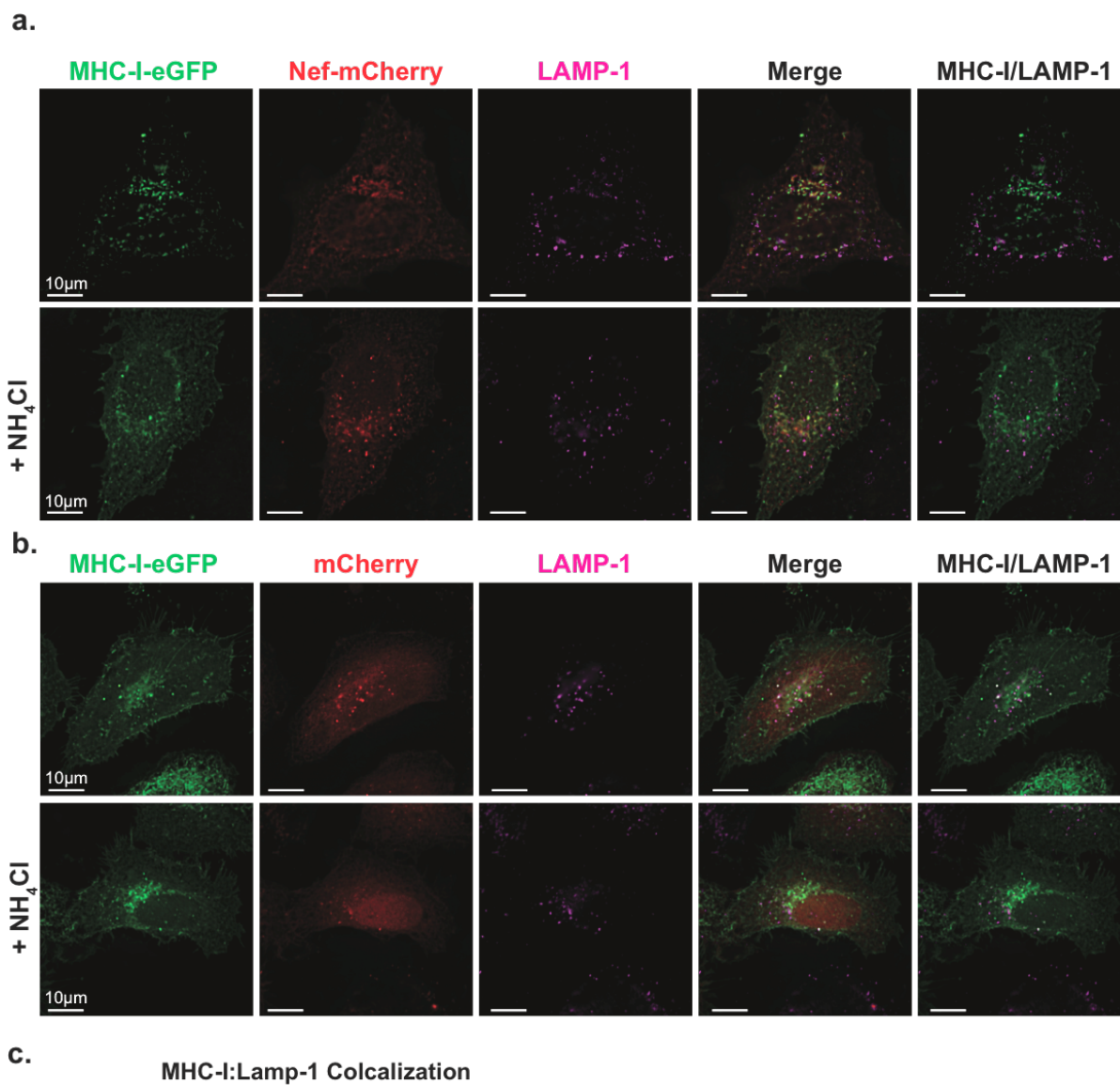


**Figure 3.7: Nef:MHC-I interaction does not occur in lysosomes.**

(A) HeLa cells were co-transfected with Nef-VC and MHC-I-VN-Flag constructs and immunostained for LAMP-1 (Panel 1), or, treated with 100mM ammonium chloride (NH<sub>4</sub>Cl) for 3 hours prior to fixation and staining (Panel 2). BiFC fluorescence (green) was visualized under the FITC channel, whereas LAMP-1 stain was visualized under the Cy5 filter settings, and pseudo-colored red. Nuclei were stained with DAPI, and scale bars represent 10µm. (B) Co-localization was quantified by the Pearson's Correlation through the JaCoP Plug-in on ImageJ. Error bars were calculated by quantification of at least 25 cells between 3 independent experiments. (C, D) HeLa cells were treated with

PBS, or 100mM of ammonium chloride for 3 hours, and then treated with 10 $\mu$ M LysoTracker Deep Red for 5 minutes. Live cells were then imaged at 37°C in 5% CO<sub>2</sub> and quantified for LysoTracker fluorescence. Error bars were calculated by quantification of at least 25 cells between 3 independent experiments. (\*\* Indicates p-value < 0.01). (E) Sup-T1 cells were infected with F2A MHC-I-Flag-Nef/ $\Delta$ Nef or F2A-CD4-Flag- $\Delta$ Vpu-Nef/ $\Delta$ Nef viruses. 48 hours post infection, cells were lysed and analyzed by Western blot. Anti-Flag detected total MHC-I-Flag and CD4-Flag, whereas anti-Nef antibody marked the presence or absence of Nef. Anti-p24 and anti-actin antibodies were used as infection and loading controls, respectively. A representative Western blot from 3 independent experiments is shown.



**c.** MHC-I:Lamp-1 Colocalization

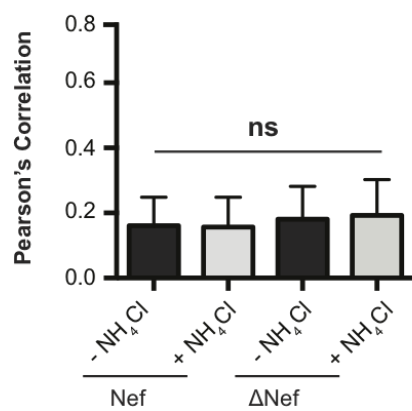




**Figure 3.8: Lysosomal localization of MHC-I-eGFP**

- (A) HeLa cells were transfected with MHC-I-eGFP (green) and Nef-mCherry (red). Twenty hours post transfection cells were treated with 100mM ammonium chloride for 4 hours. Following treatment, cells were fixed and immunostained for LAMP-1 (magenta).
- (B) HeLa cells were transfected with MHC-I-eGFP (green) and mCherry backbone (red). 20 hours post transfection, cells were treated with 100mM Ammonium chloride for 4 hours. Following treatment, cells were fixed and immunostained for LAMP-1 (magenta).
- (C) Co-localization of MHC-I and LAMP-1 were quantified by the Pearson's correlation through the JaCoP Plug-in on ImageJ. Error bars were calculated by quantification of at least 30 cells between 3 independent experiments, (ns: not significant).

Since the Nef-MHC-I complex did not traffic to lysosomes we sought to identify an alternative subcellular localization for the complex. Previous studies have demonstrated that MHC-I is re-routed by Nef to a paranuclear compartment (39). In order to visualize this compartment relative to the Nef:MHC-I complex, we counterstained HeLa cells co-expressing Nef-V<sub>C</sub> and MHC-I-V<sub>N</sub>-Flag with a marker of the TGN, TGN46 (40)(Fig. 3.9). A high degree of co-localization was observed between the Nef:MHC-I complex and TGN46 (Fig. 3.9; Pearson's = 0.60) suggesting that the Nef:MHC-I complex traffics to the TGN (40). However, our previous work demonstrated that Nef localizes to an uncharacterized Golgi-proximal compartment that cannot be resolved from the TGN in conventional images (32, 40). As such, GSDM imaging was performed to map the localization of the Nef:MHC-I complexes with high precision. HeLa cells transfected with Nef-V<sub>C</sub> and MHC-I-V<sub>N</sub> and immunostained for the TGN marker TGN46 demonstrated the close association of the Nef:MHC-I complex with TGN46 in both the epifluorescence image, and the super-resolution image (Fig. 3.9). Quantification of this complex demonstrated a significant increase in the association between the BiFC signal of the Nef:MHC-I complex with TGN46 compared to randomized images, confirming that Nef:MHC-I complexes traffic to the TGN (Fig. 3.9D and E).

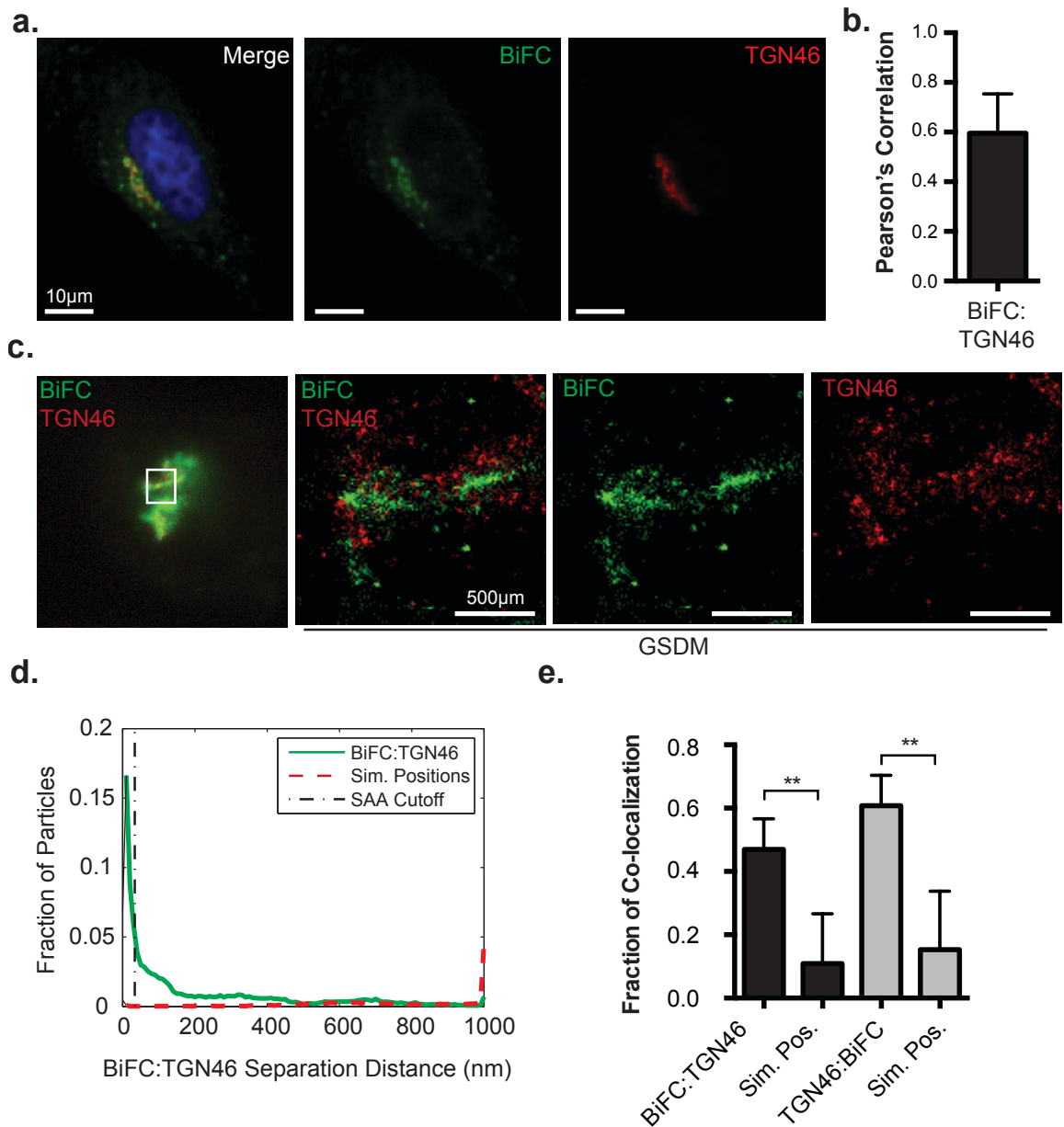


**Figure 3.9: Nef targets MHC-I for sequestration within the trans-Golgi network.**

(A) Nef- $V_C$  and MHC-I- $V_N$ -Flag were transfected into HeLa cells, and 24 hours later fixed and immunostained for TGN46. BiFC fluorescence (green) was observed under the FITC channel, and TGN46 (red) was observed under the Far-Red filters. (B) Co-localization was quantified by using the Pearson's correlation through the JaCoP Plug-in

on ImageJ. Error bars were calculated by quantification of at least 25 cells between 3 independent experiments. (\* Indicates p-value < 0.05). (C) Cells were prepared as in (A) and imaged utilizing GSDM; scale bars represent 500nm. (D) A histogram plotting the distance between the nearest neighbor, representing BiFC:TGN46 (Solid line) or BiFC:Simulated random positions (Sim. Positions; Dashed line). (E) A graphical representation of the fraction of co-localized particles observed in (D) which were observed to be under the cut-off value of ~40nm. Error bars were calculated by quantification of 8 cells in 2 independent experiments (\*\* indicates p-value < .01, \*\*\* indicates p-value < .001).

### 3.2.6 PACS-1 recruitment by Nef alters the intracellular localization of the Nef:MHC-I complex

Nef-mediated MHC-I downregulation relies on its interaction with multiple membrane trafficking regulators. The phosphofurin acidic cluster sorting protein – 1 has been identified as an important binding partner of Nef. Early studies have demonstrated the importance of the Nef:PACS-1 interaction in the downregulation of MHC-I (12, 39, 41), however, the direct impact on the distribution of MHC-I when PACS-1 fails to interact with Nef is currently unknown. To determine the role of PACS-1 in the localization of the Nef:MHC-I complex, a mutant Nef construct was produced with the E<sub>62</sub>EEE<sub>65</sub> acidic motif mutated to 4 sequential alanine residues. This mutant has previously been shown to not interact with PACS-1 (Nef (E4A)) (39). HeLa cells were co-transfected with plasmids encoding Nef-Vc (Fig. 3.10A, B, C, D) or Nef (E4A)-Vc (Fig 3-10E, F, G, H) and MHC-I-Vn-FLAG, and co-transfected with plasmids encoding mCherry-tagged Rab5 (Fig. 3.10A, E) or Rab7 (Fig 3-10B, F), or immunostained for LAMP-1 (Fig 3.10C, G) or TGN (Fig. 3.10D, H). Pearson's coefficients were calculated using the JaCoP Plug-in from ImageJ between the BiFC signals and different intracellular compartments. Interestingly, upon mutation of the Nef acidic cluster, we observed a significant 30% increase in the co-localization of Nef (E4A):MHC-I BiFC to Rab5 positive endosomes, respectively (Fig. 3.10I). Additionally, we observed a 38% decrease in the ability of the Nef-E4A mutant to localize to a TGN46-positive TGN compartment. Consistent with the previous results (Fig. 3.9), no significant difference was observed in the co-localization of wildtype or mutant BiFC signal to LAMP-1-positive lysosomes (Fig. 3.10L). These results suggest that PACS-1 promotes the sequestration of the Nef:MHC-I complex to the TGN by depleting the pool of the Nef:MHC-I complex residing in peripheral Rab5- and Rab7-positive endosomal compartments.

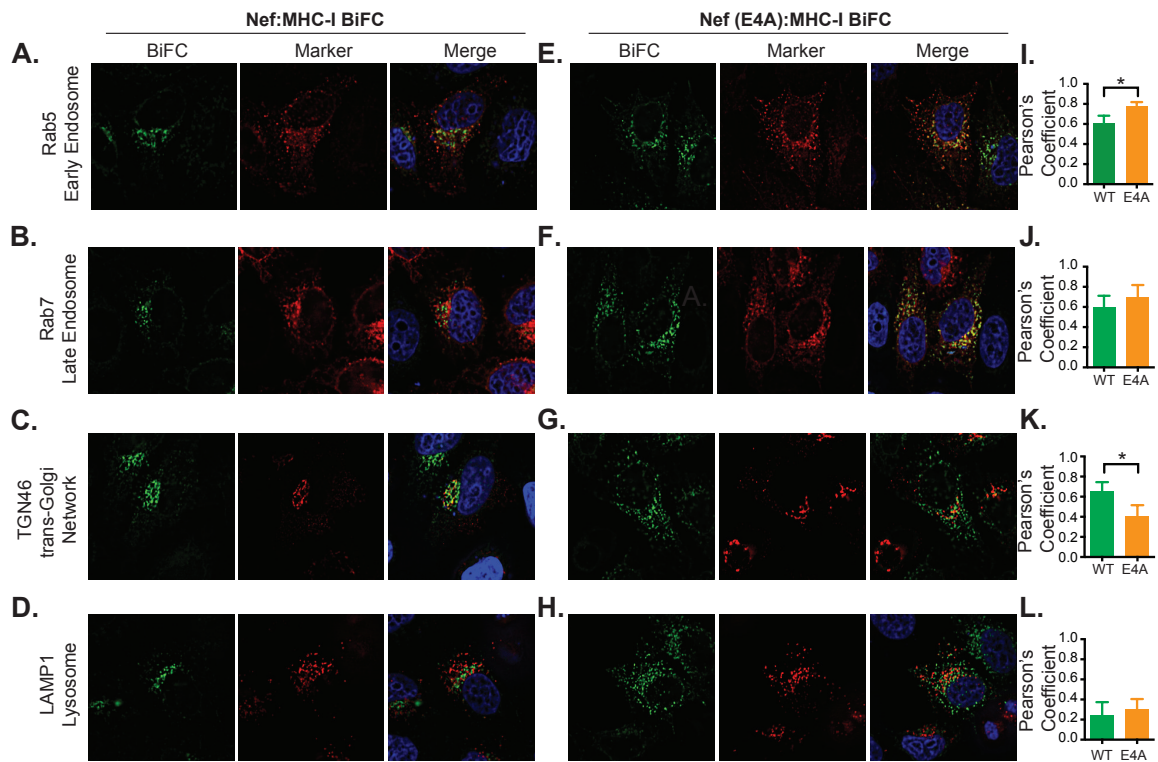


**Figure 3.10: The Nef acidic cluster mutant alters the intracellular localization of the Nef:MHC-I complex.**

(A-D) HeLa cells were co-transfected with plasmids expressing Nef- $V_C$  and MHC-I- $V_N$ -FLAG. (E-H) HeLa cells were co-transfected with plasmids expressing Nef (E4A)- $V_C$  and MHC-I- $V_N$ -FLAG. In addition to the specified BiFC constructs, HeLa cells were co-transfected with plasmids expressing the early endosomal marker Rab5 (A, E), or the late endosomal marker Rab7 (B, F), or immunostained for the TGN marker TGN46 (C, G) or immunostained for the lysosomal marker LAMP-1 (D, H). BiFC fluorescence (green) was observed under the FITC channel, mCherry-tagged constructs were visualized under Cy3 filters, and TGN46/LAMP-1 staining (red) was observed under the Far-Red filters. Nuclei were visualized under the DAPI channel (blue). Scale bar represents 10  $\mu$ m. (I-L)

Co-localization of BiFC fluorescence to each sub-cellular compartment was quantified using Pearson's coefficient calculated by the JaCoP Plug-in on ImageJ. Error bars were calculated using at least 30 cells between 3 independent experiments. (\*Indicates p-value < 0.05).

### 3.2.7 Adaptor Protein -1 recruitment is enhanced by the Nef acidic cluster

The movement of cargo between endosomes and the TGN relies on the ability of PACS-1 to act as a connector molecule to recruit AP-1 to the cytoplasmic tail of itinerant cargo (12). Previous *in vitro* crystal structure studies revealed that MHC-I lacks the classical Yxx $\theta$  AP-1 interaction motif, however, Nef interacts with the cytoplasmic tail of MHC-I to provide enhanced binding of AP-1 to the complex (26). Due to the role of PACS-1 in connecting cargo molecules to adaptor proteins, we hypothesized that the PACS-1:Nef interaction promotes AP-1 recruitment to the complex. To test the role of PACS-1 in the recruitment of AP-1 to the Nef:MHC-I complex, we examined the colocalization of AP-1 to either the wildtype Nef:MHC-I complex, or the mutant Nef(E4A):MHC-I BiFC complex. Accordingly, HeLa cells were co-transfected with plasmids expressing Nef-Vc or Nef(E4A)-Vc and MHC-I-V<sub>N</sub>-FLAG. Twenty-four hours post-transfection, cells were fixed, immunostained for the  $\gamma$  subunit of AP-1 (Fig. 3.11A). Consistent with previous findings (Fig. 2.8), AP-1 had a high degree of co-localization with the wild-type Nef:MHC-I interaction (Fig. 3.11B; Pearson's = 0.715). Conversely, abolishing the Nef:PACS-1 interaction through the Nef acidic cluster mutation resulted in a significant reduction in AP-1 co-localization with the Nef:MHC-I complex (Fig. 3.11B; Pearson's = .470; ). As a negative control, we assessed the ability of the wildtype or mutant BiFC complexes to localize to AP-2. AP-2 is a related, clathrin adaptor, and functions by downregulating CD4 by forming a ternary complex with Nef and CD4 (Fig 3.11C, D)(42). AP-2 co-localization did not significantly differ between Nef:MHC-I BiFC and Nef (E4A):MHC-I BiFC (Fig. 3.11D; Pearson's = 0.173 and Pearson's = 0.140, respectively). Overall, this supports a role for Nef's E<sub>62</sub>EEE<sub>65</sub> acidic motif, in the recruitment of AP-1 to the Nef:MHC-I complex.

To confirm the role of PACS-1 recruitment by the E<sub>62</sub>EEE<sub>65</sub> acidic motif in Nef on the co-localization of the host trafficking molecule AP-1 to the Nef:MHC-I complex, BiFC was also analyzed using super resolution ground state depletion microscopy (GSDM). HeLa cells were co-transfected with Nef-V<sub>C</sub> and MHC-I-V<sub>N</sub>-FLAG (Fig. 3.12A). In parallel, HeLa cells were co-transfected with Nef (E4A)-V<sub>C</sub> and MHC-V<sub>N</sub>-FLAG (Fig.



3.12B). All cells were subsequently fixed and immunostained 24 hours post-transfections for the  $\gamma$  subunit of AP-1. Consistent with results represented in Figure 3.11, AP-1 and Nef:MHC-I BiFC were localized to discrete vesicles (Fig. 3.11A), whereas, Nef(E4A):MHC-I BiFC and AP-1 did not closely associate (Fig. 3.12B). To define their association to each other, distances between Nef:MHC-I complexes and the stained adapter proteins were quantified using spatial association analysis (43). We observed that a significantly greater fraction of co-localized particles were present with the wildtype Nef:MHC-I BiFC, compared to the mutant interaction (Fig. 3.12C). Additionally, we determined that AP-1 was, on average, at a 2-fold greater distance away from the Nef(E4A):MHC-I BiFC complex than the wildtype (Fig. 3.12D; 75 nm and 35 nm, respectively), reinforcing our previous finding that Nef requires its interaction with PACS-1 to recruit AP-1 to the Nef:MHC-I complex (Fig. 3.11).

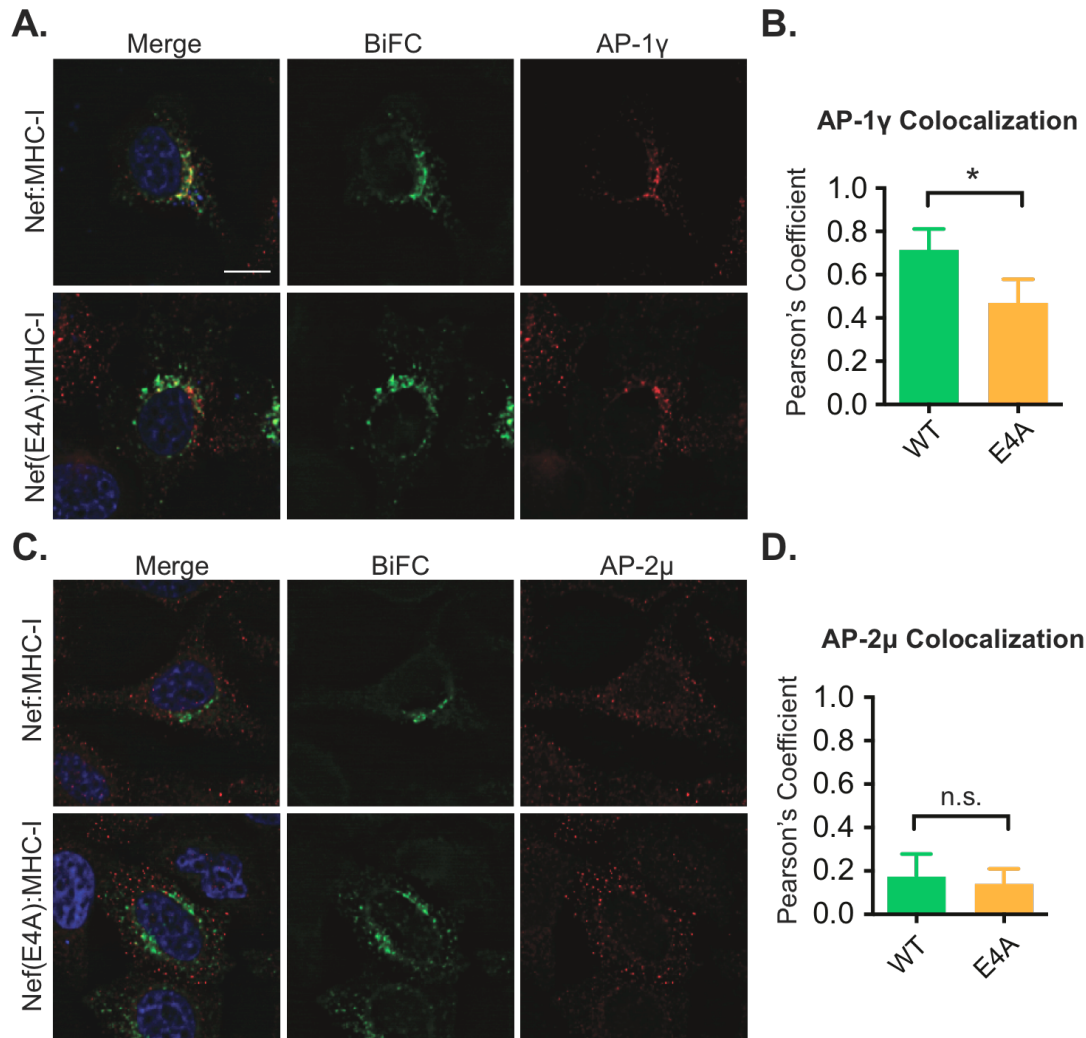


**Figure 3.11: Wide-field microscopy demonstrates that PACS-1 recruitment by Nef enhances the co-localization of AP-1 to the Nef:MHC-I complex.**

(A) HeLa cells were co-transfected with Nef-Vc or Nef (E4A)-V<sub>C</sub> and MHC-I-V<sub>N</sub>-FLAG. Twenty-four hours post transfection cells were fixed and immunostained for AP-1. (B) The co-localization between BiFC (green) and AP-1 $\gamma$  (red) was quantified between green and red signals using Pearson's correlation calculated by the JaCoP Plug-in on ImageJ. (C) Similarly, HeLa cells were co-transfected with Nef-Vc or Nef (E4A)-V<sub>C</sub> and MHC-I-V<sub>N</sub>-FLAG, and were subsequently fixed and immunostained for AP-2 $\mu$ . (D) The co-localization between BiFC (green) and AP-2 $\mu$  (red) was quantified between green and red signals using Pearson's correlation calculated by the JaCoP Plug-in on ImageJ. All

cells were mounted with DAPI Fluoromount-G. BiFC fluorescent signal (green) was visualized using the FITC channel. Both AP-1 $\gamma$  and AP-2 $\mu$  (red) were observed using the Far-Red filter. Nuclei were visualized under the DAPI channel (blue). Scale bar represents 10  $\mu$ m. Error bars were calculated by quantification of at least 20 cells from 2 independent experiments (\*Indicates p-value <0.05).

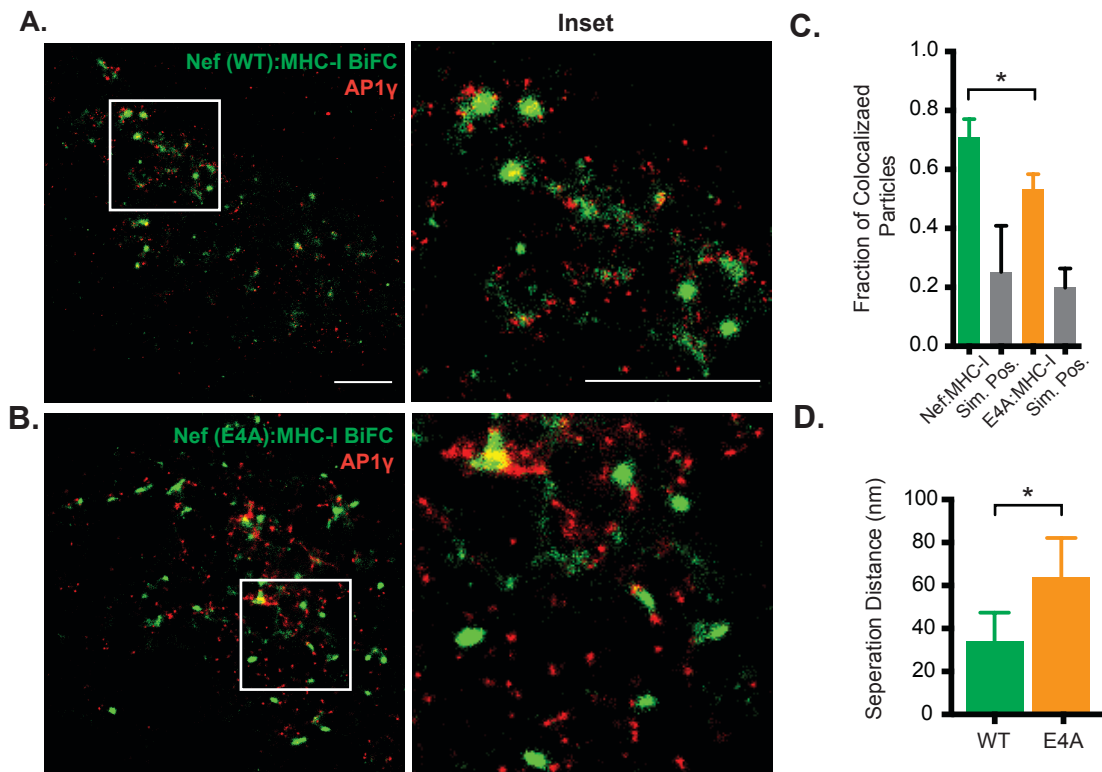


**Figure 3.12: Ground state depletion microscopy (GSDM) demonstrates that PACS-1 recruitment by Nef enhances the localization of AP-1 to the Nef:MHC-I complex.**

(A-B) HeLa cells were co-transfected with Nef-V<sub>C</sub> or Nef (E4A)-V<sub>C</sub> and MHC-I-V<sub>N</sub>-FLAG, and were subsequently immunostained for AP-1 $\gamma$  24 hours later. Magnified insets are shown (right panel). BiFC fluorescent signal (green) was visualized using the 488 nm laser line. AP-1 $\gamma$  (red) was observed using a 647 nm laser line. Scale bars represent 2.5 $\mu$ m. (C) A graphical representation of the fraction of co-localized particles was calculated between BiFC complex (green) and AP-1 $\gamma$  using the nearest-neighbour algorithm in the MIISR software as previously described (28). (D) A graphical representation of the mean separation distance between the BiFC complex (green) and AP-1 $\gamma$  (red). Error bars were calculated by quantification of 5 cells between 2 independent experiments. All images were validated by comparing the observed degree of colocalization to that observed in 10 images containing the same number of particles randomly scattered on an image of equal area. (\* Indicates p-value < 0.05).

### 3.2.8 PACS-1 directly facilitates localization of MHC-I to the trans-Golgi Network

To further investigate the mechanism of AP-1 recruitment to the Nef:MHC-I complex we conducted additional experiments to directly test the role of PACS-1. To test this, Nef:MHC-I BiFC fluorescence microscopy experiments were performed in conjunction with a dominant negative mutant of PACS-1 (ADMUT), which is unable to bind AP-1 but can still bind to acidic clusters, and Nef (22). HeLa cells were co-transfected with plasmids expressing Nef-V<sub>C</sub>, MHC-I-V<sub>N</sub>-FLAG and mCherry-tagged PACS-1 or mCherry-tagged ADMUT. Twenty-four hours post-transfection, cells were fixed, immunostained for TGN46, and imaged (Fig. 3.13A). Indeed, expression of the Nef:MHC-I BiFC constructs with the wildtype mCherry-tagged PACS-1 exhibited a robust TGN localization (Fig. 3.13A). In contrast, upon expression of the dominant negative ADMUT, numerous BiFC-positive peripheral vesicles became apparent (Fig. 3.13B). The co-localization between the Nef:MHC-I BiFC complex (green), and the TGN46 marker (magenta), were quantified in PACS-1/ADMUT-positive cells by the Pearson's coefficient. We observed a modest, but significant 11% reduction in the ability of ADMUT expressing cell to localize the Nef:MHC-I complex to the TGN (Fig. 3.13C; Pearson's = 0.562 and Pearson's = 0.635, respectively). In parallel, the expression of Nef-V<sub>C</sub>, MHC-I-V<sub>N</sub>-FLAG, and PACS-1/ADMUT-mCherry constructs were confirmed using Western blots (Fig. 3.13D). Overall, these results demonstrate the key role of PACS-1 as a connector molecule to AP-1, thereby mediating the efficient trafficking of MHC-I to the TGN.

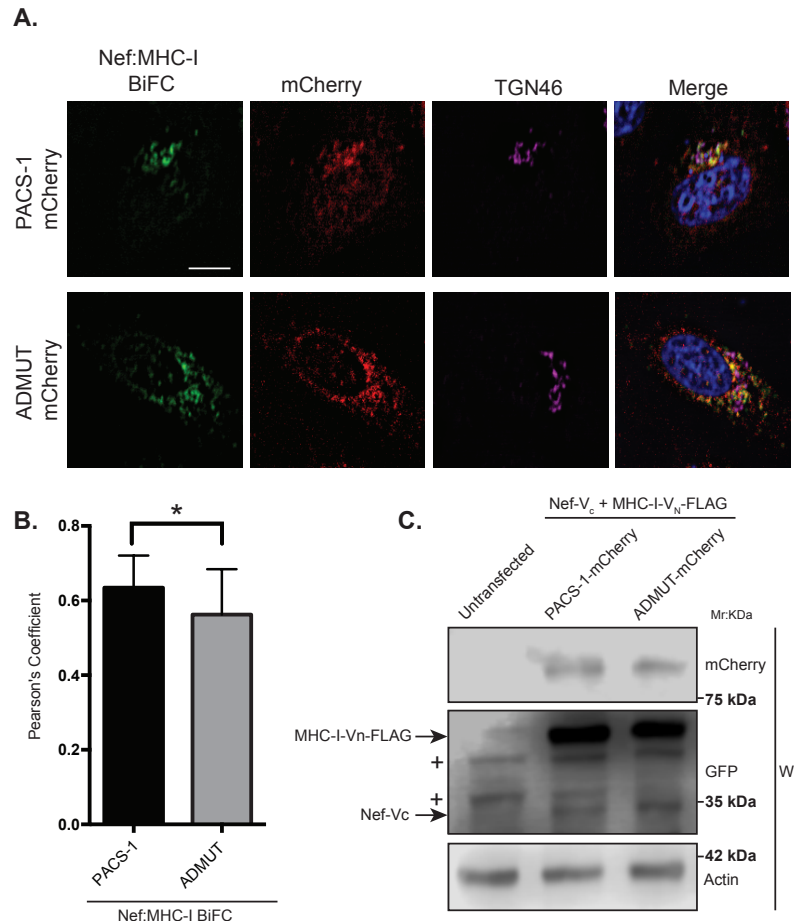


**Figure 3.13: PACS-1:Adaptor Protein interaction promotes TGN localization of Nef and MHC-I**

(A) HeLa cells were co-transfected with Nef- $V_C$  and MHC-I- $V_N$  – FLAG BiFC constructs along with either mCherry-tagged PACS-1 or ADMUT. Cells were fixed, and immunostained for the TGN marker TGN46 with AlexaFluor 647 secondary antibody, and mounted in Fluoromount G-DAPI mounting media. BiFC fluorescence (green), mCherry (red), TGN46 (magenta) and DAPI (blue) were detected using FITC, Cy3, Cy5 and DAPI filter settings, respectively. (B) Colocalization of the BiFC (green) and TGN46 (magenta) were calculated using the Pearson's coefficient using the JaCOP plugin in ImageJ. Error bars were calculated based on at least 20 cells from 2 independent experiments (\* indicates  $p < 0.05$ ). (C) In parallel, western blots were conducted to ensure expression of all fusion proteins in each condition. Both Nef- $V_C$  and MHC-I- $V_N$

constructs were detected using an anti-GFP antibody, mCherry-tagged PACS-1 and ADMUT constructs were detected using an mCherry specific western blot, and an actin specific western blot was used as a loading control. Untransfected cells were used as a negative control for antibody binding (\* indicates non-specific antibody binding).

### 3.3 Discussion

In the present study, we have tracked a complex between the HIV-1 protein Nef and MHC-I within the endosomal network. Our results demonstrate that a Nef:MHC-I complex traffics to both early and late endosomes in addition to the paranuclear TGN compartment. Furthermore, Nef impedes MHC-I from recycling to the cell surface by re-routing MHC-I through both early endosomes and late endosomes and subsequently to the TGN. Additionally, we provide evidence supporting the role of PACS-1 in facilitating the endosome-to-Golgi trafficking step of the Nef:MHC-I complex. Overall, this mechanism inhibits MHC-I molecules from presenting antigens extracellularly, contributing to the ability of HIV-1 to evade host immune surveillance (14).

Nef has the capability to disrupt the normal membrane trafficking events that occur within cells. Indeed, Nef downregulates the cell surface expression of over 36 surface receptors (44). Interestingly, there is some degree of specificity within this seemingly non-discriminatory razing of the cell surface topography. This specificity lies within the host membrane adaptor molecules that are used by Nef to internalize specific receptors. For example, the membrane adaptor molecule AP-1 interacts with MHC-I and is implicated in the Nef-dependent internalization of MHC-I (8). Conversely, the related membrane adaptor molecule, AP-2, is critical for the Nef-dependent internalization of CD4 (45). Overall, these adaptor molecules are indispensable for the ability of Nef to bind and downregulate MHC-I and CD4 receptors. Structural studies have revealed that the cytoplasmic tails of MHC-I and CD4 mediate this specificity with adaptor molecules(10). Specifically, AP-1 recognizes the Yxx $\theta$  motif (where  $\theta$  represents a bulky hydrophobic residue) in the MHC-I cytoplasmic tail, as demonstrated by the complex crystal structure between Nef:MHC-I and the  $\mu$ -1 subunit of AP-1 (10). In contrast, structural modeling of the CD4 cytoplasmic tail has implicated the canonical di-leucine motif of CD4 to be necessary for its downregulation by Nef (42). In this study, residues Y<sub>320</sub> and D<sub>327</sub> in the MHC-I cytoplasmic tail were deemed critical to maintain the Nef:MHC-I complex in cells (Fig. 3.1). As these residues were implicated in interacting with both AP-1 and Nef within crystal structures, this supports the formation of a



Nef:MHC-1:AP-1 ternary complex within cells, in agreement with previous studies utilizing co-immunoprecipitation (8, 46).

Functionally, the differences in Nef dependent internalization of CD4 and MHC-I are linked to the distinction that AP-2 dependent trafficking is linked to degradative compartments whereas AP-1 dependent trafficking is not (7, 45, 47). We confirmed this assertion as Nef and MHC-I complexes were not directed to degradative compartments (Fig. 3.7A) and MHC-I was not degraded (Fig. 3.7E), whereas Nef mediated the degradation of CD4 as previously described (Fig. 3.7E and (45)).

BiFC is a powerful technique that demonstrates the interaction or close proximity of two proteins within a cell. Previously, BiFC was used to illustrate the interaction between Nef and the membrane trafficking regulator PACS proteins, PACS-1 and PACS-2, in late and early endosomes, respectively (2). Thus, the BiFC interaction between Nef and MHC-I provides a platform to study the various models of Nef-dependent MHC-I downregulation. Our results demonstrate that newly endocytosed MHC-I originating from the cell surface is targeted by Nef (Fig. 3.3C and D). Further experiments highlight the presence of the Nef:MHC-I complex throughout the early and late endosomes, and demonstrate the importance of the early endosomal effector molecule Rab5 in this process (Fig. 3.4 and Fig. 3.5). As Rab5 functions to sort cargo early upon endocytosis (48), it is logical that the expression of Rab5-CA, which disrupts the maturation of endosomes (48), disrupts Nef-dependent MHC-I cell surface downregulation (49). A possible mechanism governing this trafficking step may rely on a ternary complex between Nef, MHC-I and the PACS proteins, as previously demonstrated biochemically for PACS-1 (2). Specifically, we highlight the role of PACS-1 in the TGN sequestration step of Nef and MHC-I, as when PACS-1 is unable to interact with the acidic cluster of Nef, MHC-I is no longer able to trafficking to the TGN (Figure 3.10)(2, 49). Such a trafficking defect is similar to that of an acidic cluster mutant of the cellular protease furin (50-52). Indeed, mutation of the furin acidic cluster results in a peripheral endosomal localization(50-52). PACS-1 often acts as a connector molecule between cytoplasmic tails of cargo and AP-1. Consistent with this, we observed that the acidic cluster of Nef drastically reduces the AP-1 recruitment to the complex (Figure 3.11 &

3.12). Additionally, over expression of a mutant PACS-1 unable to interact with AP-1 also reduced the ability for the Nef:MHC-I complex to transit to the Golgi from peripheral endosomes. Interestingly, expression of the Nef (E4A):MHC-I complex was still visible despite the reduced recruitment of AP-1 complex, which was inconsistent with the mutational analysis of the MHC-I cytoplasmic tail aimed to disrupt the interaction between Nef, MHC-I, and AP-1. This suggests that different protein complexes may be required at different endosomal locations to ensure MHC-I downregulation. Overall, these results highlight the importance of different motifs involved in the recruitment of AP-1 to the cytoplasmic tail of MHC-I. Indeed, different motifs may be required within different locals of the cell.

Interestingly, our results are directly linked to the signaling model of Nef-dependent MHC-I downregulation (7), which is dependent on the PACS protein dependent endocytosis of MHC-I from the cell surface and not a block of MHC-I trafficking from the endoplasmic reticulum to plasma membrane which is linked to the Nef-dependent degradation of MHC-I in lysosomes (53). We failed to observe the localization of the Nef:MHC-I complex in lysosomes even upon rendering these compartments more basic (Fig. 3.7A, B and C), suggesting that our experiments closely mimicked early time points in an infection (7). This trafficking route would not result in the degradation of MHC-I, a phenomenon observed readily in other viral infections, such as Kaposi-sarcoma related herpesvirus infections, which mediates degradation of MHC-I by the K3 and K5 proteins (54). Instead, the Nef:MHC-I complex was routed from Rab5 positive early endosomes to Rab7 positive late endosomes and the TGN and these interactions were observed at the 20nm resolution offered by GSDM, unequivocally defining the subcellular route undertaken by MHC-I in the presence of Nef (Figs. 3.4, 3.6 and 3.9). Moreover, the localization of the Nef-MHC-I complex in Rab7 positive late endosomes is reminiscent of the Nef dependent-localization of SERINC5 within this compartment (55, 56). SERINC5 was recently identified as a host cellular antiretroviral factor that inhibits HIV-1 replication (56). Thus, it appears that Rab7-positive late endosomes are used by Nef to block both infectivity and the CTL response. Overall, Rab7-positive late endosomes are compartments used by multiple viruses for various steps of the viral infectious cycle including entry (57, 58) and would also represent a central compartment used by Nef to

enable key HIV-1 functions such as the sequestration of MHC-I in an intracellular compartment.

The Nef:MHC-I interaction was also observed in the TGN, consistent with the Nef and AP-1 dependent sequestration of MHC-I in a paranuclear compartment (Fig. 3.9A)(39, 49). We postulate that this compartment contains the re-routed MHC-I that has been pulled away by Nef from the cell surface. Previous studies by Blagoveshchenskaya *et al.* demonstrated that Nef increased the rates of endocytosed MHC-I in an Arf6 dependent manner (3). Herein, we demonstrate that this endocytosed MHC-I localizes to the TGN in complex with Nef (Fig. 3.9). Indeed, we show that MHC-I is excluded from Rab11-positive recycling endosomes when in complex with Nef, suggesting that this represents a membrane trafficking junction point that differs between cells that do or do not express Nef (Fig. 3.3A and B). In uninfected cells, normal MHC-I recycling occurs via Rab11-positive compartments to enable antigen cross presentation, while maintaining physiological MHC-I levels on the cell surface (59, 60).

Overall, we propose a model for the Nef-dependent downregulation of cell surface MHC-I that highlights the cellular compartments that are subverted by Nef in order to coordinate the removal of MHC-I away from the cell surface. Our results demonstrate that a Nef:MHC-I complex traffics to both early and late endosomes in addition to the paranuclear TGN compartment in a PACS-1 and AP-1-dependent manner. Further studies will be aimed at determining whether the transition between early and late endosomes is required for MHC-I sequestration, or if sequestration of MHC-I is independent of endosomal maturation. This work builds on the model of Nef-mediated MHC-I downregulation by identifying key cellular compartments in which Nef targets MHC-I. Understanding how Nef targets MHC-I will lead to new insights into how viruses mediate immune evasion, and specifically how HIV-1 persists within the infected host.

## 3.4 Methods

### 3.4.1 Cells

HeLa and HEK-293T cells (ATCC, Manassas, VA) were grown in complete DMEM (HyClone, Logan, UT) containing 10% fetal bovine serum (FBS) (Wisent, Montreal,

Canada) and 100µg/ml penicillin-streptomycin (HyClone). Sup-T1 cells were grown in complete RPMI (HyClone) containing 10% FBS and 10µM L-Glutamine (HyClone). All cell lines were grown at 37°C in the presence of 5% CO<sub>2</sub> and sub-cultured in accordance with supplier's recommendations.

### 3.4.2 Plasmids

HLA-A2 cDNA (provided by Dr. G. Thomas, University of Pittsburgh Medical School) was subcloned into a pcDNA 3.1 (+) plasmid encoding the N-terminal portion of the Venus fluorophore (V<sub>N</sub> 1-173), as previously described (24). NL4.3 *nef* was subcloned into a pV<sub>C</sub>-N1 backbone plasmid encoding the C-terminal portion of the split Venus fluorophore (V<sub>C</sub> 155-273). Overlap PCR mutagenesis was performed to mutate Nef EEEE<sub>65</sub> to AAAA<sub>65</sub>. HLA-A2 mutants were generated using overlap extension polymerase chain reaction. Expression vectors encoding mCherry-Rab5, mCherry-Rab5-DN, mCherry-Rab5-CA, mCherry-Rab7, mCherry-Rab7-DN, dsRed-Rab11a were provided by Dr. R. Flanagan, UWO and were previously described(30, 61). PACS-1 cDNA was sub cloned into a pmCherry-N1 vector. Primer overlap extension PCR was performed to mutate PACS-1 168-175 to alanines. The MHC-I-eGFP plasmid was generated by subcloning the HLA-A2 gene into a peGFP-N1 (Clontech) using EcoRI and BamHI restriction digest enzymes. Viral vectors: pNL4.3 F2A-CD4-Flag Δvpu Nef/ΔNef and pNL4.3 F2A MHC-I-MHC-I-Flag Nef/ΔNef were generated by sub cloning MHC-I-Flag and CD4-Flag into the previously described base vector pNL4.3 F2A-X-Nef/ΔNef(24).

### 3.4.3 Transfections

For BiFC and subcellular localization studies, 2.5x10<sup>5</sup> HeLa cells were seeded onto coverslips and 24 hours later plasmids were transfected into cells at equal molar ratios using PolyJet transfection reagent (FroggaBio, Toronto, Canada). Twenty-four hours post transfection cells were incubated for one hour at room temperature to allow for fluorophore maturation, as described previously(24). Subsequently, cells were fixed in 4% PFA and prepared for immunofluorescence as described below.

### 3.4.4 Western Blots

For analysis of BiFC protein expression, HeLa cells were transfected with the specified BiFC vectors, incubated for 24 hours, washed once with phosphate buffered saline (PBS) and lysed in lysis buffer (0.5M HEPES, 1.25M NaCl, 1M MgCl<sub>2</sub>, 0.25M EDTA, 0.1% Triton X-100, 1X complete Protease inhibitor Tablets (Roche, Indianapolis, IN)). Cells were incubated on a rotator for 20 minutes at 4°C before removing insoluble cellular debris by centrifugation at 20,000xg for 20 minutes. Lysates were boiled at 98°C in 5X SDS-PAGE sample buffer (0.312M Tris pH 6.8, 25% 2-Mercaptoethanol, 50% glycerol, 10% SDS) and proteins were separated on a 12% SDS-PAGE gel and subsequently transferred to nitrocellulose membranes. Membranes were blocked in 5% non-fat skimmed milk (BioShop Canada, Burlington, Canada) in TBST containing 0.1% Triton X-100 for 1 hour, then incubated overnight at 4°C with various antibodies: rabbit anti-Nef polyclonal antibody (1:2000; catalog number 2949, NIH AIDS Research and Reference Reagent Program, USA (62), rat anti-DYKDDDK monoclonal IgG (1:2500; BioLegend, San Diego, CA), anti-p24 (1:800; catalog number 4121, NIH AIDS Research and Reference Reagent Program, USA) and anti-Actin (1:2000; Thermo Scientific). Membranes were then washed and incubated for two hours with the appropriate species-specific HRP-conjugated antibodies (1:3000; Thermo Scientific). All blots were developed and quantified using ECL substrates (Millipore Inc., Billerica, MA) and a C-DiGit chemiluminescence Western blot scanner (LI-COR Biosciences, Lincoln, NE). To test Nef's ability to mediate MHC-I or CD4 expression, we utilized our previously described viral vector system(24) to express MHC-I-Flag or CD4-Flag, in the presence or absence of Nef. The resulting vectors: pNL4.3 F2A MHC-I-Flag Nef/ $\Delta$ Nef or pNL4.3 F2A CD4-Flag  $\Delta$ vpu Nef/ $\Delta$ Nef were used to generate pseudoviral particles as previously described(24). Sup-T1 cells were subsequently infected, and 48 hours post infection, cells were lysed and levels of MHC-I and CD4 were analyzed by Western blot as described above.

### 3.4.5 Immunofluorescence

For subcellular localization studies, transfections were performed as described above. Cells used in BiFC studies were incubated at room temperature for 1 hour prior to

fixation to allow the reconstituted fluorophore to mature(24). All cells were fixed by washing twice with PBS, incubating for 20 minutes in 4% PFA and subsequently washing three times in PBS. To stain for the split fluorophore halves and various intracellular compartments, fixed HeLa cells were incubated in permeabilization/blocking buffer (5% BSA in PBS and 0.2% Triton X-100) for 1 hour. Cells were then incubated with the appropriate antibodies diluted in blocking buffer for 2 hours (anti-Rab5 (Cell Signaling); 1:200, anti-Rab7 (Santa-Cruz); 1:100, anti-LAMP-1 (DSHB); 1:200, anti-TGN46 (Sigma Aldrich); 1:200, anti-Flag (Biolegend): 1:400, anti-AP-1 $\gamma$  1:100 (Sigma Aldrich), anti-AP-2 $\mu$  (Santa-Cruz)). Cells were subsequently washed three times in blocking buffer and incubated with the appropriate secondary antibody diluted in blocking buffer (donkey anti-rabbit AlexaFluor 647 or donkey anti-mouse AlexaFluor 647 (1:1000; Jackson ImmunoResearch)) for 2 hours at room temperature. Finally, cells were washed three times in PBS (3 minute each) and mounted onto glass slides using Fluormount-G or DAPI-fluoromount-G (Southern Biotech, Birmingham, AL). Fluorescence intensity of the BiFC signal was measured by selecting cells positive for both Nef and Flag-tagged MHC-I, then subtracting the background fluorescence using ImageJ(63, 64). To test the localization of MHC-I-eGFP with LAMP-1, cells were transfected with MHC-I-eGFP with Nef-mCherry or mCherry and immunostained as above. Co-localization of MHC-I-eGFP and LAMP-I was then measured in cells expressing either Nef-mCherry or mCherry in the presence or absence of ammonium chloride.

### 3.4.6 Antibody Uptake

HeLa cells were transfected with equal molar amounts of MHC-I-V<sub>N</sub>-Flag and Nef-V<sub>C</sub>. Twenty-four hours post-transfection cells were washed with ice cold PBS, and subsequently anti-HLA-A2 (BB7.2; Biolegend) antibody was added at a dilution of 1:300. Antibody was allowed to bind for 20 minutes at 4°C. Following antibody binding, cells were washed 3X with cold PBS, and either fixed (time 0 minutes), or supplemented with warm complete media and incubated for 90 minutes at 37°C. Cells were then fixed, permeabilized, and immunostained with donkey anti-mouse AlexaFluor 647 (1:400;

Jackson ImmunoResearch) secondary antibody for 2 hours to detect the internalized antibody. Coverslips were then washed 3X in PBS and mounted using DAPI-Fluoromount-G (Southern Biotech).

#### 3.4.7 Ammonium chloride treatment of cells to assess lysosomal trafficking

For assessing lysosomal subcellular localization, staining was performed as described above with anti-human LAMP-1 1:200 (Developmental Studies Hybridoma Bank; Iowa City, IA). Ammonium chloride was added to a concentration of 100mM to prevent lysosomal acidification for 4 hours. To ensure the ammonium chloride treatment affected lysosomal acidification, HeLa cells treated in an equivalent manner were stained with LysoTracker DeepRed (10 $\mu$ M; Life Technologies). Live cells were then imaged, and mean fluorescence intensity was measured using ImageJ.

#### 3.4.8 Microscopy

Cells were viewed on a Leica DMI6000 B at 63X or 100X magnification using the FITC, Cy3, CY5 and DAPI filter settings and imaged with a Hamamatsu Photometrics Delta Evolve camera. Images were subsequently deconvolved using the Advanced Fluorescence Deconvolution (Lecia, Wetzlar, Germany) application on the Leica Application Suite software. Co-localization analysis was conducted using Pearson's Correlation from the ImageJ plugin JACoP, as described previously(65).

Super-resolution imaging was performed as previously described(32). Briefly, HeLa cells were transfected with plasmid DNA, and 24 hours later immunostained as described above. Prior to imaging, cells were mounted in a depression slide containing 100mM cysteamine (Sigma) buffer in PBS. Coverslips were sealed with Twinsil (Picodent), and imaged within 4 hours of mounting. All images were acquired using a Lecia SR GSD microscope with the 100X/1.43 NA objective lens containing an additional 1.6X magnifier. Fluorophores were excited using 125mW-250mW lasers (488, 532 and 647nm) and a 30mW backpumping 405nm laser. Channels were acquired sequentially at 100fps for 7,000 – 15,000 frames, with minor adjustments on laser power and backpumping to maintain 10 to 30 active fluorophores per frame. The resulting images

were exported and molecule position files were converted to ASCII for analysis. Intermolecular interactions and localization within labeled endocytic compartments was quantified using spatial association analysis (SAA), performed using our custom-written MliSR software(32), with datasets filtered to remove molecules detected with a precision of <25 nm prior to analysis. All interactions were validated by comparing the observed degree of interaction to that observed in 10 images containing the same number of particles randomly scattered in an image of equal area.

### 3.4.9 Flow cytometry

To test the functional significance of disrupting Rab5, HeLa cells were transfected with mCherry-tagged Rab5-CA or Rab5 (wt) constructs in conjunction with Nef-eGFP or empty eGFP encoding backbone. Twenty-four hours post transfection, cells were trypsinized, washed twice with PBS and fixed in 2% PFA for 15 minutes. Following fixation, cells were washed in FACS buffer (0.5% FBS and 50mM EDTA in PBS) and stained with W6/32 anti-MHC-I (1:4000) antibody for 30 minutes (provided by D. Johnson, Oregon Health and Science University). Cells were then washed twice and stained with donkey anti-mouse AlexaFluor 647 (1:1000) for 20 minutes, followed by two more washes in FACS buffer. Flow cytometry was then performed using a BD FACSCanto (BD Biosciences) and the geometric mean fluorescence intensity of AlexaFluor 647 (MHC-I) was determined for mCherry and eGFP positive cells.

To test the functionality of the MHC-I-V<sub>N</sub>-Flag fusion proteins, we transfected HeLa cells with vectors encoding MHC-I-V<sub>N</sub>-Flag or MHC-I-Y<sub>320A</sub>/D<sub>327N</sub>-V<sub>N</sub>-Flag in combination with either Nef-eGFP or eGFP alone. Twenty-four hours post transfection cells, were stained with BB7.2 anti-HLA-A2 (1:4000) and donkey anti-mouse AlexaFluor 647 (1:2000), as above, to specifically detect cell surface MHC-I fusion proteins. Cells were then analyzed by flow cytometry as above and geometric mean fluorescence intensity of AlexaFluor 647 (MHC-I) was determined for eGFP and AlexaFluor 647 positive cells.

To test the functionality of Nef-V<sub>C</sub>, HeLa cells were transfected with vectors encoding Nef-V<sub>C</sub> and eGFP as a transfection control, or a vector encoding eGFP alone. GFP



positive cells were subsequently analyzed for cell surface MHC-I levels by flow cytometry using W6/32 anti-MHC-I antibody as described above.

### 3.4.10 Statistics

All statistics were conducted using a paired T-test, or a one-way ANOVA where indicated on Graph Pad Prism (Graph Pad Software Inc., La Jolla, CA).

### 3.5 References

- 1     Malim, M. H. & Emerman, M. HIV-1 accessory proteins--ensuring viral survival in a hostile environment. *Cell Host Microbe* **3**, 388-398, doi:S1931-3128(08)00126-1 [pii] 10.1016/j.chom.2008.04.008 (2008).
- 2     Dikeakos, J. D. *et al.* An interdomain binding site on HIV-1 Nef interacts with PACS-1 and PACS-2 on endosomes to down-regulate MHC-I. *Molecular biology of the cell* **23**, 2184-2197, doi:mbc.E11-11-0928 [pii] 10.1091/mbc.E11-11-0928 (2012).
- 3     Blagoveshchenskaya, A. D., Thomas, L., Feliciangeli, S. F., Hung, C. H. & Thomas, G. HIV-1 Nef downregulates MHC-I by a PACS-1- and PI3K-regulated ARF6 endocytic pathway. *Cell* **111**, 853-866, doi:S0092867402011625 [pii] (2002).
- 4     Collins, D. R. & Collins, K. L. HIV-1 accessory proteins adapt cellular adaptors to facilitate immune evasion. *PLoS Pathog* **10**, e1003851, doi:10.1371/journal.ppat.1003851 PPATHOGENS-D-13-02746 [pii] (2014).
- 5     Collins, K. L., Chen, B. K., Kalams, S. A., Walker, B. D. & Baltimore, D. HIV-1 Nef protein protects infected primary cells against killing by cytotoxic T lymphocytes. *Nature* **391**, 397-401, doi:10.1038/34929 (1998).
- 6     Pawlak, E. N. & Dikeakos, J. D. HIV-1 Nef: A Master Manipulator of the Membrane Trafficking Machinery Mediating Immune Evasion. *Biochimica et Biophysica Acta (BBA)-General Subjects* (2015).
- 7     Dikeakos, J. D. *et al.* Small molecule inhibition of HIV-1-induced MHC-I down-regulation identifies a temporally regulated switch in Nef action. *Molecular biology of the cell* **21**, 3279-3292, doi:E10-05-0470 [pii] 10.1091/mbc.E10-05-0470 (2010).
- 8     Roeth, J. F., Williams, M., Kasper, M. R., Filzen, T. M. & Collins, K. L. HIV-1 Nef disrupts MHC-I trafficking by recruiting AP-1 to the MHC-I cytoplasmic tail. *J Cell Biol* **167**, 903-913, doi:jcb.200407031 [pii] 10.1083/jcb.200407031 (2004).
- 9     Wan, L. *et al.* PACS-1 defines a novel gene family of cytosolic sorting proteins required for trans-Golgi network localization. *Cell* **94**, 205-216 (1998).
- 10    Jia, X. *et al.* Structural basis of evasion of cellular adaptive immunity by HIV-1 Nef. *Nat Struct Mol Biol* **19**, 701-706, doi:nsmb.2328 [pii] 10.1038/nsmb.2328 (2012).
- 11    Schaefer, M. R., Wonderlich, E. R., Roeth, J. F., Leonard, J. A. & Collins, K. L. HIV-1 Nef targets MHC-I and CD4 for degradation via a final common beta-

- COP-dependent pathway in T cells. *PLoS Pathog* **4**, e1000131, doi:10.1371/journal.ppat.1000131 (2008).
- 12 Tokarev, A. & Guatelli, J. Misdirection of membrane trafficking by HIV-1 Vpu and Nef: Keys to viral virulence and persistence. *Cell Logist* **1**, 90-102, doi:10.4161/cl.1.3.16708 2159-2780-1-3-4 [pii] (2011).
  - 13 Schwartz, O., Maréchal, V., Le Gall, S., Lemonnier, F. & Heard, J.-M. Endocytosis of major histocompatibility complex class I molecules is induced by the HIV-1 Nef protein. *Nature medicine* **2**, 338-342 (1996).
  - 14 Stoorvogel, W., Strous, G. J., Geuze, H. J., Oorschot, V. & Schwartz, A. L. Late endosomes derive from early endosomes by maturation. *Cell* **65**, 417-427 (1991).
  - 15 Rink, J., Ghigo, E., Kalaidzidis, Y. & Zerial, M. Rab conversion as a mechanism of progression from early to late endosomes. *Cell* **122**, 735-749 (2005).
  - 16 Bucci, C., Thomsen, P., Nicoziani, P., McCarthy, J. & van Deurs, B. Rab7: a key to lysosome biogenesis. *Molecular biology of the cell* **11**, 467-480 (2000).
  - 17 Maxfield, F. R. & McGraw, T. E. Endocytic recycling. *Nature reviews Molecular cell biology* **5**, 121-132 (2004).
  - 18 Zerial, M. & McBride, H. Rab proteins as membrane organizers. *Nature reviews Molecular cell biology* **2**, 107-117 (2001).
  - 19 Kerppola, T. K. Bimolecular fluorescence complementation (BiFC) analysis as a probe of protein interactions in living cells. *Annu Rev Biophys* **37**, 465-487, doi:10.1146/annurev.biophys.37.032807.125842 (2008).
  - 20 Kerppola, T. K. Design and implementation of bimolecular fluorescence complementation (BiFC) assays for the visualization of protein interactions in living cells. *Nature protocols* **1**, 1278-1286 (2006).
  - 21 Dirk, B. S., Heit, B. & Dikeakos, J. D. Visualizing Interactions Between HIV-1 Nef and Host Cellular Proteins Using Ground-State Depletion Microscopy. *AIDS research and human retroviruses* **31**, 671-672 (2015).
  - 22 Dirk, B. S. *et al.* Viral Bimolecular Fluorescence Complementation: A Novel Tool to Study Intracellular Vesicular Trafficking Pathways. *PloS one* **10**, e0125619 (2015).
  - 23 Ye, H., Choi, H. J., Poe, J. & Smithgall, T. E. Oligomerization is required for HIV-1 Nef-induced activation of the Src family protein-tyrosine kinase, Hck. *Biochemistry* **43**, 15775-15784, doi:10.1021/bi048712f (2004).
  - 24 Jia, X. *et al.* Structural basis of evasion of cellular adaptive immunity by HIV-1 Nef. *Nature structural & molecular biology* **19**, 701-706 (2012).
  - 25 Donaldson, J. G. & Williams, D. B. Intracellular assembly and trafficking of MHC class I molecules. *Traffic* **10**, 1745-1752 (2009).
  - 26 Ullrich, O., Reinsch, S., Urbé, S., Zerial, M. & Parton, R. G. Rab11 regulates recycling through the pericentriolar recycling endosome. *The Journal of cell*

- biology* **135**, 913-924 (1996).
- 27 Huotari, J. & Helenius, A. Endosome maturation. *The EMBO journal* **30**, 3481-3500 (2011).
  - 28 Stenmark, H. *et al.* Inhibition of rab5 GTPase activity stimulates membrane fusion in endocytosis. *The EMBO journal* **13**, 1287 (1994).
  - 29 Hell, S. W. & Kroug, M. Ground-state-depletion fluorescence microscopy: A concept for breaking the diffraction resolution limit. *Applied Physics B* **60**, 495-497 (1995).
  - 30 Caetano, F. A. *et al.* MliSR: Molecular Interactions in Super-Resolution Imaging Enables the Analysis of Protein Interactions, Dynamics and Formation of Multi-protein Structures. *PLoS Comput Biol* **11**, e1004634 (2015).
  - 31 Mukhopadhyay, A., Funato, K. & Stahl, P. D. Rab7 regulates transport from early to late endocytic compartments in *Xenopus* oocytes. *Journal of Biological Chemistry* **272**, 13055-13059 (1997).
  - 32 Choudhury, A. *et al.* Rab proteins mediate Golgi transport of caveola-internalized glycosphingolipids and correct lipid trafficking in Niemann-Pick C cells. *The Journal of clinical investigation* **109**, 1541-1550 (2002).
  - 33 Rohrer, J., Schweizer, A., Russell, D. & Kornfeld, S. The targeting of Lamp1 to lysosomes is dependent on the spacing of its cytoplasmic tail tyrosine sorting motif relative to the membrane. *The Journal of cell biology* **132**, 565-576 (1996).
  - 34 Segal, H. L. & Doyle, D. J. *Protein turnover and lysosome function*. (Academic Press, 2014).
  - 35 Cardelli, J., Richardson, J. & Miers, D. Role of acidic intracellular compartments in the biosynthesis of *Dictyostelium* lysosomal enzymes. The weak bases ammonium chloride and chloroquine differentially affect proteolytic processing and sorting. *Journal of Biological Chemistry* **264**, 3454-3463 (1989).
  - 36 Piguet, V. *et al.* Nef-induced CD4 degradation: a diacidic-based motif in Nef functions as a lysosomal targeting signal through the binding of  $\beta$ -COP in endosomes. *Cell* **97**, 63-73 (1999).
  - 37 Piguet, V. *et al.* HIV-1 Nef protein binds to the cellular protein PACS-1 to downregulate class I major histocompatibility complexes. *Nature cell biology* **2**, 163-167 (2000).
  - 38 Prescott, A., Lucocq, J. & Pannambalam, V. TGN46 is localised in distinct domains of the HeLa cell Golgi apparatus. *Eur. J. Cell Biol* **72**, 238-246 (1997).
  - 39 Haller, C. *et al.* HIV-1 Nef and Vpu are functionally redundant broad-spectrum modulators of cell surface receptors, including tetraspanins. *Journal of virology* **88**, 14241-14257 (2014).
  - 40 Chaudhuri, R., Lindwasser, O. W., Smith, W. J., Hurley, J. H. & Bonifacino, J. S. Downregulation of CD4 by human immunodeficiency virus type 1 Nef is dependent on clathrin and involves direct interaction of Nef with the AP2 clathrin

- adaptor. *J Virol* **81**, 3877-3890, doi:JVI.02725-06 [pii]  
10.1128/JVI.02725-06 (2007).
- 41 Ren, X., Park, S. Y., Bonifacino, J. S. & Hurley, J. H. How HIV-1 Nef hijacks the AP-2 clathrin adaptor to downregulate CD4. *Elife* **3**, e01754 (2014).
  - 42 Wonderlich, E. R., Williams, M. & Collins, K. L. The tyrosine binding pocket in the adaptor protein 1 (AP-1)  $\mu$ 1 subunit is necessary for Nef to recruit AP-1 to the major histocompatibility complex class I cytoplasmic tail. *Journal of Biological Chemistry* **283**, 3011-3022 (2008).
  - 43 Janvier, K. & Bonifacino, J. S. Role of the endocytic machinery in the sorting of lysosome-associated membrane proteins. *Molecular biology of the cell* **16**, 4231-4242, doi:10.1091/mbc.E05-03-0213 (2005).
  - 44 Roberts, R. *et al.* Endosome fusion in living cells overexpressing GFP-rab5. *Journal of cell science* **112**, 3667-3675 (1999).
  - 45 Blagoveshchenskaya, A. D., Thomas, L., Feliciangeli, S. F., Hung, C.-H. & Thomas, G. HIV-1 Nef downregulates MHC-I by a PACS-1-and PI3K-regulated ARF6 endocytic pathway. *Cell* **111**, 853-866 (2002).
  - 46 Kasper, M. R. *et al.* HIV-1 Nef disrupts antigen presentation early in the secretory pathway. *Journal of Biological Chemistry* **280**, 12840-12848 (2005).
  - 47 Ishido, S., Wang, C., Lee, B.-S., Cohen, G. B. & Jung, J. Downregulation of major histocompatibility complex class I molecules by Kaposi's sarcoma-associated herpesvirus K3 and K5 proteins. *Journal of Virology* **74**, 5300-5309 (2000).
  - 48 Usami, Y., Wu, Y. & Göttlinger, H. G. SERINC3 and SERINC5 restrict HIV-1 infectivity and are counteracted by Nef. *Nature* **526**, 218-223 (2015).
  - 49 Rosa, A. *et al.* HIV-1 Nef promotes infection by excluding SERINC5 from virion incorporation. *Nature* **526**, 212-217 (2015).
  - 50 Saeed, M. F., Kolokoltsov, A. A., Albrecht, T. & Davey, R. A. Cellular entry of ebola virus involves uptake by a macropinocytosis-like mechanism and subsequent trafficking through early and late endosomes. *PLoS Pathog* **6**, e1001110 (2010).
  - 51 Chu, J. & Ng, M. Infectious entry of West Nile virus occurs through a clathrin-mediated endocytic pathway. *Journal of virology* **78**, 10543-10555 (2004).
  - 52 Nair-Gupta, P. *et al.* TLR signals induce phagosomal MHC-I delivery from the endosomal recycling compartment to allow cross-presentation. *Cell* **158**, 506-521 (2014).
  - 53 Grommé, M. *et al.* Recycling MHC class I molecules and endosomal peptide loading. *Proceedings of the National Academy of Sciences* **96**, 10326-10331 (1999).
  - 54 Rojas, R. *et al.* Regulation of retromer recruitment to endosomes by sequential action of Rab5 and Rab7. *The Journal of cell biology* **183**, 513-526 (2008).

- 55 Shugars, D. C. *et al.* Analysis of human immunodeficiency virus type 1 nef gene sequences present in vivo. *Journal of virology* **67**, 4639-4650 (1993).
- 56 Schneider, C. A., Rasband, W. S. & Eliceiri, K. W. NIH Image to ImageJ: 25 years of image analysis. *Nat methods* **9**, 671-675 (2012).
- 57 Abràmoff, M. D., Magalhães, P. J. & Ram, S. J. Image processing with ImageJ. *Biophotonics international* **11**, 36-42 (2004).
- 58 Bolte, S. & Cordelieres, F. A guided tour into subcellular colocalization analysis in light microscopy. *Journal of microscopy* **224**, 213-232 (2006).

## Chapter 4

### 4 PACS-1 and Adaptor Protein 1 mediate ACTH trafficking to the regulated secretory pathway

#### 4.1 Introduction

In addition to the constitutive secretion of proteins into the extracellular milieu, endocrine and neuroendocrine cells also possess a specialized form of secretion termed “regulated secretion” (1-3). The latter pathway is a controlled cellular process that ensures the release of intracellular contents, such as hormones in response to the appropriate physiological stimuli (4). Interestingly, regulated secretion is often preceded by the specific targeting of unprocessed pro-hormones to a specialized subcellular storage organelle termed the dense core secretory granule (DCSG) (5, 6). Within DCSGs, pro-hormones and their substrates can be processed into their active forms. Upon receiving the appropriate physiological stimulus, vesicles containing DCSG resident cargo fuse with the plasma membrane, and are secreted into the extracellular milieu (6).

Pro-opiomelanocortin (POMC) is a pro-hormone that undergoes proteolytic cleavage to produce smaller active peptide hormones within DCSGs (7-9). This activity requires the co-targeting of both POMC, and the pro-hormone convertases (PC) family of enzymes to DCSGs where they mediate the conversion of POMC to its active forms ((10) and reviewed in (11)). The products generated upon the proteolytic processing of the POMC precursor in pituitary DCSGs induce drastic sympathetic and cellular responses upon their regulated secretion (12). Products generated from POMC cleavage by PCs include peptide hormones, such as  $\alpha/\beta/\gamma$  melanotropin; which regulate skin pigmentation (13),  $\beta$ -endorphin; an endogenous opioid (14), and adrenocorticotrophic hormone (ACTH); a key mediator in hypothalamic-pituitary-adrenal signaling (12). ACTH specifically controls the release of additional steroid hormones and cholesterol from the adrenal glands. Importantly, the mis-sorting of POMC and its processing enzymes away from DCSGs has been associated with various disease states, such as Addison’s disease (15), Cushing’s disease (16), and Hermansky-Pudlak syndromes (17).

Multiple membrane trafficking proteins have been described as playing distinct roles in the sorting and processing of peptide hormones, however it remains unknown if these proteins affect the sorting of POMC to DCSGs. A critical membrane trafficking protein family is the heterotetrameric clathrin adaptor proteins (APs), AP-1 and AP-3, which mediate key stages of DCSG formation and release (18). AP-1 is critical in selectively removing cargo from the maturing DCSGs, such as the Vesicular Associated Membrane Protein-4 (VAMP4) (19), Calcium Independent-Mannose-6-Phosphate Receptor (CI-MPR) (20) and furin (21). Furthermore, knockdown of the AP-3 $\delta$  subunit in *C. elegans* results in defects in DCSG density, size, and number (22). Interestingly, the regulation of AP-1 and AP-3 relies on their ability to interact with the multifunctional membrane trafficking regulator Phosphofurin Acidic Cluster Sorting protein 1 (PACS-1) (23). Specifically, the PACS-1:AP-1 interaction is mediated through PACS-1 residues 174-182, and facilitates the removal of VAMP4 from immature secretory granules through the VAMP4 motif (E<sub>27</sub>DDSDEEED) located in the VAMP4 cytoplasmic tail (19, 23). Furthermore, sorting of the cellular endopeptidase furin away from maturing secretory vesicles is mediated through PACS-1 and AP-1 (21). Additionally, the tight regulation of CI-MPR trafficking mediated by PACS-1 and AP-1 aids in the targeting of lysosomal hydrolases to endosomes, thereby decreasing luminal pH (24), a phenomenon that is associated with the regulation of DCSG formation and proper sorting of ACTH to the regulated secretory pathway (25, 26). Thus, through its ability to regulate AP-mediated trafficking, PACS-1 regulates multiple membrane trafficking steps within the cell, making it a hub for membrane trafficking, including cargo in the regulated secretory pathway.

Herein, we provide evidence that identifies PACS-1 and AP-1 as key mediators in the sorting of POMC to the regulated secretory pathway. We observed that mutation of the PACS-1: AP binding site decreases the ability of PACS-1 to co-localize with ACTH-positive DCSGs. Furthermore, knockdown of PACS-1 and AP-1 decreases DCSG formation, decreases intracellular ACTH storage, and increases extracellular ACTH levels in the absence of stimuli. Importantly, upon knockdown of PACS-1 and AP-1, we observed a significant increase in ACTH localized to the unregulated secretory pathway.



## 4.2 Results

### 4.2.1 PACS-1 and AP-1 promote intracellular storage of POMC

PACS-1 mediates trafficking of multiple proteins to and from the TGN (TGN) through its ability to recruit AP-1 and AP-3 (23). Thus, we sought to test for a role of PACS-1, AP-1, and AP-3 in the sorting of POMC to DCSGs by performing knockdown studies in mouse pituitary AtT-20 cells, which endogenously expresses POMC (7). Transfection of siRNAs targeting the *PACS-1*, *AP-1*, or *AP-3* genes resulted in approximately 50% knockdown relative to non-specific siRNA, as determined by qRT-PCR, confirming that our knockdowns were effective (Fig. 4.1A). Subsequent to siRNA transfection, intracellular levels of POMC and its intermediates were assessed by Western blotting (Fig. 4.1B). Specifically, we utilized the previously described antibody that recognizes residues 1-18 of the POMC-derived ACTH peptide, thus detecting the ACTH-containing processed forms from full length POMC (27). Total intracellular POMC cleavage products detected by Western blot were quantified using densitometry (Fig. 4.1C). Strikingly, upon knockdown of PACS-1, we observed a 50% reduction in intracellular POMC-derived peptides compared to that of the non-specific siRNA. The knockdown of AP-1 resulted in a similar reduction of intracellular POMC, however, knockdown of AP-3 did not significantly alter the intracellular storage levels of POMC (Fig. 4.1C).

Upon external stimulation, DCSGs undergo fusion with the plasma membrane to release their contents into the extracellular environment via exocytosis (4). Therefore, we next sought to determine if the observed decrease in intracellular storage of POMC-derived peptides upon knockdown of PACS-1 or AP-1 is the result of increased secretion of the POMC-derived peptide, ACTH, in the absence of external stimulation. To test this, we transfected AtT-20 cells with siRNA towards PACS-1, AP-1, AP-3 or a non-specific control and subjected the cell culture supernatants to MAGPIX analysis. These experiments were conducted in the absence of stimulus and thus represent the constitutive, or unregulated secretion of ACTH. We observed 1.5 fold and 1.25 fold increases in ACTH in the cell culture supernatant upon knockdown of PACS-1 and AP-1, respectively, compared to the non-specific control siRNA (Fig. 4.1D). In contrast, increased levels of extracellular ACTH were not detected in cell culture supernatants

from AP-3 knockdown cells (Fig. 4.1D). These findings indicate that upon knockdown of PACS-1 or AP-1 unregulated secretion of ACTH occurs, suggesting that sorting of POMC to the regulated secretory pathway is dependent on the membrane trafficking proteins PACS-1 and AP-1, but not necessarily AP-3.

To further assess the role of PACS-1 and its binding partners AP-1 and AP-3 in the sorting of POMC-derived peptides to DCSGs, we visualized the localization of ACTH in AtT-20 cells using widefield microscopy (Fig. 4.2). Accordingly, we co-transfected siRNA against PACS-1, AP-1, AP-3 or a non-specific sequence with a plasmid expressing a fluorescently labeled marker of the unregulated secretory pathway, the transferrin receptor (TfnR) (28), and examined the cells via microscopy (Fig. 4.2A). We subsequently compared the co-localization of POMC/ACTH with GFP-tagged TfnR (TfnR-GFP) in the presence or absence of siRNA targeting the various trafficking proteins (Fig. 4.2B). Interestingly, our results suggest that in PACS-1 knockdown cells, POMC/ACTH is shunted to the unregulated secretory pathway, as we observed an increased co-localization of POMC/ACTH with TfnR-GFP (siPACS-1; Fig. 4.2B & C; Pearson's Coefficient = 0.49), compared to the scrambled siRNA control (siNS; Fig. 4.2B & C; Pearson's Coefficient = 0.32). Similarly, knockdown of AP-1 or AP-3 resulted in a significant increase in the co-localization of ACTH with TfnR-GFP (Pearson's Coefficient = 0.46, 0.49, respectively). Taken together, these results support the hypothesis that PACS-1 and Adaptor Proteins play important roles in the trafficking of POMC/ACTH away from the unregulated secretory pathway.

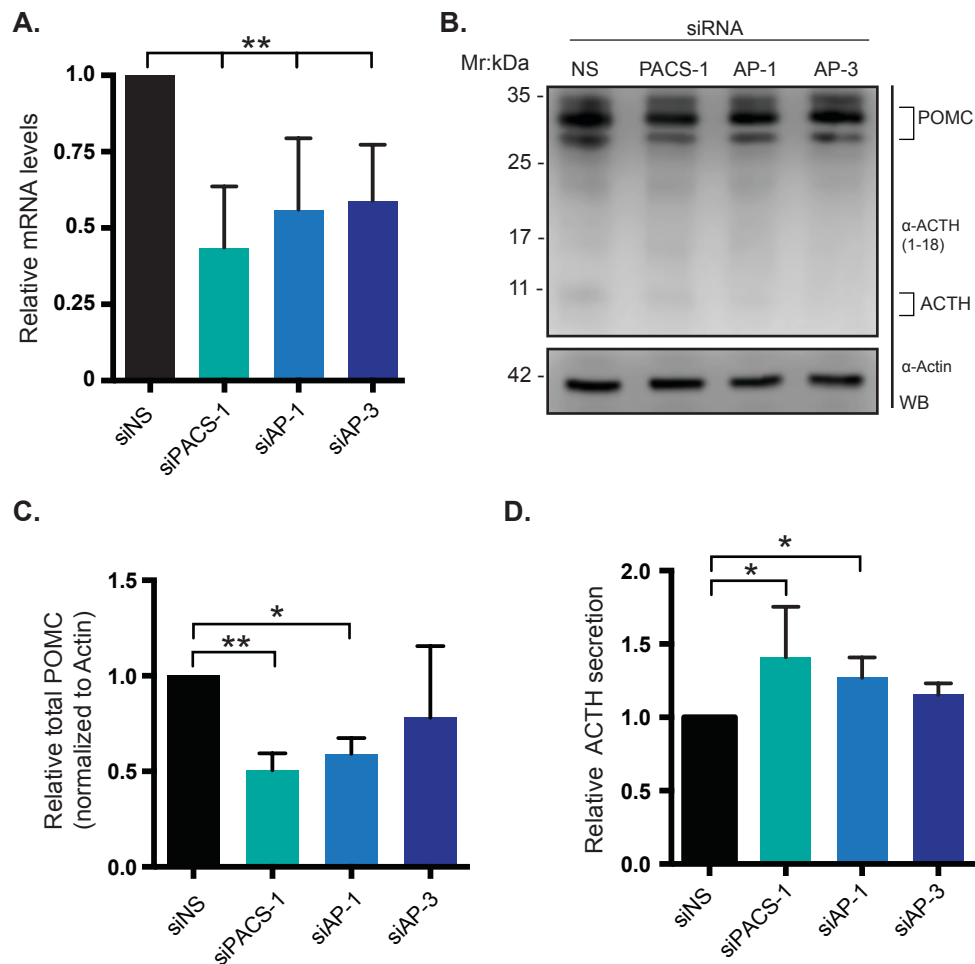


**Figure 4.1: Intracellular storage of POMC is regulated by PACS-1 and AP-1.**

AtT-20 cells were transfected with siRNA targeting *PACS-1*, *AP-1*, *AP-3* or scrambled control. Forty-eight hours post transfection, cell-associated and cell culture supernatant-associated POMC was quantified. (A) Knockdown efficiency of siRNA transfections was determined by reverse transcription of cellular RNA to cDNA followed by quantification of siRNA target cDNA via qRT-PCR. Percent knockdown was calculated by comparing relative cDNA levels within cells transfected with targeting siRNA versus the scrambled control (n=6). (B) AtT-20 cell lysates were subjected to Western blot 48 hours post siRNA transfection with antibodies targeting ACTH 1-18, and the loading control Actin. (C) Quantification of mean ( $\pm$  standard error) intracellular POMC protein levels was

completed following Western blot quantification. Levels of POMC were calculated relative to actin and subsequently normalized to that of POMC in the scrambled control siRNA treated cells. Shown is the quantification of 5 independent experiments (n=5). (D) Supernatants of siRNA transfected cells were subjected to quantification of secreted extracellular ACTH using a MAGPIX assay. Mean relative extracellular ACTH (+/- standard error), compared to scrambled control siRNA, was calculated from 3 independent experiments (n=3). (\* Indicates p-value <0.05, \*\* p-value <0.01; WB: Western blot).

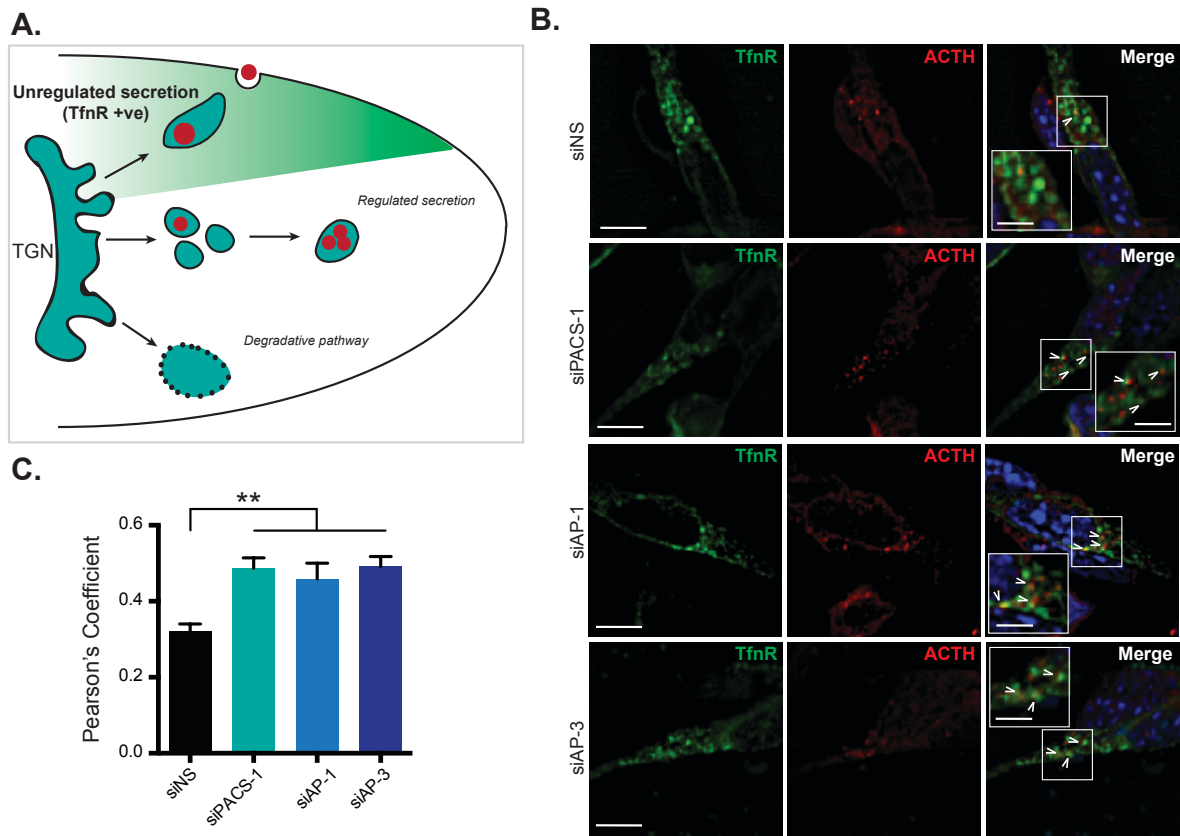


**Figure 4.2: PACS-1, AP-1 and AP-3 are required for the sorting of ACTH to the regulated secretory pathway.**

AtT-20 cells were co-transfected with siRNA targeting *PACS-1*, *AP-1*, *AP-3* or a scrambled control and GFP-tagged transferrin receptor (TfnR-GFP). Forty-eight hours post transfection cells were immunostained for ACTH 1-18 and imaged via widefield microscopy. (A) Schematic of potential fates of POMC-derived peptides in neuroendocrine cells. Highlighted is the constitutive secretory pathway wherein TfnR<sup>+</sup> vesicles are present. (B) Representative images of cells co-transfected with siRNA targeting *PACS-1* (siPACS-1), *AP-1* (siAP-1), *AP-3* (siAP-3) or a scrambled control (siNS), and TfnR-GFP. Shown are TfnR-GFP (Green), ACTH (Red) and DAPI (Blue). Scale bar represent 10 μm, inset scale bars represent 5 μm. (C) The co-localization between TfnR-GFP and ACTH was determined by calculating the mean (+/- standard

error) Pearson's correlation coefficient in at least 30 cells from 3 independent experiments. (\*\* Indicates  $p\text{-value} > 0.01$ ).

#### 4.2.2 ACTH is not directed to a lysosomal degradation pathway

We next tested if the reduced intracellular storage of POMC-derived peptides upon PACS-1 and AP-1 silencing could be attributed to the trafficking of POMC molecules to a degradative lysosomal compartment. To assess this, we analyzed ACTH co-localization with the lysosomal marker LAMP-1 in the presence of PACS-1, AP-1, AP-3 or control siRNA (Fig. 4.3A). Forty-eight hours post transfection, cells were fixed and immunostained for ACTH (Red; Fig. 4.3B) and the lysosomal marker LAMP1 (Green; Fig. 4.3B). Co-localization analysis between LAMP1 and ACTH revealed that decreased expression of PACS-1, AP-1 or AP-3 does not result in the trafficking of ACTH to a lysosomal compartment, compared to control siRNA (Fig. 4.3C). Taken together, these results suggest that the observed decrease in intracellular storage of POMC-derived peptides is not driven through the degradation of ACTH, but rather through mis-trafficking to the unregulated secretory pathway.

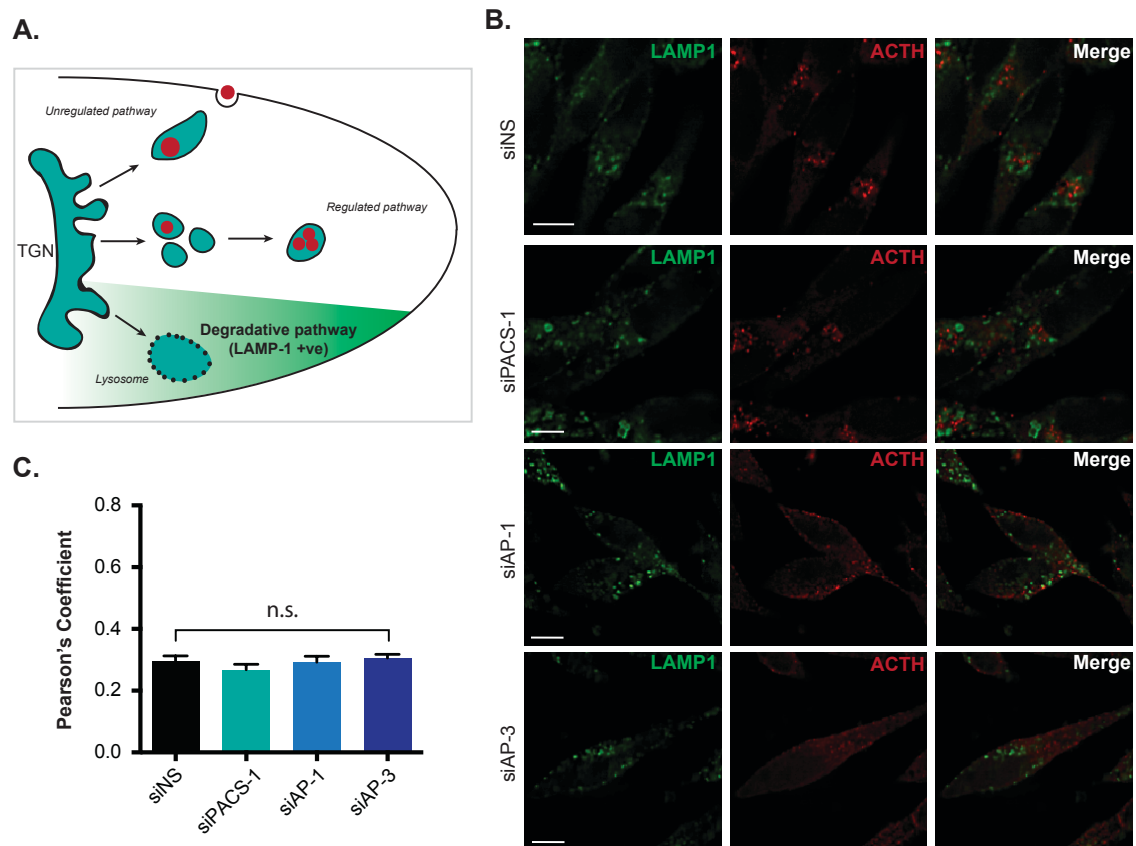


**Figure 4.3: ACTH is not targeted to the degradative lysosomal compartment.**

AtT-20 cells were transfected with siRNA towards *PACS-1*, *AP-1*, *AP-3* and scrambled control. Forty-eight hours post transfection, AtT-20 cells were immunostained for LAMP1 and ACTH. (A) Schematic of potential fates of POMC-derived peptides in neuroendocrine cells. Highlighted is the degradative pathway wherein LAMP1<sup>+</sup> lysosomes are present. (B) Representative images of cells transfected with siRNA targeting *PACS-1* (siPACS-1), *AP-1* (siAP-1), *AP-3* (siAP-3) or a scrambled control (siNS). Cells are stained for LAMP1 (Green) and ACTH (Red). Scale bar represent 10  $\mu$ m. (C) Co-localization between LAMP1 and ACTH staining was scored by calculating the mean (+/- standard error) Pearson's correlation coefficient by quantification of at least 40 cells in 3 independent experiments. (n.s. represents not significant, LAMP1; Lysosomal associated membrane protein - 1).



### 4.2.3 PACS-1: Adaptor Protein interactions modulate PACS-1:ACTH co-localization

Both PACS-1 and AP-1 act in concert to recognize cargo and modulate their localization within cells. Alteration of the AP-1 binding site on PACS-1 can modify the trafficking of itinerant cargo (23). For example, expression of a dominant-negative form of PACS-1, which is defective in AP-1/3 binding (termed ADMUT; **A**daptor Protein binding **M**utant), alters the localization AP-1, preventing Furin trafficking from endosomes to the TGN (23). Our findings demonstrate that PACS-1, AP-1, and AP-3 are critical in the sorting of POMC, and its derivatives, to the regulated secretory pathway (Fig. 4.2). Therefore, we sought to determine if PACS-1 co-localized with POMC-positive vesicles in an Adaptor Protein dependent manner. To test this, we transfected expression vectors encoding wildtype PACS-1-GFP (Green; Fig. 4.4A) into AtT-20 cells, or the dominant negative mutant of PACS-1, ADMUT-GFP (Green; Fig. 4.4B), and immunostained for ACTH (Red, Fig 4.4A and B). We subsequently examined co-localization between PACS-1/ADMUT and ACTH through super-resolution ground-state depletion microscopy (GSDM) using nearest neighbor spatial association analysis (29, 30) (SAA; Fig. 4.4). GSDM allows for a 10-fold increase in resolution compared to conventional widefield or confocal microscopy, and therefore enables the quantitative measurement of intermolecular distances between acquisition channels to determine the ability of fluorescently labeled proteins to associate (30). Interestingly, we observed that over 60% of ACTH co-localized with PACS-1-GFP (Fig. 4.4A and D). Furthermore, SAA revealed that this co-localization occurred at a much greater rate than expected of randomly positioned molecules, suggesting that PACS-1 is within close proximity to ACTH vesicles, whereby it may be exerting its sorting function (Fig. 4.4C and D). Upon expression of ADMUT-GFP we observed a 30% reduction in co-localization of ACTH and ADMUT-GFP compared to wildtype PACS-1-GFP, as determined via super-resolution nearest-neighbor analysis (Fig. 4.4B and D). Overall, these results indicate that the interaction between PACS-1 and Adaptor Proteins, such as AP-1, facilitate localization of PACS-1 to ACTH containing compartments.

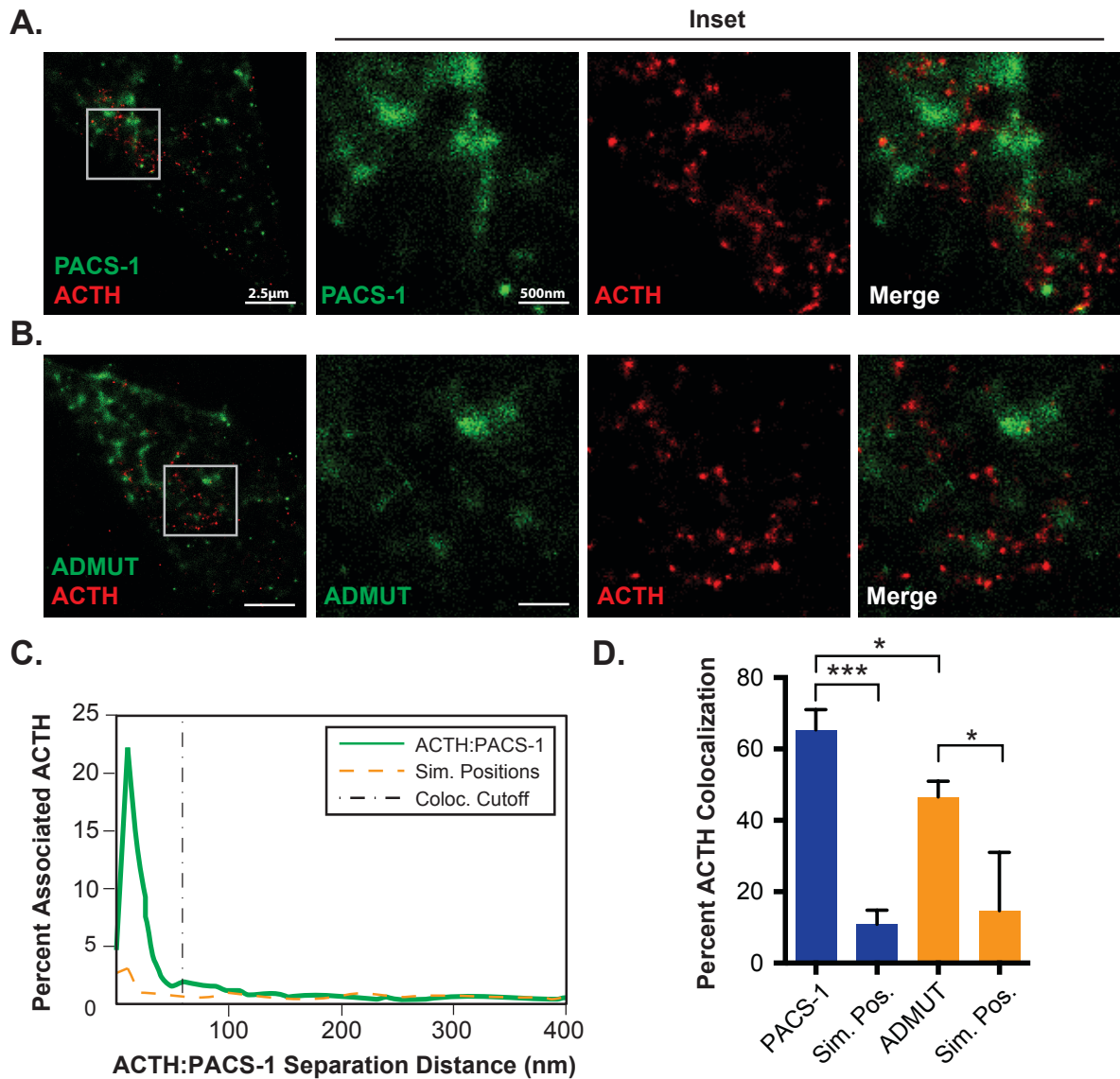


**Figure 4.4: PACS-1 co-localizes to POMC+ vesicles in AtT-20 cells.**

AtT-20 cells were transfected with PACS-1-GFP or ADMUT-GFP and forty-eight hours post transfection, cells were fixed, immunostained for ACTH, and imaged using ground-state depletion super-resolution microscopy. (A+B) Representative images of AtT-20 cells transfected with PACS-1-GFP (A; Green) or ADMUT-GFP (B; Green) and immunostained for ACTH (Red) (scale bars represent 2.5 $\mu$ m, inset scale bars represent 500nm). (C) A representative histogram mapping the intermolecular distances between

ACTH and PACS-1 (Green) or simulated random position (Orange). Co-localization cut-off is illustrated (black dashed line). (D) A graphical representation of the mean ( $\pm$  standard error) percent of ACTH co-localized to PACS-1 or ADMUT-GFP, or ACTH co-localized to randomly simulated positions. Error bars were calculated by quantification of 6 cells in 2 independent experiments. (\* p-value < 0.05; \*\*\* p-value < 0.001)

#### 4.2.4 PACS-1 facilitates the trafficking of ACTH to mature secretory granules

We next sought to define if PACS-1 and Adaptor Proteins specifically mediate the targeting of ACTH to DCSGs. To ascertain this, we used the vesicular associated membrane protein 2 (VAMP2) as a marker for DCSGs (31). Due to the observed increase in constitutive secretion of ACTH upon knockdown of PACS-1 and AP-1 (Fig. 4.1D), we investigated the ability for ACTH to be targeted to VAMP2 positive DCSGs in the presence or absence of siRNA targeting PACS-1, AP-1 or AP-3 (Fig. 4.5A). To test this, we co-transfected AtT-20 cells with siRNA targeting PACS-1, AP-1, AP-3 or a scrambled control siRNA and a GFP-tagged VAMP2 (Green). Cells were imaged by widefield fluorescence microscopy and scored for ACTH (Red) and VAMP2 (Green) co-localization through the Pearson's Coefficient (Fig. 4.5B and C). We observed a robust co-localization in control cells (Pearson's Coefficient  $\sim 0.41$ ), consistent with the storage of the ACTH peptide hormone within mature granules. Strikingly, upon knockdown of PACS-1, we observed a significant reduction in the ability of ACTH to be localized to a VAMP2-positive compartment (Fig. 4.5C), highlighting the role of PACS-1 in sorting ACTH to mature granules. Furthermore, knockdown of AP-1 resulted in an even greater reduction of ACTH localization to VAMP2-positive compartments (Fig. 4.5B and C). However, knockdown of AP-3 did not have a significant effect on VAMP2 co-localization, consistent with our previous secretion assay results (Fig. 4.1D). Taken together, the results demonstrate the importance of PACS-1 and AP-1 in sorting ACTH containing vesicles to mature secretory granules.

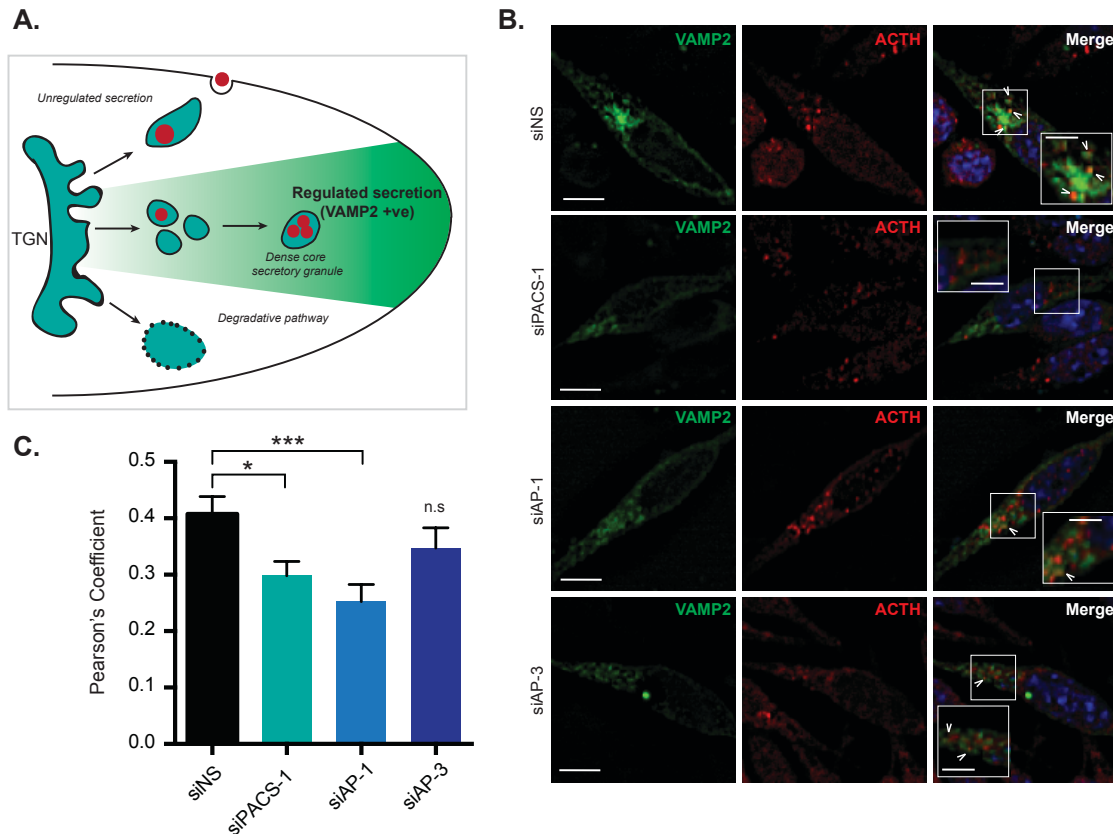


**Figure 4.5: PACS-1 and AP-1 facilitate the sorting of POMC to mature secretory granules.**

AtT-20 cells were co-transfected with siRNA against *PACS-1*, *AP-1*, *AP-3* or scrambled control and a plasmid encoding GFP-tagged Vesicular Associated Membrane Protein – 2 (VAMP2-GFP). Forty-eight hours post transfection cells were fixed and immunostained for ACTH. (A) Schematic of potential fates of POMC-derived peptides in neuroendocrine cells. Highlighted is the regulated secretory pathway wherein VAMP2<sup>+</sup> mature secretory vesicles / DCSGs are present. (B) Shown are representative images illustrating VAMP2-GFP (Green), ACTH (Red) and DAPI (Blue) in cells transfected with siRNA targeting *PACS-1* (siPACS-1), *AP-1* (siAP-1), *AP-3* (siAP-3) or a scrambled control (siNS). Scale bar represent 10µm, inset scale bars represent 5µm. (C) The mean (+/- standard error) co-localization between ACTH and VAMP2-GFP was scored by calculating the Pearson's correlation coefficient using the JACoP plugin on ImageJ from the quantification of at

least 25 cells from 3 independent experiments. (\* indicates  $p\text{-value} < 0.05$ ; \*\*\*  $p\text{-value} < 0.001$ ; n.s. represents not significant).

### 4.3 Discussion

In the current report, we demonstrate that the membrane trafficking regulator proteins PACS-1 and AP-1 regulate trafficking of the peptide hormone ACTH to DCSGs. We observed decreased DCSG sorting of ACTH upon PACS-1 and AP-1 depletion (Fig. 4.5). Moreover, in the absence of PACS-1 and AP-1, ACTH was secreted into the extracellular environment in the absence of a stimulus (Fig. 4.1D).

The role of PACS-1 in the trafficking of cellular cargo is essential for cellular homeostasis. To achieve this, PACS-1 has been described as a multifunctional connector molecule that bridges itinerant cargo to Adaptor Proteins, such as AP-1 (23). These protein-protein interactions are assured by binding sites that are primarily located in the PACS-1 binding site for the prototypical PACS-1 cargo protein, furin, known as the furin binding region (32). Characterizing these PACS-1 protein-binding sites had previously enabled a preliminary understanding its role in the secretory pathway. Indeed, mutational analysis of the protein-binding sites in PACS-1 demonstrated that PACS-1 retrieves furin from immature secretory granules and traffics it to the TGN (21). Furthermore, trafficking of furin away from immature secretory granules was blocked in the presence of PACS-1 ADMUT, demonstrating the importance of the PACS-1:AP-1 interaction on targeting proteins to the secretory pathway, consistent with our determination of a role for PACS-1:AP-1 interaction in sorting ACTH to DCSGs (Fig. 4.4) (32). Interestingly, PACS-1 also serves an important role in HIV-1 mediated immune evasion by acting as a connector molecule between the viral accessory protein Nef and AP-1 to downregulate the antiviral molecule MHC-I from the surface of immune cells (33-35). Thus, viruses, such as HIV-1, have also evolved to use PACS-1 and AP-1 to shuttle cargo to diverse locations (36).

Here, we present data identifying novel membrane trafficking proteins that mediate sorting of the ACTH precursor protein POMC. Processing of POMC is mediated by prohormone convertase- 1 and 2 (PC-1 and PC-2)(9). The cleavage events that activate POMC can occur at both early stages in the regulated secretory pathway, within the TGN, and at later stages within acidic DCSG compartments (7, 9, 37, 38). Thus, processing to produce ACTH and other peptide hormones requires the correct sorting of POMC, PC1,

and PC2 to the TGN and subsequently DCSGs (11, 39). Defects in the processing ability of POMC can be observed upon knockout of PC1 or PC2, or mutation of POMC itself (38). Interestingly, the processing of POMC was not affected when PACS-1 or Adaptor Protein levels were reduced (Fig. 4.1). This is consistent with the notion that PACS-1 may mediate sorting of POMC-derived peptides following PC cleavage. Alternatively, upon depletion of PACS-1 and AP-1, PCs and POMC may mis-localize to the same compartment, wherein POMC can still be cleaved into active components, yet is secreted in an unregulated fashion. Therefore, in future experiments it would be interesting to examine localization of PC-1 and PC-2 upon knockdown of PACS-1 or AP-1.

Nonetheless, our results demonstrate a distinct role of PACS-1 and AP-1 in routing POMC-derived ACTH toward the regulated secretory pathway as knockdown of PACS-1 and AP-1 resulted in shuttling of ACTH toward the unregulated secretory pathway (Fig. 4.2), and away from DCSGs (Fig. 4.5). Interestingly, similar defects in ACTH trafficking have been observed when endosomes have been globally de-acidified through  $\text{NH}_4\text{Cl}$  treatment or inhibition of vacuolar ATPase activity (25, 26). This suggests that PACS-1 may be impacting the acidification of secretory granules through the altered trafficking of a cellular ATPase.

Cleavage and activation of POMC is also achieved by the peptidase Carboxypeptidase E (CPE) (40, 41). CPE itself has also been proposed to assist in the targeting of POMC-derived hormones, such as ACTH, to the secretory pathway (42). Indeed, CPE knockout mice exhibit decreased ability to process POMC (42). Furthermore, the POMC-derived peptides that became processed were unable to be properly stored within granules, resulting in these mice containing elevated serum levels of ACTH (43). These results are akin to our data, whereby upon reduced expression of PACS-1 and AP-1 we observed a striking defect in POMC storage and increased ACTH secretion, even in the absence of stimuli (Fig. 4.1). This data suggests that PACS-1 and AP-1 may be impacting trafficking and sorting steps similar to those mediated by CPE, or alternatively may act in concert with CPE. However, it is unlikely that PACS-1 or Adaptor Proteins directly affect CPE itself given that it lacks a canonical PACS-1 recognition motif and may not be accessible to the cytosolic PACS-1 protein (44, 45).



Previous studies utilizing a siRNA knockdown model identified a role for AP-3 in mediating specific sorting steps of cargo into storage granules, as well as inducing their ability to fuse with the plasma membrane upon stimulation (22). However, little is known about the specific role of AP-3 in the sorting of diverse cargo, such as POMC. AP-3 is responsible for the localization of vesicle fusion proteins to neuronal synapses (46), and is required for efficient release of neurotransmitters (47). Likewise, AP-3 also facilitates trafficking of fusion proteins to cytolytic granules in CD8 positive T cells (48). Moreover, loss of AP-3 function can lead to impairment in these processes and development of diseased states (17). Interestingly, knockdown of AP-3 has been associated with the routing of the DCSG-resident protein, Secretogranin II, to the unregulated secretory pathway (22). In agreement with these findings, we observed that knockdown of AP-3 resulted in an increase in ACTH localization to the constitutive pathway (Fig. 4.2C). However, we did not observe a corresponding decrease in sorting of ACTH into VAMP2 positive granules (Fig. 4.5C), nor did we observe an increase in extracellular ACTH secretion upon AP-3 knockdown (Fig. 4.1D). It is possible that AP-3 knockdown results in the compensation by other adaptor protein molecules, or that ACTH does not follow the AP-3 dependent pathway previously described. Indeed, not all DCSGs contain the same cargo, suggesting that different adaptors can modulate cargo differently (49).

Overall, we provide evidence supporting the key role of PACS-1 and AP-1 in controlling peptide hormone storage within AtT-20 cells. We also highlight the role of the PACS-1: Adaptor Protein interaction in the recruitment of PACS-1 to ACTH positive vesicles, and the role of PACS-1 and AP-1 in the storage of ACTH within cells. Controlling the release of peptide hormones is an important physiological process, which requires multiple proteins. Studying how these proteins work together is fundamental to understanding how different pathways can be altered in homeostasis and disease.

## 4.4 Materials and Methods

### 4.4.1 Cell Culture

AtT-20 cells (ATCC; catalog #CCL-89) were cultured in complete Dulbecco's Modified Eagle's Medium (DMEM; Hyclone, Logan, UT) supplemented with 10% fetal bovine serum (Wisent, Montreal, Canada), 10 $\mu$ M L-Glutamine (HyClone), and 100 $\mu$ M penicillin and streptomycin (Hyclone). Cells were grown at 37 °C in the presence of 5% CO<sub>2</sub> and sub-cultured in accordance with supplier's recommendations.

### 4.4.2 Plasmids and siRNA

Plasmids encoding VAMP2-GFP-C3 and GFP-tagged transferrin receptor were obtained as a kind gift by Thierry Galli (French Institute for Health and Medical Research; Addgene plasmid #42308) (50), and by Dr. Ron Flanagan (Western University), respectively. PACS-1 cDNA was provided by Dr. Gary Thomas (University of Pittsburgh), and was sub-cloned into the pEGFP-N1 vector to yield a C-terminally GFP-tagged PACS-1 construct. Additionally, ADMUT-GFP was generated by PCR overlap mutagenesis (Primers in Table 1). For knockdown experiments, siRNA against PACS-1 (CCUUAGCUGUGGGACUCAUTT), AP-1  $\mu$ -1 (GUAUCGGAAGAAUGAAGUATT), AP-3  $\delta$ -1 (GCGAUGAACUGCUCACCAATT) and a scrambled control were obtained from Life Technologies (Carlsbad, California, USA).

### 4.4.3 Transfections

To quantify intracellular and extracellular levels of ACTH, 3 x 10<sup>5</sup> AtT-20 cells were seeded into 12 well dishes and 24 hours later, cells were transfected with 2.5 $\mu$ M siRNA using PepMute<sup>TM</sup> siRNA Transfection Reagent (FroggaBio, North York, Canada) in accordance with the manufacturers' recommendations. Twenty-four hours post transfection, media was replaced with complete DMEM, and 48 hours post-transfection cells lysates and supernatants were collected for Western blot and MAGPIX analysis, respectively. For microscopy experiments, 3 x 10<sup>5</sup> AtT-20 cells were seeded on coverslips, and 24 hours later, cells were transfected with 2.5 $\mu$ M siRNA and 1 $\mu$ g of the

appropriate plasmid DNA using PepMute™ siRNA transfection Reagent. Forty-eight hours post transfection, cells were fixed and prepared for imaging. For ground-state-depletion imaging, cells were seeded on coverslips as previously described above. Cells were then transfected with plasmids encoding GFP-tagged PACS-1 or GFP-tagged ADMUT using PolyJet™ In Vitro DNA Transfection Reagent (FroggaBio), in accordance with manufacturers' recommendations. Forty-eight hours post transfection, cells were prepared for imaging and analysis.

#### 4.4.4 qRT-PCR

AtT-20 cells were transfected with siRNA, as described above. Cells were collected 48 hours post transfection, and RNA was extracted using Ambion RNA extraction kit (Life Technologies), as per the supplier's instructions. First strand cDNA synthesis was performed using the Superscript III RT cDNA synthesis kit (Life Technologies). Primer sequences for reverse-transcription quantitative PCR are outlined in Table 3.

Subsequently, cDNA was subjected to quantitative PCR using the SensiFast Probe Hi-Rox Kit (Bioline, Taunton, MA) and the Applied Biosystems QuantStudio 5 Real-time PCR system (Thermo Fisher Scientific, Waltham, Massachusetts, USA). Using *actin* as the reference gene, fold change in expression of the target gene was calculated using the delta CT ( $\text{actin}/\text{target}$ ), and compared to that of scrambled control siRNA. Fold change expression =  $1 - 2^{-(\text{CT}_{\text{actin}}_{\text{target}} - \text{CT}_{\text{siRNA}}_{\text{target}}) - (\text{CT}_{\text{actin}}_{\text{control}} - \text{CT}_{\text{siRNA}}_{\text{control}})}$ .

#### 4.4.5 Western Blots

To assess intracellular protein levels in siRNA transfected cells, forty-eight hours post-transfection cells were washed 2X with phosphate buffered saline (PBS), and lysed on ice with lysis buffer (0.5M HEPES, 1.25M NaCl, 1M MgCl<sub>2</sub>, 0.25M EDTA, 0.1% Triton X-100, 1X complete protease inhibitor tablets (Roche, Indianapolis, IN)). Cells were incubated on a rotator for 20 minutes at 4°C prior to centrifugation at 20,000 x g at 4°C for 30 minutes. Supernatants were collected and boiled for 10 minutes after addition of 5X SDS-PAGE sample buffer (5X Sample Buffer; 0.312M Tris pH 6.8, 25% 2-Mercaptoethanol, 50% glycerol and 10% SDS). Samples were run on a 14% SDS-PAGE gel and transferred onto a nitrocellulose membrane. Membranes were blocked in 5%

skim milk powder in TBST for 1 hour, and incubated overnight at 4°C with antibodies specific for the ACTH peptide residues 1-18 (1:1000; generously provided by Dr. Lindberg, University of Maryland) or Actin (1:3000; Thermo Scientific). Membranes were then washed 3X in TBST, incubated in species-specific HRP-conjugated secondary antibodies for 2 hours (1:2000; Thermo Scientific), and washed 3X in TBST. All blots were imaged using the C-Digit chemiluminescence Western blot scanner (LI-COR Biosciences, Lincoln, NE) with Crescendo ECL substrates (Millipore Inc.; Billerica, MA). Band intensities corresponding to peptides of 29 kDa, 26 kDa, and 9 kDa were quantified using the ImageQuant Studio software (LI-COR) and normalized to the Actin loading control.

#### 4.4.6 Extracellular ACTH Quantification

To quantify basal extracellular levels of ACTH, cells were transfected with siRNA, as described above. Forty-eight hours post transfection, cell culture media was removed and 250µl of fresh complete DMEM was added. Cells were then incubated at 37°C for 2 hours. Subsequently, cell supernatants were collected and centrifuged at 10 000 x g to remove particulate matter and supernatants were then subjected to MAGPIX analysis. Specifically, cell culture supernatants were subjected to the ACTH MILLIPLEX MAP mouse pituitary magnetic bead panel (Millipore, Burlington, Massachusetts) to quantify extracellular ACTH, as per the suppliers' protocol. Experimental samples were conducted in duplicate, and average values were reported as fold increase over the scrambled siRNA control treated cells.

#### 4.4.7 Widefield microscopy

Forty-eight hours post transfection, cells were washed 3X in PBS, fixed in 4% paraformaldehyde for 15 minutes, and subsequently washed 3X with PBS. All cells were blocked for 1 hour in blocking buffer (5% bovine serum albumin and 0.1% Triton X-100 in PBS). Cells were then incubated with rabbit anti-ACTH antibody diluted in blocking buffer (1:200;) and/or mouse anti-LAMP1 (1:100; clone 1D4B; Developmental Studies Hybridoma Bank; Iowa, USA) for 2 hours. Cells were washed 2X with blocking buffer, and incubated with the Goat-anti-mouse Cy3, or Goat-anti-Rabbit Alexafluor 647

secondary antibody (1:800; Jackson ImmunoResearch) for 1.5 hours. Following secondary antibody staining, cells were washed 3X with PBS, and mounted on Fluoromount-G mounting media containing DAPI nuclear stain. Cells were viewed on a Leica DMI6000B at 63X or 100X magnification using the FITC, CY5 and DAPI filter settings, and imaged with a Hamamatsu Photometrics Delta Evolve camera (Leica, Wetzlar, Germany). Images were deconvolved using the advanced fluorescence (Leica) application on the Leica Application Suite software. Co-localization analysis was performed using the Pearson's correlation coefficient from the ImageJ plugin JACoP, as described previously (51).

#### 4.4.8 Ground-state depletion microscopy

Super-Resolution imaging was performed as described previously (51). Briefly, cells were mounted, and imaged in a depression slide containing 100mM cysteamine (Sigma Aldrich). All images were acquired using a Leica SR GSD microscope with a 100X/1.43 NA objective lens containing a 1.6X magnifier. GFP and AlexaFluor 647 fluorophores were excited using 488nm and 647 nm laser lines respectively, and back pumped with a 30 mW 405 laser line. Resulting images were quantified using the spatial association analysis MliSR software as previously described (51) (Available for download: <http://phagocytes.ca/miisr/>). Co-localization between the two channels was quantified as percent association of ACTH to PACS-1/ADMUT.

#### 4.4.9 Statistics

All statistics were conducted using the unpaired t-test or the one-way ANOVA with multiple comparisons where indicated using Graph Pad Prism (Graph Pad Software Inc., La Jolla, CA).

**Table 3 Primers for mutagenesis and qRT-PCR**

Target	Primer ID	Sequence 5'→3'
<i>ADMUT forward</i>	JD-136	CTTCCAGCTAGTGGACTGGTGGCAGCAG CGGCCGCAGCAGCCGCCTCCCTTCAGTA CCCTCATTTCCTT
<i>ADMUT reverse</i>	JD-137	AAGGAAATGAGGGTACTGAAGGGAGGC GGCTGCTGCGGCCGCTGCTGCCACCAGT CCACTAGCTGGAAG
<i>pacsl forward</i>	JD-706	TTGTATGCTACCTGGGAGGTG
<i>pacsl reverse</i>	JD-707	AAATGAGGGTACTGGAGGGAG
<i>ap1m1 forward</i>	JD-712	TGGTGGCGTTCGTTTCATGT
<i>ap1m1 reverse</i>	JD-713	GCAGCTCGTAGATGATGACAAA
<i>ap3d1 forward</i>	JD-708	CGACCGCATGTTCGATAAGAA
<i>ap3d1 reverse</i>	JD-709	GCTTGATCTCGTCAATGCACTG
<i>actin forward</i>	JD-702	TCCTTCGTTGCCGGTCCACA
<i>actin reverse</i>	JD-703	CGTCTCCGGAGTCCATCACA

## 4.5 References

1. Kelly, R. B. (1985) Pathways of protein secretion in eukaryotes, *Science*. **230**, 25-32.
2. Burgess, T. L. & Kelly, R. B. (1987) Constitutive and regulated secretion of proteins, *Annual review of cell biology*. **3**, 243-293.
3. Moore, H. & Kelly, R. B. (1985) Secretory protein targeting in a pituitary cell line: differential transport of foreign secretory proteins to distinct secretory pathways, *The Journal of cell biology*. **101**, 1773-1781.
4. Emanuel, R. L., Adler, G. K., Kifor, O., Quinn, S. J., Fuller, F., Krapcho, K. & Brown, E. M. (1996) Calcium-sensing receptor expression and regulation by extracellular calcium in the AtT-20 pituitary cell line, *Molecular Endocrinology*. **10**, 555-565.
5. Orci, L., Ravazzola, M., Amherdt, M., Madsen, O., Perrelet, A., Vassalli, J.-D. & Anderson, R. (1986) Conversion of proinsulin to insulin occurs coordinately with

- acidification of maturing secretory vesicles, *The Journal of Cell Biology*. **103**, 2273-2281.
6. Schmidt, W. & Moore, H. (1995) Ionic milieu controls the compartment-specific activation of pro-opiomelanocortin processing in AtT-20 cells, *Molecular biology of the cell*. **6**, 1271-1285.
  7. Schnabel, E., Mains, R. E. & Farquhar, M. G. (1989) Proteolytic processing of pro-ACTH/endorphin begins in the Golgi complex of pituitary corticotropes and AtT-20 cells, *Molecular Endocrinology*. **3**, 1223-1235.
  8. Thomas, L., Leduc, R., Thorne, B. A., Smeekens, S. P., Steiner, D. F. & Thomas, G. (1991) Kex2-like endoproteases PC2 and PC3 accurately cleave a model prohormone in mammalian cells: evidence for a common core of neuroendocrine processing enzymes, *Proceedings of the National Academy of Sciences*. **88**, 5297-5301.
  9. Benjannet, S., Rondeau, N., Day, R., Chretien, M. & Seidah, N. (1991) PC1 and PC2 are proprotein convertases capable of cleaving proopiomelanocortin at distinct pairs of basic residues, *Proceedings of the National Academy of Sciences*. **88**, 3564-3568.
  10. Rabah, N., Gauthier, D., Dikeakos, J. D., Reudelhuber, T. L. & Lazure, C. (2007) The C-terminal region of the proprotein convertase 1/3 (PC1/3) exerts a bimodal regulation of the enzyme activity in vitro, *The FEBS journal*. **274**, 3482-3491.
  11. Dikeakos, J. D. & Reudelhuber, T. L. (2007) Sending proteins to dense core secretory granules: still a lot to sort out, *The Journal of cell biology*. **177**, 191-196.
  12. Tsigos, C. & Chrousos, G. P. (2002) Hypothalamic-pituitary-adrenal axis, neuroendocrine factors and stress, *Journal of psychosomatic research*. **53**, 865-871.
  13. Gantz, I. & Fong, T. M. (2003) The melanocortin system, *American Journal of Physiology-Endocrinology And Metabolism*. **284**, E468-E474.
  14. Mains, R. E., Eipper, B. A. & Ling, N. (1977) Common precursor to corticotropins and endorphins, *Proceedings of the National Academy of Sciences*. **74**, 3014-3018.
  15. Ten, S., New, M. & Maclaren, N. (2001) Addison's disease 2001, *The Journal of Clinical Endocrinology & Metabolism*. **86**, 2909-2922.
  16. Salgado, L. R., Machado, M. C., Cukiert, A., Liberman, B., Kanamura, C. T. & Alves, V. A. F. (2006) Cushing's disease arising from a clinically nonfunctioning pituitary adenoma, *Endocrine pathology*. **17**, 191-199.
  17. Dell'Angelica, E. C., Shotelersuk, V., Aguilar, R. C., Gahl, W. A. & Bonifacino, J. S. (1999) Altered trafficking of lysosomal proteins in Hermansky-Pudlak syndrome due to mutations in the  $\beta$ 3A subunit of the AP-3 adaptor, *Molecular cell*. **3**, 11-21.
  18. Tooze, S. A. (1998) Biogenesis of secretory granules in the trans-Golgi network of neuroendocrine and endocrine cells, *Biochimica et Biophysica Acta (BBA)-Molecular Cell Research*. **1404**, 231-244.
  19. Hinners, I., Wendler, F., Fei, H., Thomas, L., Thomas, G. & Tooze, S. A. (2003) AP-1 recruitment to VAMP4 is modulated by phosphorylation-dependent binding of PACS-1, *EMBO reports*. **4**, 1182-1189.

20. Klumperman, J., Kuliawat, R., Griffith, J. M., Geuze, H. J. & Arvan, P. (1998) Mannose 6-phosphate receptors are sorted from immature secretory granules via adaptor protein AP-1, clathrin, and syntaxin 6-positive vesicles, *The Journal of cell biology*. **141**, 359-371.
21. Dittié, A. S., Klumperman, J. & Tooze, S. A. (1999) Differential distribution of mannose-6-phosphate receptors and furin in immature secretory granules, *J Cell Sci*. **112**, 3955-3966.
22. Asensio, C. S., Sirkis, D. W. & Edwards, R. H. (2010) RNAi screen identifies a role for adaptor protein AP-3 in sorting to the regulated secretory pathway, *The Journal of cell biology*. **191**, 1173-1187.
23. Crump, C. M., Xiang, Y., Thomas, L., Gu, F., Austin, C., Tooze, S. A. & Thomas, G. (2001) PACS-1 binding to adaptors is required for acidic cluster motif-mediated protein traffic, *The EMBO journal*. **20**, 2191-2201.
24. Munier-Lehmann, H., Mauxion, F. & Hoflack, B. (1996) Function of the two mannose 6-phosphate receptors in lysosomal enzyme transport in, Portland Press Limited,
25. Moore, H.-P., Gumbiner, B. & Kelly, R. B. (1983) Chloroquine diverts ACTH from a regulated to a constitutive secretory pathway in AtT-20 cells, *Nature*. **302**, 434.
26. Dyken, J. J. & Sambanis, A. (1994) Ammonium selectively inhibits the regulated pathway of protein secretion in two endocrine cell lines, *Enzyme and microbial technology*. **16**, 90-98.
27. Martinez-Arca, S., Rudge, R., Vacca, M., Raposo, G., Camonis, J., Proux-Gillardeaux, V., Daviet, L., Formstecher, E., Hamburger, A. & Filippini, F. (2003) A dual mechanism controlling the localization and function of exocytic v-SNAREs, *Proceedings of the National Academy of Sciences*. **100**, 9011-9016.
28. Dirk, B. S., Pawlak, E. N., Johnson, A. L., Van Nynatten, L. R., Jacob, R. A., Heit, B. & Dikeakos, J. D. (2016) HIV-1 Nef sequesters MHC-I intracellularly by targeting early stages of endocytosis and recycling, *Scientific reports*. **6**, 37021.
29. Cawley, N. X., Li, Z. & Loh, Y. P. (2016) 60 YEARS OF POMC: Biosynthesis, trafficking, and secretion of pro-opiomelanocortin-derived peptides, *Journal of molecular endocrinology*. **56**, T77-T97.
30. Futter, C. E., Connolly, C. N., Cutler, D. F. & Hopkins, C. R. (1995) Newly synthesized transferrin receptors can be detected in the endosome before they appear on the cell surface, *Journal of Biological Chemistry*. **270**, 10999-11003.
31. Hell, S. W. & Kroug, M. (1995) Ground-state-depletion fluorescence microscopy: A concept for breaking the diffraction resolution limit, *Applied Physics B*. **60**, 495-497.
32. Caetano, F. A., Dirk, B. S., Tam, J. H., Cavanagh, P. C., Goiko, M., Ferguson, S. S., Pasternak, S. H., Dikeakos, J. D., de Bruyn, J. R. & Heit, B. (2015) MliSR: molecular interactions in super-resolution imaging enables the analysis of protein interactions, dynamics and formation of multi-protein structures, *PLoS computational biology*. **11**,



e1004634.

33. Papini, E., Rossetto, O. & Cutler, D. F. (1995) Vesicle-associated membrane protein (VAMP)/synaptobrevin-2 is associated with dense core secretory granules in PC12 neuroendocrine cells, *Journal of Biological Chemistry*. **270**, 1332-1336.
34. Wan, L., Molloy, S. S., Thomas, L., Liu, G., Xiang, Y., Rybak, S. L. & Thomas, G. (1998) PACS-1 defines a novel gene family of cytosolic sorting proteins required for trans-Golgi network localization, *Cell*. **94**, 205-216.
35. Blagoveshchenskaya, A. D., Thomas, L., Feliciangeli, S. F., Hung, C.-H. & Thomas, G. (2002) HIV-1 Nef downregulates MHC-I by a PACS-1-and PI3K-regulated ARF6 endocytic pathway, *Cell*. **111**, 853-866.
36. Dikeakos, J. D., Thomas, L., Kwon, G., Elferich, J., Shinde, U. & Thomas, G. (2012) An interdomain binding site on HIV-1 Nef interacts with PACS-1 and PACS-2 on endosomes to down-regulate MHC-I, *Molecular biology of the cell*. **23**, 2184-2197.
37. Dirk, B. S., Jacob, R. A., Johnson, A. L., Pawlak, E. N., Cavanagh, P. C., Van Nynatten, L., Haeryfar, S. M. & Dikeakos, J. D. (2015) Viral bimolecular fluorescence complementation: a novel tool to study intracellular vesicular trafficking pathways, *PLoS One*. **10**, e0125619.
38. Pawlak, E. N. & Dikeakos, J. D. (2015) HIV-1 Nef: a master manipulator of the membrane trafficking machinery mediating immune evasion, *Biochimica et Biophysica Acta (BBA)-General Subjects*. **1850**, 733-741.
39. Zhou, Y. & Lindberg, I. (1993) Purification and characterization of the prohormone convertase PC1 (PC3), *Journal of Biological Chemistry*. **268**, 5615-5623.
40. Zhou, A., Bloomquist, B. T. & Mains, R. E. (1993) The prohormone convertases PC1 and PC2 mediate distinct endoproteolytic cleavages in a strict temporal order during proopiomelanocortin biosynthetic processing, *Journal of Biological Chemistry*. **268**, 1763-1769.
41. Dikeakos, J. D., Di Lello, P., Lacombe, M.-J., Ghirlando, R., Legault, P., Reudelhuber, T. L. & Omichinski, J. G. (2009) Functional and structural characterization of a dense core secretory granule sorting domain from the PC1/3 protease, *Proceedings of the National Academy of Sciences*. **106**, 7408-7413.
42. Hook, V. & Loh, Y. P. (1984) Carboxypeptidase B-like converting enzyme activity in secretory granules of rat pituitary, *Proceedings of the National Academy of Sciences*. **81**, 2776-2780.
43. Che, F. Y., Biswas, R. & Fricker, L. D. (2005) Relative quantitation of peptides in wild-type and Cpefat/fat mouse pituitary using stable isotopic tags and mass spectrometry, *Journal of mass spectrometry*. **40**, 227-237.
44. Cool, D. R., Normant, E., Shen, F.-s., Chen, H.-C., Pannell, L., Zhang, Y. & Loh, Y. P. (1997) Carboxypeptidase E is a regulated secretory pathway sorting receptor: genetic obliteration leads to endocrine disorders in Cpefat mice, *Cell*. **88**, 73-83.
45. Cawley, N. X., Yanik, T., Woronowicz, A., Chang, W., Marini, J. C. & Loh, Y. P.

- (2010) Obese carboxypeptidase E knockout mice exhibit multiple defects in peptide hormone processing contributing to low bone mineral density, *American Journal of Physiology-Endocrinology and Metabolism*. **299**, E189-E197.
46. Thiele, C., Gerdes, H.-H. & Huttner, W. B. (1997) Protein secretion: puzzling receptors, *Current Biology*. **7**, R496-R500.
  47. Varlamov, O. & Fricker, L. D. (1996) The C-terminal region of carboxypeptidase E involved in membrane binding is distinct from the region involved with intracellular routing, *Journal of Biological Chemistry*. **271**, 6077-6083.
  48. Faúndez, V., Horng, J.-T. & Kelly, R. B. (1998) A function for the AP3 coat complex in synaptic vesicle formation from endosomes, *Cell*. **93**, 423-432.
  49. Newell-Litwa, K., Seong, E., Burmeister, M. & Faundez, V. (2007) Neuronal and non-neuronal functions of the AP-3 sorting machinery, *J Cell Sci*. **120**, 531-541.
  50. de Saint Basile, G., Ménasché, G. & Fischer, A. (2010) Molecular mechanisms of biogenesis and exocytosis of cytotoxic granules, *Nature Reviews Immunology*. **10**, 568.
  51. Sobota, J. A., Ferraro, F., Bäck, N., Eipper, B. A. & Mains, R. E. (2006) Not all secretory granules are created equal: Partitioning of soluble content proteins, *Molecular biology of the cell*. **17**, 5038-5052.

## Chapter 5

### 5 Thesis Overview

#### 5.1 Discussion

##### 5.1.1 General Discussion Overview

This dissertation highlights the importance of trafficking cellular cargo to precise subcellular locations. Examples of cargo that were highlighted include a cellular receptor critical for the immune response, MHC-I (1), and the peptide hormone, ACTH, that mediates multiple physiological responses (2, 3). In both cases, PACS-1 was a membrane trafficking regulator protein pivotal in ensuring the correct localization of both cargo and was thus the primary focus of this dissertation. In addition, it was observed that PACS-1 requires the recruitment of APs to ensure the sorting of both MHC-I and ACTH (Fig. 4.4), thereby demonstrating that PACS-1-dependent sorting steps are also dependent on AP-1. Overall, in the presence of HIV-1 Nef, disruption of the Nef:PACS-1 or PACS-1:AP-1 interactions resulted in a drastic redistribution of MHC-I within the cell (Fig. 3.10). Similarly, mutation of the PACS-1:AP-1 binding site also impaired the ability of PACS-1 to localize to ACTH-positive vesicles (Fig. 4.4). Lastly, these studies also highlight the importance of quantitative fluorescence microscopy to visualize protein-protein interactions and associations within cells.

##### 5.1.2 Summary of Findings

HIV-1 is a master of hijacking the cell to permit its own replication. A primary contributor enabling this success is the Nef protein (4-8). As a small non-enzymatic viral protein, Nef relies almost exclusively on its ability to interact with a multitude of host cellular proteins to circumvent their functions. Most notably, Nef mediates the downregulation or upregulation of upwards of 35 cell surface molecules (9). To study Nef's role in hijacking host cellular proteins, I employed a novel tool that we defined as viral BiFC in Chapter 2 of this dissertation. Viral BiFC enables the detection of an association between putative protein partners expressed from the same vector. In addition, this technique permits the localization of this interaction to a precise subcellular

locale by counterstaining for vesicular markers. This novel experimental tool enabled the identification of the Nef:PACS-1 (Fig. 2.5), Nef:MHC-I (Fig. 2.7) and Nef:SNX-18 (Fig. 2.7) interactions which were observed throughout the endosomal network. Importantly, these interactions were described within the context of a viral infection. These studies represented the first demonstration of a Nef:PACS-1 interaction in cells in the context of viral infection, and the first visualization of a Nef:MHC-I interaction within cells. Moreover, we demonstrated the first reported interaction of the SNX18 protein with Nef, a protein which is believed to localize within the same vesicular structure as PACS-1 and AP-1 (10).

Nef's function during MHC-I downregulation has been previously explored however a complete understanding of the molecular players involved and the location of their activities remains unknown. Two major models exist to explain Nef-mediated MHC-I downregulation (6, 11). The first describes a process in which newly synthesized MHC-I is blocked from reaching the cell surface (11-13). The second identifies an endocytic event leading to the sequestration of MHC-I within the cell, which is dependent on the cellular PACS proteins (6, 11, 14-16). In Chapter 3, I outlined the detailed trafficking itinerary for the Nef MHC-I complex which is endocytosed from the cell surface. Importantly, this work identified the distinct endosomal localization for the interaction, and the Nef-dependent sequestration of MHC-I within the TGN. Furthermore, I discovered that Nef hijacks early recycling pathways of MHC-I trafficking, and requires Nef's acidic cluster (EEEE<sub>62-65</sub>) to recruit PACS-1, and subsequently AP-1 to the Nef:MHC-I complex. By perturbing the regulation of the early endosomal marker, Rab5, by over expressing a constitutively active mutant of Rab5 (Rab5-Q67L; Fig. 3.5), we abrogated MHC-I downregulation by Nef. This long-hypothesized sequence of events had never been previously visualized in cells. Moreover, the use of super-resolution imaging greatly aided in the identification of the role of PACS-1 in the recruitment of AP-1, and the localization of the Nef:MHC-I complex to discrete sub cellular compartments (Fig. 3.12). These data directly support the molecular events encompassed within the signaling model of MHC-I downregulation (14, 15, 17). More specifically, MHC-I was not found to traffic to the lysosome, and PACS-1 was identified to mediate the retrograde transport of MHC-I from endosomes to TGN (Fig. 3.10). Importantly,

these results further support the importance of a Nef:MHC-I:AP-1 complex, but add an additional layer of complexity by incorporating PACS-1 as an additional protein to this complex. Additional co-immunoprecipitation experiments will be needed to confirm this biochemically, but the extensive microscopic data provided in Chapter 3 strongly supports this assertion.

The data presented in Chapter 4 identified a previously unidentified role of PACS-1. PACS-1 has multiple cellular functions (11, 18-22). It is critical in the early development of the human embryo, during the trafficking of the cellular protease furin, and has been recently described as a protein that when expressed in a mutant form in humans causes cranial malformations and growth defects (23, 24). The latter disease is termed PACS-1 syndrome. Thus, we aimed to study PACS-1's role in a different cellular process: the packaging and storage of ACTH with specialized storage granules in anterior pituitary cells. The role of PACS-1 in this process has not been fully studied, rather, had focused on the role of adaptor proteins AP-1 and AP-3 in the sorting of proteins and receptors to synaptic and storage vesicles within neuroendocrine cells (25-28). In Chapter 4, I implicated PACS-1, through both knockdown and mutational analysis in the storage of ACTH within neuroendocrine cells (Fig. 4.1). Through super-resolution imaging, I determined that PACS-1 localizes to ACTH positive vesicles, which is dependent on its interaction with APs (Fig. 4.4). Moreover, upon knockdown of PACS-1 or AP-1, ACTH undergoes unregulated release into the extracellular environment (Fig 4.1). Overall, we propose a role for PACS-1 in the sorting of ACTH towards the regulated secretory pathway.

### 5.1.3 Interrogating Nef's interacting partners during MHC-I downregulation

Viruses are small genomic machines which have optimized their protein coding capacity to optimize their replication within host cells. Their genome size is limited by a number of factors including, but not limited to, the size of the viral capsid, the stability of their genome, and their sensitivity to mutation (29). Because of this, viral proteins have evolved to be multifunctional and thereby mediate a variety of diverse functions within the cell to optimize viral replication. Thus, viral proteins hijack the function of a plethora

of proteins by forming specific protein-protein interactions. To adapt to such a wide range of protein-protein interactions, viral proteins are often intrinsically disordered; lacking a defined tertiary structure (30, 31). In doing so, they can undergo conformational changes necessary to interact with host proteins. Often, viruses employ strategies known as ‘viral mimicry’ to imitate binding motifs of host cellular proteins (32-34). Notably, the adenovirus E1A protein employs this strategy to hijack the cellular protein PKR to enhance nuclear localization and viral transcription (35). HIV-1 accessory proteins are no exception to this, as the Nef protein can regulate the cell surface expression of over 35 different receptors, mediate apoptosis pathways, and alter cellular activation (9).

Nef employs multiple short yet well conserved motifs often located in flexible regions of the protein, thereby optimizing its ability to bind multiple protein partners (36). The Nef-encoded dileucine (LL<sub>164-165</sub>) motif, for example, mimics the recognition motif of AP-2 to downregulate the viral receptor CD4 from the cell surface of virally infected cells (37-40). The Nef poly-proline PxxP<sub>75</sub> motif bears similarity to the cellular PxxP motif present in host cell proteins which recognizes SH3 domains (11, 16). In the context of HIV-1 infection, Nef interacts with Src-family kinases at the TGN via the PxxP<sub>75</sub> motif to initiate a signaling cascade resulting in MHC-I endocytosis. The SNX18 protein also contains an SH3 domain within its N-terminus (41), and could represent a potential binding interface involving Nef PxxP<sub>75</sub> (Figure 2.8). Extensively investigated in Chapter 3, the Nef acidic cluster (EEEE<sub>65</sub>) mimics the cellular acidic cluster found in the cytoplasmic tail of multiple cellular receptors; furin, CI-MPR, VAMP4 and sortilin, among others (18, 19, 42-46). The acidic cluster serves as a canonical recognition motif to the PACS family of proteins (43). Much like the well-described endosome-to-Golgi trafficking of cellular receptors, we demonstrated a similar Nef-dependent trafficking of MHC-I by hijacking PACS-1. Moreover, we demonstrated the importance of PACS-1 to recruit AP-1 to the cytoplasmic tail of MHC-I.

Multiple studies have aimed to decipher the precise mechanism of Nef-mediated MHC-I downregulation. Multiple studies have demonstrated roles for Nef and PACS-2- in the activation of SFKs and PI3K (11, 14). These data convincingly demonstrated that within PBMCs, SFK and PI3K activation is a requirement for MHC-I downregulation (11, 14).

Further supporting this data is the fact that putative Nef inhibitors targeting the Nef:SFK interaction drastically increased MHC-I on the cell surface (11, 47). Other reports questioned this hypothesis; however, these results were primarily conducted in PTEN deficient cell lines, which bypass the requirement of PI3K activation (48-50). Therefore, in these circumstances, PACS-2 involvement may be dispensable. The specific contribution of PACS-1 has also been unclear. The interaction of PACS-1 and Nef has been demonstrated convincingly in both yeast-2-hybrid, co-immunoprecipitation, and BiFC assays (51, 52). Moreover, multiple studies have re-capitulated the importance of the Nef:PACS-1 interaction along with the PACS-1:AP-1 interactions in the downregulation of MHC-I (14, 15, 20). However, it remained unknown if these protein complexes were interconnected, and what trafficking steps they regulated. In Chapter 3, we propose a role for PACS-1 in the retrograde transport of the Nef:MHC-I complex from the peripheral endosomal compartments to the TGN for sequestration (Fig. 3.10 and 3.13). These studies were made possible using the BiFC assay combined with GSDM imaging. Indeed, with the 10-fold gain in resolution we demonstrated the requirement of the Nef:PACS-1 interaction in the recruitment of AP-1 to the cytoplasmic tail of MHC-I (Fig. 3.12), highlighting the role of a possible Nef:PACS-1:AP-1:MHC-I quaternary complex .

The identification of SNX18 as a potential Nef binding partner in Chapter 2 is also intriguing. The sorting nexin family of proteins is implicated in a wide variety of cellular sorting pathways, from endocytosis, to Golgi trafficking (10, 41). SNX18 can directly interact with AP-1, and co-localizes with PACS-1 in uninfected cells (10). In this context, SNX18 can also bind to curved membranes and interact with the membrane scission protein dynamin to pinch off newly budded vesicles (53, 54). The contribution of SNX18 to the downregulation of receptors by Nef is not fully known, but is currently under investigation within our laboratory (55). An attractive hypothesis includes the assembly of a multi-protein complex, in which SNX18 is recruited to sites of Nef and MHC-I, thereby facilitating the scission event required for Nef to shuttle MHC-I from one cellular location to another.

#### 5.1.4 Role of PACS-1 and AP-1 in protein sorting

Separate from the PACS-1 dependent trafficking steps in HIV-1 Nef-expressing cells, is the role of PACS-1 in uninfected cells. The role of PACS-1 in the regulated secretory pathway has evolved around its function in trafficking the endopeptidase furin (56-58). The coordinated trafficking of furin by PACS-1 allows the cleavage of multiple substrates such as the pro-parathyroid hormone, the pro-nerve growth factor and the von Willebrand factor in specialized secretory compartments (56). DCSGs are one such compartment where inactive proteins are activated via processing events (59). The maturation process of immature secretory granules to DCSGs is still not well understood, including how different cargo proteins become targeted to such specialized compartments (60). In Chapter 4, we present data which highlights the role of PACS-1 in the sorting of ACTH to the regulated secretory pathway. This study revealed that upon knockdown of PACS-1, ACTH is routed to the unregulated secretion pathway, resulting in the constitutive secretion of ACTH (Fig. 4.1). Moreover, we identified that PACS-1 co-localizes with ACTH in an AP-1 dependent fashion (Fig 4.4). It is still unclear to how PACS-1 may exert its sorting function on ACTH, as ACTH does not possess a cytoplasmic tail. This trafficking event may be a by-product of the mis-trafficking of an unknown cellular receptor mediating the formation of the DCSGs. Both PACS-1 and AP-1 are capable of interacting with the tethering protein VAMP4, which is present at the TGN, and aids in the docking of vesicles within endosomal compartments (44, 61). It is unknown if knockdown of VAMP4 prevents proper docking of ACTH positive vesicles to the immature secretory granule, but such a possibility warrants further investigation.

We did not observe a significant effect on ACTH secretion upon knockdown of AP-3. PACS-1 can interact with both AP-1 and AP-3 via the same PACS-1 motif (43, 46). The role of AP-3 in regulated DCSG release at the plasma membrane has been previously observed. The mechanism by which this occurs is not fully elucidated, but it is hypothesized to involve the calcium sensing receptor synaptotagmin-1 (SYT1) (27). SYT1 has a regulatory role in controlling the fusion of DSCGs and with the plasma membrane upon calcium stimulation due to its ability to signal the fusion of SNARE complexes (62-64). Although a knockdown of AP-3 did not result in a significant



unregulated release of ACTH akin to the knockdown of PACS-1 and AP-1 (Fig. 4.1), knockdown of AP-3 has been demonstrated to impact the fusion of DCSGs to the plasma membrane (27, 28). The precise trafficking itinerary of STY1 is not known, however, it does possess a canonical acidic cluster along with a tyrosine sorting motif, which suggests that it may also be trafficked by PACS-1. Interestingly, a preliminary analysis of PACS-1 interaction partners by our lab has identified SYT1 as a potential interaction partner (65).

### 5.1.5 Concluding remarks

Overall, the data contained within this thesis represents two fascinating fields of research: HIV-1 pathogenesis and fundamental cell biology. I bridged these fields with a focused role for PACS-1 in regulating cellular membrane trafficking. In the context of HIV-1, I provided an unprecedented view of virus-host interactions. I generated a viral vector which enabled the study of Nef-interacting partners within the cell, and provided a platform to identify novel interactions (55, 66). Moreover, these studies led to the direct visualization of the Nef:MHC-I complex within the cell. MHC-I downregulation is an important process required to evade immune detection. Thus, understanding the PACS-1-dependent mechanisms governing this process provides an important piece of the puzzle in determining how to more effectively treat HIV-1 infections (67). Importantly, we took a step back to evaluate the role of PACS-1 in protein trafficking during the uninfected state. The recent identification of *de novo* mutations in *pacs-1* (23), leading to PACS-1 syndrome, highlights the important physiological role of PACS-1 in growth and development. Overall, I believe that an enhanced understanding of PACS-1 biology during regulated secretion will aid in understanding the complexities and importance of membrane trafficking in cellular homeostasis and disease.

## 5.2 References

1. Jondal M, Schirmbeck R, Reimann J. MHC class I-restricted CTL responses to exogenous antigens. *Immunity*. 1996;5(4):295-302.
2. Moore H-P, Gumbiner B, Kelly RB. Chloroquine diverts ACTH from a regulated to a constitutive secretory pathway in AtT-20 cells. *Nature*. 1983;302(5907):434.
3. Wyllie A, Kerr J, Macaskill I, Currie A, Currie A. Adrenocortical cell deletion: the role of ACTH. *The Journal of pathology*. 1973;111(2):85-94.
4. Fackler OT, Baur AS. Live and let die: Nef functions beyond HIV replication. *Immunity*. 2002;16(4):493-497.
5. Leonard JA, Filzen T, Carter CC, Schaefer M, Collins KL. HIV-1 Nef disrupts intracellular trafficking of major histocompatibility complex class I, CD4, CD8, and CD28 by distinct pathways that share common elements. *J Virol*. 2011;85(14):6867-6881.
6. Pawlak EN, Dikeakos JD. HIV-1 Nef: A Master Manipulator of the Membrane Trafficking Machinery Mediating Immune Evasion. *Biochimica et Biophysica Acta (BBA)-General Subjects*. 2015.
7. Renkema GH, Saksela K. Interactions of HIV-1 NEF with cellular signal transducing proteins. *Front Biosci*. 2000;5:D268-283.
8. Tokarev A, Guatelli J. Misdirection of membrane trafficking by HIV-1 Vpu and Nef: Keys to viral virulence and persistence. *Cell Logist*. 2011;1(3):90-102.
9. Haller C, Müller B, Fritz JV, Lamas-Murua M, Stolp B, Pujol FM, et al. HIV-1 Nef and Vpu are functionally redundant broad-spectrum modulators of cell surface receptors, including tetraspanins. *Journal of virology*. 2014;88(24):14241-14257.
10. Håberg K, Lundmark R, Carlsson SR. SNX18 is an SNX9 paralog that acts as a membrane tubulator in AP-1-positive endosomal trafficking. *Journal of cell science*. 2008;121(9):1495-1505.
11. Dikeakos JD, Atkins KM, Thomas L, Emert-Sedlak L, Byeon IJ, Jung J, et al. Small molecule inhibition of HIV-1-induced MHC-I down-regulation identifies a temporally regulated switch in Nef action. *Molecular biology of the cell*. 2010;21(19):3279-3292.
12. Kasper MR, Roeth JF, Williams M, Filzen TM, Fleis RI, Collins KL. HIV-1 Nef disrupts antigen presentation early in the secretory pathway. *Journal of Biological Chemistry*. 2005;280(13):12840-12848.
13. Wonderlich ER, Williams M, Collins KL. The tyrosine binding pocket in the adaptor protein 1 (AP-1)  $\mu$ 1 subunit is necessary for Nef to recruit AP-1 to the major histocompatibility complex class I cytoplasmic tail. *Journal of Biological Chemistry*. 2008;283(6):3011-3022.
14. Atkins KM, Thomas L, Youker RT, Harrieff MJ, Pissani F, You H, et al. HIV-1 Nef Binds PACS-2 to Assemble a Multikinase Cascade That Triggers Major Histocompatibility Complex Class I (MHC-I) Down-regulation ANALYSIS USING SHORT INTERFERING RNA AND KNOCK-OUT MICE. *Journal of Biological Chemistry*. 2008;283(17):11772-11784.
15. Blagoveshchenskaya AD, Thomas L, Feliciangeli SF, Hung C-H, Thomas G. HIV-1 Nef downregulates MHC-I by a PACS-1-and PI3K-regulated ARF6 endocytic pathway. *Cell*. 2002;111(6):853-866.

16. Hung CH, Thomas L, Ruby CE, Atkins KM, Morris NP, Knight ZA, et al. HIV-1 Nef assembles a Src family kinase-ZAP-70/Syk-PI3K cascade to downregulate cell-surface MHC-I. *Cell Host Microbe*. 2007;1(2):121-133.
17. Schwartz O, Maréchal V, Le Gall S, Lemonnier F, Heard J-M. Endocytosis of major histocompatibility complex class I molecules is induced by the HIV-1 Nef protein. *Nature medicine*. 1996;2(3):338-342.
18. Schermer B, Höpker K, Omran H, Ghenoïu C, Fliegau M, Fekete A, et al. Phosphorylation by casein kinase 2 induces PACS-1 binding of nephrocystin and targeting to cilia. *The EMBO journal*. 2005;24(24):4415-4424.
19. Scott GK, Fei H, Thomas L, Medigeshi GR, Thomas G. A PACS-1, GGA3 and CK2 complex regulates CI-MPR trafficking. *The EMBO journal*. 2006;25(19):4423-4435.
20. Scott GK, Gu F, Crump CM, Thomas L, Wan L, Xiang Y, et al. The phosphorylation state of an autoregulatory domain controls PACS-1-directed protein traffic. *The EMBO journal*. 2003;22(23):6234-6244.
21. Thomas G, Aslan JE, Thomas L, Shinde P, Shinde U, Simmen T. Caught in the act—protein adaptation and the expanding roles of the PACS proteins in tissue homeostasis and disease. *J Cell Sci*. 2017;jcs. 199463.
22. Youker R, Shinde U, Day R, Thomas G. At the crossroads of homeostasis and disease: roles of the PACS proteins in membrane traffic and apoptosis. *Biochem J*. 2009;421:1-15.
23. Schuurs-Hoeijmakers JH, Oh EC, Vissers LE, Swinkels ME, Gilissen C, Willemsen MA, et al. Recurrent de novo mutations in PACS1 cause defective cranial-neural-crest migration and define a recognizable intellectual-disability syndrome. *The American Journal of Human Genetics*. 2012;91(6):1122-1127.
24. Schuurs-Hoeijmakers JH, Landsverk ML, Foulds N, Kukolich MK, Gavrilova RH, Greville-Heygate S, et al. Clinical delineation of the PACS1-related syndrome—Report on 19 patients. *American Journal of Medical Genetics Part A*. 2016;170(3):670-675.
25. Dittié AS, Thomas L, Thomas G, Tooze SA. Interaction of furin in immature secretory granules from neuroendocrine cells with the AP-1 adaptor complex is modulated by casein kinase II phosphorylation. *The EMBO Journal*. 1997;16(16):4859-4870.
26. Nakatsu F, Ohno H. Adaptor protein complexes as the key regulators of protein sorting in the post-Golgi network. *Cell structure and function*. 2003;28(5):419-429.
27. Asensio CS, Sirkis DW, Edwards RH. RNAi screen identifies a role for adaptor protein AP-3 in sorting to the regulated secretory pathway. *The Journal of cell biology*. 2010;191(6):1173-1187.
28. Newell-Litwa K, Seong E, Burmeister M, Faundez V. Neuronal and non-neuronal functions of the AP-3 sorting machinery. *J Cell Sci*. 2007;120(4):531-541.
29. Brandes N, Linial M. Gene overlapping and size constraints in the viral world. *Biology direct*. 2016;11(1):26.
30. King CR. Functional and Structural Mimicry of A-Kinase Anchoring Proteins by

- Human Adenovirus E1A. 2018.
31. Fuxreiter M, Tompa P, Simon I. Local structural disorder imparts plasticity on linear motifs. *Bioinformatics*. 2007;23(8):950-956.
  32. Alcamí A. Viral mimicry of cytokines, chemokines and their receptors. *Nature Reviews Immunology*. 2003;3(1):36.
  33. Wimmer P, Schreiner S. Viral mimicry to usurp ubiquitin and SUMO host pathways. *Viruses*. 2015;7(9):4854-4872.
  34. Chemes LB, de Prat-Gay G, Sánchez IE. Convergent evolution and mimicry of protein linear motifs in host–pathogen interactions. *Current opinion in structural biology*. 2015;32:91-101.
  35. King CR, Cohen MJ, Fonseca GJ, Dirk BS, Dikeakos JD, Mymryk JS. Functional and structural mimicry of cellular protein kinase A anchoring proteins by a viral oncoprotein. *PLoS pathogens*. 2016;12(5):e1005621.
  36. Pawlak EN, Dikeakos JD. HIV-1 Nef: a master manipulator of the membrane trafficking machinery mediating immune evasion. *Biochimica et Biophysica Acta (BBA)-General Subjects*. 2015;1850(4):733-741.
  37. Aiken C, Konner J, Landau NR, Lenburg ME, Trono D. Nef induces CD4 endocytosis: requirement for a critical dileucine motif in the membrane-proximal CD4 cytoplasmic domain. *Cell*. 1994;76(5):853-864.
  38. Bresnahan PA, Yonemoto W, Ferrell S, Williams-Herman D, Geleziunas R, Greene WC. A dileucine motif in HIV-1 Nef acts as an internalization signal for CD4 downregulation and binds the AP-1 clathrin adaptor. *Current biology*. 1998;8(22):1235-S1231.
  39. Lu X, Yu H, Liu S-H, Brodsky FM, Peterlin BM. Interactions between HIV1 Nef and vacuolar ATPase facilitate the internalization of CD4. *Immunity*. 1998;8(5):647-656.
  40. Ren X, Park SY, Bonifacino JS, Hurley JH. How HIV-1 Nef hijacks the AP-2 clathrin adaptor to downregulate CD4. *Elife*. 2014;3:e01754.
  41. Park J, Kim Y, Lee S, Park JJ, Park ZY, Sun W, et al. SNX18 shares a redundant role with SNX9 and modulates endocytic trafficking at the plasma membrane. *Journal of cell science*. 2010;jcs. 064170.
  42. Crump CM, Hung C-H, Thomas L, Wan L, Thomas G. Role of PACS-1 in trafficking of human cytomegalovirus glycoprotein B and virus production. *Journal of virology*. 2003;77(20):11105-11113.
  43. Crump CM, Xiang Y, Thomas L, Gu F, Austin C, Tooze SA, et al. PACS-1 binding to adaptors is required for acidic cluster motif-mediated protein traffic. *The EMBO journal*. 2001;20(9):2191-2201.
  44. Hinners I, Wendler F, Fei H, Thomas L, Thomas G, Tooze SA. AP-1 recruitment to VAMP4 is modulated by phosphorylation-dependent binding of PACS-1. *EMBO reports*. 2003;4(12):1182-1189.
  45. Köttgen M, Benzing T, Simmen T, Tauber R, Buchholz B, Feliciangeli S, et al. Trafficking of TRPP2 by PACS proteins represents a novel mechanism of ion channel regulation. *The EMBO journal*. 2005;24(4):705-716.
  46. Wan L, Molloy SS, Thomas L, Liu G, Xiang Y, Rybak SL, et al. PACS-1 defines a novel gene family of cytosolic sorting proteins required for trans-Golgi network

- localization. *Cell*. 1998;94(2):205-216.
47. Mujib S, Saiyed A, Fadel S, Bozorgzad A, Aidarus N, Yue FY, et al. Pharmacologic HIV-1 Nef blockade promotes CD8 T cell-mediated elimination of latently HIV-1-infected cells in vitro. *JCI insight*. 2017;2(17).
  48. Larsen JE, Massol RH, Nieland TJ, Kirchhausen T. HIV Nef-mediated major histocompatibility complex class I down-modulation is independent of Arf6 activity. *Molecular biology of the cell*. 2004;15(1):323-331.
  49. Casartelli N, Giolo G, Neri F, Haller C, Potestà M, Rossi P, et al. The Pro78 residue regulates the capacity of the human immunodeficiency virus type 1 Nef protein to inhibit recycling of major histocompatibility complex class I molecules in an SH3-independent manner. *Journal of general virology*. 2006;87(8):2291-2296.
  50. Schaefer MR, Wonderlich ER, Roeth JF, Leonard JA, Collins KL. HIV-1 Nef targets MHC-I and CD4 for degradation via a final common  $\beta$ -COP-dependent pathway in T cells. *PLoS pathogens*. 2008;4(8):e1000131.
  51. Piguet V, Wan L, Borel C, Mangasarian A, Demarex N, Thomas G, et al. HIV-1 Nef protein binds to the cellular protein PACS-1 to downregulate class I major histocompatibility complexes. *Nature cell biology*. 2000;2(3):163-167.
  52. Dikeakos JD, Thomas L, Kwon G, Elferich J, Shinde U, Thomas G. An interdomain binding site on HIV-1 Nef interacts with PACS-1 and PACS-2 on endosomes to down-regulate MHC-I. *Molecular biology of the cell*. 2012;23(11):2184-2197.
  53. Sørensen K, Munson MJ, Lamb CA, Bjørndal GT, Pankiv S, Carlsson SR, et al. SNX18 regulates ATG9A trafficking from recycling endosomes by recruiting Dynamin-2. *EMBO reports*. 2018:e44837.
  54. Hinshaw JE, Schmid SL. Dynamin self-assembles into rings suggesting a mechanism for coated vesicle budding. *Nature*. 1995;374(6518):190.
  55. Dirk BS, Jacob RA, Johnson AL, Pawlak EN, Cavanagh PC, Van Nynatten L, et al. Viral Bimolecular Fluorescence Complementation: A Novel Tool to Study Intracellular Vesicular Trafficking Pathways. *PloS one*. 2015;10(4):e0125619.
  56. Anderson ED, Molloy SS, Jean F, Fei H, Shimamura S, Thomas G. The ordered and compartment-specific autoproteolytic removal of the furin intramolecular chaperone is required for enzyme activation. *Journal of Biological Chemistry*. 2002;277(15):12879-12890.
  57. Dittie AS, Klumperman J, Tooze SA. Differential distribution of mannose-6-phosphate receptors and furin in immature secretory granules. *J Cell Sci*. 1999;112(22):3955-3966.
  58. Dittie AS, Thomas L, Thomas G, Tooze SA. Interaction of furin in immature secretory granules from neuroendocrine cells with the AP-1 adaptor complex is modulated by casein kinase II phosphorylation. *The EMBO Journal*. 1997;16(16):4859-4870.
  59. Schmidt W, Moore H. Ionic milieu controls the compartment-specific activation of pro-opiomelanocortin processing in AtT-20 cells. *Molecular biology of the cell*. 1995;6(10):1271-1285.
  60. Sobota JA, Ferraro F, Bäck N, Eipper BA, Mains RE. Not all secretory granules are created equal: Partitioning of soluble content proteins. *Molecular biology of*

- the cell. 2006;17(12):5038-5052.
61. Wendler F, Page L, Urbé S, Tooze SA. Homotypic fusion of immature secretory granules during maturation requires syntaxin 6. *Molecular biology of the cell*. 2001;12(6):1699-1709.
  62. Leguia M, Conner S, Berg L, Wessel GM. Synaptotagmin I is involved in the regulation of cortical granule exocytosis in the sea urchin. *Molecular Reproduction and Development: Incorporating Gamete Research*. 2006;73(7):895-905.
  63. Lynch KL, Gerona RR, Kielar DM, Martens S, McMahon HT, Martin TF. Synaptotagmin-1 utilizes membrane bending and SNARE binding to drive fusion pore expansion. *Molecular biology of the cell*. 2008;19(12):5093-5103.
  64. Fox MA, Sanes JR. Synaptotagmin I and II are present in distinct subsets of central synapses. *Journal of Comparative Neurology*. 2007;503(2):280-296.
  65. Johnson AL. Understanding the impact of HIV-1 genetic diversity on the function of Nef and its role in SERINC5 antagonism. 2018.
  66. Dirk BS, Heit B, Dikeakos JD. Visualizing Interactions Between HIV-1 Nef and Host Cellular Proteins Using Ground-State Depletion Microscopy. *AIDS research and human retroviruses*. 2015;31(7):671-672.
  67. Dirk BS, Pawlak EN, Johnson AL, Van Nynatten LR, Jacob RA, Heit B, et al. HIV-1 Nef sequesters MHC-I intracellularly by targeting early stages of endocytosis and recycling. *Scientific reports*. 2016;6:37021.

## Appendix

### Permissions

Data presented in Chapter 2 was published in PLoS ONE.

#### May I Use Article Content I Previously Published in Another Journal?

Many authors assume that if they previously published a paper through another publisher, they own the rights to that content and they can freely use that content in their PLOS paper, but that's not necessarily the case – it depends on the license that covers the other paper. Some publishers allow free and unrestricted re-use of article content they own, such as under the CC BY license. Other publishers use licenses that allow re-use only if the same license is applied by the person or publisher re-using the content.

If the paper was published under a CC BY license or another license that allows free and unrestricted use, you may use the content in your PLOS paper provided that you give proper attribution, as explained above.

If the content was published under a more restrictive license, you must ascertain what rights you have under that license. At a minimum, review the license to make sure you can use the content. Contact that publisher if you have any questions about the license terms – PLOS staff cannot give you legal advice about your rights to use third-party content. If the license does not permit you to use the content in a paper that will be covered by an unrestricted license, you must obtain written permission from the publisher to use the content in your PLOS paper. Please do not include any content in your PLOS paper which you do not have rights to use, and always [give proper attribution](#).

A portion of the data presented in Chapter 3 was published in Scientific Reports

#### Get permission to reuse Springer Nature content online

##### Permission requests from authors

The author of articles published by SpringerNature do not usually need to seek permission for re-use of their material as long as the journal is credited with initial publication.

Ownership of copyright in original research articles remains with the Author, and provided that, when reproducing the contribution or extracts from it or from the Supplementary Information, the Author acknowledges first and reference publication in the Journal, the Author retains the following non-exclusive rights:

To reproduce the contribution in whole or in part in any printed volume (book or thesis) of which they are the author(s).

The author and any academic institution where they work at the time may reproduce the contribution for the purpose of course teaching.

To reuse figures or tables created by the Author and contained in the Contribution in oral presentations and other works created by them.

To post a copy of the contribution as accepted for publication after peer review (in locked Word processing file, of a PDF version thereof) on the Author's own web site, or the Author's institutional repository, or the Author's funding body's archive, six months after publication of the printed or online edition of the Journal, provided that they also link to the contribution on the publisher's website.

The above use of the term 'Contribution' refers to the author's own version, not the final version as published in the Journal.

A portion of the data presented in Chapter 4 was published in Biochemical and Biophysical Communications



The screenshot shows a web browser window with the URL <https://www.elsevier.com/about/policies/copyright/permissions>. The browser's address bar and tabs are visible. The page header includes the Elsevier logo (a tree) and the word "ELSEVIER". To the right of the logo is a search bar with a magnifying glass icon and the word "SEARCH". Below the header, the main content area displays the question "Can I include/use my article in my thesis/dissertation? –" followed by the answer: "Yes. Authors can include their articles in full or in part in a thesis or dissertation for non-commercial purposes."

← → ↻ <https://www.elsevier.com/about/policies/copyright/permissions>

Apps Welcome! | LinkedIn | Lab Bookings | EasyWeb | Google Scholar | Sign In | Present Yourself! ...

 **ELSEVIER**

 **SEARCH** 

[Can I include/use my article in my thesis/dissertation? –](#)

Yes. Authors can include their articles in full or in part in a thesis or dissertation for non-commercial purposes.



## Curriculum Vitae

<b>Name:</b>	Brennan Dirk
<b>Post-secondary Education and Degrees:</b>	<p>University of Guelph Guelph, Ontario, Canada 2009-2013 BSc. Honours Microbiology</p> <p>The University of Western Ontario London, Ontario, Canada 2013-2018 Ph.D. Microbiology &amp; Immunology</p>
<b>Honours and Awards:</b>	<p>Canadian Institutes of Health Research (CIHR) Doctoral Research Award 2017-2020</p> <p>The University of Western Ontario Nellie Farthing Fellowship in Medical Sciences 2017</p> <p>Canadian Association for HIV Research Academic Scholarship in Vaccine Design 2017</p> <p>Province of Ontario Graduate Scholarship 2016-2017, 2017-2018 (declined)</p> <p>The University of Western Ontario FW Luney Graduate Fellowship 2015</p> <p>The University of Western Ontario Dean's MSc to PhD Transfer Award 2015-2016, 2016-2017 (declined), 2017-2018 (declined)</p> <p><i>Travel Awards</i></p> <ul style="list-style-type: none"> <li>- American Society for Virology - June 2016</li> <li>- Canadian Society for Virology - June 2016 &amp; June 2017</li> <li>- CIHR Community Support Travel Award- March 2016</li> </ul>
<b>Related Work Experience</b>	<p>Guest Lecturer: "Respiratory Viruses" The University of Western Ontario November 22, 2017</p>

Partners in Education Co-op Student Supervisor  
The University of Western Ontario  
2014-2017

Teaching Assistant (MIRO/IMM 2500A, 3100A)  
The University of Western Ontario  
2014-2017

Let's Talk Science Representative  
The University of Western Ontario  
2013-2015

Infection and Immunity Research Forum Organizational  
Committee Chair  
The University of Western Ontario  
2015-2016

### **Publications:**

1. **Dirk BS**, End C, Pawlak EN, Van Nynatten LR, Jacob RA, Heit B, Dikeakos JD. 2018. PACS-1 and adaptor proteins – 1 mediate ACTH trafficking to the regulated secretory pathway. *Biochem Biophys Res Commun.* (in press).
2. Van Nynatten,LR., Johnson AL., **Dirk BS**, Pawlak EN., Jacob RA., Haeryfar SMM., & Dikeakos JD. 2018. Identification of Novel Subcellular Localization and Trafficking of HIV-1 Nef Variants from Reference Strains G (F1.93.HH8793) and H (BE.93.VI997). *Viruses*, Sep 13;10(9)
3. Pawlak EN, **Dirk BS**, Jacob RA, Johnson AL, Dikeakos JD. 2018. The HIV-1 accessory proteins Nef and Vpu downregulate total and cell surface CD28 in CD4+ T cells. *Retrovirology*. Jan 12;15(1):6.
4. Jacobs RA, Johnson AL, Pawlak EN, **Dirk BS**, Van Nynatten LR, Haeryfar SMM, Dikeakos JD. 2017. The interaction between HIV-1 Nef and adaptor protein-2 reduces Nef-mediated CD4 T cell apoptosis. *Virology*. 509:1-10.
5. Evans AL, Blackburn JWD, Taruc K, Kipp A, **Dirk BS**, Hunt NR, Barr SD, Dikeakos JD, Heit B. 2017. Antagonistic Coevolution of MER tyrosine kinase expression and function. *Mol Biol Evol.* 34(7):1613-1628.
6. **Dirk BS**, Pawlak EN, Johnson AL, Van Nynatten LR, Dr. Jacob RA, Heit B & Dikeakos JD. 2016. HIV-1 Nef sequesters MHC-I intracellularly by targeting early stages of endocytosis and recycling. *Scientific Reports*. 6:37021
7. Johnson AL, **Dirk BS**, Coutu M, Haeryfar SMM, Arts EJ, Finzi A & Dikeakos JD. 2016. Highly Conserved residue in HIV-1 Nef alpha helix-2 modulates protein expression. *mSphere*. 1(6) pii: e00288-16.
8. **Dirk BS**, Van Nynatten LR & Dikeakos JD. 2016. Where in the cell are you? Probing HIV-1-Host interactions through advanced imaging techniques. *Viruses*. 8(10), 288.
9. Asmal M, Lane S, Tian M, Nickle G, Venner CM, **Dirk B**, Dikeakos JD, Luedemann C, Mach L, Balachandran H, Buzbe A, Rao S, Letvin N, Gao Y &

- Arts EJ. 2016. Pathogenic infection of Rhesus macaques by an evolving SIV-HIV derived from CCR5-using envelope genes of acute HIV-1 infections. *Virology*. 499:298-312.
10. King CR, Cohen MJ, Fonseca JG, **Dirk BS** Dikeakos JD & Mymryk JS. 2016. Functional and structural mimicry of cellular protein kinase A anchoring proteins by a viral oncoprotein. *PLOS Pathog*. 12(5):e1005621.
  11. Caetano FA, **Dirk BS**, Tam JHK, Cavanagh PC, Ferguson SG, Pasternak SH, Dikeakos JD, de Bruyn JR, & Heit B. 2015. Super-Resolution Imaging as a Quantitative Analysis Method Enabling the Study of Protein Interactions, Dynamics and Formation of Multi-protein Structures. *PLoS Comput. Biol*. 11(12): e1004634
  12. **Dirk BS**, Heit B & Dikeakos JD. 2015. Visualizing interactions between HIV-1 Nef and host cellular proteins using ground state depletion microscopy. *AIDS Research and Human Retroviruses*. 31(7):671-672.
  13. **Dirk BS\***, Jacob RA\*, Johnson AL, Pawlak EN, Cavanagh CP, Van Nynatten L, Haeryfar SM, & Dikeakos JD. 2015. Viral bimolecular fluorescence complementation: A Novel Tool to Study Intracellular Vesicular Trafficking Pathways. *PLoS ONE*. 10(4) doi:e0125619 – \*Co-first Author

### Oral Presentations

1. **Dirk BS**, End C, Dikeakos JD. ‘Seeing is believing: identifying intermolecular protein complexes mediating HIV immune evasion through microscopy.’ 2<sup>nd</sup> Meeting for the Canadian Society for Virology. Halifax, Nova Scotia. June 13-15, 2018.
2. **Dirk BS**, End C, Dikeakos JD. ‘Seeing is believing: identifying intermolecular protein complexes mediating HIV immune evasion through microscopy.’ 27<sup>th</sup> Annual Canadian Conference on HIV/AIDS Research. Vancouver, British Columbia. April 27-31, 2018.
3. **Dirk BS**, Pawlak EP, Johnson AL, Van Nynatten L, Jacob RA, Dikeakos JD. ‘Hide and seek with HIV-1 Nef: Gaining super-resolution insights to viral immune evasion.’ 26<sup>th</sup> Annual Canadian Conference on HIV/AIDS Research. Montreal, Quebec. April 6-7, 2017.
4. **Dirk BS**, Pawlak EP, Johnson AL, Van Nynatten L, Jacob RA, Dikeakos JD. ‘Hide and seek with HIV-1 Nef: Gaining super-resolution insights to viral immune evasion.’ London Health Research Day. London, Ontario. March 30, 2017.
5. **Dirk BS**, Van Nynatten LV, Heit B & Dikeakos JD. ‘HIV Nef targets MHC-I for Sequestration by hijacking early endocytic events.’ 35<sup>th</sup> Meeting for the American Society for Virology. Blacksburg, VA, USA. June 18-22, 2016.
6. **Dirk BS**, Van Nynatten LV, Heit B & Dikeakos JD. ‘HIV Nef targets MHC-I for Sequestration by hijacking early endocytic events.’ 1<sup>st</sup> Annual Canadian Society for Virology Workshop. Blacksburg, VA, USA. June 18, 2016.
7. **Dirk BS**, Van Nynatten LV, Heit B & Dikeakos JD. ‘HIV Nef targets MHC-I for Sequestration by hijacking early endocytic events.’ London Health Research Day. London Ontario, Canada. March 29, 2016.

8. **Dirk BS**, Heit B & Dikeakos JD. 'Examining the role of the PACS-1/AP-1 interaction in Nef mediated MHC-I downregulation by super-resolution microscopy', 34<sup>th</sup> Meeting for the American Society for Virology. Western University, London, ON, Canada. July 11-15, 2015.

### **Poster Presentations**

1. Dirk BS, C End, Dikeakos JD. 'Seeing is believing: identifying intermolecular protein complexes mediating HIV immune evasion through microscopy.' London Health Research Day 2018. London, ON. May 10, 2018.
2. **Dirk BS**, Van Nynatten L & Dikeakos JD. 'HIV Nef targets MHC-I for Sequestration by hijacking early endocytic events. Keystone Symposia X7 HIV Persistence: Pathogenesis and Eradication. Resort at Squaw Creek, Olympic Valley, CA. March 20-24, 2016.
3. **Dirk BS**, Jacob RA, Johnson AL, Pawlak EN, Cavanagh CP, Van Nynatten L, Haeryfar SM & Dikeakos JD. Viral bimolecular fluorescence complementation: A Novel Tool to Study Intracellular Vesicular Trafficking Pathways.' 24<sup>th</sup> Annual Canadian Conference for HIV/AIDS Research-CAHR 2015. Toronto, ON. April 30-May 3, 2015.
4. **Dirk BS**, Cavanagh C, Dikeakos JD. 'Examining the subcellular localization of HIV-1 Nef and MHC-I through the endocytic network. London Health Research Day 2014. London Ontario. March 2014.